Universidad de Cantabria (UC)

Facultad de Medicina

Departamento de Biología Molecular

Instituto de Biomedicina y Biotecnología de Cantabria (IBBTEC)

Departamento de Microbiología y Genómica

Lípidos de valor añadido en bacterias genéticamente modificadas

Tesis Doctoral presentada por

Beatriz Lázaro Pinto

para optar al Grado de Doctor por la Universidad de Cantabria

Santander, 2016

University of Cantabria (UC)

School of Medicine

Molecular Biology Department

Institute of Biomedicine and Biotechnology of Cantabria (IBBTEC)

Department of Microbiology and Genomics

Added-value oils in genetically engineered bacteria

Beatriz Lázaro Pinto

Santander, 2016

Don Gabriel Moncalian Montes, Profesor Titular de Genética, perteneciente al Departamento de Biología Molecular de la Universidad de Cantabria,

CERTIFICA: Que Dña. Beatriz Lázaro Pinto ha realizado bajo su dirección el trabajo que lleva por título "Lípidos de valor añadido en bacterias genéticamente modificadas".

Considero que dicho trabajo se encuentra terminado y reúne los requisitos necesarios para su presentación como Memoria de Doctorado, al objeto de poder optar al grado de Doctor.

Santander, a 6 de Junio de 2016

Fdo. Gabriel Moncalian Montes

El presente trabajo ha sido realizado entre el Departamento de Biología Molecular de la Universidad de Cantabria y el Departamento de Microbiología y Genómica del Instituto de Biomedicina y Biotecnología de Cantabria, bajo la dirección del Dr. Gabriel Moncalián Montes, gracias a un contrato de la Universidad de Cantabria asociado a los proyectos “Aceites a la carta: bioingeniería de la síntesis de monoésteres y triglicéridos en microorganismos” (BIO2010-14809, del Ministerio de Ciencia e Innovación) y “Producción de aceites de interés comercial en microorganismos modificados genéticamente” (2014).

Durante este periodo se ha realizado una estancia de diez meses en el laboratorio de la Dra. Cintia D. F. Milagre (Instituto de Química, Universidad Estatal Paulista "Júlio de Mesquita Filho"– UNESP –, Araraquara, Brasil), gracias a una ayuda de la Comisión Europea (Programa Erasmus Mundus, Proyecto iBrasil, 2014/2015).

"No temas a las dificultades:
lo mejor surge de ellas."

Rita Levi-Montalcini

"...tantas cosas que decir... ¡prometo estarte agradecido!"

Como no quiero que esta sea la parte más larga de este documento, intentaré sintetizar, aunque temo que eso implica dejarme en el tintero muchos nombres...de cualquier forma me gustaría agradecer a todos y cada uno de los que me habéis ayudado de alguna manera, en el terreno profesional o psicológico, durante estos años de trabajo. Además del esfuerzo dedicado, la realización de esta Tesis Doctoral no habría sido posible sin la colaboración de mucha gente.

En primer lugar quería agradecer a mi jefe Gabi la oportunidad de realizar esta Tesis en su laboratorio, todas las indicaciones y consejos gracias a los que he llegado hasta aquí y lo aprendido en esta etapa. A Fernando, a Iñaki y a Elena, por vuestro interés por mi trabajo, por vuestras ideas y por todo lo aprendido en cada una de las discusiones y reuniones, ¡muchas gracias!

Muito obrigada à minha orientadora da estadia no Brasil, a Profa. Cíntia, por me abrir a porta do seu laboratório e do seu grupo de pesquisa, por me apresentar aos colegas que colaboraram nestre trabalho e pela ajuda toda, desde antes da estadia até o fim da Tese.

A la empresa "Biomar Microbial Technologies" (León) por los análisis GC y por las interesantes discusiones sobre los proyectos en común.

Al Dr. Olimpio Montero (Centro para el Desarrollo de la Biotecnología, CSIC; Boecillo, Valladolid) por los análisis UPLC/MS.

Thanks to Dr. Okuyama (Graduate School of Environmental Earth Science, Hokkaido University, Sapporo, Japan) for providing the plasmid pDHA4.

À Profa. Maria Célia e ao Prof. Rubens pela sua ajuda e por me permitir trabalhar nos seus laboratórios no Câmpus de Araraquara da UNESP na purificação de proteínas.

A Dolores, por ser la insustituible guía de los doctorandos en la EDUC, por tu apoyo.

À Lucinéia V. Marconcini e ao Nivaldo Boralle pela grande ajuda com os experimentos de RMN na UNESP.

A Víctor Campa, por la asistencia en todos los experimentos de microscopía y por ayudarme en el aprendizaje del tratado de imágenes en el IBBTEC.

A María Aramburu, por ayuda técnica con la citometría de flujo en la Facultad de Medicina de la UC.

A Matí, por toda tu ayuda en el laboratorio, especialmente por tus enseñanzas en los comienzos.

A María de Toro (MdT) por la ayuda con secuenciación del plásmido pDHA4, por tus buenos ideas y consejos, por tu perspectiva.

A Rulí, por tus interesantes ideas y su ayuda, sobretodo con los experimentos de time-lapse en el IBBTEC.

A Mapi..... por resolverme las dudas tontas, por tu permanente apoyo, por estar ahí, eres una gran persona, ¡no cambies!

To Alexandra...

Gracias a todos los que en algún momento han compartido conmigo laboratorio/ lobera/ cafeses / taperes / clases y cursos varios... <u>desde los inicios en la Facultad</u>...

A Alej (EL "master of pipettes!!" sabinero experto en protectores de pantalla ;P), a Jorge ("el gallego", por esas bienvenidas mañaneras con RockFm a buen volumen sin perder nunca el ritmo de trabajo), a Lillo ("-pedía", SIEMPRE dispuesto a aportar su granito de arena), a Getino (por ofrecerme ayuda desde el primerísisimo día que nos dieron las tantas en el labo), a Inma, a Juan, a Val, a Maris, a Atha. A Sheila, Carlos, Raquel, Ana y Sandra. A Lucía, Paula, Fer, Lorena, Marcos, Pilar, Esther, Anabel, Coral, Alfonso, Javi...

A David, por toda la ayuda tanto en la parte puramente laboratoril como por ejercer de psicológo, por "pegarme" esa afición a Loquillo (sin llegar a tu nivel :P)... por estar siempre ahí.

A Vir, Palanca, Eva y Rocío, por acogerme como una más desde el principio de los tiempos, por todos los Regmas y Quebecs, por las fílmos de los domingos, las infusiones en la Escondida...

A Elena BuenA....aunque sólo compartí un año contigo... dejaste una huella imborrable! Gracias por continuar apoyándome desde la distancia. Sé que va a ir todo genial. Lo mereces.

...en cualquier rincón del ibítec....

A Jorge ("nuevo IBBTEC" -lo siento, he de confensar que mi móvil aún dice eso xd-, ¡¡no cambies nunca!!), a Litri (espero que vaya todo genial! :), a Emilio (un grande! gracias por esa sonrisa contagiosa), a Jusep, a Dalia, a Fuen, a Raquel (temo que descubrí tarde el departamento de Farma)...

A Omar (por tener siempre ese comentario-locura que te saca una sonrisa...); a Lorena (aunque apenas hayamos coincidido, estoy segura de que todo va a ir sobre ruedas)

A Laura, puedes considerarte incluida en cualquiera de los agracecimientos (desde Biomar y el labo de Santander hasta la estancia y la recta final de la tesis, pasando por la EOI...), vamos... que te mereces un enooOoorme GRACIAS (y una visita al indio... xd).

A los compas (y profes) de las EOIses, en especial a Juan y Luz, que a pesar de distancias, ahí están, com seus narizes e com vontade de comer uma boa dose de queijo comigo ;P

...o al otro lado del charco....

Muito obrigada à Karina pelas indicações no começo; ao Bruno, pelos bons conselhos, pelo apoio e pela ajuda com o MestreNova, à Raquel.... por tudo, você foi un apoio muito importante lá! À Ana, à Veridiana, ao João. À Juliana, gratidão pela gentileza e a ajuda, espero que esteja dando tudo certo! A Pablo, gracias por esa disposición para echarme una mano en el labo (y tomar un pão de queijo en la cafetería).

A los "gringos com fome", a Abraham (tener vecinos de labo y amigos así no tiene precio), a Rúben (porque Rubén me suena raro, y porque às vezes aún son 20 para las 3... jeje), a Ana (por tu optimismo y espontaneidad), a Pigüi (por tener siempre una palabra amable), à Amber (um exemplo de independência), a Teddy (por estar siempre ahí, por tu apoyo), à Cintia (pela sua alegria e grande sorriso). À todos meus professores forrozeiros, à Fernanda, à Anna, a Borja, ao Lukas, ao Armin... À a Elaise e ao Lucas e às suas famílias, vocês foram muito amáveis comigo, não vou esquecer.

Muchiiiísimas gracias a los que siempre estuvieron ahí, ni me acuerdo ya desde cuando, y siguen al pie del cañón sin importar distancias...Sofi, Tama, Leti, Moni, Kike, Julia, Sergio (Carni), Patri, Elena (BuenO), Nuria (un par de millones de gracias a mayores por aquí!), Leyre... y los que me han aguantado en esta última etapa... Javi, Zara, Jorge, Vane...

A Diego, Juan y Marce.

Por último en orden, pero no en importancia, a mi familia, y en especial a mis padres, por la infinita paciencia, comprensión y apoyo incondicional.

¡¡GRACIAS!! VALEU!!

A mis padres, a mi abuela.

Index

Abbreviations

1D	One-dimensional
1D TOCSY	One-dimensional total correlation spectroscopy (^{1}H NMR)
^{1}H NMR	Proton nuclear magnetic resonance
2D	Two-dimensional
2D H-H COSY	Two-dimensional homonuclear H correlation spectroscopy (^{1}H NMR)
3D	Three-dimensional
aa	Amino acid
AA	Arachidonic acid
ACC	Acetyl-CoA carboxylase complex
ACP	Acyl carrier protein
AFU	Arbitrary fluorescence units
ALA	α-linolenic acid
Ap	Ampicillin
AT	Acyltransferase
BCIP	5-bromo-4-chloro-3-indolyl-phosphate
bp	Base pair
BPI	Base peak ion
BSA	Bovine serum albumin
CAT	Chloramphenicol acetyltransferase
$CDCl_3$	Deuterated chloroform
CHD	Coronary heart diseases
CL	Cardiolipin diphosphatidylglycerol
CLF	Chain length factor
Cm	Chloramphenicol
CoA	Coenzyme A
Ct	Terminal carboxyl end
d	Doublet
D_2O	Deuterium oxide
DAG	Diacylglycerol
DCC	Dry-Column Flash Chromatography
dd	Doublet of doublets
DEAE	Diethylaminoethanol
DGAT	Diacylglycerol acyltransferase
DH/I	Dehydrase/isomerase
DHA	Docosahexaenoic acid
DMSO	Dimethyl sulfoxide

DMSO-d_6	Deuterated dimethyl sulfoxide
DNA	Deoxyribonucleic acid
dNTP	Deoxyribonucleotide triphosphate
DPA	Docosapentaenoic acid
dpi	Dots per inch
EDTA	Ethylenediaminetetraacetic acid
EFAs	Essential fatty acids
EIC	Extracted ion chromatogram
Em	Erythromycin
EPA	Eicosapentaenoic acid
ER	Enoyl reductase
ESI	Electrospray
FA	Fatty acid
FABEs	Fatty acid butyl esters
FAEE	Fatty acid ethyl ester
FAME	Fatty acid methyl esters
FAS	Fatty acid synthase
FFA	Free fatty acid
GC	Gas chromatography
gDNA	Genomic DNA
GLA	γ-linolenic acid
Gm	Gentamicin sulphate
GRAVY	Grand average of hydropathy
HTC	High-throughput conjugation
Hz	Hertz
IPTG	Isopropyl-β-D-thiogalactopyranoside
Kb	Kilobase
kDa	Kilodalton
Km	Kanamycin monosulphate
KR	Ketoacyl reductase
KS	Ketoacyl synthase
LA	*cis*-linoleic acid
LB	Luria-Bertani broth medium
LC-PUFA	Long chain- polyunsaturated fatty acids
LDs	Lipid droplets
LPA	Lysophosphatidic acid
LPB	Lipid-prebody
m	Multiplet

Ma2	WS/DGAT from *Marinobacter hydrocarbonoclasticus*
MAG	Monoacylglycerol
MAT	Malonyl transferase
MDO	Membrane-derived oligosaccharides
MHz	Megahertz
MM	Minimal medium
MSA	Multiple sequence alignment
MUFA	Monounsaturated fatty acid
NADH	Nicotinamide adenine dinucleotide
NADPH	Nicotinamide adenine dinucleotide phosphate
NBT	Nitro blue tetrazolium
NMR	Nuclear magnetic resonance
NOE	Nuclear Overhauser Effect
nt	Nucleotide
Nt	Terminal amino end
Nx	Nalidixic acid
o/n	Overnight
OA	Oleic acid
OD	Optical density
ORF	Open reading frame
oriT	Origin of transfer
***oriT*$_{R388}$**	R388 *oriT*
PA	Palmitic acid
PBS	Phosphate-buffered saline
PCR	Polimerase chain reaction
PDAT	Phospholipid : diacylglycerol acyltransferase
PE	Phosphatidylethanolamine
PG	Phosphatidylglycerol
PHA	Polyhydroxyalkanoate
PhA	Phosphatidic acid
pI	Isoelectric point
PKS	Polyketide Synthase
PL	Phospholipids
PMSF	Phenylmethylsulfonyl fluoride
PO	Palmitoleic acid
ppm	Parts per million
PPTase	Phosphopantetheinyl transferase
PUFAs	Polyunsaturated fatty acids

r.p.m.	Revolutions per minute
rf	Radiofrequency
Rf	Rifampicin
RM	Rich medium
ROS	Reactive oxygen species
RT	Retention time
s	Singlet
SCO	Single cell oil
SDS-PAGE	Sodium dodecyl sulphate polyacrylamide gel electrophoresis
SFA	Saturated fatty acid
SLD	Small lipid droplet
Sm	Streptomycin
Sp	Spectinomycin
SPB	Sorensen's phosphate buffer
STD-NMR	Saturated Transfer Difference - Nuclear Magnetic Resonance
t	Triplet
TAG	Triacyilglycerol
TBE	Tris/Borate/EDTA
TBST	Tris-buffered saline with Tween 20
Tc	Tetracycline
tDGAT	WS/DGAT from *Thermomonospora curvata*
TEM	Transmission electron microscopy
TLC	Thin Layer Chromatography
Tp	Trimethoprim
Tp	Trimethoprim
Tyr	Tyrosine
U	Enzyme unit
UFA	Unsaturated fatty acid
UPLC/MS	Ultra Pressure Liquid Chromatography/Mass Spectrometry
UV	Ultraviolet light
v/v	Volume/ volume
VC	*cis* vaccenic acid
w/v	Weight/ volume
WE	Wax ester
WS/DGAT	Wax ester synthase/acyl-CoA : diacylglycerol acyltransferase
wt	Wild-type

INTRODUCTION

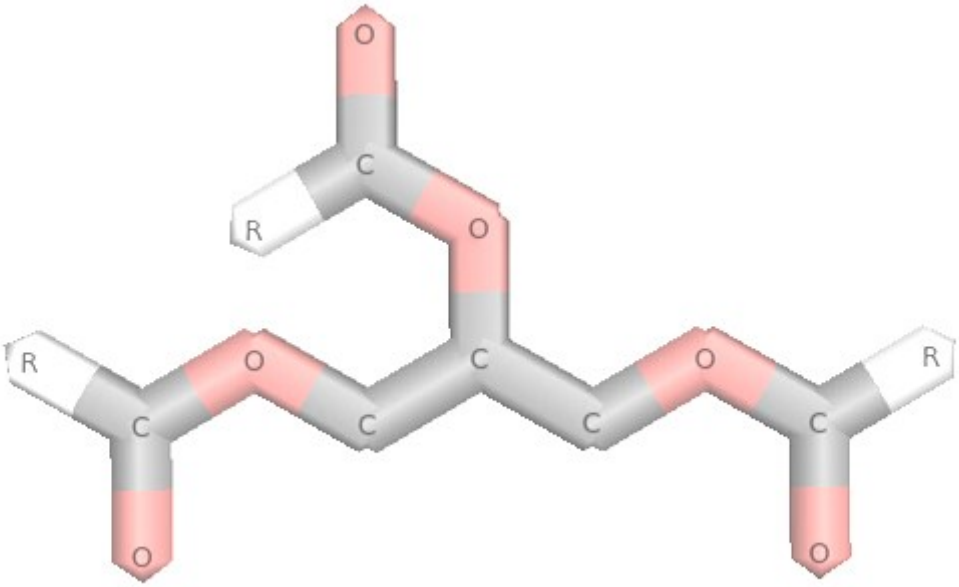

1. Introduction

1.1. Lipid synthesis in prokaryotes

According to the classic description, lipids are defined as a chemically heterogeneous group of substances insoluble in water, but soluble in non-polar solvents such as chloroform, hydrocarbons or alcohols. This definition, still acceptable and habitual, is based in physical properties and embraces a wide range of fatty substances occurring in microorganisms, higher plants and animals whose major roles are structural, storage and metabolic (Gurr and Harwood, 1991).

Among the three domains of life, significant differences are found in the lipid chemistry of the predominant building blocks (e.g., L-glycerol vs D-glycerol, ester vs ether linkages, among others). As a whole, lipids can be divided according to two basic biosynthetic groups. The first involves the carbanion-based condensation of acyl thioester intermediates, giving rise to diverse classes of lipids that contain fatty acyl chains, including fatty acids (FA), phospholipids (PL) and glycerolipids. The second involves the condensation of branched-chain 5-carbon pyrophosphate intermediates and a carbocation intermediate, leading to all lipids that are present in the Archaea domain and a large number of lipids in the Bacteria and Eukarya domains such as the steroids, polyisoprenoids and highly pigmented molecules such as the carotenoids (Brown and Marnett, 2011; Brown and Murphy, 2009; Fahy et al., 2005).

In contrast with the wide knowledge of neutral lipid synthesis in eukaryotes, our understanding about lipid metabolism in prokaryotes is still limited, specially with respect to neutral lipid biosynthesis. The key enzymes involved in lipid metabolism in prokaryotes differ from the situation in eukaryotes (Brown and Murphy, 2009; Heath, Richard J. et al., 2002). Fig I-1 shows an overview of lipid metabolism in bacteria, with schematic illustrations of the main pathways (see the following Tables for more information on the represented genes).

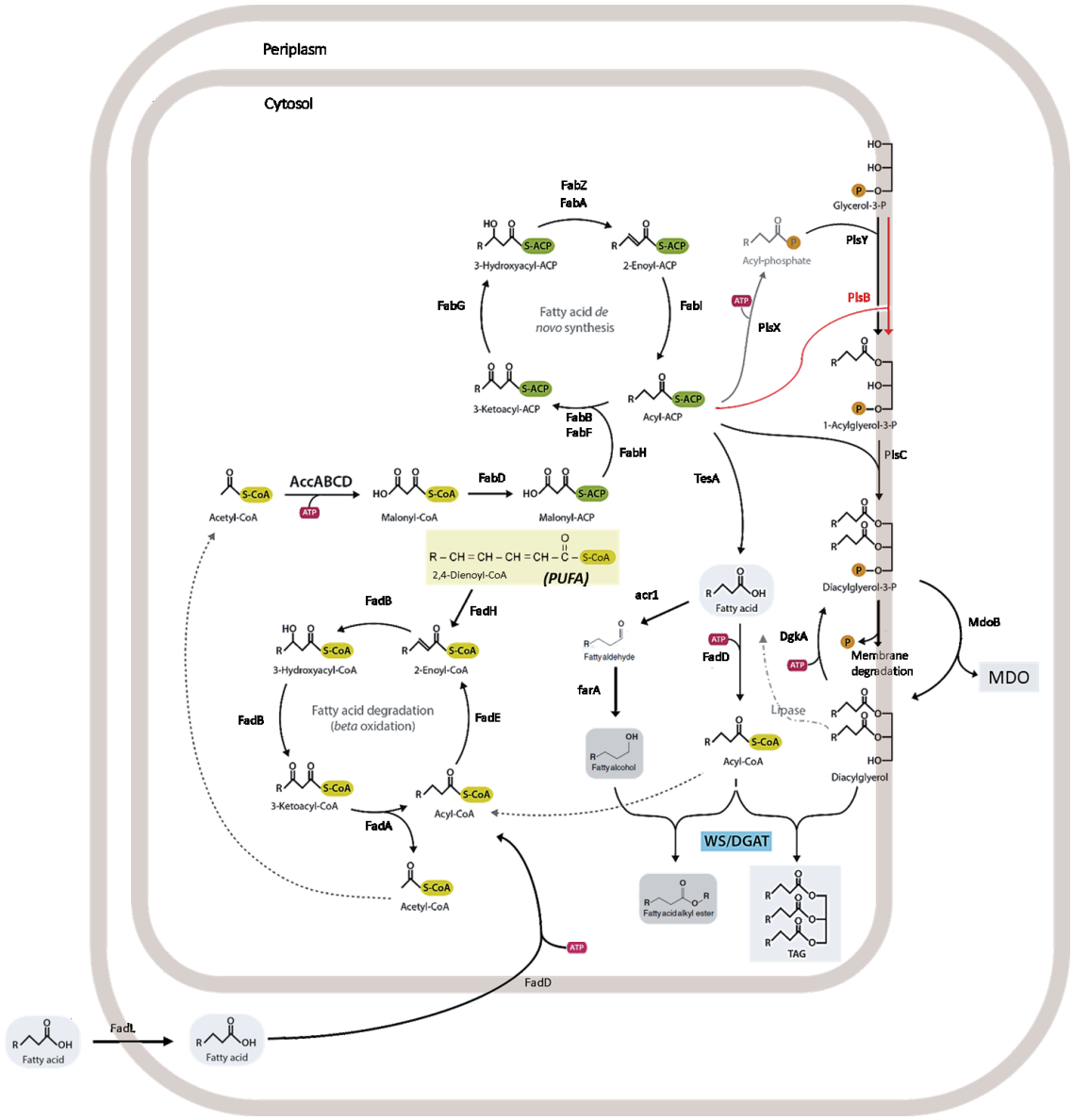

Figure I-1. Outline of some main pathways of lipid metabolism in bacteria. Fab and Fad genes codify for enzymes responsible for FA biosynthesis and degradation, respectively; Pls genes are implied in phospholipid metabolism and WS/DGAT in the biosynthesis of neutral lipids such as triacylglycerols. Sources: Janßen and Steinbüchel, 2014; Röttig and Steinbüchel, 2013; Röttig et al., 2015.

1.1.1. Fatty acids in prokaryotes

FA are lipid molecules that can adopt a huge number of possible configurations in living systems due to its continuous thermal motion and the free rotation about the carbon-carbon bonds. However, steric hindrance and interactions with other molecules reduce the mobility of FFAs and the acyl chains of acyl lipids (i.e. lipids consisting of FA esterified with other molecules). The physical properties of complex lipids are therefore affected by their individual FA, being the melting point an evident one. The larger the number of double bonds (higher degree of unsaturation), the lower the melting point of the acyl chains. For example, the melting point of stearic acid (C18:0) is 69.6°C, whereas that of oleic acid (OA, C18:1, with one *cis* double bond) is 13.4°C. The melting points of polyunsaturated fatty acids (PUFA) of the C18 series are even lower. Within the groups of saturated fatty acids (SFA), the melting point is also lowered as the chain length decreases or if the chain is branched (especially in the anteiso form). In this way, the melting temperature of palmitic acid (PA, C16:0) and anteisoheptanoic acid (15-Me C17:0, FA with 18C in total) are 63.1 and 36.8 °C respectively. In general, FA do not exist as free fatty acids (FFA) in living organisms because of their marked affinity for many proteins (one result of this is an inhibitory action on many enzymes). In fact, where FA are reported as major tissue constituents they are usually artefacts due to cell damage which allows lipases to break down the endogenous acyl lipids (Knothe and Dunn, 2009; Berg, JM et al., 2002; Gurr and Harwood, 1991; Kaneda, 1991).

For most of the metabolic reactions in which FA take part, whether they are anabolic (synthetic) or catabolic (degradative), thermodynamic considerations dictate that the acids must be 'activated'. For these reactions thiol esters are generally employed. The active form is usually the thiol ester of the FA with the complex nucleotide, coenzyme A (CoA) or the small protein known as acyl carrier protein (ACP), both of them showing a pantetheine arm for thioester formation. The presence of the ACP, the small (8.86 kDa), acidic and highly soluble product of the *acpP* gene, is a unique feature of FA synthesis in bacteria. In normally growing cells the ACP pool is approximately one-eighth the CoA pool. ACP also plays other roles in cell physiology, donating acyl chains to membrane-derived oligosaccharides, lipoic acid and quorum sensors (Heath, Richard J. et al., 2002).

In general, there are two basic routes to provide FA: (i) via *de novo* FA synthesis from the central metabolite acetyl-CoA, yielding acyl-ACPs, or (ii) via uptake of exogenous FA, or other compounds that are converted to FA such as alkanes, and their conversion to acyl-CoAs by acyl-CoA synthetases (Röttig and Steinbüchel, 2013).

Fatty acid biosynthesis in bacteria

Like all organisms, prokaryotes make FA using an organized array of several enzyme activities, trivially known as fatty acid synthase (FAS). Nonetheless, bacteria have evolved the capacity for FA biosynthesis for subsequent incorporation into membrane PLs in three distinct ways (Shulse and Allen, 2011).

- Some bacteria have a Type I FAS composed of a large, multifunctional biosynthetic complex containing all enzymatic domains necessary for acyl chain elongation and functional derivatization to which ACP is covalently bound (see scheme in Fig I-2.A). FAS I is responsible for the production of both membrane phospholipid FA chains as well as precursor FA molecules for elongation to long-chain mycolic acids in members of the Corynebacteriaceae, Mycobacteriaceae and Nocardiaceae families. This enzymatic complex, also found in animals and plants, synthesize only SFA products (Schweizer and Hofmann, 2004; Shulse and Allen, 2011).

- In contrast, in most bacteria the biosynthesis of these lipid molecules is usually carried out by a dissociable multienzyme complex (a Type II FAS). In this system individual enzymatic activities reside on discrete enzyme products, encoded by the FA biosynthesis, or *fab*, genes (see Fig I-2.B). The intermediates are covalently bound to ACP as they undergo successive cycles of condensation, reduction, dehydration and reduction for each 2C-unit added from malonyl-ACP. FAS II can synthesize a mixture of SFA and monounsaturated fatty acid (MUFA) products (being the last process known as the "anaerobic pathway" to reflect the proper reaction mechanism for FA, which does not involve oxygen directly). In other respects, to form methyl-branched-chain FAs, many

Gram-positive bacteria use the same FAS system, but employing branched-chain primer molecules derived from amino acids (by deamination and activation with CoA) (Heath, Richard J. et al., 2002; Russell and Nichols, 1999).

- The third recognized mechanism of bacterial FA biosynthesis consists of a multi-enzymatic domain complex similar to Type I FAS and Polyketide Synthase (PKS) arrangements (see Fig I-2.C). PKS systems are involved in the *de novo* biosynthesis of long chain – polyunsaturated fatty acids (LC-PUFAs), such as eicosapentaenoic acid (EPA, C20:5 ω-3) and docosahexaenoic acid (DHA, C22:6 ω-3), and coexists with the aforementioned Type II FAS in certain species of marine Gammaproteobacteria (Bergé and Barnathan, 2005; Metz et al., 2001; Shulse and Allen, 2011).

A joint evolution process of these FA biosynthetic pathways has been revealed by means of the comprehensive phylogenetic analysis of FAS and PKS from diverse organism groups based on the highly conserved ketoacyl synthase (KS) domains (Jenke-Kodama et al., 2005). This enzymatic activity will be further explained below.

The three systems have in common the 4'-phosphopantetheinyl transferases (PPTases), which are responsible for catalyzing the post-translational modification of carrier proteins (Orikasa et al., 2006a).

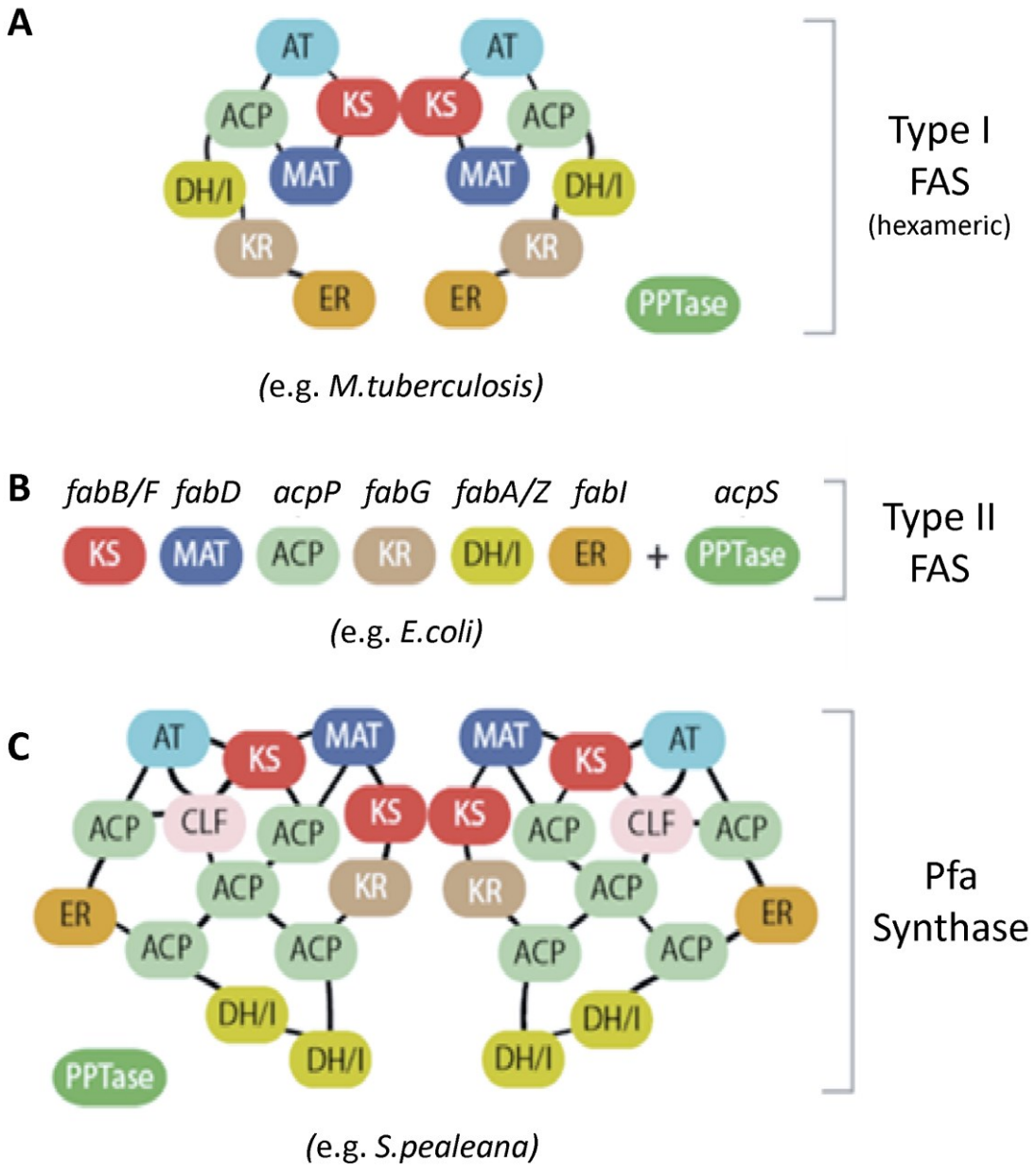

Figure I-2. Schematic illustration of the three types of FAS found in bacteria. Abbreviations: KS, ketoacyl synthase; MAT, Malonyl transferase; ACP, acyl carrier protein; KR, ketoacyl reductase; DH/I, dehydrase/isomerase; ER, enoyl reductase; PPTase, phosphopantetheinyl transferase; AT, acyltransferase; CLF, chain length factor (Fernandez, 2011).

The most important genes implied in FA synthesis in bacteria are listed in Table I-1.

Table I-1. Most important genes implied in FA synthesis in bacteria. Sources: DiRusso et al., 1992; Heath, Richard J. et al., 2002; Hofvander et al., 2011; Röttig and Steinbüchel, 2013.

Metabolic pathway	Gene(s)	Protein	Function
FAS Type II	*acpP*	Acyl carrier protein (ACP)	Interact specifically and transiently with all of the enzymes of FA biosynthesis (except acetyl-CoA carboxylase).
	acpS	Acyl carrier protein synthase	PPTase, modify the ACP.
	accA-D	Acetyl-CoA carboxylase complex	First step of FA biosynthesis: conversion of acetyl-CoA to malonyl-CoA.
	fabD	Malonyl-CoA:ACP transacylase	Transfer of malonyl-CoA to malonyl-ACP.
	fabG	β-ketoacyl-ACP reductase	Reduction of the ketoester formed by the two-carbon unit addition to the growing acyl-ACP.
	fabH	β-ketoacyl-ACP synthase III	Initial condensation reaction in FA biosynthesis.
		Acetyl-CoA : ACP transacylase	Transfer of Acetyl-ACP to Acetyl-CoA.
	fabB	β-Ketoacyl-ACP synthase I	Addition of a two-carbon unit from malonyl-ACP to the growing acyl-ACP in the elongation of FA.
	fabF	β-Ketoacyl-ACP synthase II	
	fabA	β-hydroxyacyl-ACP dehydrase	Remove a water molecule from the β-HydroxyacyI-ACP in the elongation cycle of FA biosynthesis.
	fabZ		
	fabI	Enoyl-ACP reductase	Form a saturated acyl-ACP.
FAS Type I	*FAS1*	Subunit β of Type I FAS	FA biosynthesis
	FAS2	Subunit α of Type I FAS	
Aerobic PUFA synthesis	*desA*	Desaturase	Use activated molecular oxygen to remove two hydrogens from a hydrocarbon chain.
Anaerobic PUFA synthesis	*pfaA-E*	Pfa synthase or PKS multienzymatic complex	Synthesize LC-PUFA from acetyl-CoA and malonyl-CoA

Saturated fatty acid (SFA) synthesis

Both Type I and II FAS make use of highly conserved enzyme activities encoded respectively on integrated domains or autonomous monofunctional gene products to accomplish the cycle of condensation, reduction, dehydration, and reduction necessary to produce a final FA product. Generally, the primer molecule is acetyl-ACP, which after seven elongation rounds with malonyl extender units gives PA as the straight-chain product. Thus, the first committed step in FA biosynthesis consists in the conversion of acetyl-CoA to malonyl-CoA catalyzed by the acetyl-CoA carboxylase complex (ACC) (Heath, Richard J. et al., 2002; Polyak et al., 2011; Shulse and Allen, 2011).

The discrete enzymes constituting Type II FAS are encoded by different genes (see Table I-1). They are scattered along the genome with only two clusters, the minimal *accBC* operon and the *fab* cluster. In this system ACC is a distinct component that assembles as a multisubunit complex, with each of the reactions performed by a separate enzyme. All intermediates in FA synthesis are shuttled through the cytosol as thioesters of the ACP. For the malonate group to be used for FA synthesis, it must first be transferred from malonyl-CoA to malonyl-ACP by the malonyl-CoA : ACP transacylase (encoded by *fabD*). Then, FabH produces the first condensation reaction responsible for the formation of the four carbon acetoacetyl-ACP from acetyl-CoA and malonyl-ACP with the consequent loss of CO_2 (Heath, Richard J. et al., 2002; Schweizer and Hofmann, 2004).

Four enzyme activities constitute each iterative cycle of chain elongation (see Fig I-3), placing the first two carbons introduced into the nascent chain in the methyl end of the carboxylic acid and adding the next in the opposite end:

1. The Claisen condensation is catalyzed by a KS. The products of the *fabB* and *fabF* genes are responsible for this reaction in Type II FAS, where a two-carbon unit is added from malonyl-ACP to the growing acyl-ACP.

2. The resulting ketoester is then reduced by the ketoacyl reductase (KR). In Type II FAS the gene for the β-ketoacyl-ACP reductase (*fabG*) is located within the *fab* gene cluster between the *fabD* and *acpP* genes and is cotranscribed with *acpP*.

3. Next, a water molecule is removed by a β-hydroxyacyl dehydrase/isomerase (DH/I). There are two β-hydroxyacyl-ACP dehydrases (more properly termed dehydratases) in bacteria with Type II FAS: one is encoded by *fabZ*, and is active on all chain lengths of saturated and unsaturated intermediates; the FabA enzyme dehydrates saturated, but not unsaturated, FA intermediates.

The final step in each round of fatty acyl elongation is the NADH-dependent reduction of the *trans* double bond, catalyzed by the NADH-dependent enoyl reductase (ER). This enzyme is generally encoded by *fabI* in Type II FAS, although there are different isoforms (FabK and FabL) in some Gram-positive bacteria.

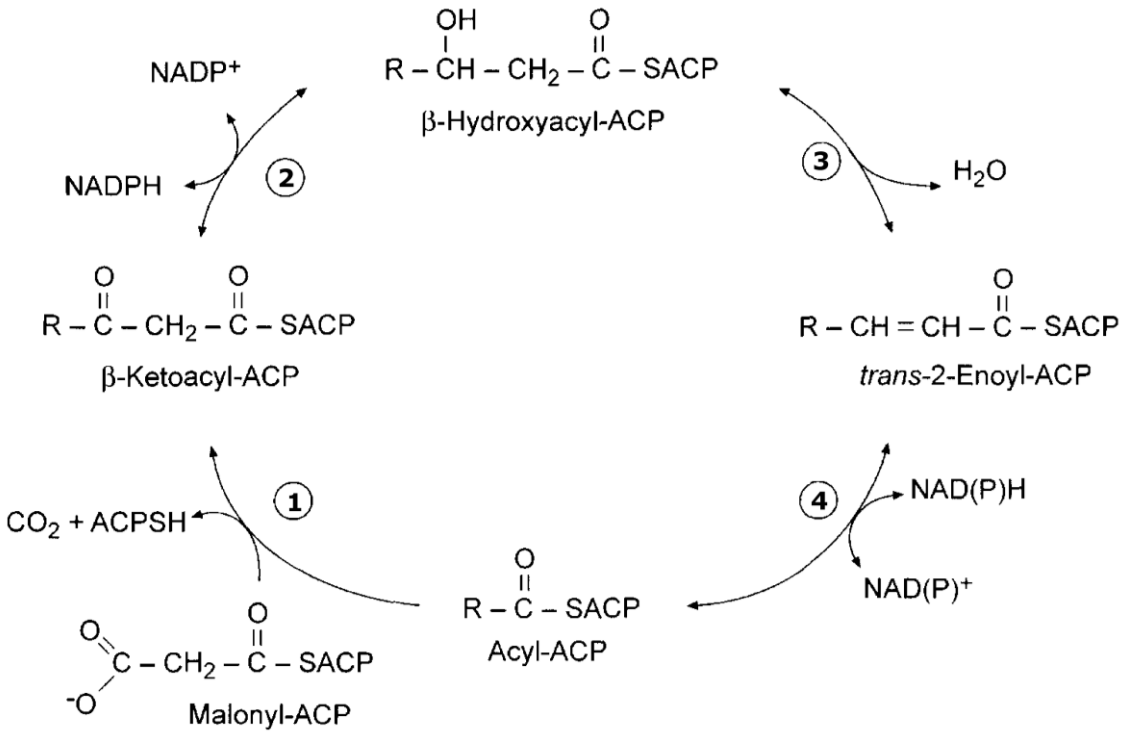

Figure I-3. Elongation cycles in FA biosynthesis with the corresponding enzyme activities: (1) β-Ketoacyl synthase (KS); (2) β-Ketoacyl reductase (KR); (3) β-Hydroxyacyl dehydrase (DH/I); (4) *trans*-2-Enoyl reductase (ER). Adapted from Heath, Richard J. et al., 2002.

An important characteristic of every FAS is the specificity of its chain termination reaction, which determines both the chain length and the acceptor of the FAS product. This property is believed to mainly depend on inherent properties of every FAS, even though external factors may interfere with the elongation process too. In some bacteria with Type II FAS, such as *E.coli*, long acyl chains are transacylated directly to the membrane PLs by specific glycerol phosphate transacylases (encoded by *plsB* and *plsC*). Alternatively, certain shorter-chain intermediates may be diverted from the elongation process for other reactions such as lipopolysaccharide or coenzyme biosynthesis.

Besides, biosynthesis of the heteromultimeric Type I FASs requires the coordinate expression of two genes, *FAS1* and *FAS2*, which encode subunits β (*FAS1*) and α (*FAS2*) of the $\beta_6\alpha_6$ FAS complex. In this system, all ACC components reside in a single polypeptide chain and are part of the multienzymatic complex. The MAT domain is responsible for transferring the initial malonyl to the ACP domain, which will remain bound to the ongoing intermediate for the whole synthesis process. The acyl-transferase (AT) component iniciates FA biosynthesis loading the initial acyl primer, generally acetate, from CoA to a specific binding site on the FAS. After several cycles of elongation, termination of the process occurs by removing the product from FAS either by transesterification to an appropriate acceptor or by hydrolysis. Nevertheless, the structural basis for this final reaction and the determination of the chain length is still elusive in both systems (Heath, Richard J. et al., 2002; Polyak et al., 2011; Schweizer and Hofmann, 2004; Shulse and Allen, 2011).

Mono unsaturated fatty acid (MUFA) synthesis

All organisms regulate the fluidity of their membranes to maintain a membrane bilayer in a largely fluid state. As temperatures are lowered, membranes undergo a reversible change from a fluid (disordered) to a non-fluid (ordered) state. As explained above, the temperature of the transition point depends on the FA composition of the membrane PLs. Although gram-positive bacteria often use branched chain FA to modulate membrane fluidity, the main mechanism to regulate membrane fluidity in bacteria relies on the production of straight chain unsaturated fatty acids (UFA, Heath, Richard J. et al., 2002; Suutari and Laakso, 1994).

MUFA: Aerobic pathway

Bacteria whose FAS only synthesize SFAs make UFA by subsequently desaturating the FAS products using separate and mechanistically distinct desaturase enzymes which involve the use of molecular oxygen as the terminal acceptor in an aerobic process schematized in Fig I-4.A. Reducing equivalents from NADPH are passed through a short series of redox proteins ending in the desaturase enzyme, which uses them to reduce molecular oxygen to water. Although this cycle may be repeated with MUFA products being the substrates for further rounds of desaturation with desaturases having different positional specificities to give PUFA products, generally bacteria have only a single type of desaturase enzyme and only make MUFA acids (these enzymes are specific for the position of the double bond which they 'insert'). An example of FA desaturase reaction is shown in Fig I-4.B. A $2e^-$ and O_2-dependent dehydrogenation is catalysed at an unactivated position of PA, resulting in *cis*-double bond formation, giving rise to palmitoleic acid (PO, 16:1Δ9) and releasing two water molecules. These enzymes are generally located in membranes. Some desaturases have been shown to be regulated through cold-shock which could be a way to selectively increment the proportion of MUFA in the membrane when needed.

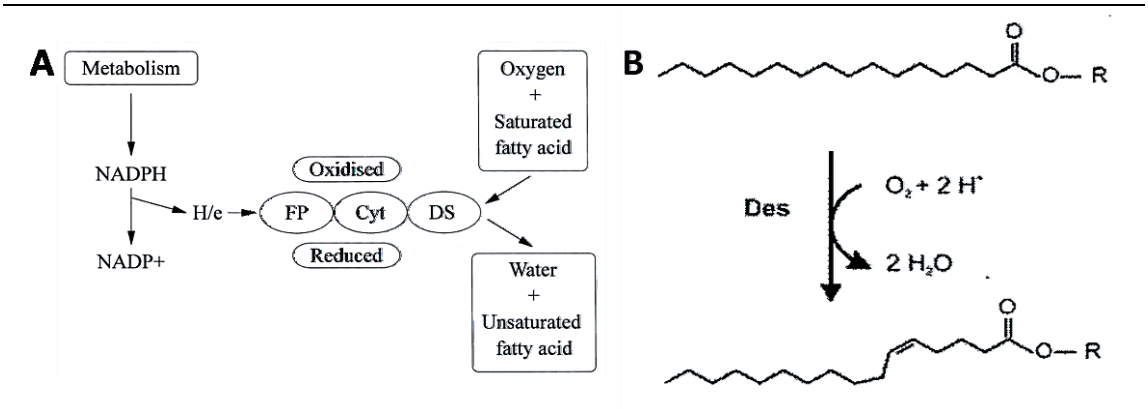

Figure I-4. A) Generic outline of the mechanism of formation of UFA by aerobic desaturation. Abbreviations: FP, flavoprotein; Cyt, cytochrome; DS, desaturase enzyme. Image from Russell and Nichols, 1999. B) Reactants and products of a representative FA desaturase reaction. R represents CoA for free acyl chains or a PL for acyl chains of lipids in the membrane. Image from Mansilla et al., 2004.

MUFA: Anaerobic pathway

Biosynthesis of UFA in prokaryotes carrying out the "anaerobic pathway", like the model microorganism *E.coli*, starts according to the same process explained for SFAs until eventually the pathway bifurcates in the fourth cycle. FabA is a bifunctional enzyme that catalyzes both the removal of water to generate *trans*-β-decenoyl-ACP (as in all the cycles of the elongation process previously explained) and the isomerization of this intermediate to *cis*-β -decenol-ACP. The acyl-ACP with the *cis* configuration in the double bound is a substrate only for the enzyme encoded by *fabB* (not recognized by *FabI*), which provokes its direct elongation and the diversification of FA biosynthesis (see Fig I-5.A), although both compounds will then continue with a number of elongation cycles in the same way. Thus, a mixture of SFA and MUFA is made by Type II FAS. Competition between FabI and FabB is partly responsible for the ratio of SFA/MUFA. On the other hand, while FabB enzyme is required for the elongation of these unsaturated acyl-ACP intermediates, FabF participates in SFA synthesis and in the elongation of palmitoleoyl-ACP to *cis*-vaccenoyl-ACP. As shown in Fig I-5.B, the reactivity of this enzyme toward palmitoleoyl-ACP is increased after a temperature downshift. That leads to increased amounts of more fluid membrane PLs at lower temperatures. This anaerobic pathway is limited to the production of MUFA only (Heath, Richard J. et al., 2002; Mansilla et al., 2004).

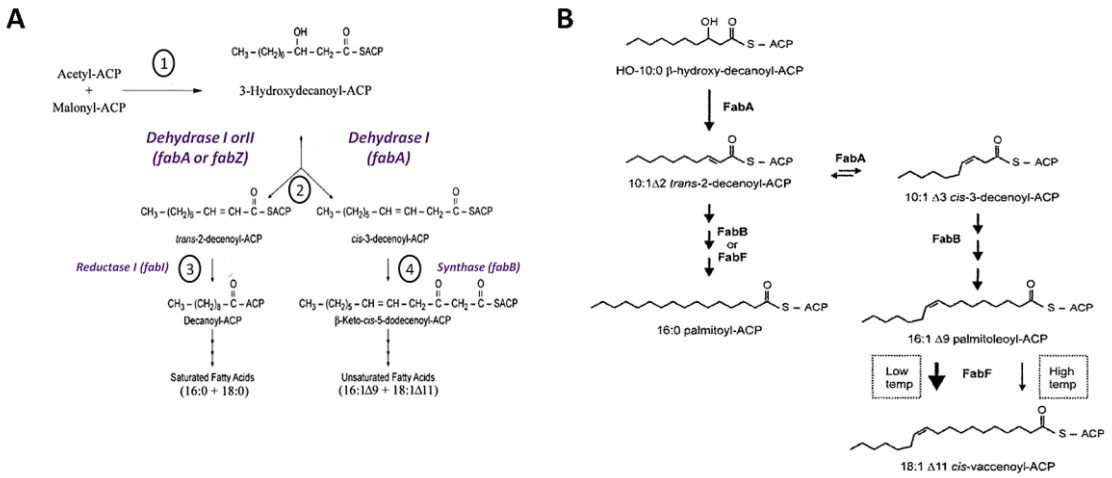

Figure I-5. A) General overview of the two pathways of FA biosynthesis developed in bacteria with the Type II FAS. The following steps are depicted: 1--> 3, FAS producing only SFA; 1--> 3 and 1--> 4, FAS producing a mixture of SFA and MUFA ('anaerobic pathway'). Adapted from Heath, Richard J. et al., 2002 and Russell and Nichols, 1999. B) UFA biosynthesis: key step in UFA production catalysed by FabA (which introduces the double bond into the acyl chain at the 10-carbon intermediate) and regulation of the activity of the enzyme encoded by *FabF* by growth temperature of the bacteria. Imagen from Mansilla et al., 2004. Abbreviations: ACP, acyl carrier protein; temp, temperature.

Interestingly, in the Type II FAS system overproduction of FabB has two effects: an increased amount of *cis*-vaccenic acid in PLs; and resistance to the antibiotics thiolactomycin and cerulenin. FabF is also inhibited by cerulenin and thiolactomycin. Although FabF is not essential for growth in *E.coli*, it is essential for the regulation of FA composition in response to temperature fluctuations (Heath, Richard J. et al., 2002).

Anaerobic bacteria must use the anaerobic pathway of FA biosynthesis, but aerobic bacteria may use either route. Both biosynthetic pathways could operate simultaneously in aerobic bacteria. Nevertheless, it is important to remark that only bacteria expressing the specific dehydrase for the formation of the *cis*-3-ene intermediate can produce MUFA through the anaerobic pathway. This is relevant to PUFA synthesis in bacteria, as discussed below (Heath, Richard J. et al., 2002; Russell and Nichols, 1999).

Long-chain polyunsaturated fatty acids (LC-PUFA) synthesis.

PUFAs are molecules composed of a hydrocarbon chain and a terminal carboxylate group containing at least two methylene-interrupted double bonds in the *cis* position. When the FA chain has 18 carbons or more in length they are called LC-PUFAs. Their long chain length and unsaturation degree distinguishes these FA products from those directly produced by FAS II (≤18 carbons). As a matter of fact, to distinguish these products from those synthesized via core, or primary FA biosynthetic mechanisms and simultaneously emphasize its accessory nature, these specialized lipid molecules and collectively denominated "secondary lipids" (Russell and Nichols, 1999; Shulse and Allen, 2011).

PUFAs can be grouped into different families depending on the position of the first double bond proximate to the methyl end of FA. The two main families are ω-6 (or n-6, series derived from cis-linoleic acid (LA, C18:2) and ω-3 (or n-3, FAs derived from α-linolenic acid, ALA, C18:3) (see Fig I-6.A for main examples). Other families are ω-9 (or n-9, derived from OA), ω-7 (or n-7, derived from PO), ω-4 (or n-4) and ω-1 (or n-1). As explained in Fig I-6.B, double bonds in PUFAs may also be counted from the carboxylate group and are then represented by the symbol Δ (Huang et al., 2004; Sakuradani et al., 2009; Sijtsma and de Swaaf, 2004).

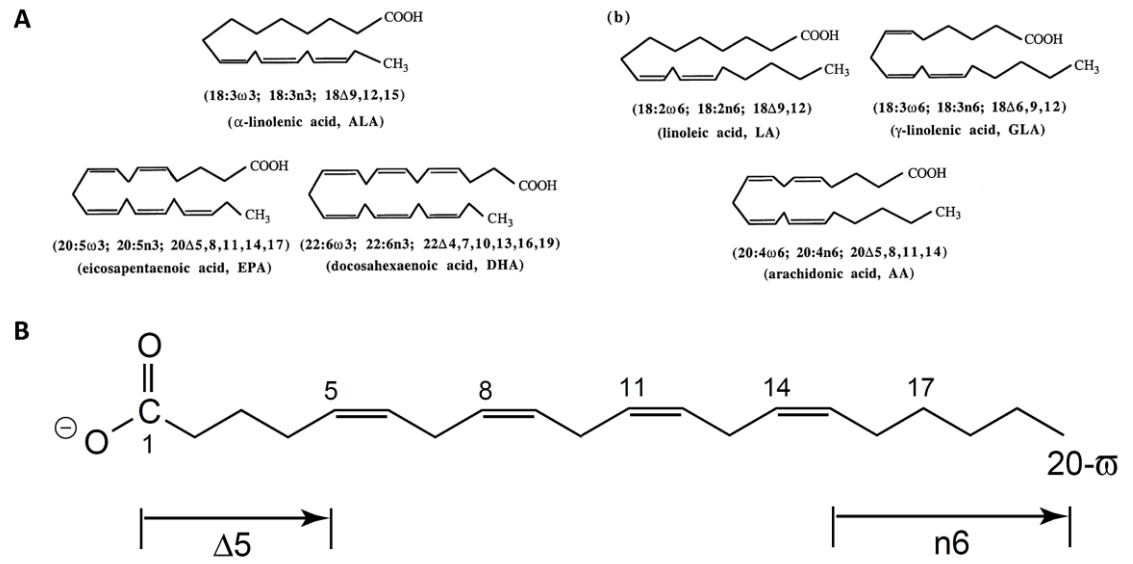

Figure I-6. A) Skeletal formula of the major ω-3 (left) and ω-6 (right) LC-PUFA occurring in nature (Images from Russell and Nichols, 1999). B) Detailed representation of the simplified nomenclature for PUFA, showing arachidonic acid as example (Wallis et al., 2002).

A schematic model of the potential reaction pathways for the biosynthesis of membrane lipids containing PUFA acyl chains is represented in Fig I-7. Saturated acyl lipids in the membrane may also be desaturated to give monounsaturated lipids, but neither of the two types of monounsaturated lipids (i.e. those derived from MUFA from aerobic or anaerobic desaturation) is capable of direct conversion to PUFAs because of the need for elongation (Russell and Nichols, 1999).

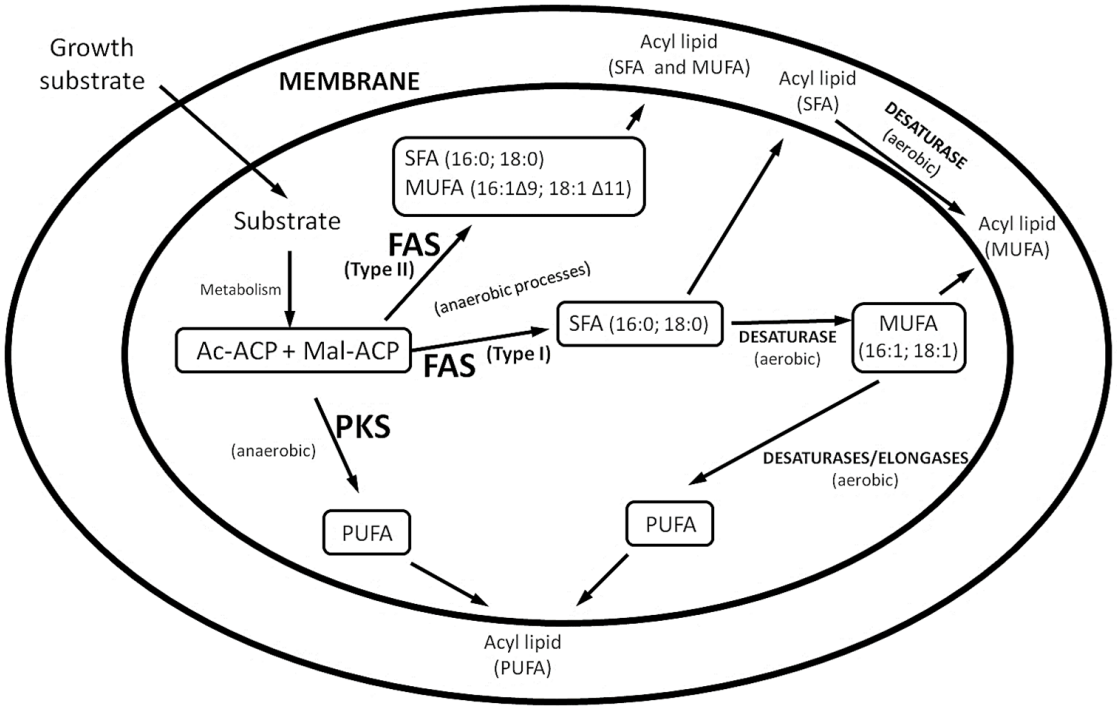

Figure I-7. Summary of possible pathways for the biosynthetic origin of fatty acyl chains in bacterial membrane lipids. Ac-ACP, acetyl-acyl carrier protein; Mal-ACP, malonyl-acyl carrier protein. Adapted from Russell and Nichols, 1999.

LC-PUFA: Front and methyl-end desaturases

In organisms that make PUFAs through the most common pathway, there are distinct desaturases for inserting the different double bonds by the oxygen-dependent modification of SFA precursors that all organisms produce through the FAS (Russell and Nichols, 1999). As explained before, a desaturase is a special type of oxygenase that can use activated molecular oxygen to remove two hydrogens from a hydrocarbon chain, especially from a FA chain, catalyzing the formation of a double bond in the substrate and creating a molecule of water. Desaturases are denominated as Δx desaturase referring to the position from the carboxyl end of a FA where it selectively introduces the double bound or nx referred to the position from the methyl end (Meesapyodsuk and Qiu, 2012). The first double bond is often inserted at approximately the middle position of a FA chain. Nonetheless, the most relevant desaturases required for PUFA biosynthesis are the so-called “front-end” desaturases that introduce a new double bond between a pre-existing one and the carboxyl end of the acyl group, while a "methyl-end" desaturase inserts a double bound between the pre-existing one and the methyl-end. Δ12 and Δ15 and are examples of methyl-end desaturases, while desaturases widely spread in microorganisms such as Δ4, Δ5, Δ6 and Δ8 belong to front-end desaturases (Bergé and Barnathan, 2005; Meesapyodsuk and Qiu, 2012).

While desaturase enzymes insert double bonds at specific carbon atoms in the FA chain, the FA elongation system elongates the precursors by two-carbon increments, giving rise through different pathways to every LC-PUFA. Although aerobic pathways for biosynthesis of ω-3 and ω-6 LC-PUFA are identical until the production of arachidonic acid (AA, C20:4 ω-6) and EPA, they split after that point (see an overview in Fig I-8). The simplest sequence to transform EPA into DHA consists of one elongation step followed by the addition of a double bound by the Δ4 desaturase. Some organisms (such as mammals) lack Δ4 desaturase activity and use an alternative pathway, called "the retro-conversion pathway" or the Sprecher pathway, consisting of two succeeding elongation cycles (leading to 24:5n-3) followed by a Δ6 desaturation and a specific β-oxidation chain-shortening to the C22 product (see Fig I-8; Bergé and Barnathan, 2005; Sprecher et al., 1995; Wallis et al., 2002). By this route, the synthesis of DHA, 22:6n3 from acetyl-CoA requires about 30 distinct enzyme activities and nearly 70 reactions, including the four repetitive steps of the FA synthesis cycle (Metz et al., 2001).

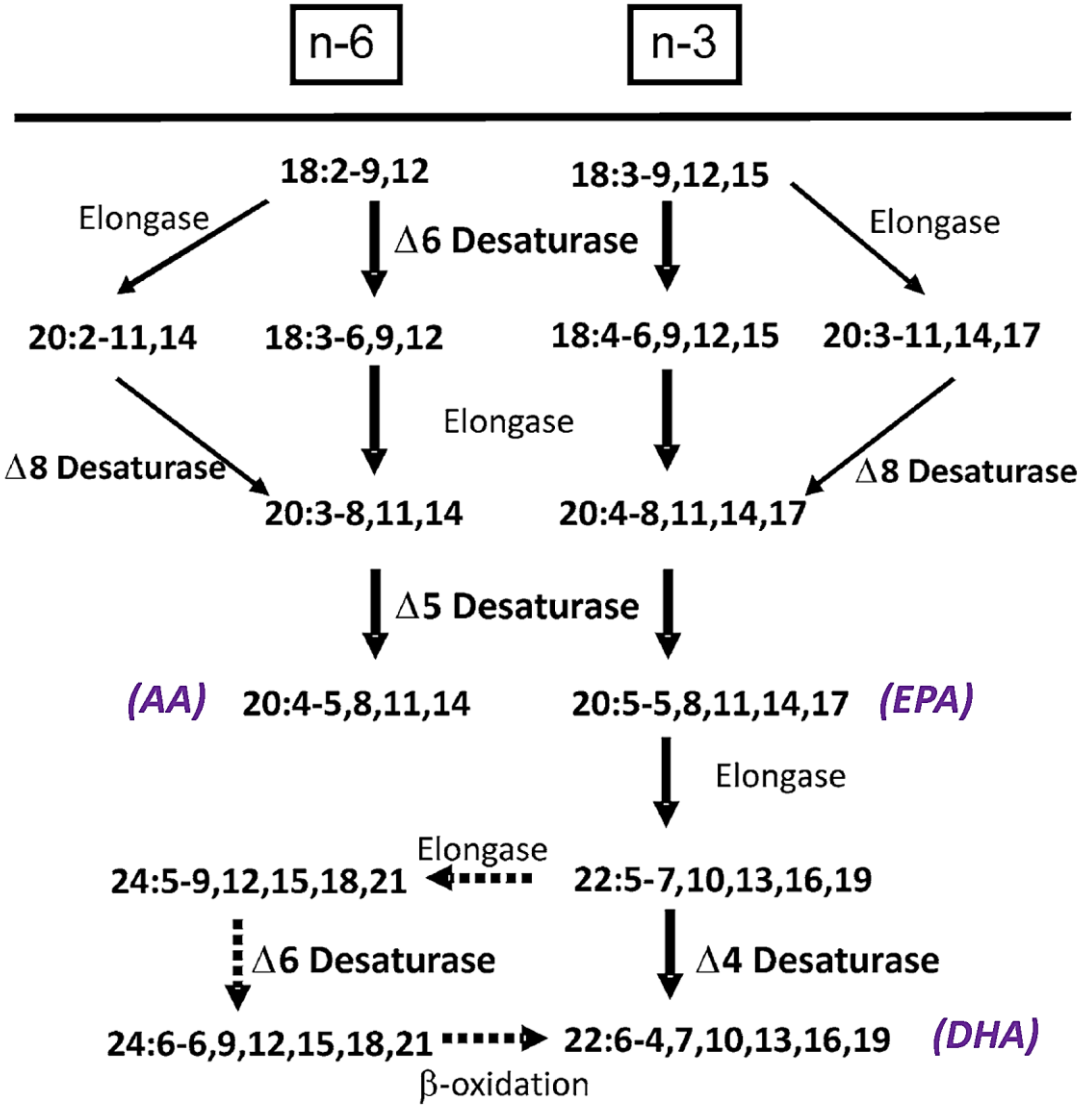

Figure I-8. Front-end desaturases involved in the biosynthesis of LC-PUFA. The dotted arrow indicates Sprecher's pathway for DHA biosynthesis Adapted from Meesapyodsuk and Qiu, 2012.

A case of methyl-end desaturases for LC-PUFA biosynthesis: Desaturases in cyanobacteria

Cyanobacteria, a class of photosynthetic prokaryotes occurring in the phytoplankton, produce C18 PUFA esterified to polar lipids, but they do not biosynthesize EPA or DHA (Bergé and Barnathan, 2005). Generally, unicellular types of cyanobacteria lack PUFA, while most of the filamentous species contain high levels of di- and trienoic FA (Quintana et al., 2011). Anabaena is a genus of filamentous nitrogen-fixing cyanobacteria that introduce double bonds at the Δ9, Δ12, and Δ15 (ω3) positions of C18 FA since its genome contains the genes for Δ9, Δ 12 and Δ15 desaturases (Chi et al., 2008).

LC-PUFA: Pfa synthases

Nature has overcome the enormous energetic cost and the complexity of the aerobic biosynthesis of very long-chain PUFA using a fundamentally different pathway catalyzed by a specialized PKS found in both prokaryotic and eukaryotic marine microbes. Unlike the elongation/desaturation pathway, in this metabolic route molecular oxygen is not required for introducing several double bonds into the existing acyl chain. Instead, unsaturation is introduced during the process of a specialized FA synthesis. Regardless of its ''anaerobic'' nature, the pathway can take place under aerobic conditions. (Huang et al., 2004; Qiu, 2003).

Like the traditionally known FA synthesis in bacteria, this PKS system, also known as "Pfa synthase", uses ACP as a covalent attachment for chain synthesis, proceeding with reiterative cycles with the acyl chain growing by two-carbon units with each round. Although the enzymes involved are different, the biochemical reactions of FAS elongation and PKS synthesis are the same. A four-step process is initiated by the condensation of malonate and a FA with release of a CO_2 molecule. The C=O double bond at C3 of the ketoacyl is reduced using NAD(P)H. The subsequent dehydration generates the enoyl substrate for the final reduction that employs NAD(P)H as co-factor, giving rise to a FA that has been extended by two carbon atoms (like in Fig I-3). Unlike FAS and FA elongation, the PKS pathway is distinguished by its propensity to terminate the biosynthetic process at diverse points within the reaction series, producing carbon chain products with keto and hydroxy groups. As examples, this mechanism is responsible for the C26 to C32 FA alkyl chains containing hydroxyl or ketone moieties found in the heterocyst glycolipids of filamentous nitrogen-fixing cyanobacteria such as *Nostoc punctiforme* and the C22 to C26 FA of phenolic lipids comprising the dormant cysts of the Gram-negative bacteria *Azotobacter vinelandii* (Shulse and Allen, 2011; Wallis et al., 2002).

The PKS pathway consists of iterative large, multi-domain protein complexes responsible for *de novo* production of LC-PUFAs (see Fig I-2). The genes encoding for these enzyme activities, designated *pfaA–E*, are known to be present sequentially on long (20–30 kb) open reading frames (ORFs) in bacteria (see Fig I-9). These genetic clusters gives rise to multiple FA biosynthetic enzyme activities as integrated domains within operon-encoded gene products (Hoffmann et al., 2008; Shulse and Allen, 2011).

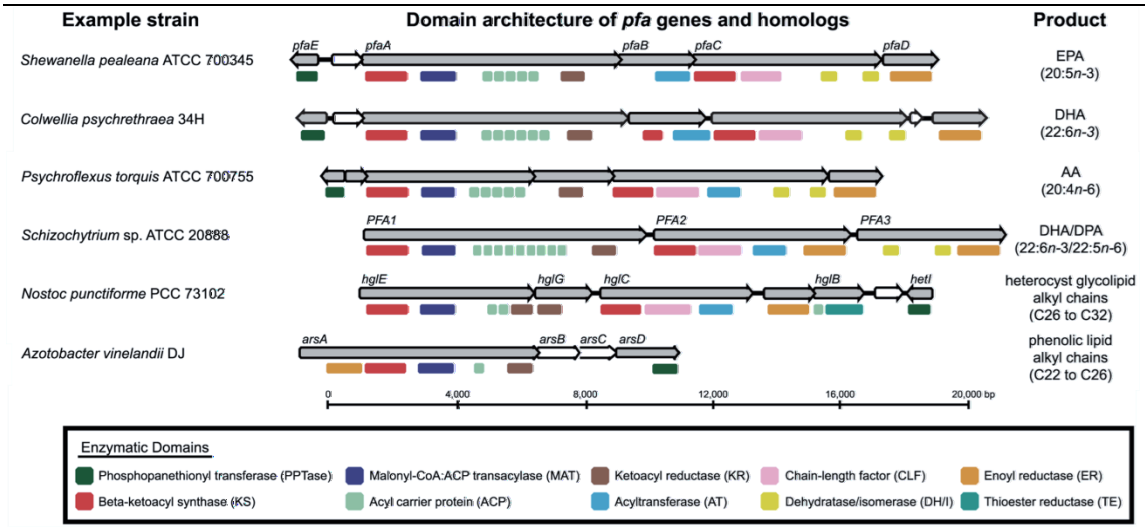

Figure I-9. Diversity of *pfa* gene clusters occurring in marine microorganisms. Source: Shulse and Allen, 2011.

In this multienzyme system, a total of five genes have been found to be required for the production of PUFA (see Fig I-10.A):

- *pfaA* which contains sequences corresponding to a KS domain, an AT domain, a stretch containing multiple ACP domains and finally a KR domain;
- *pfaB* consists of a KS-AT domain in species such as *Colwellia psychrethraea* or *Moritella marina* or a single AT domain in *Shewanella* sp;
- *pfaC* contains one KS, one CLF and two DH domains;
- *pfaD* contains a single ER domain;
- *pfaE* encodes for a PPTase which is typically required for the activation of the ACP domains.

The tandem ACP arrangement is a defining feature of the marine PKS. Most PUFA producers contain between 2–9 ACP domains in tandem. It has been shown that an increase in the number of ACPs in Pfa synthases is related to an increment in its ability to produce higher yields of PUFA (additive effect). Structural stabilization of the multidomain protein (synergistic effect) was also suggested to be influenced by the length of this fragment. In Fig I-10.B a comparison among the ACP domains repeated in tandem along the sequence of *pfaA* in diverse marine microorganisms is shown (Shulse and Allen, 2011; Trujillo et al., 2013).

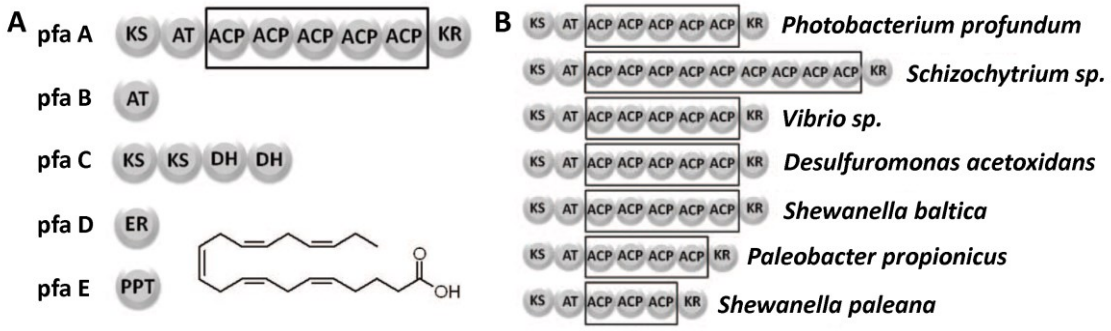

Figure I-10. A) PKS domain structure responsible of EPA production; B) Evolutionary conservation of the tandem ACP domain. Images from Trujillo et al., 2013.

A final component specific to Pfa synthases is the chain length factor (CLF) domain, which determine the ultimate chain length of the reaction product (Shulse and Allen, 2011). CLF domains, which has been suggested to have malonyl-ACP decarboxylase activity, are homologous to KS domains but the KS active site has a conserved cysteine residue whereas in CLF a glutamine residue exists (Allen and Bartlett, 2002).

Studying traditional PKS, the multienzimatic complexes that make other secondary metabolites such as antibiotics, we find different kinds. Each of the classes resembles one of the classes of FAS: the type I PKS possess a multidomain architecture similar to the Type I FAS while Type II PKS carry each catalytic site on a separate protein, like occurs in Type II FAS. The majority of bacterial PKS I consists of multiple sets of domains, or modules, that normally correspond to the number of acyl units in the product. A minimal module is composed of a KS, AT and ACP domain. Frequently KR, DH and ER domains are also embedded in the multifunctional megasynthases (Jenke-Kodama et al., 2005).

The organization of Pfa gene clusters is divided into three types, as illustrated in Fig I-11. Type I, which is represented by *Shewanella pneumatophor*i SCRC-2738, is a gene cluster including all five *pfa* genes in similar vicinity. Type II consists of a cluster of the four genes *pfaABCD*, with *pfaE* separate from the other genes. This type of cluster is represented by *M.marina* MP-1. In type III, *pfaE* is integrated into *pfaC*/E, and the cluster is considered to consist of four genes, *PfaA*, *PfaB*, *PfaC/E* and *PfaD*. The third type of cluster has been reported for *Pseudoalteromonas* sp. strain DS-12 only (Okuyama et al., 2007).

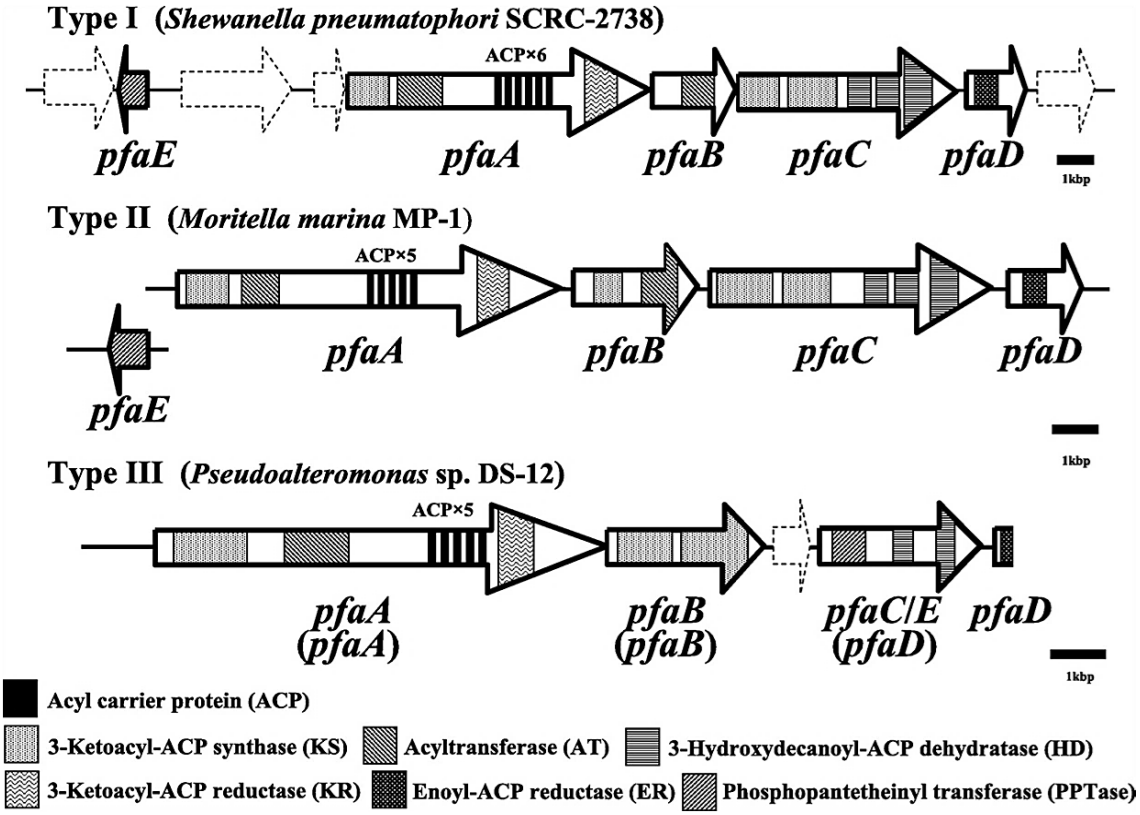

Figure I-11. Organization of genes responsible for bacterial EPA and DHA biosynthesis and domain structures of individual genes (Okuyama et al., 2007). GenBank accession: ABF00130.

Most bacteria possessing the archetypal PKS multienzymatic system also possess a complete FAS II (even though an exception, *Schizochytrium* sp., was reported by (Hauvermale and co-workers., 2006). Both FA synthetic pathways start from the same intracellular pool of precursor molecules for their activities, which make the relationship between them an interesting target of study. In those organisms, PUFA are normally produced as a small percentage of their total FA, with SFA and MUFA comprising the majority of their PLs. However, some interesting exceptions exist among the bacteria harboring putative secondary lipid synthases, such as the fish patogen *Renibacterium salmoninarum* that needs to incorporate exogenous FA for growing (Shulse and Allen, 2011).

A case of Pfa synthase for LC-PUFA biosynthesis: DHA biosynthesis in *Moritella marina*.

The marine psychrophilic and piezophilic Gammaproteobacteria *M. marina* MP-1, originally known as *Vibrio marinus*, is particularly interesting due to the presence of significant DHA in its membrane lipids as fatty acyl components (e.g. 11% of the total FA content in squid-based culture medium according to Morita and coworkers, 2005). As previously stated, the genome of the bacteria *M.marina* MP-1 possesses a Pfa synthase encoded by a gene cluster with type II organization (i.e. with *pfaE* separated from the other four ORFs) responsible for the production of DHA (Okuyama et al., 2007; Shulse and Allen, 2011).

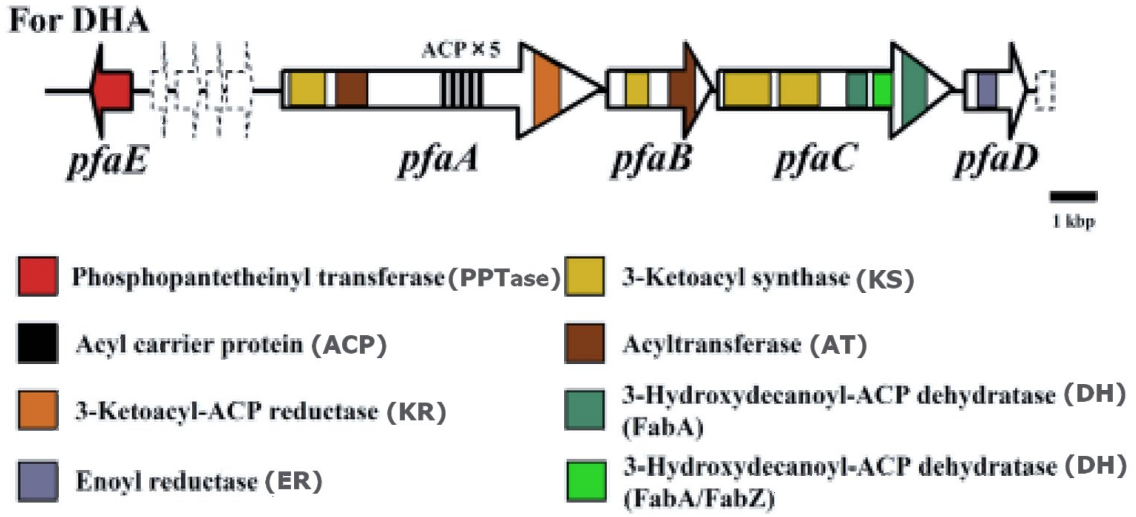

Figure I-12. Gene cluster for DHA-production-PKS from *M. marina* MP-1 (Orikasa et al., 2009).

As shown in Fig I-12, five repeated ACP-homologous regions were found in *pfaA* gene of *M.marina*, which also contained KS, AT and KR domains. In *M.marina*, *pfaB* has a region homologous to the carboxilic terminal (Ct) domain of KS but lacks an active-site sequence (Allen and Bartlett, 2002). The second KS domain in *pfaC* was considered to be a CLF (Okuyama et al., 2007).

Degradation of fatty acids

Exogenous FA needs to become activated to be degraded and employed as carbon source for cell growth (i.e. esterified to CoA). This reaction is catalyzed by the acyl-CoA synthetase, encoded by *fadD*.

FA degradation occurs through the β-oxidation pathway, which consist in repeated cycles of reactions that are basically the reverse of the reactions of FA biosynthesis. Nonetheless, β-oxidation utilizes acyl-CoA thioesters instead of acyl-ACPs, the β-hydroxy intermediates have the opposite stereochemistry (L in β-oxidation and D in synthesis) and the enzymes of β-oxidation share no homology with those of synthesis. The main proteins implied in FA catabolism in bacteria are enumerated in Table I-2 (Heath, Richard J. et al., 2002).

Table I-2. Some genes implied in FA degradation in bacteria. Sources: DiRusso et al., 1992; Heath, Richard J. et al., 2002; Hofvander et al., 2011; Röttig and Steinbüchel, 2013.

Metabolic pathway	Gene(s)	Protein	Function
β-oxidation	*fadD*	Acyl-CoA synthetase	CoA activates exogenous FA in Gamma-proteobacteria
	fadL	Long-chain FA transport protein precursor	Take up FA greater than 10 carbon-length.
	fadR	Global transcriptional regulator	Regulates FA Metabolism.
	yahF or fad E-F	acyl-CoA dehydrogenase	Dehydrogenation of acyl-CoA (first step in β-oxidation).
	fadE	electron transferring flavoprotein	Associates to the acyl-CoA dehydrogenase.
	fadB	enoyl-CoA hydratase	Reduction of the double bound.
		β-hydroxyacyl-CoA dehydrogenase	Removes a water molecule.
		cis-β-enoyl-CoA isomerase	Isomerization of *cis*-unsaturated FA to *trans*.
	fadA	thiolase	Releases acetyl-CoA from the β-ketoacyl-CoA to form an acyl-CoA.
	fadH	2,4-dienoyl-CoA reductase	Reduce PUFA double bounds.
	cfa	Cylcopropane synthase	Post-synthetically convert fatty acyl chains to their cyclopropane derivatives.
	tesA	Thioesterase I	Cleave the thioester bond of acyl-CoA molecules to produce CoA and FFA with a substrate specificity for acyl chains > 12 carbon atoms.
	tesB	Thioesterase II	Cleaves acyl-CoAs of >6 carbons and β-hydroxyacyl-CoAs, but is unable to cleave acyl-pantetheine thioesters.

1.1.2. Phospholipids

PLs in *E.coli* and other Gram-negative bacteria are used in the construction of the inner and outer membranes. Its biosynthesis requires significant investment by the cell, and the advantages of maintaining fine control over the pathway are obvious. Between the inner and outer membranes there is an osmotically active compartment called the periplasmic space. Membrane-derived oligosaccharides (MDOs), peptidoglycan, and binding proteins involved in metabolite transport are found in this compartment. MDOs are composed of *sn*-glycerol-1-phosphate (derived from phosphatidylglycerol, PG), glucose and (usually) succinate moieties. Gram-positive bacteria do not possess an outer membrane (Heath, Richard J. et al., 2002).

Glycerophospholipids are usually the major constituents of bacterial membranes. They are normally enriched with SFA at the *sn*-1 position and with UFA at the *sn*-2 position. PG is frequently the major PL in most species of bacteria (Gunstone et al., 2007). For instance, the three major PL species in *E.coli* membranes are phosphatidylethanolamine (PE, which comprises the bulk of the PLs, 75%), with PG and cardiolipin (CL, diphosphatidylglycerol).

The scheme for the synthesis of membrane PLs follows the classic Kennedy pathway (see Fig I-13). Phosphatidic acid (PhA), synthesized from glycerol phosphate and two FA by the acyltransferases, is transformed into the key activated intermediate in PL biosynthesis, CDP-diacylglycerol, by a phosphatidate cytidyltrasferase. Then the biosynthesis pathway splits for the production of PE or PG/CL.

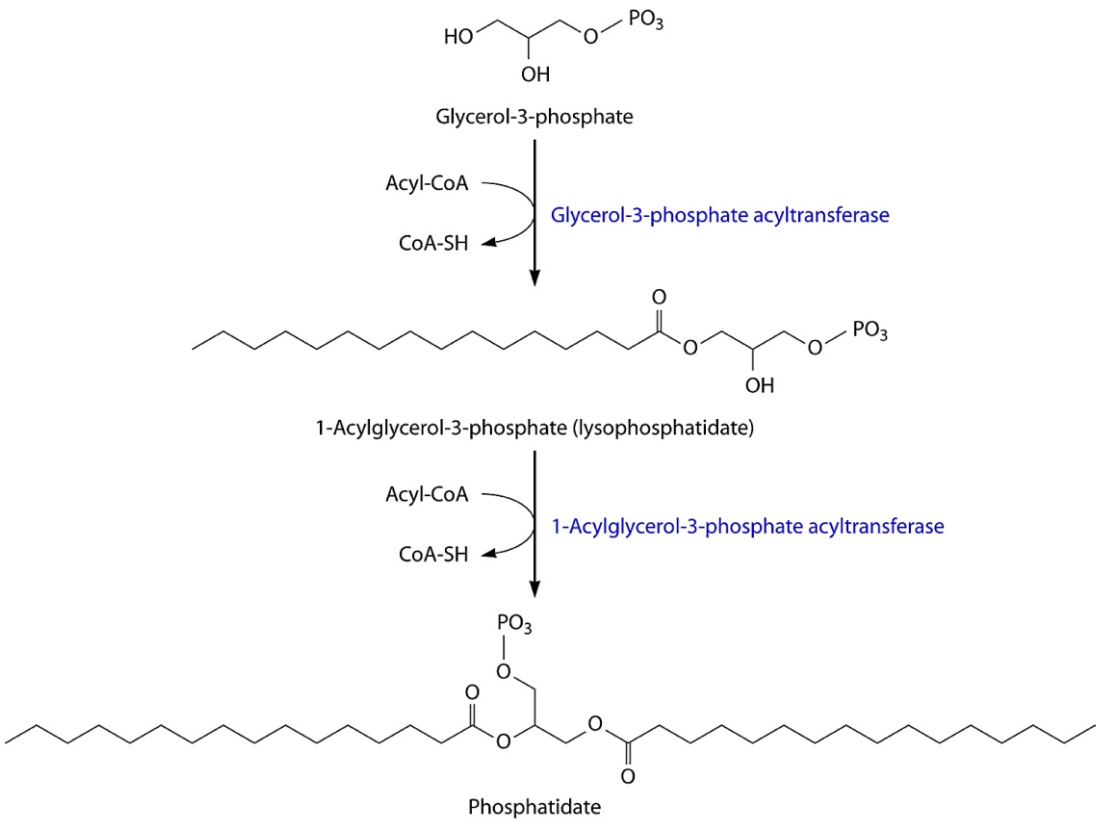

Figure I-13. First two acylation steps in membrane lipid and triacylglycerol synthesis from glycerol-3-phosphate to the central intermediate phosphatidate (Kennedy pathway). Enzymes are labelled in blue and molecule names in black. Source: Röttig and Steinbüchel, 2013.

PL degradation is performed by different phospholipases that catalyze the hydrolysis of acyl chains from PLs, while thioesterases cleave the thioester bond of acyl-CoA molecules to produce CoA and FFAs.

Alternatively, FA attached to membrane PLs can be post-synthetically converted to their cyclopropane derivatives by the product of the *cfa* gene during the stationary phase of bacterial growth. This more stable molecule protects the reactive double bond from adverse reactions (Heath, Richard J. et al., 2002).

Phospholipid turnover: the diacylglycerol cycle

In the synthesis of MDOs in Gram-negative bacteria, the *sn*-glycerol-1-phosphate polar head-group of PG is transferred to the oligosaccharide, being 1,2- diacylglycerol (DAG) the other product of the reaction. This reaction, catalyzed by the product of *mdoB,* is regulated by the osmotic pressure of the growth medium. Therefore, decreased osmotic pressure gives an increased rate of MDO and DAG synthesis. This DAG is phosphorylated by the diacylglycerol kinase (encoded by *dgkA*) to form PhA, which can reenter the PL biosynthetic pathway to complete the DAG cycle (as reflected in Fig I-14). The rate of accumulation of DAG in strains lacking the *dgkA* gene correlates with the presence of both the oligosacccharide acceptor and the osmolarity on the growth medium (Heath, Richard J. et al., 2002; Lin et al., 2013; Ridgway and McLeod, 2015).

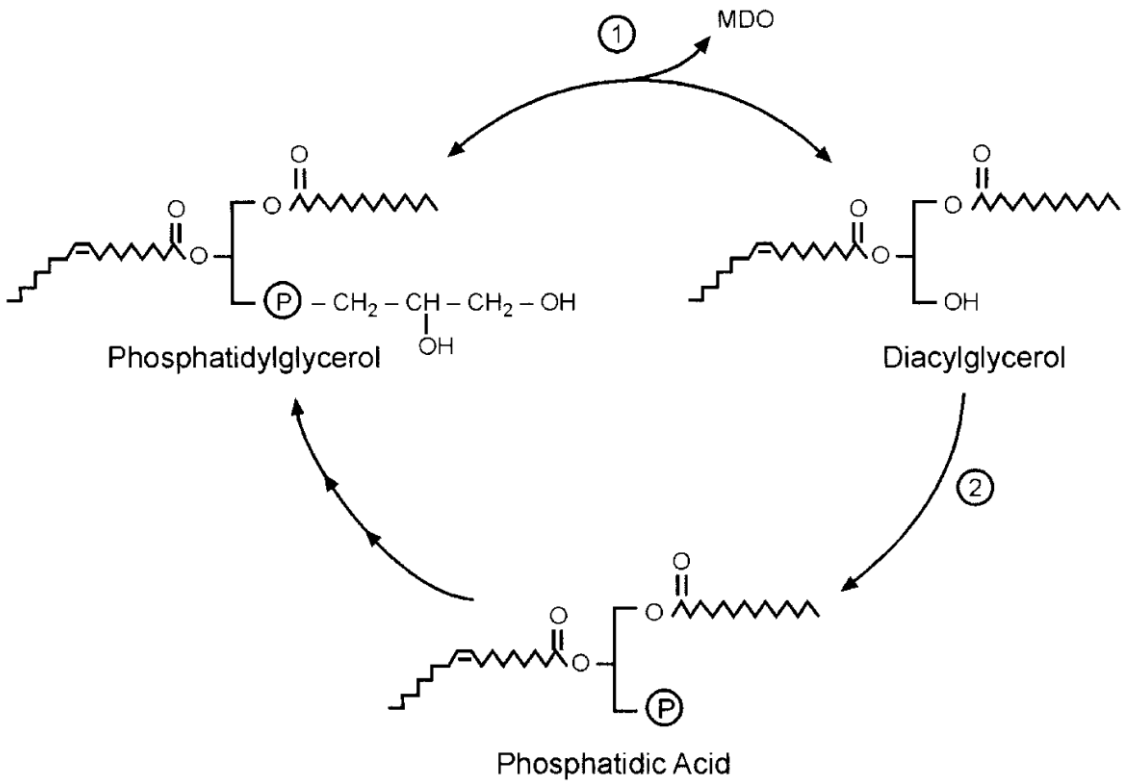

Figure I-14. Phospholipid turnover. The 1,2-diacylglycerol kinase cycle involves (1) the transfer of the *sn*-1-glycerol-phosphate moiety from PG to MDO by the enzyme MdoB. (2) Diacylglycerol kinase converts the DAG to PhA, which can regenerate the PG. Abbrebiations: PG, phosphatidylglycerol; PhA, phosphatidic acid. Source: Heath, Richard J. et al., 2002.

In Gram-positive bacteria, an analogous DAG cycle is constitutively active. Synthesis of lipoteichoic acid (constituted by the addition of about 25 sn-1-glycerolplosphate moieties from PG molecules to the head group of glucosyl-diacylglycerols) in these organisms yields DAG as co-product. This DAG is reintroduced into the PL biosynthetic pathway (Ridgway and McLeod, 2015).

The main genes related with PL metabolism are listed in Table I-3.

Table I-3. Some genes implied or affecting PL metabolism in bacteria. Sources: DiRusso et al., 1992; Heath, Richard J. et al., 2002; Hofvander et al., 2011; Röttig and Steinbüchel, 2013.

Metabolic pathway	Gene(s)	Protein	Function
PlsX/PlsY System for PL synthesis	*plsB*	Glycerol-3-phosphate acyltransferase	Transfer of fatty acyl groups to the 1 position of *sn*-glycerol-3-phosphate.
	plsC	1-Acylglycerol-3-phosphate acyltransferase	Transfer of fatty acyl groups to the 2-position of 1-acylglycerol-3-phosphate.
	plsX	Phosphotransacetylase	Catalyzes the formation of acyl-phosphate from acyl-ACP.
	plsY	Glycerol-phosphate acyltransferase	Transfer of fatty acyl groups to the 1 position of *sn*-glycerol-3-phosphate. It is inhibited by acyl-CoA and uses acyl-phosphate as its unique acyl donor.
Diacylglycerol cycle	mdoB	Phosphoglycerol transferase	Transfer the *sn*-1-glycerol-phosphate moiety from PG to MDO.
	dgk	Diacylglycerol kinase	Phosphorylates DAG to form phosphatidic acid.
	cds	Phosphatidate cytidyltrasferase	Conversion of phosphatidic acid to a mixture of CDP-diacylglycerol and dCDP-diacylglycerol.
PL degradation	*pldA*	Phospholipase A1	Hydrolyzes FA from PL and mono- and diacylglycerols in the outer membrane of a Gram-negative bacteria.
	pldB	Lysophospholipase L2	Hydrolyzes some PL and catalyzes the transfer of FA to others in the inner membrane of Gram-negative bacteria.

1.1.3. Accumulation of neutral lipids

The ability to deposit intracellular carbon storage compounds means an advantage over competitors in the habitat when growth substrates become scarce. Consequently, nearly all prokaryotes known so far are able to accumulate at least one type of storage compound. The accumulation of lipid droplets (LDs) or granules in prokaryotes is normally a facultative response to nutrient depletion. The few exceptions of prokaryotes lacking the natural capability to accumulate lipids (e.g. Enterobacteriaceae) exist in nutrient-rich habitats, in which accumulation of lipids does not provide an advantage. Those lipids constitute the ideal reserve materials, as they are highly calorific, water insoluble, and osmotically inert. The most common lipophilic storage compounds in prokaryotes consist of esterified (hydroxy)- FA and can be divided into polymeric lipids (polyhydroxyalkanoates, PHAs, a complex class of storage polyesters with a great variety of hydroxialkanoic acids as constituents), and non-polymeric neutral lipids (TAGs, FA-triesters of glycerol and wax esters, WEs, oxoesters of long-chain FA esterified with long-chain alcohols, see Fig I-15) (Murphy, 2012; Röttig and Steinbüchel, 2013; Wältermann and Steinbüchel, 2005).

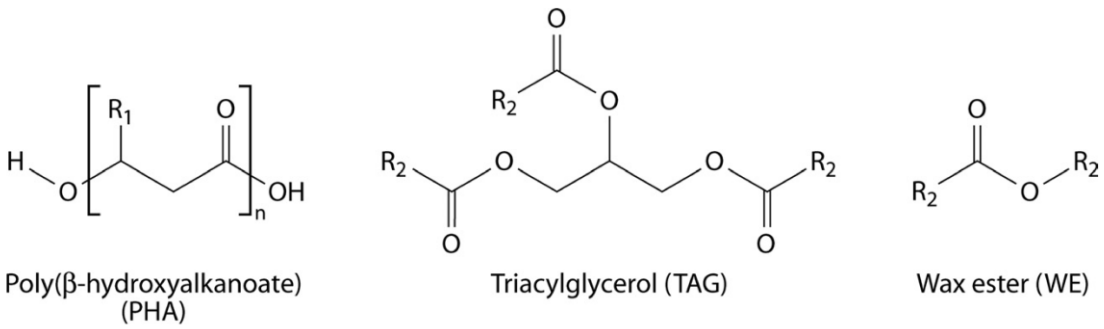

Figure I-15. Chemical structures of common lipophilic storage compounds in prokaryotes: poly (3-hydroxyalkanoate) (PHA), triacylglycerol (TAG), and wax ester (WE). R_1, alkyl chain with a length ranging from C1 to C13; R_2, saturated or unsaturated long-chain-length alkyl residue. Images from Röttig and Steinbüchel, 2013.

LDs consist on spherical cellular structures constituted by a neutral lipid core, a monolayer PL membrane and numerous proteins. Those lipid inclusions accumulate in bacteria in discrete, intracellular granules. Even though their structure seems relatively simple, interesting differences between the diverse types of inclusions (TAG, WE or PHA) can be distinguished by transmission electron microscopy (TEM). Similar to lipid bodies in cultured mammalian cells, bacterial TAG inclusions split into numerous internal fracture planes when freeze-fractured, leading to a lamellar internal view of the hydrophobic core. In contrast, PHA granules exhibit needle-like or mushroom-like artifacts, which occur owing to a plastic deformation process. Besides, WE droplets show a wide variety of different morphologies ranging from spherical and ellipsoid to disc-like structures or even rectangular shapes (Liu et al., 2013; Wältermann and Steinbüchel, 2006).

The fundamental mechanisms in the formation of LDs in bacteria were analyzed by Wältermann and co-workers in 2005, who studied the process in the known oleogenic microorganism *Rhodococcus opacus* PD630 (see Fig I-16.A) and presented the model displayed in Fig I-16.B. Neutral lipid-body formation starts at peripheral lipid domains close to the cytoplasm membrane, with attachment of WS/DGAT. Initially, small lipid droplets remain associated with this protein due to hydrophobic interactions between the enzyme and the synthesized lipids, while hydrophilic regions between them would allow normal membrane-associated metabolic processes of the cell, such as lipid biosynthesis itself. This rather unstable small-lipid-droplet-emulsion accumulates in an oleogenous layer at the cytoplasm membrane at certain parts of the cell, coated by a by a half-unit membrane of PLs, to form lipid-prebodies. The latter are then released into the cytoplasm after reaching a critical size and matured lipid bodies are formed (Wältermann et al., 2005).

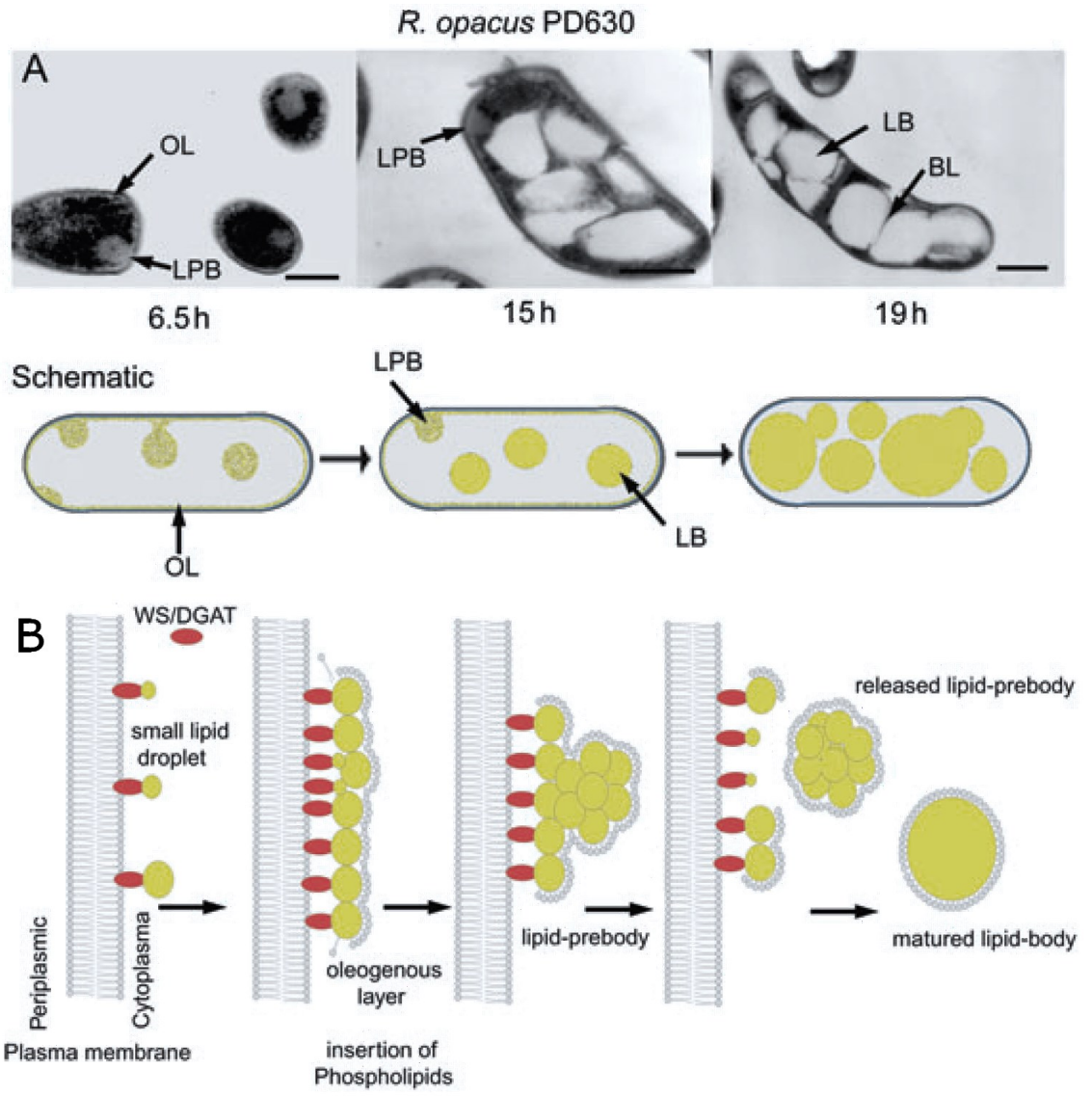

Figure I-16. A) Morphological characterization of lipid-body formation: TEM micrographs of *Rhodococcus opacus* PD630 and scheme of the same cells grown under storage conditionsfor 6.5, 15 and 19 hours. B) Model proposed for TAG- and WE-body formation in prokaryotes by Wältermann and co-workers in 2005. Scale bar = 0.2 mm. Abbreviations: BL, boundary layer; LB, lipid-body; LPB, lipid-prebody; OL, oleogenous layer.

While the occurrence of intracellular TAG reservoirs is widespread in many eukaryotes, its accumulation in prokaryotes is restricted only to a few aerobic heterotrophic bacteria and some cyanobacteria. Biosynthesis of TAGs is a common property of species belonging to the Gram-positive actinomycetes group (such as *Mycobacterium* sp., *Nocardia* sp., *Rhodococcus* sp., *Micromonospora* sp., *Dietzia* sp., *Gordonia* sp. and streptomycetes), which might be defined as oleaginous organisms since they can accumulate lipids to more than 20% of their dry weight. TAG inclusions have been also reported for Gram-negative proteobacteria like *Alcanivorax* sp., *Marinobacter* sp. or *Acinetobacter* sp., though the amounts are small in these species. For their part, WEs accumulates in few prokaryotic species, acting in some (such as *Acinetobacter baylyi*) as the main storage compound. In contrast, PHAs are common in the entire bacteria spectrum (Alvarez and Steinbüchel, 2002; Wältermann and Steinbüchel, 2005).

In addition to its role as storage molecules, these lipid bodies are a both a source of signaling molecules and substrates for membrane biogenesis and a deposit for reducing equivalents, toxic FFAs,

alkanes and alcohols or useless FA. Accordingly, regulation of cellular membrane fluidity by keeping certain FA away from PL biosynthesis has been discussed as key function of those lipophilic molecules (Alvarez and Steinbüchel, 2002; Lin et al., 2013; Wältermann and Steinbüchel, 2005).

Biosynthesis of WE and TAG in prokaryotes

The crucial final step in the most common pathway for TAG biosynthesis in bacteria is catalyzed by a key enzyme named wax ester synthase/acyl-CoA : diacylglycerol acyltransferase (WS/DGAT). This family of promiscuous enzymes mediates both WEs and TAGs formation, as presented in Fig I-17. Formation of TAGs by WS/DGAT depends on the presence of DAGs, produced by *de novo* biosynthesis by sequential acylation of glycerol-3-phosphate, and acyl donors, derived by *de novo* biosynthesis from unrelated carbon sources like glucose or from exogenous sources. Fatty alcohols needed for WE synthesis are naturally produced in some bacteria from acyl-ACP/acyl-CoA (Hofvander et al., 2011; Kalscheuer and Steinbüchel, 2003; Wältermann et al., 2007).

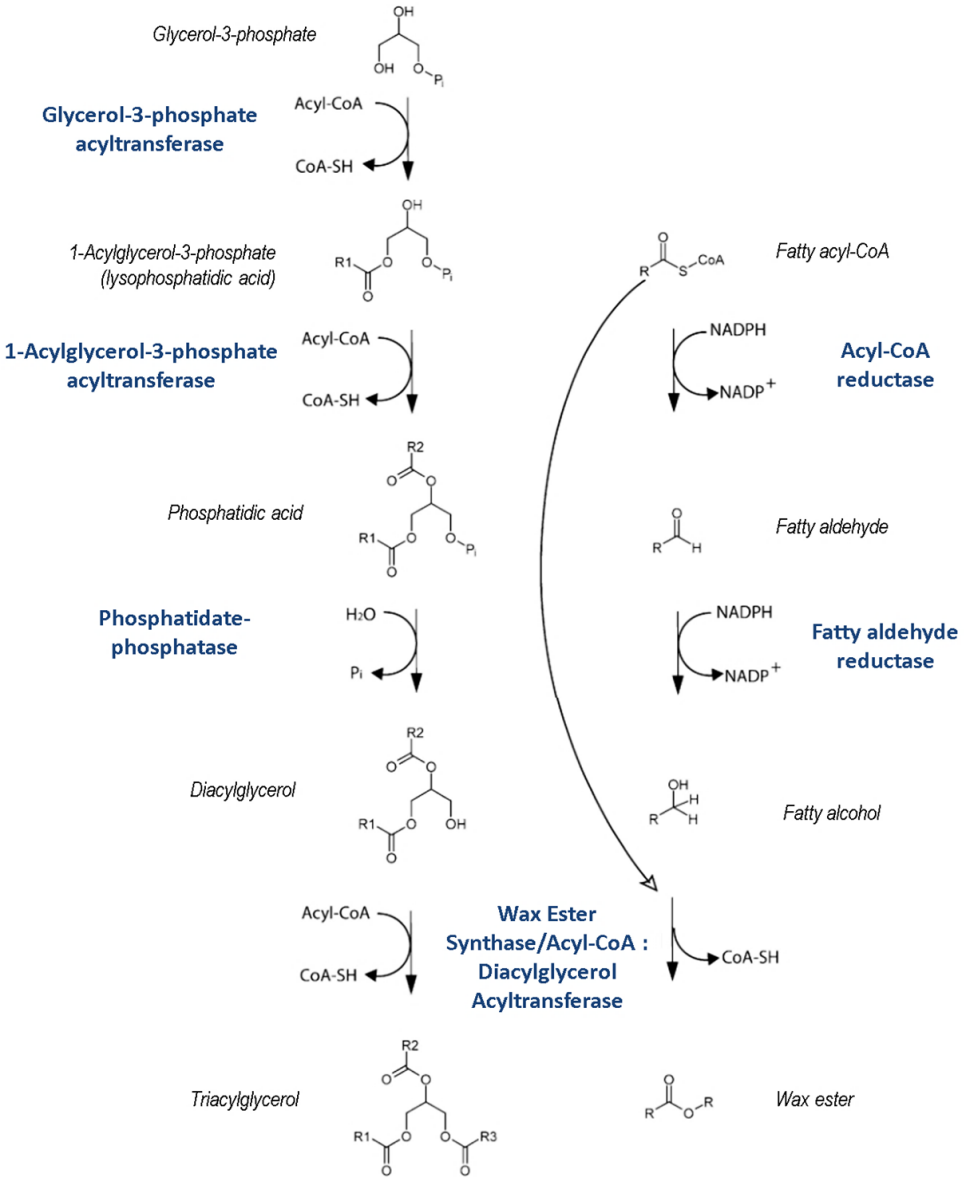

Figure I-17. Main pathways for biosynthesis of WEs and TAGs through a WS/DGAT enzyme. Enzymes are named in blue and molecule names in black. Adapted from Wältermann et al. (2007).

As already mentioned, biosynthesis of TAG in bacteria is strongly related to the metabolism of PLs, both sharing common intermediates. A schematic overview of the main pathways for the synthesis of glycerophospholipids and TAG in bacteria is illustrated in Fig I-18.A, showing that PhA is the precursor for both membrane PLs and TAG synthesis. The pathways for the biosynthesis of those lipid metabolites in different types of bacteria are distinguished in the outline presented in Fig I-18.B. While in gammaproteobacteria glycerol-3-phosphate is acylated to LPA by PlsB, there exists an alternative for the first acylation step in the vast majority of bacteria: the PlsX/PlsY pathway. Together with the different PlsC proteins in both groups (using both acyl-ACP and acyl-CoA or dependent on acyl-ACP as the essential acyl donor), that implies that most gammaproteobacteria can incorporate exogenous FA into their lipids, whereas the remaining bacteria depend on *de novo* FA synthesis as a source for membrane synthesis.

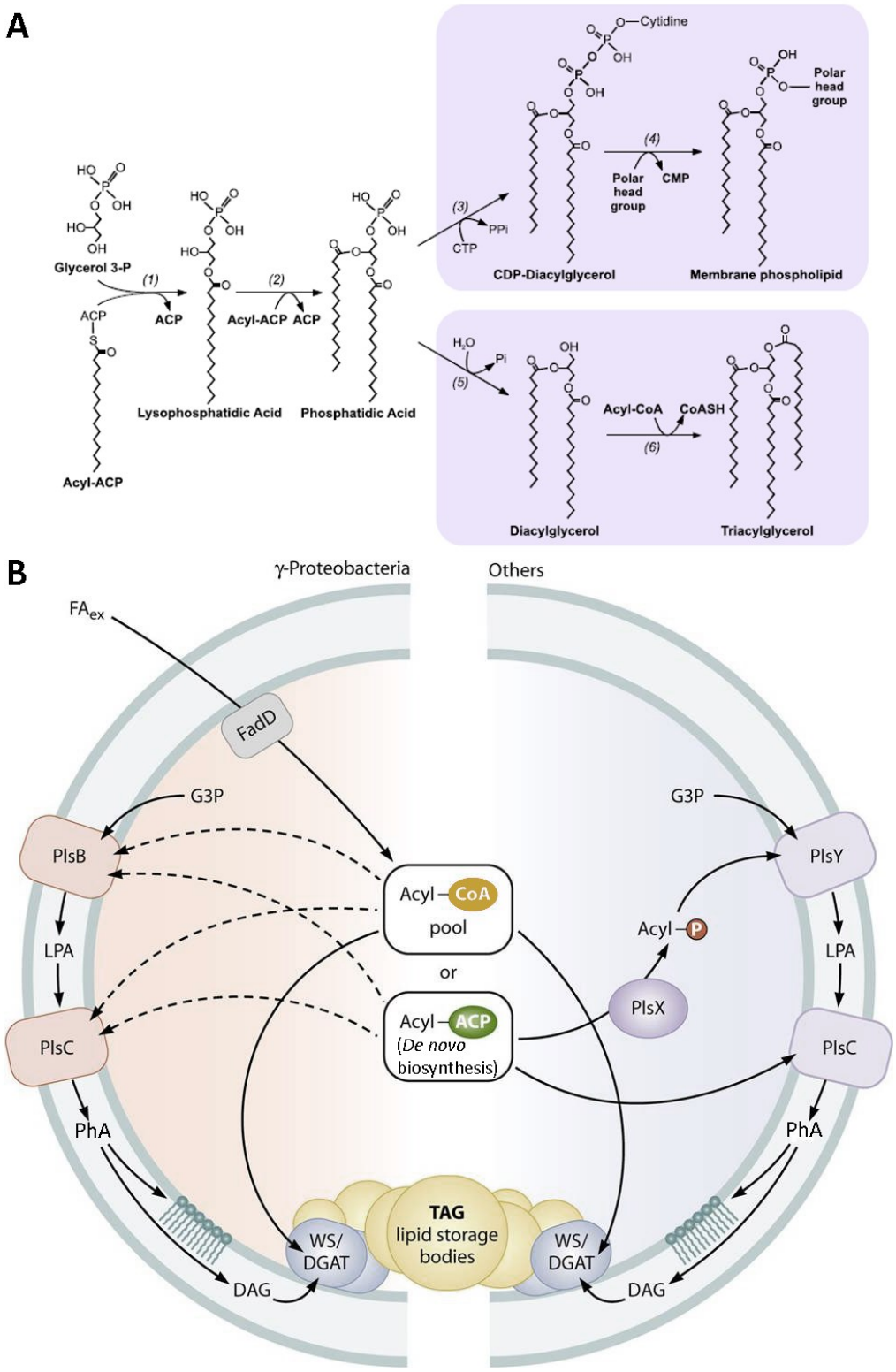

Figure I-18. A) Schematic representation of the major biosynthesis pathways for membrane glycerophospholipids and TAGs in bacteria producing these neutral lipids. PhA is the metabolic branch point dividing glycerophospholipid and TAG biosynthesis. (1) Glycerol-3-Phosphate acyltransferase. (2) Lisophosphatidic acid acyltransferase. (3) Phosphatidatecytidyly ltransferase. (4) Phosphatidyl transferase. (5) Phosphatic acid phosphatase. (6) Diacylglycerol: acyl-CoA acyltransferase. Adapted from Comba et al. (2013). B) Overview of pathways for membrane PL and TAG biosynthesis in bacteria. G3P, glycerol-3-phosphate; FAex, exogenous fatty acids; LPA, lysophosphatidic acid; PhA, phosphatidic acid; DAG, diacylglycerol; TAG, triacylglycerol. Adapted from Röttig and Steinbüchel (2013).

Furthermore, some reports indicate there are alternative acyl-CoA-independent pathways for TAG synthesis with a rather low contribution to the overall TAG content. A mechanism implying a DAG : DAG transacylase which utilizes DAG as both the acyl donor and acceptor has been described in plants and animals, although a responsible gene product has not been identified yet. Besides, the eukaryotic sterol : acyl-CoA acyltransferase from *Saccharomyces cerevisiae* also exhibits a certain DGAT side activity (Röttig and Steinbüchel, 2013). Moreover, the pathway mediated by a phospholipid : diacylglycerol acyltrasferase (PDAT) that uses PLs as acyl donors and DAG as acyl acceptors, which had already been described in yeast and plants, has been demonstrated to occur both in *Alcanivorax borkumensis* and *Streptomyces coelicolor*. In addition to the role of the latter enzymes in neutral lipid accumulation, the employment of PLs as substrates lead to the hypothesis that this proteins are modulators of membrane composition (Arabolaza et al., 2008; Kalscheuer et al., 2007).

WS/DGAT family of proteins. Current knowledge about structure and specificity

The family of promiscuous enzymes WS/DGAT mediates both WE and TAG formation from long-chain acyl-coenzyme A (CoA) molecules as acyl donors and long-chain fatty alcohols or DAGs as respective acyl acceptors in bacteria (see Fig I-19).These proteins are partly distributed in the cytoplasm, whereas there is a proportion associated with the membrane or lipid inclusions (Röttig and Steinbüchel, 2013; Stöveken et al., 2005). When they are found attached to the membrane, this is due to electrostatic interactions rather than by an integral conformation. WS/DGATs have anamphiphilic character, with hydrophobic regions necessary for its interaction with hydrophobic substrates and a charge in an environment with a neutral pH due to its non-neutral isoelectric point. More so, it can be speculated that its activity and/or substrate specificity might be influenced depending on whether it is exposed to a hydrophilic (cytoplasm) or hydrophobic (membrane-associated) environment (Röttig and Steinbüchel, 2013; Stöveken et al., 2005; Wältermann et al., 2005).

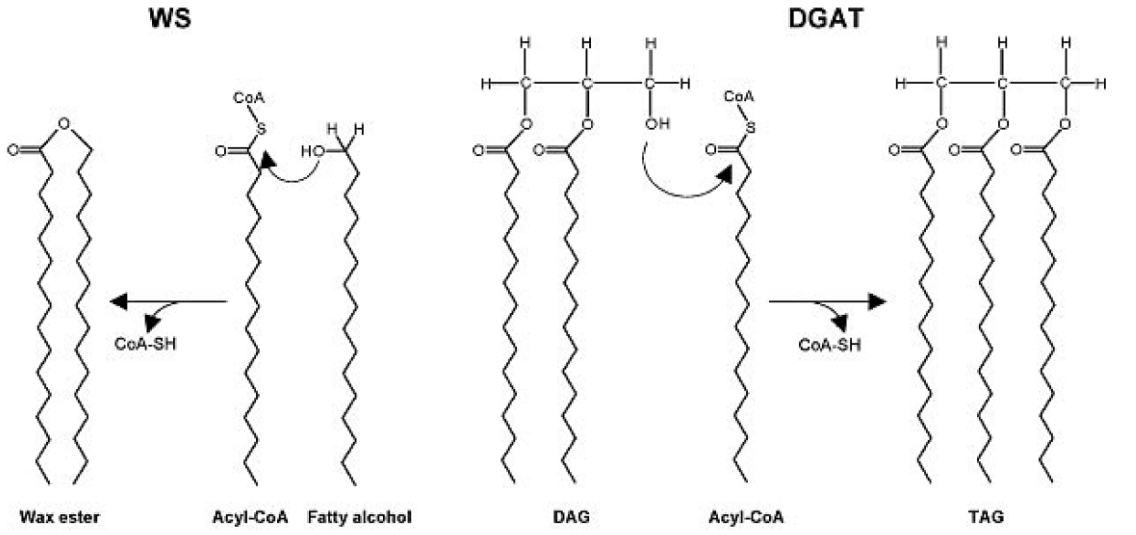

Figure I-19. Chemical reactions catalyzed by the bi-functional WS/DGAT enzyme for the synthesis of WE or TAG from acyl-CoA and fatty alcohol or DAG, respectively. Image from Kalscheuer and Steinbüchel (2003).

Sequence analysis of several homologs of the WS/DGAT underscored a highly conserved motif occurring in all members of that family as well as in other acyl–CoA-dependent acyltransferases: "HHXXXDG" (see Fig I-20). The second histidine residue in this putative active-site motif is strictly conserved and was firstly demonstrated to be essential for catalytic activity in nonribosomal peptide bond formation (Stachelhaus et al., 1998) and later for WS/DGAT enzymes (Arabolaza et al., 2008; Kalscheuer et al., 2007). Nevertheless, both histidines were reported to be necessary for maximal activity in enzymes belonging to the WS/DGAT family. Although the other two highly conserved residues were reported not to be of major importance for the activity of the WS/DGAT from *A.baylyi* ADP1 (Stöveken et al., 2009), the aspartate showed to be crucial for activity in other enzymes of this family such as the one from *Marinobacter hydrocarbonoclasticus* VT8 (Ma2, Villa et al., 2014).

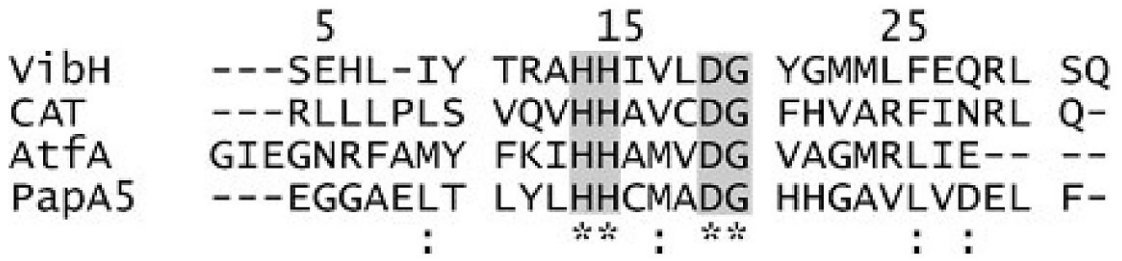

Figure I-20. Multiple sequence alignment of the highly conserved HHXXXDG motif from different types of bacterial acyltransferases. VibH, non-ribosomal peptide synthetase condensation domain from *Vibrio cholerae*; CAT, chloramphenicol acetyltransferase from *E.coli*; AtfA, WS/DGAT from *A.baylyi ADP1*; PapA5, phthiocerol dimycocerosyl transferase from *M.tuberculosis* (Stöveken et al., 2009).

In general, enzymes with this motif share the ability to transfer thioester-activated acyl substrates to a hydroxyl or amine acceptor to form an ester or amide bond, such as acyltransferases that synthesize glycerolipids, nonribosomal peptide synthetases, acyltransferases involved in lipid biosynthesis, polyketide-associated acyltransferases, or chloramphenicol acetyltransferase (CAT). The catalytically active histidine initiates the deprotonation of a hydroxyl group to enable the nucleophilic attack on the acyl donor (Röttig and Steinbüchel, 2013). The assumed mechanism for WS/DGAT enzymes was first described in 2009 by Stöveken and co-workers, who proposed that both histidine residues in this amino acid sequence are able to act as general base and deprotonate the hydroxyl group of the fatty alcohol or the DAG, respectively. Then, the resulting oxoanion acts as nucleophile and interacts with the carbon atom of the thioester bond of acyl-CoA (see Fig I-21). This results in the formation of the oxoester bond of the WE or TAG and in the release of CoA-S^-. The protonated histidine is subsequently regenerated by transferring the received proton back to $CoAS^-$, yielding free CoA-SH.

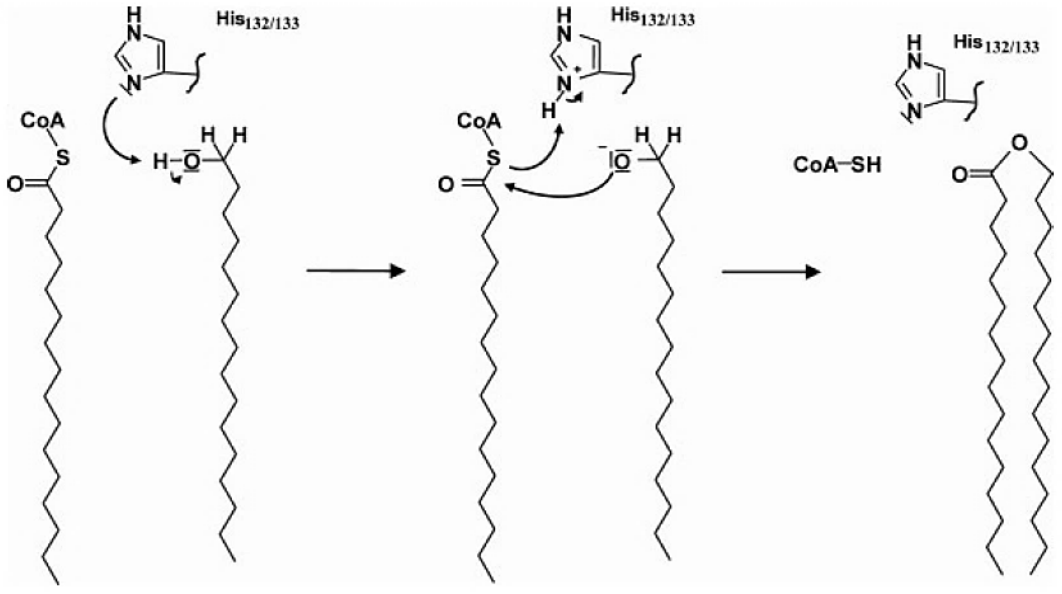

Figure I-21. Catalysis mechanism proposed in 2009 by Stöveken and co-workers for the WS/DGAT from *Acinetobacter baylyi* ADP1 exemplarily demonstrated for the WE synthesis reaction. Only one catalytically active histidine residue of WS/DGAT is shown.

Besides, other two conserved motifs characteristic of WS/DGAT enzymes were also reported to be essential for acyltransferase activity, as seen by site-directed mutagenesis by Villa and co-workers

(2014). The mutation of some residue of the motif I (PLW) reduced drastically the enzymatic activity of the WS/DGAT from *M. hydrocarbonoclasticus* VT8, while a significant decrease was also seen upon mutation any of the residues from motif II (ND). Both motifs seemed to be involved in the proper conformation of the active site according to its location in the tridimensional model.

Limited proteolysis demonstrated the presence of two structural domains within the protein, which give rise to WS/DGAT activity when co-expressed as independent polypeptides. This was related to the tri-dimensional (3D) model prediction that suggested two domains (Nt and Ct domains) connected by a helical linker (see Fig I-22), similar to several other HHxxxDG acyltransferases whose structures have been solved (Villa et al., 2014). As previously suggested (Röttig and Steinbüchel, 2013; Stöveken et al., 2009), its catalytic center would be located in a hydrophobic pocket or channel, restricting the accessibility for hydrophilic molecules.

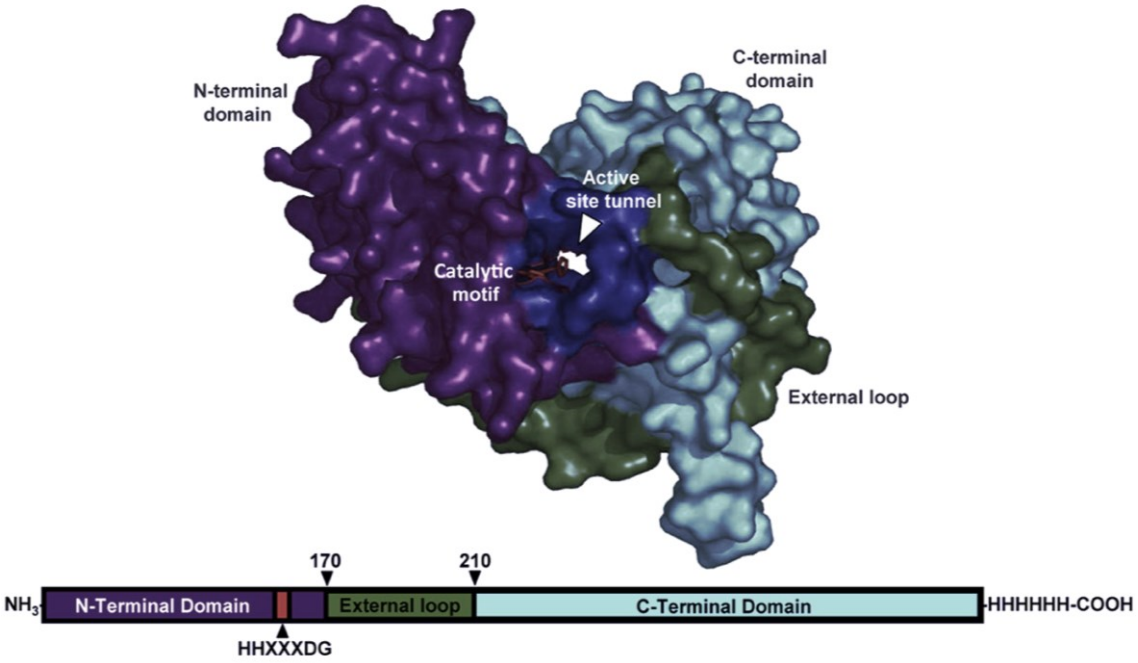

Figure I-22. Locations of the C-terminal (purple) and N-terminal (cyan) domains in modelled structure and in the primary sequence of the WS/DGAT from *Marinobacter hydrocarbonoclasticus*. The external loop (linker) is coloured in green and the position of the active site motif HHxxxDG is shown in red in the central channel (dark blue in the 3D structure). Source: Villa et al., 2014.

WS/DGAT has been reported to have a remarkably broad spectrum (see Fig I-23). The first enzyme characterized from this family, the protein from *Acinetobacter* sp. Strain ADP1, accepted a wide range of substrates in *in vitro* experiments. The highest activity was obtained for medium-chain-length alcohols (C14 to C18) and palmitoyl-CoA. However, both alcohols and acyl-CoAs with different lengths were also accepted although not with the same efficiency. Likewise, a terminal hydroxy group in fatty alcohols showed to be more accessible to the enzyme than other isomers. Additionally, the substrate range of WS/DGAT was successfully evaluated for cyclic and aromatic alcohols and both the formation of thio WEs and wax diesters were also demonstrated. Besides, various mono-, di-, and oligosaccharides, some amino acids and other molecules were tested as acyl acceptors with no detectable WS/DGAT-mediated acylation. This wide spectrum has leaded to the presumption that only the provision of hydrophobic substrates limits the products synthesized by this enzyme (Stöveken and Steinbüchel, 2008; Stöveken et al., 2005).

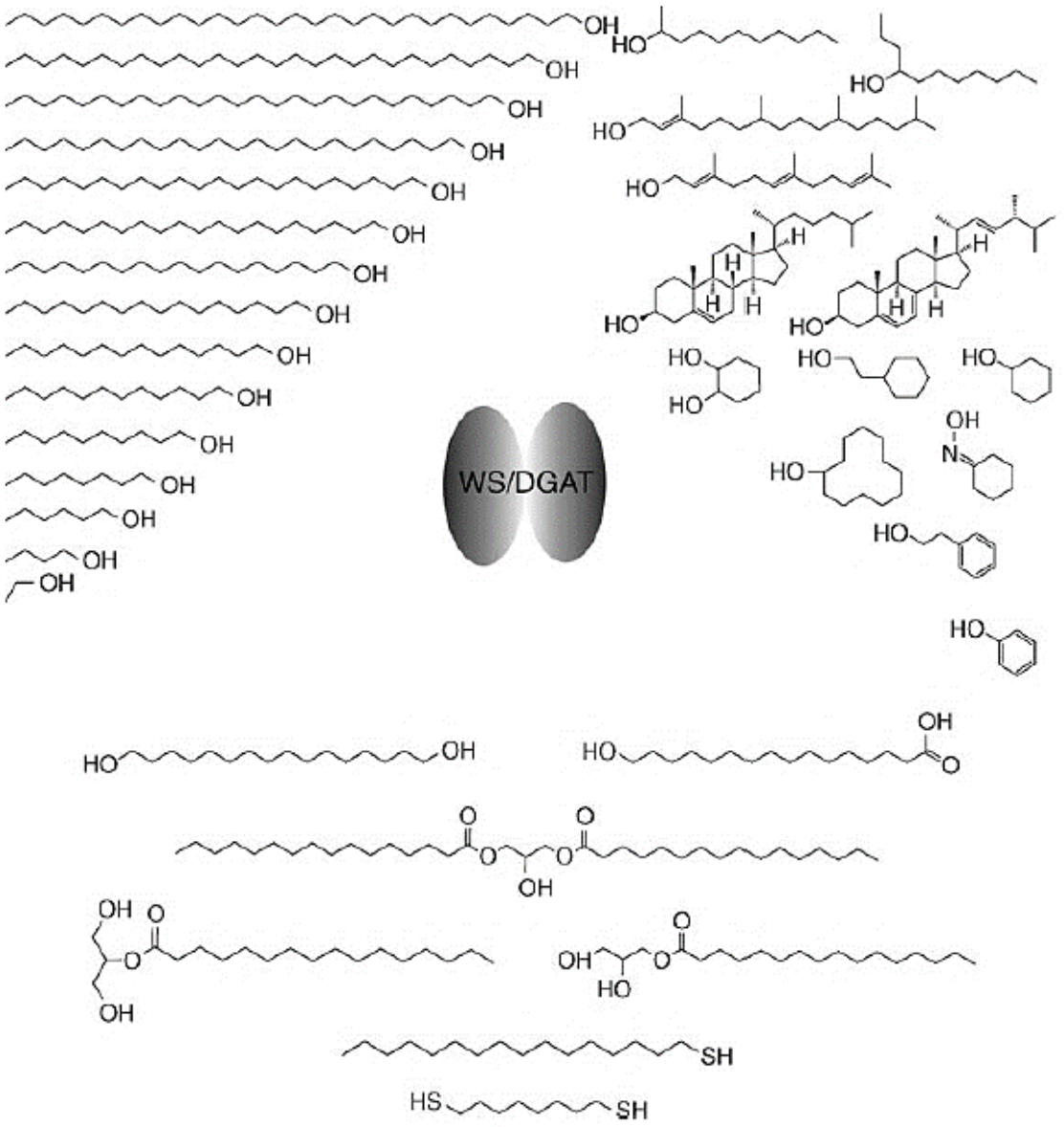

Figure I-23. Overview of hydroxy-group-containing substrates for bacterial acyltransferases belonging to the WS/DGAT family (Stöveken and Steinbüchel, 2008).

Stöveken and co-workers (2005) also reported the inactivation of the WS/DGAT at high temperatures and saw that free CoA, which was released during the WS/DGAT-mediated acyltransferase reaction, significantly inhibited WS/DGAT-mediated WE formation.

In other respects, Röttig and Steinbüchel reported in 2013 the wide variety of homologs belonging to the WS/DGAT family, which diverge substantially in size, sequence, or specific activities in natural or artificial hosts. The vast majority of these members were descryed in prokaryotes, although two members were also identified in plants and homologous sequences have been found in plants (from monocotyledons and gymnosperms to important crops such as wheat, barley, rice, jojoba or soybean), protists and animals (cnidaria, arthropoda, or hemichordate) as well. Among prokarytes, it is important to remark the high number of orthologous genes belonging to this family in actinobacteria species, which suggests a great importance of these enzymes for their survival. Phylogenetic analysis of representative homologs carried out by Villa and co-workers in 2014 show that while most proteobacterial members of the family are

phylogenetically related, actinomycete ones are disperse along the bacterial clusters. Besides, a recent report point to the need of search for new members of this protein family in environmental samples rather than only bacterial isolates to broaden the knowledge on its diversity and find new activities such as the production of unusual lipids (Lanfranconi et al., 2015).

Since MAG also served as substrate, DAG synthesis was discussed to be not exclusively occurring via the Kennedy pathway by sequential acylation of glycerol-3-phosphate, but also by a possible involvement of WS/DGAT in the formation of DAGs *in vivo* as well (Stöveken and Steinbüchel, 2008).

Summarizing, some genes implied in neutral lipid metabolism are listed in Table I-4.

Table I-4. Some genes related to neutral lipid metabolism in bacteria. Sources: DiRusso et al., 1992; Heath, Richard J. et al., 2002; Hofvander et al., 2011; Icho and Raetz, 1983; Röttig and Steinbüchel, 2013; Wältermann et al., 2007.

Metabolic pathway	Gene(s)	Protein	Function
	pgpB	Phosphatidate-phosphatase	Dephosphorylate phosphatidate to forme DAG.
	WS/DGAT	Wax ester synthase/Acyl-CoA : diacylglycerol acyltransferase.	Catalize the crucial final step in the most common pathway for TAG biosynthesis and WE formation.
Fatty alcohol formation	*acr1*	Acyl-CoA reductase	Reduction of acyl-CoA/acyl-ACP to fatty aldehydes.
	farA	Fatty Aldehyde Reductase	Reduction of the fatty aldehyde to the corresponding fatty alcohol.

TAGs as a FA source.

Certain FA such as LC-PUFA are essential cellular components in several organisms. However, FFA are found in very low levels in the cells, which is likely related to the diverse biological activities they show. Some can interfere with cellular energy production, inhibit certain enzyme activities, impair nutrient uptake or generate peroxidation and auto-oxidation degradation of diverse products. As a matter of fact, its antibacterial properties have been discussed, providing the ability of some FFA to inhibit the growth or even kill bacteria. Consequently, FAs in bacteria are normally either metabolized or employed as a building part of the plasma membrane, but can also be accumulated as part of TAGs in organisms capable of storing these neutral lipids. Hence, those lipid bodies become an important source of diverse FA. Microbial oil, also known as single cell oil (SCO), consists of lipids produced by oleaginous microorganisms. In SCO processes, microorganisms that are able to produce the desired oil are cultivated in a bioreactor. In addition to the continuously increasing research on its use as alternative raw material for biodiesel production, as evidence of the medical significance of oils enriched in PUFA increases the interest in enhancing the production of these molecules (Desbois and Smith, 2010; Heath, Richard J. et al., 2002; Huang et al., 2013; Sijtsma and de Swaaf, 2004).

1.2. Commercial relevance of oil generation in prokaryotes. Interest of oil production.

All living organisms require a form of energy to sustain life. Furthermore, specialized needs demand that organisms maintain a store of fuel that can be mobilized when required. Most living organisms use neutral lipids as the preferred long term form of stored energy, as their low oxidation state and high calorific value make them yield significantly more energy upon oxidation than carbohydrates and proteins. As state before, TAGs, WE and PHA are the main lipid storage compounds. Moreover, lipids are indispensable for life not only as energy source but also for their structural role and as precursors of important hormones and other signalling molecules.

TAGs, major storage compounds and source of FA in living organisms, have been employed for the production of commercially significant goods throughout history, being widely used in both industrial and healthcare applications. Diverse profitable applications of TAGs are production of biofuels, lubricants, different dietary supplements, oils for cooking or products with health benefits, including antioxidant power and ability to moisturize the skin (Alvarez and Steinbüchel, 2002; Gurr et al., 2002; Viola and Viola, 2009).

World consumption of oils and fats has grown progressively during the last 25 years. Actually, since 1995, the global consumption per capita of oils and fats has risen from 15.6 to 23.4 kg per year. Furthermore, the forecast for global demand for fats and oils during the next years consists on a continuous increment and probably to exceed world production (Alvarez, 2010).

Prokaryotic SCO display a series of advantages when compared to plants and animals as lipid sources. In addition to being more genetically accessible (e.g. single-copy genes vs. multiple genes encoding proteins with redundant enzymatic activities in FA biosynthesis), microorganisms are generally capable of producing greater diversity and storing higher percentages of lipids. Hence, their productivity per volume and energy input can become significatively higher. The numerous industrial uses of FAs and their derivatives will probably make them gain popularity as technical difficulties in their production are eased. Overall, the great demand of new bioresources for the production of all TAG-derived products provides motivation to engineer production from robust microbial platforms based in the scheme shown in Fig I-24 (Duan et al., 2011; Garay et al., 2014; Handke et al., 2011; Rucker et al., 2013).

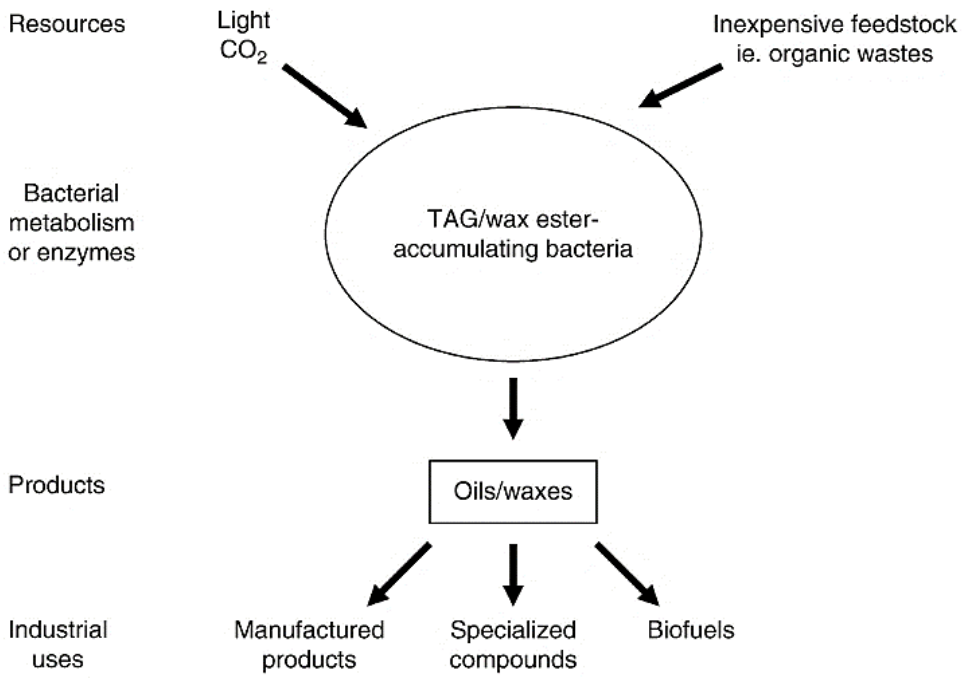

Figure I-24. Scheme of the potential use of microbial lipids for industrial purposes. Image from Alvarez, 2010.

1.2.1. Biodiesel production

Biomass fuels have been used throughout man's long history (different organic molecules or alcohols produced by the fermentation of diverse substances were employed for a variety of uses such as combustion, solvents, greases, cleaners or as basic chemicals for the emerging chemical industry) until a cheaper source was found in fossil oil. Currently, the concern on global warming (accelerated by release of fossil entombed CO_2 due to human activity), the rising prices for crude oil and increasing political instability in oil producing countries, has placed the use of bio-based alcohols as solvents or basic chemicals again under consideration (Antoni et al., 2007). Furthermore, the continued use of fossil fuels as a primary source of energy is now widely recognized to be unsustainable because of depleting resources and its accepted responsibility to climate change. Thus, fossil fuels as a source of energy should be replaced with renewable, clean energy sources to reduce carbon dioxide and greenhouse gas emissions. In addition, if the current trend of augment in the world energy needs continues at the same rhythm, the world will be confronted with an energy crisis (Ahmad et al., 2011). World energy consumption has steadily increased from 283 Quadrimillion Btu in 1980 to 552 Quadrimillion Btu in 2015 and is expected to reach 678 Quadrimillion Btu in 2030 (Fig I-25.A left). This increment is mainly due to the increment of energy consumption by China, India and other emergent countries (Fig I-25.A right). Besides, energy-related CO_2 emissions have increased more than 10 Gt in the last 24 years, being always mainly due to power generation (Fig I-25.B left). The augment is again more pronounced in these two countries, especially in China, who overtook the United States as the biggest CO_2 emitter in 2006 (Fig I-25.B right). It has been estimated that the global transportation energy use is expected to increase by an average of 1.8% per year from 2005 to 2035 and nearly all fossil fuel energy consumption in the transportation sector is from oil (97.6%) (Atabani et al., 2012).

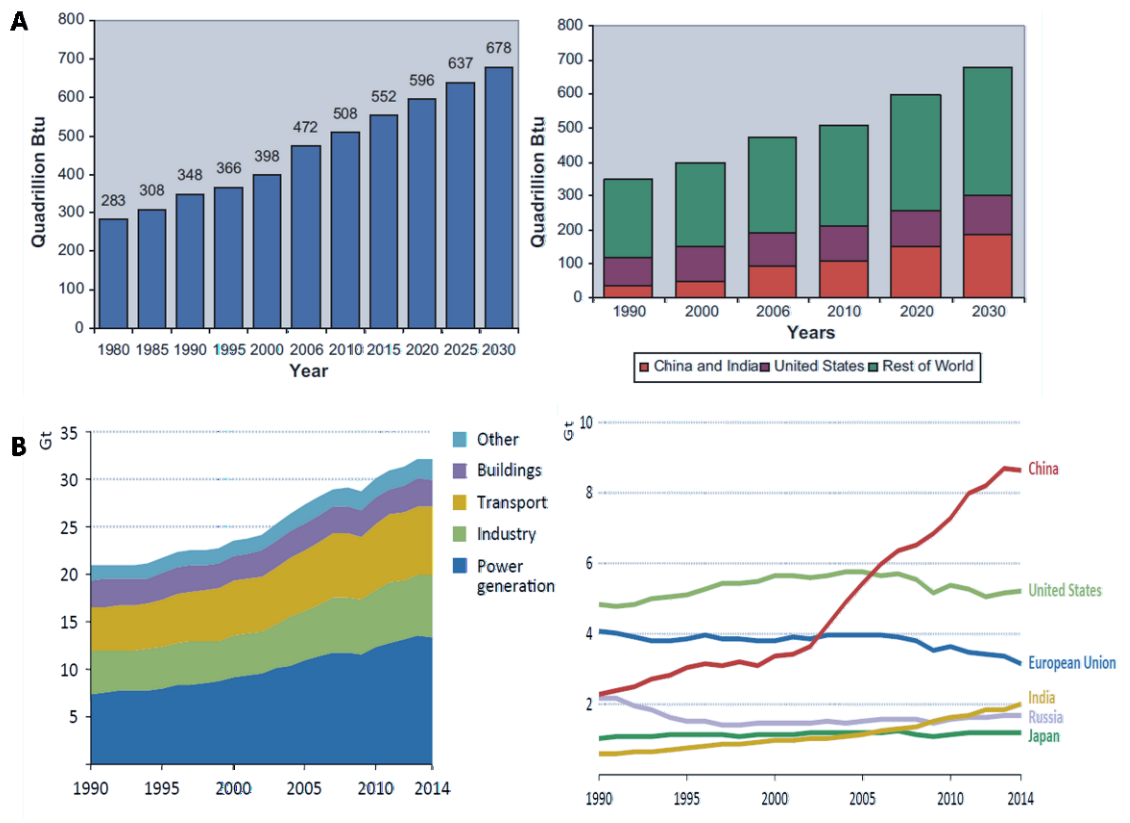

Figure I-25. A) Total world energy consumption (left) and energy use by region (right) from 1980 to the present and projected through 2030. Images from Ahmad et al. (2011); BTU: British Thermal Unit = 1055 joules. B) Global energy-related CO_2 emissions by sector (left) and region (right) between 1990 and 2014. Source: International Energy Agency (IEA), 2015. Gt: gigaton (millions of tonnes).
*"Other" includes agriculture, non-energy use (except petrochemical feedstock), oil and gas extraction and energy transformation.

In order to solve these important issues, strong research efforts are being made worldwide towards the development of technologies to allow substitution of fossil fuel with renewable energy.

Although there are diverse types of biofuels being investigated and developed (see Table I-5), bioethanol and biodiesel have been attracting great interest, especially in Europe and the United States (Lutterbach and Galvão, 2010) as they can be used in automobile engines mixed with petrol gasoline or petrol diesel, respectively. Moreover, the other biofuels have greater restrictions due to transportation or storage difficulties (e.g. for hydrogen, methane or propane), by production problems (e.g. for methanol) or by unfavourable chemical properties (e.g. the water solubility of methyl-*t*-butyl ether) (Uthoff et al., 2009). It is also worth noting that the risks of handling, transporting, and storing biodiesel are much lower than those associated with mineral diesel (Kegl et al., 2013).

Table I-5. List of selected biofuels with the required process for its production and the status of their use. Adapted from Antoni et al., 2007. ETBE, ethyl *tert*-butyl ether.

Biofuel	Process	Status
Biomethanol	Thermochemical/microbial	Pilot plant
Bioethanol	Microbial	Industrial
Biobutanol	Microbial	Pilot plant/industrial
ETBE	Chemical/microbial	Industrial
Biomethane/biogas	Microbial	Industrial
Biohydrogen	Microbial	Laboratory
Biodiesel	Physical/chemical (enzymatic)	Industrial (laboratory)

Biodiesel consists of fatty acid alkyl esters (FAAEs), including fatty acid methyl esters (FAMEs) and fatty acid ethyl esters (FAEEs). It can be obtained by chemical or enzymatically catalyzed transesterification of vegetable, animal or waste oils and fats using methanol or ethanol as acyl acceptors or esterification of FA to an alcohol (see Fig I-26; Duan et al., 2011). Although very diverse techniques have been studied by researchers, the most widely used large-scale method for chemical synthesis of biodiesel is an alkali-catalysed transesterification carried out with a reaction temperature near the boiling point of the alcohol (e.g. 60°C for methanol) and at a 6:1 molar ratio of alcohol to oil. The process is a sequence of three reversible reactions, in which the TAG molecule is converted step by step into DAG, MAG and glycerol (Al-Zuhair, 2007; Qiul et al., 2011; Ramos et al., 2009; Uthoff et al., 2009). The resulting product therefore can contain not only the desired alkyl ester product but also unreacted starting material (TAG), residual alcohol, and residual catalyst. Glycerol is formed as by-product (see Fig I-26.A) and separated from biodiesel in the production process, although traces can be found in the final biodiesel product. Since transesterification is a stepwise process, monoacylglycerol (MAG) and DAG formed as intermediates can also be found in biodiesel. Accordingly, these aspects have been addressed in biodiesel standards in addition to the physico-chemical properties, storage and handling issues (Knothe, 2006). FA chain length and saturation degree of the FAAE structures determine the properties of the bio-combustible: the calorific value, fluidity at low temperatures, oxidative stability and the nitrogen oxide emissions (Duan et al., 2011). Moreover, in spite of the high reaction rates of the established reaction process, it has a few limitations such as its sensitivity towards the presence of water and FFA in the feedstock oil. Consequently, although waste oils and fats are useable sources of biodiesel, their high contents of FFA and polymerization products as well as their high viscosity may require a cost-intensive treatment to clean such oils inevitable prior to transesterification. Besides, most of the currently produced biodiesel is obtained by means of reactions using methanol as alcohol moiety. This alcohol is cheap, easily available, highly reactive and more volatile than ethanol, but it is toxic, and its production is non-sustainable as it is synthesized from non-renewable sources such as coal

or natural gas, what prevent the resulting biodiesel from meeting the demands of a totally 'green' fuel production (Handke et al., 2011; Janßen and Steinbüchel, 2014a; Uthoff et al., 2009).

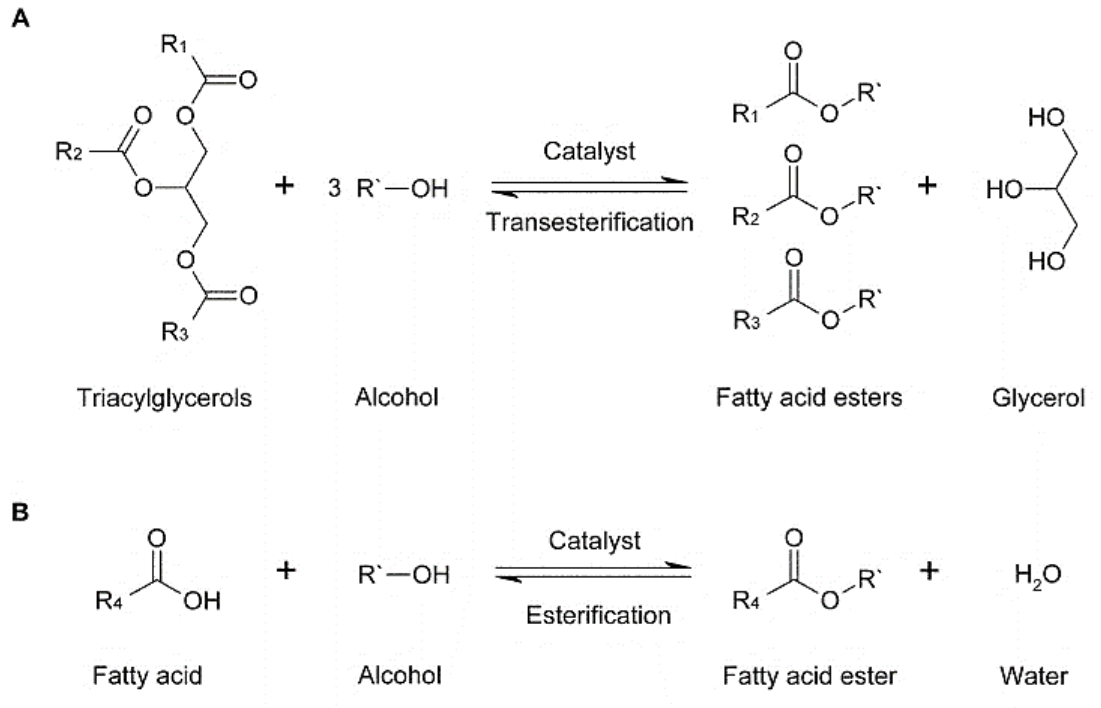

Figure I-26. Transesterification (A) and esterification (B) reactions carried out during biodiesel production from TAG or FFA, respectively, in presence of a chemical or biological catalyst and a short-chain alcohol. R1 to R4 represent the FA side-chains, whereas R' indicates the alcohol side-chains. Image from Uthoff et al., 2009.

Conventional biodiesel, made from edible oil, is also known as first generation biodiesel. Its production relies on feedstock oil whose origin depends much on the regional situation and on its availability. Currently, more than 95% of the world biodiesel is produced from edible oils such as rapeseed (84%), sunflower oil (13%), palm oil (1%), soybean oil and others (2%) (Atabani et al., 2012). It has been widely reported the possibility of a ''food versus fuel'' world crisis due to the employment of food crops to produce oil in the large-scale production of biodiesel, since that could bring a serious imbalance to the global food market. Furthermore, most studies conclude that the overall environmental impact of biodiesel is currently negative, due to the high requirement of arable land, which leads to monocultures and has an impact on biodiversity, adding the use of fertilizers for growing the oil plants to the energy and chemicals employed for the transesterification process (Kegl et al., 2013; Liu et al., 2014; Uthoff et al., 2009).

Production of biodiesel from non-edible oil crops has been extensively investigated over the past decade: second generation biodiesel feedstocks do not directly compete with food, and reduce the need for agricultural land since they can be grown in wastelands. Animal fats such as beef tallow, poultry fat and pork lard, waste oils and grease are also considered second generation feedstocks. However, they may not be abundant enough to replace much of our total transportation fuels (Atabani et al., 2012).

In addition to the need of developing an alternative more sustainable process for obtaining biodiesel, the optimization of a model to produce FAAEs with optimal characteristics for diesel engines has gained relevance. It is known that not every FA is similar for biodiesel production. Biodiesel properties such as ignition quality, heat of combustion, cold flow, oxidative stability, viscosity and lubricity are determined by the structure of its component fatty esters (Knothe, 2005). A highly efficient production of oil enriched in MUFA would be the doorway towards the production of a perfect biodiesel. High levels of PUFA in the oil source negatively impacts the oxidative stability of the biofuel and increase nitrogen oxide exhaust emissions, which do not suit diesel engines. On the other hand, biodiesel proceeding from TAGs just

constituted by SFA have good oxidative stability, but are not appropriate either due to its bad properties at low temperatures (because of the higher freezing point of its fatty esters) and its high cetane number (i.e. bad ignition properties) (Cao et al., 2014; Lu et al., 2009; Ramos et al., 2009). In that respect, plant-based oils are similar to one another in terms of FA composition, containing primarily C16 and C18 FA with varying degrees of unsaturation (Wahlen et al., 2013). Table I-3 show some examples of the FA composition of several commonly employed oil feedstocks. As we can observe, TAG resources derived from vegetal origin and animal fats often present a noteworthy content in PUFAs and SFAs, which is known to be a disadvantage for the production of biodiesel (Wahlen et al., 2013). Ultimately, a sustainable supply of TAGs is the main bottleneck for current biodiesel production (Duan et al., 2011).

All in all, the unsustainability of the traditional plant-based oil production model, considered until recently as a clean-burning alternative fuel has turned crucial the development of alternatives. New generation biodiesel feedstocks, which are derived from algal and microbial oil have emerged as one the most promising alternative renewable sources of lipid for use in biodiesel production (Ahmad et al., 2011; Janßen and Steinbüchel, 2014a). The FA composition of microbial oils can differ significatively from these derived from animals and vegetables and may contain uncommon FA that differ in both chain length and structure, as can be noticed in the examples presented in Table I-6. Studies examining the effect of branched or hydroxylated FA (especially typical of bacterial oil) could aid cold flow properties without negatively affecting emissions and cause biodiesel fuels to have higher viscosity. There are very few reports available about the performance of biodiesel from microbial oil, but data obtained to the moment indicate that they are an optimal alternative that can effectively displace both petroleum diesel and biodiesel produced from plant oils (Wahlen et al., 2013). Furthermore, to become cost and energy effective, these processes must utilize organisms that can be optimized to efficiently produce candidate fuels from a variety of feedstocks. Actually, the conversion and utilization of carbon substrate is a major issue in the process of microbial oil accumulation. It has been well recognized that many oleaginous microorganisms have the ability to convert multiple carbon sources into microbial oils. Therefore, the development of processes for microbial oil production that reduces carbon emissions by using CO_2 or utilizes diverse organic waste compounds and by-products from industries as substrates results really attractive and has been widely studied. Hence, both carbon-source utilization and biofuel synthesis processes need to be improved for a sustainable industrial production (Alvarez, 2016; Clomburg and Gonzalez, 2010; Janßen and Steinbüchel, 2014a; Xu et al., 2013).

Table I-6. Lipid accumulation and FA profiles of selected oils from plants, animals and oleaginous microorganisms. Recycled greases can be classified according to its FFA content: yellow greases (<15% (w/w), produced from heated animal fats and vegetable oils collected from commercial and industrial cooking business) and brown greases (>15%). Sources: Banković-Ilić et al. (2014); Cao et al. (2014); Thevenieau and Nicaud (2013); Wahlen et al. (2013); Xu et al. (2013).

		Fatty acid compostion (% w/w)							
	Lipid content	SFA			MUFA		PUFA		
	(% w/w)	C14:0	C16:0	C18:0	C16:1	C18:1	C18:2	C18:3	Other
Vegetable oils									
Rapeseed	45		5.51	2.17		58.33	19.89	9.13	C22:1 (4.59%)
Sunflower	45		7	5		19	68	1	
Soybean	20		11	4		23.4	53.2	7.8	C20:0 (0.2%); C20:1 (0.2%); C22:0 (0.3%)
Coconut	50	18	9	3		6	2		C4-C10 (15%); C12:0 (47%)
Olive	6kg/l		13	3	1	71	10	1	C20 (1%)
Palm	50	1	44	4		38	10	1	C4-C10 (1%); C12:0 (1%)
Animal fats									
Chicken fat		0.5	24	5.8	5.8	38.2	23.8	1.9	
Recycled greases									
Yellow grease		2.43	23.24	12.96	3.79	44.32	6.97	0.67	
Brown grease		1.66	22.83	12.54	3.13	42.36	12.09	0.82	
Microorganisms									
Microalgae									
Chlorella vulgaris			26.1	1.3		24.8	47.8		
Chaetoceros gracilis		10.3	26.8	0.5	29.9	3.7	2.2	4.1	C16:2 (6.9%); C16:3 (8.6%); C20:4 (0.6%); C20:5 (5.8%)
Schizochytrium linacinum	50-77	3-4	54-60	1-4					C22:5:2 (4–6%); C22:6 (29–35%)
Fungi									
Rhodotorula glutinis	72		37	3	1	47	8		
Cryptococcus curvatus			15.3	18	0.2	59.8	5.3	0.3	C20:0 (0.5%); C22:0 (0.2%); C24:0 (0.4%)
Yarrowia lipolytica	36		5.7	0.8	6	55.3	20.9		
Mortierella isabellina	50		29	3		55	3	3(n-6)	
Pythium ultimum	48		15	2		20	16	1	C4-C10 (7%); C20:1 (4%); C20:4 (15%); C20:5 (12%)
Aspergillus terreus		2	23			14	40		C21 n-3 (21%)
Claviceps purpurea			23	2		19	8		12-OH-C18:1 (42%)
Bacteria									
Rhodococcus opacus	19-80	1.9	33.9	3	8.9	23.9			C19:1 (0.6%); C18:0 OH (0.1%); C18:1 CH_3 (0.2%); C16:0 CH_3 (5.4%); C16:1 CH_3 (16.6%); C14:1 (0.2%); C14:0 CH_3 (0.2); SFA<C14 (0.3%)

As there are two mechanisms for producing biodiesel, different approaches have been addressed by researchers.

Transesterification of microbial oils

Recently, the development of processes to produce SCO as raw material for biodiesel production by subsequent transesterification (see Fig I-27) has triggered significant attention. However, it has not been still established an economic process for microbial production of TAGs at an industrial level.

On one hand, autotrophic organisms such as microalgae are photosynthetic microorganisms that efficiently convert sunlight, water and CO_2 to algal biomass, which represents a very promising feedstock with higher growth rates, productivity and oil content than first and second generation biodiesel feedstocks (Atabani et al., 2012).

On the other hand diverse heterotrophic oleaginous have emerged as potential SCO producers. These organisms accumulate lipids, mostly consisting of TAGs that form the storage fraction of the cell. Among heterotrophic microorganisms, oleaginous fungi, including both molds and yeasts, are increasingly being reported as good TAG producers (Rossi et al., 2011). Some bacterial species are also capable of synthesize those lipids. In general, bacterial species capable of synthesizing sufficient yields of those lipids require strict culture conditions, show low carbon source flexibilities, lack efficient genetic modification tools and in some cases poses safety concerns. For the achievement of an optimal process, genetic engineering could be used to obtain an industrially appropriate oleogenic microorganism to carry out a process like the one displayed in Fig I-27 (Thevenieau and Nicaud, 2013).

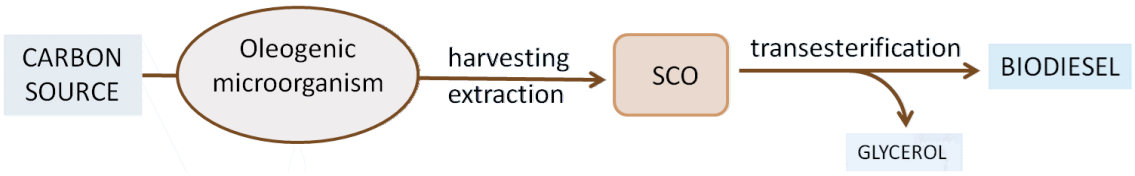

Figure I-27. Schematic representation of the production of biodiesel throughout oil-producing microorganisms.

Remarkably, one of the major differences between autotrophic and heterotrophic microorganisms is that the scaling up for autotrophic microalgaes is more complicated, since light is needed during the cultivation process. This leaded to heterotrophic microalgae. One interesting example is *Chlorella pototheco*ides, which although usually works as autotrophic microalgae, increases about four times its oil content when using organic carbon sources (Li et al., 2008).

In other respects, increasing environmental and economic concern about the residual glycerol originated as by-product in biodiesel production through transesterification has motivated some research. Its use as a substrate for microbial fermentation has been studied by several groups (Nwachukwu et al., 2013; Rossi et al., 2012).

A practical case of SCO generation for transesterification to yield biodiesel: production of TAG in Escherichia coli.

Although TAG can already be produced and accumulated naturally by many microbes, only the combination of a high TAG-accumulation with a fast growth could lead to a competitive process (Janßen and Steinbüchel, 2014a). The well-known model bacteria *E.coli* presents many genetic, technical, and biotechnological advantages over native oleaginous bacteria (Comba et al., 2014). Moreover, the feasibility of the production of diverse lipid compounds such as jojoba oil-like WEs , fatty acid butyl esters (FABEs), FAEEs and FA-derived hydrocarbons has been studied in this microorganism in the last years (Kalscheuer et al., 2006a, 2006b; Schirmer et al., 2010).

TAG production has also been reported in diverse *E.coli* strains by means of the over-expression of the enzyme WS/DGAT from other Gram-negative non-oleogenic microorganisms (Janßen and Steinbüchel, 2014b; Kalscheuer and Steinbüchel, 2003; Lin et al., 2013; Röttig et al., 2015; Rucker et al., 2013) or from Gram-positive actinomycetes (Arabolaza et al., 2008; Comba et al., 2013, 2014; Daniel et al., 2004; Lin et al., 2013; Moncalián et al., 2014). However, the yield of TAG production by recombinant *E.coli* is still low compared with those of natural oleaginous producers, especially considering the productivities reported for fed-batch fermentations (Comba et al., 2014).

Enzymatic esterification of intracellular FA

In nature, there are diverse organisms capable of synthesize different long- or medium-chain alcohol esters of FA. Nonetheless, an organism that naturally produces biodiesel compounds, i.e. short-alcohol esters of FA, is not known. The transesterification process required to obtain FAAE-based biodiesel from SCO and the subsequent purification steps are cost intensive and energy consuming, thereby reducing the possible energy yield and increasing the price. Hence, the construction of a recombinant microorganism capable of directly producing FAAES while feeding on different substrates (see Fig I-28) would mean an optimal step towards the development of a sustainable process for biodiesel production (Janßen and Steinbüchel, 2014a; Kalscheuer et al., 2007).

Due to its low toxicity for the production organism, compared to methanol or butanol, and the ease of its microbial production, ethanol is preferred as alcohol moiety. Howbeit, WS/DGAT activity has been reported to be considerably lower towards ethanol than towards the natural substrates such as DAG or long chain-length alcohols (Stöveken et al., 2005). With the purpose of overcoming this possible bottleneck the activity of five WS/DGAT enzymes from different organisms expressed in *S.cerevisiae* were tested towards FAEE production *in vitro*, using palmitoyl-CoA as the acyl donor and alcohols ranging from ethanol to octadecanol. In addition to confirm the general preference of WS/DGAT proteins for long-chain alcohols, the WS/DGAT from *M.hydrocarbonoclasticus* was suggested for further research (Janßen and Steinbüchel, 2014a; Shi et al., 2012).

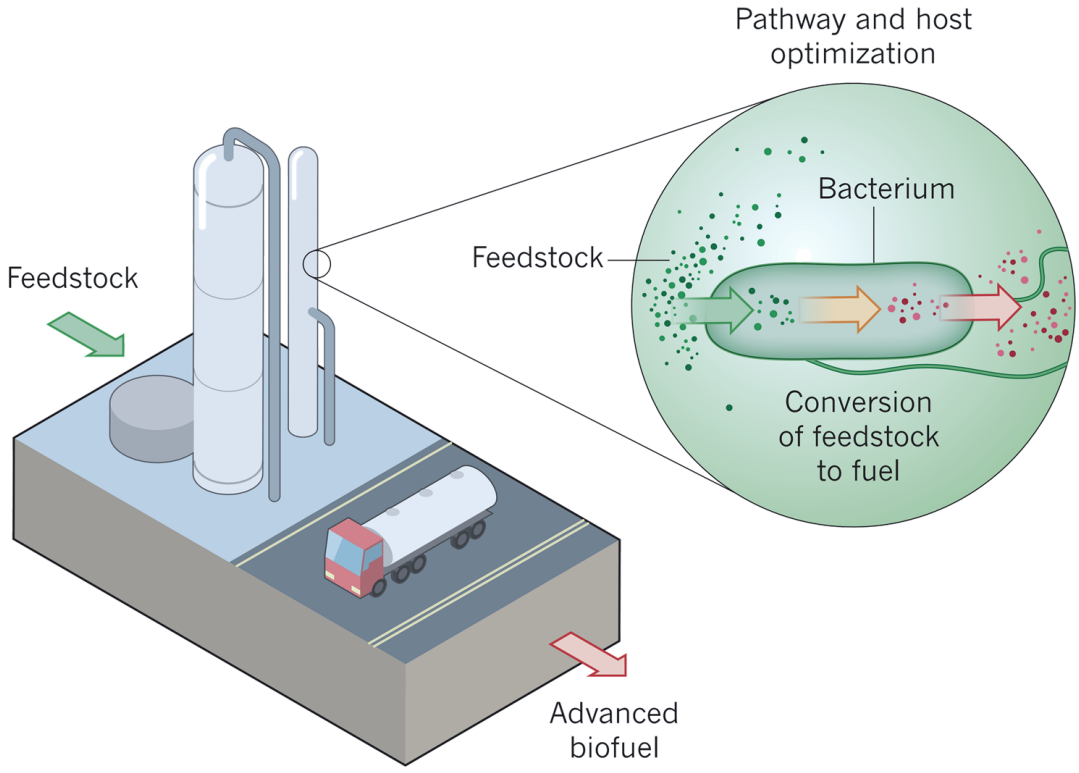

Figure I-28. Schematic representation of the production of advanced biofuels. Engineering of bacteria or yeast species through data- or synthetic-biology-driven techniques optimizes the production of advanced biofuelsfrom feedstocks (ideally non-food resources such as lignocellulosic biomass, greenhouse gases and algal biomass) (Peralta-Yahya et al., 2012).

Nonetheless, production of biodiesel directly *in vivo* has already been proved. The first study to report production of FAEE-based biodiesel in *E.coli* was performed by Kalscheuer and co-workers (2006a), who called the product *microdiesel*. Since ethanol levels naturally occurring in this bacteria under anaerobic conditions are not sufficient to support formation of significant amounts of this compound, they co-expressed the *Zymomonas mobilis* pyruvate decarboxylase (*pdc*) and alcohol dehydrogenase B (*adhB*) to produce ethanol, together with the *Acinetobacter baylyi* ADP1 WS/DGAT (*AtfA*), though a plasmid construction named "pMicrodiesel" in TOP10 *E.coli* cells (see Fig I-29.A). This construction allowed the production of esters consisting of ethanol and a FA in a culture media supplemented with 0.1 - 0.2% (w/v) of OA (see Fig I-29.B).

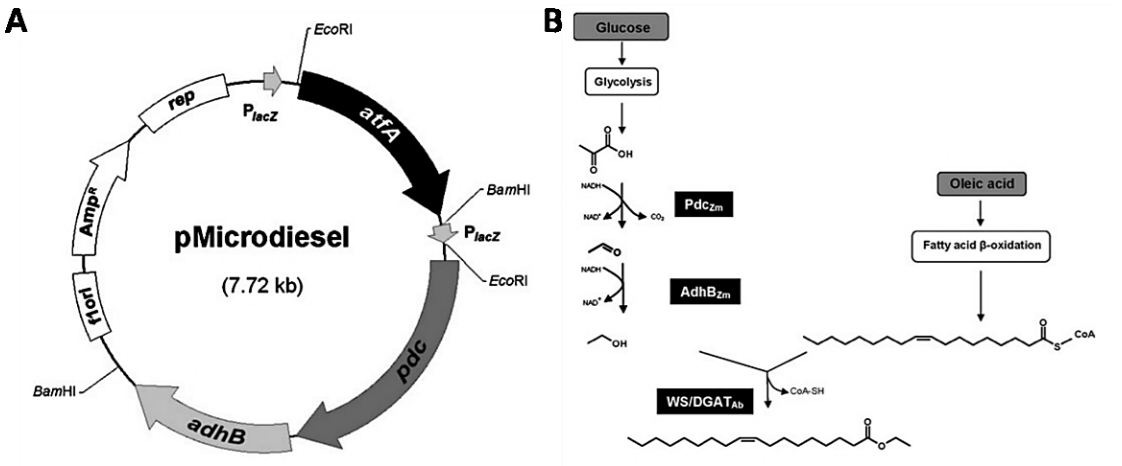

Figure I-29. A) Map of plasmid pMicrodiesel. Relevant characteristics: *rep*, origin of replication; Amp^R, ampicillin-resistance gene; P_{lacZ}, *lacZ* promoter; *pdc*, pyruvate decarboxylase gene from *Z.mobilis*; *adhB*, alcohol dehydrogenase gene from *Z.mobilis*; *atfA*, WS/DGAT gene from *A.baylyi* strain ADP1. B) Pathway of FAEE biosynthesis in recombinant *E coli* (Kalscheuer et al., 2006a).

The fed-batch process was further optimized by Elbahloul and Steinbüchel (2010). However, these two studies used OA that was externally added to the culture medium and did not rely on endogenously produced FA. To overcome that, Steen and colleagues (2010) combined the natural FA synthetic ability of *E.coli* with new biochemical reactions through synthetic biology. As the substrate of microbial FA biosynthesis is acyl-ACP while this of the WS/DGAT is predominantly acyl-CoA (although Kaiser and coworkers reported some exception in 2013), the over-expression of a thioesterase and an acyl-CoA ligase need to be combined with ethanol production and WS/DGAT expression. In addition to hydrolyze these acyl-ACPs, the activity of the thioesterase provokes a deregulation of FA biosynthesis due to the decrease of acyl-ACP feedback (which otherwise would inhibit FA biosynthesis). With further engineering of enzymes for the hydrolysis of hemicelullose and the metabolism of xilose they demonstrated the microbial production of FAAE-based biodiesel compounds directly from cellulosic plant biomass. Duan and co-workers optimized the process to produce microdiesel from glucose in 2011 and subsequent studies have been published about enhance of the FA production (Dellomonaco et al., 2011; Zhang et al., 2012). Nonetheless, the titers are still far too low for commercial purposes and further research is still required to achieve industrial yields.

1.2.2. High value fatty acids

Some LC-PUFA are both essential membrane components that confer fluidity, flexibility and selective permeability in higher eukaryotes for adaptation to special conditions like cold temperatures (by becoming part of the PLs, see Fig I-30) and are the precursors of many lipid-derived signalling molecules such as eicosanoids (prostaglandins, thromboxanes and leukotrienes), growth regulators and hormones. (Das, 2006; Huang et al., 2004; Sakuradani et al., 2009; Sijtsma and de Swaaf, 2004).

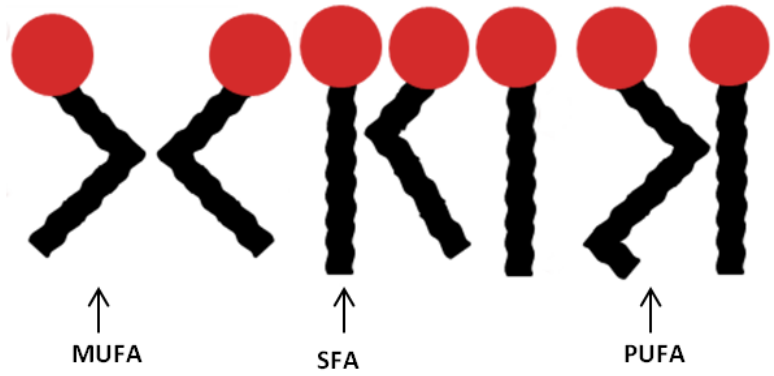

Figure I-30. Simulation of how the structural differences of the FA constituting the PLs may affect the physical and chemical behaviour of a membrane (Adapted from Valenzuela and Valenzuela, 2013). Abbreviations: SFA, saturated fatty acids; MUFA, mono-unsaturated fatty acids; PUFA, poly-unsaturated fatty acids.

In bacteria, PUFA incorporation into membrane PLs has been reported to be typically enhanced when cultivation temperature is decreased and/or pressure increased. This modulation is thought to maintain appropriate membrane physical structure (Allen and Bartlett, 2002; Russell and Nichols, 1999). Although growth at high pressure and low temperature does not depend upon PUFA synthesis (Allen et al., 1999), the enrichment of PUFA-producing strains in those environmental conditions has led to speculation that PUFA synthesis is an important adaptation for countering the effects of those extreme surroundings on membrane fluidity or phase (Allen and Bartlett, 2002).

In humans, LC-PUFAs have profound effects on health (Simopoulos, 2002a). Since they are essential constituents of all cell membranes and alter membrane fluidity, the behaviour of membrane-bound enzymes and receptors are influenced and determined by them. In several diseases such as obesity, hypertension, diabetes mellitus, coronary heart disease, alcoholism, schizophrenia, Alzheimer's disease, atherosclerosis, and cancer the metabolism of LC-PUFAs is altered. Thus, LC-PUFAs have significant clinical implications (Das, 2006). As an example, according to a FAO / WHO report from 2011 fish in the diet of women giving birth to children lowers the risk of suboptimal development of the brain and neural system compared to children of women not eating fish. Strong evidence also underlines how consumption of fish, and in particular oily fish, lowers the risk of death (36 percent reduction) caused by coronary heart diseases (CHD) - a particularly growing health problem in developing countries.

Moreover, ω-3 LC-PUFA such as EPA and DHA, are precursors of potent anti-inflammatory compounds, some due to a decrease of oxidative stress as assessed by lower reactive oxygen species (ROS) formation. As they are highly oxidable because of their double bounds, they could serve also as biomarkers of oxidative stress. However, a bimodal effect of those molecules, with antioxidant and pro-oxidant effects at low and high concentrations, respectively, has been also reported. At low supplementation levels DHA might be a target for free radicals but once oxidation reached a threshold level, the free radical chain reaction of lipid peroxidation might have exceeded the protection supplied by DHA, leading to pro-oxidant effects (Galano et al., 2015; Guichardant et al., 2015).

Human are incapable of synthesizing the simpler PUFAs of the two main families due to lack of the Δ12 and Δ15 (or n3) desaturases. Therefore, humans need to incorporate ω-3 and ω-6 LC-PUFAs from the diet. Consequently, LC-PUFAs belonging to these two groups are considered essential fatty acids (EFAs). However, humans can metabolize these two types of EFAs obtained from external sources to form longer and more unsaturated PUFAs through a series of desaturation and elongation steps (see Fig I-31). Normally, most of the EFAs in healthy subjects, are β-oxidized to provide energy and only a small portion of them (3.0% and 1.5%, respectively) are converted to longer LC-PUFAs (Das, 2006; Huang et al., 2004).

The diet on which human beings evolved and their genetic patterns were established were based in wild and free-range food animals with much higher contents of ω-3 PUFA than do the present-day commercial livestock. Hence, western diets have a very high ω-6 /ω-3 PUFA ratio (about 15-16-fold the ideal 1:1 relation) since currently, most consumed LC-PUFAs originate from plant oils and belong to the ω-6 group. Many reports have signalled that this unbalanced proportion promote the pathogenesis of many diseases, including cardiovascular disease, cancer, and inflammatory and autoimmune diseases, whereas increased levels of ω-3 LC-PUFA (a low ω-6/ ω-3 ratio) have been reported to show suppressive effects. In order to redress the FA balance generally seen as optimal for human health, an increase in ω-3 LC-PUFA consumption and a reduction in ω-6 LC-PUFAs is needed (Sijtsma and de Swaaf, 2004; Simopoulos, 2002a, 2002b; Wallis et al., 2002). Moreover, increasing clinical evidence has shown that dietary supplementation of LC-PUFAs, such as γ-linolenic acid (GLA, C18:3 ω-6), EPA and DHA can provide beneficial effects and downregulate inflammatory pathways that are known to be activated in chronic diseases such as rheumatoid arthritis, obesity, and type 2 diabetes, among others. At the same time, inclusion of adequate average requirements of AA and DHA in infant formula has been reported to be beneficial to the growth and visual development in pre-term infants. In the same way, the brain is particularly rich in LC-PUFAs, especially DHA, a ligand for the retinoid X receptor (Huang et al., 2004; Simopoulos, 2002a; Ward and Singh, 2005).

Summarizing, beneficial effects on human health have been related to the presence of adequate quantities of every LC-PUFA in the diet. While the average daily intake of EFAs, in general, is around 7-15g/day in Europe and USA (Das, 2006), a daily intake of 250-500 mg EPA plus DHA per day in adults is recommended by the Food and Agriculture Organization of the United Nations (2014) to get an optimal protection against CHD. For optimal brain development in children, the daily requirement is only 150 mg. The average daily intake of AA is estimated to be in the region of 100-200 mg/day, more than enough to account for the total daily production of eicosanoids, which is estimated to be about 1 mg/day (Das, 2006). These findings have prompted the use of these LC-PUFAs as supplements in the past few years, demand that cannot be sustainably met by fish-derived oils (Horrocks and Yeo, 1999; Huang et al., 2004; Kautharapu et al., 2013; Simopoulos, 2002a).

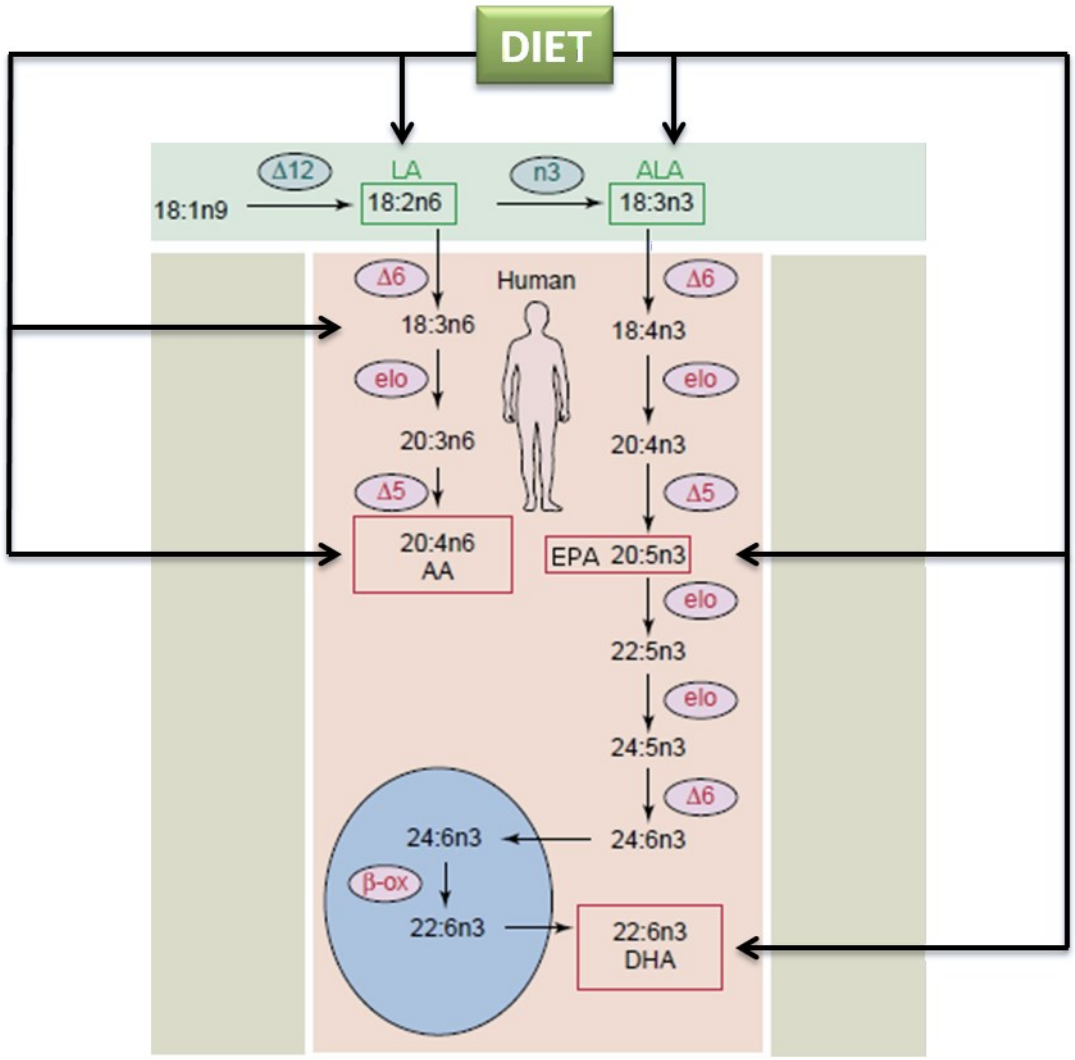

Figure I-31. Pathways for LC-PUFA synthesis in humans. The FA humans cannot synthesize are outside the pink box, where a schema of the reactions that might occur in this mammalians is shown. The synthesis of DHA is carried out in the peroxisome (blue) through the Sprecher pathway (see Fig I-8 and text above for further explanation). Abbreviations: LA, cis-linoleic acid; ALA, α-linoleic acid; AA, arachidonic acid; β-ox, β oxidation; EPA, eicosapentaenoic acid; DHA, docosahexaenoicacid; elo, FA elongase; EPA, eicosapentaenoic acid. Adapted from Wallis et al., 2002.

The most common sources of EFA in human diet, listed in Table I-7, have a vegetal or fish origin, although some have animal origin. However, the main sources of those important compounds definitely proceed from aquatic environments (Meyer et al., 2003). Nowadays, oils extracted from marine fish such as mackerel, herring, salmon and sardines are the richest sources of ω3-PUFAs, such as EPA and DHA (Hoffmann et al., 2008). Although marine fish and mammals have some capacity for de novo biosynthesis of ω-3 PUFAs, the majority of the PUFAs in their body originates from their diet: wild fish obtain their PUFAs by consuming PUFA-rich marine microorganisms (in particular phytoplankton, marine algae and fungi, which are thought to be the primary producers of ω-3 PUFAs in the marine food chain); and in the case of farmed fish, PUFAs source is fish oil supplied in their diet. The quality of the fish oil, however, is usteady and depends on several variables such as fish species, season and location of catching sites (Food and Agriculture Organization of the United Nations, 2014; Sijtsma and de Swaaf, 2004).

Table I-7. Sources of the main LC-PUFAs in human diet (Das, 2006).

LC-PUFA name	Main dietary sources
LA	Cereals, eggs, poultry, most vegetable oils, whole-grain breads, baked goods, and margarine. Sunflower, saffola, and corn oils. Human milk is rich in LA. Thus, breast fed babies get significant amounts.
ALA	Canola oil, flaxseed oil, linseed and rapeseed oils, walnuts, and leafy green vegetables. Human milk is rich in ALA.
GLA	Human milk contains 0.3-1.0% of its fat as GLA. Evening primrose oil, borage oil, black currant oil and hemp seed oil contain substantial amounts of GLA, also found in some fungal sources.
AA	Human milk contains modest amounts and cow's milk small amounts. Meat, egg yolks, some seaweeds, and some shrimps contain substantial amounts.
EPA and DHA	Currently, the major source of these two FA is marine fish. Human milk is rich in DHA and EPA as well.

The aquaculture sector consumed about 81 % of global fish-oil production in 2008 (see Fig I-32.A). In this year, the largest consumers of fish oil were salmons (36.6% total fish oil used in compound aquafeeds), followed by marine fishes (24.7%), trouts (16.9%), marine shrimps (12.9%), miscellaneous freshwater fishes (3.1%), freshwater crustaceans (2.6%), eels (2.6%) and milkfish (0.7%; see Fig I-32.B). In spite of the fast growing aquaculture production, this percentage seems to be declining owing to the increasing demand of fish oil for supplements and other food purposes. Actually this percentage decreased till a 75% in the year 2014. Farmed fish provides currently enough EPA plus DHA to cover the yearly needs of more than 2 billion people (see Fig I-32.B). Nonetheless, there are no good alternative sources of EPA and DHA for feeding cultured fish at present (FAO GLOBEFISH, 2011; Food and Agriculture Organization of the United Nations, 2014; Huang et al., 2004; Sijtsma and de Swaaf, 2004).

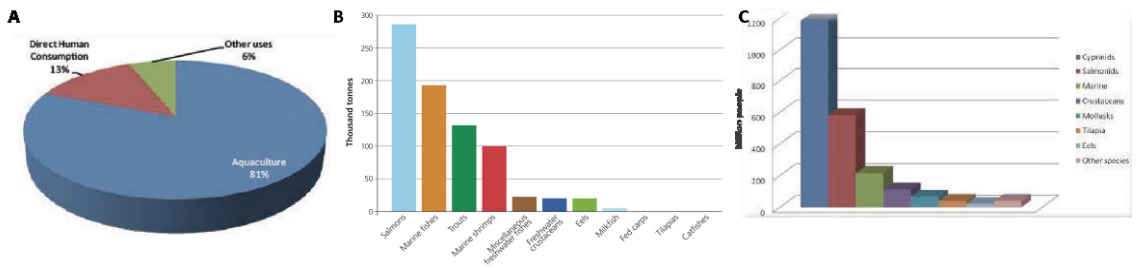

Figure I-32. A) Distribution of fish oil comsumption; B) Estimated global consumption of fish oil by major aquaculture species group; C) Estimated contribution of ω-3 PUFA oils by group of species and per million people. Sources: FAO GLOBEFISH, 2011; 2015.

In addition, the cost of production of those commercial fish oils is very high. The increasing cost involved in processing, refining, and stabilizing the fish oils, and the decreased yields due to over-fishing, have continuously driven up the cost of fish oils. Environmental contaminants in fish-derived oils arise as another important issue together with their concerns about possible socio-economic effects, such as the inability of local populations to continue to use fish as a food staple. In this situation, the development of new alternative, sustainable sources of those treasured molecules is urgently required (Hoffmann et al., 2008; Kautharapu et al., 2013). Currently, commercially available fish oils, sold in the form of gelatin capsules or oily preparations, contain around 20% to 30% EPA and DHA. Those oils can also be obtained

from single cell organisms like microalgae and fungi ω6-LC-PUFAs such as GLA can be found in plant oils. (Huang et al., 2004).

Oleaginous microorganisms can provide an economically feasible source of PUFAs, as long as most of the PUFAs occur in TAGs which is the preferred form to take lipids within the diet. Furthermore, microorganisms preferably contain one specific PUFA, rather than a mixture of various PUFAs. This gives the microbial oils an additional value as compared with fish oils, which contain mixtures of PUFAs. The first attempt to produce ω-3 PUFA for commercial purposes was the cultivation of phototrophic algae, but neither open ponds (due to contamination with bacteria and protozoa and to the high harvesting costs caused by low biomass concentrations) nor closed photobioreactors (scale-up of the process was too limited by the ability to effectively introduce enough light) were successful. Heterotrophic fermentation was then assessed. The company Omega Tech (later bought by Martek Biosciences Corporation, a component of Royal DSM NV) developed a commercial cultivation protocol to produce ω-3 PUFA: the heterotrophic fermentation of *Schizochytrium* sp., a traustrochytrid, i.e. an alga-like microorganism with very high DHA content, yet the additional presence of the ω-6 PUFA docosapentaenoic acid (DPA, C22:5n6) caused initial controversy and prevented its commercialization for human consume. Later on, they employed conventional stirred-tank fermenters to produce oils rich in DHA (with the marine dinoflagellate *Crypthecodinium cohnii*) and ARA (with fungi such as *Pythium insidiosum* or *Mortierella alpina*). Other heterotrophic algae used in aquaculture include *Ulkenia*, *Chlorella*, *Nitzschia*, *Cyclotella* and *Tetraselmis* species. Further research is ongoing on new LC-PUFA producers and improved protocols for meliorating the process have been researched in the last years (Arts et al., 2001; Ji et al., 2015; Sijtsma and de Swaaf, 2004; Ward and Singh, 2005). According to a report realized in 2012 by Packaged Facts (MarketResearch.com; USA), the global market for products fortified with EPA and DHA obtained from traditional sources (fish oils from anchovy or cod livers) or new sources (such as krill, squid or calamari and algae) reached $25.4 billion in 2011. The distribution by category and global region is shown in Fig I-33.

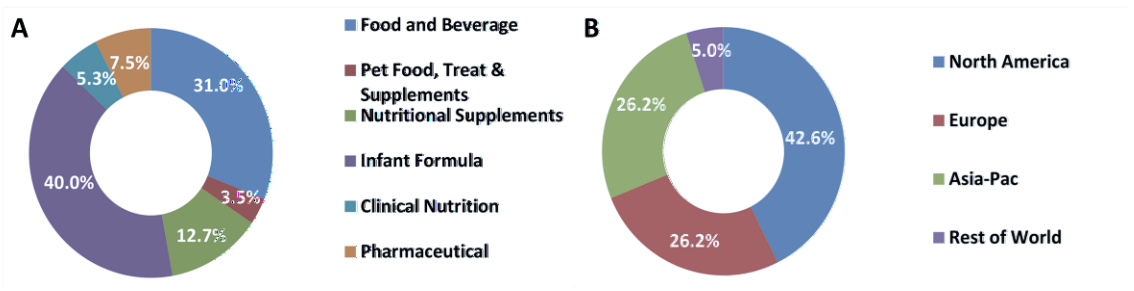

Figure I-33. Global market share of EPA/DHA ω-3 products by category (A) and global region (B) in 2011. Images from Packaged Facts, 2012.

On the other hand, genetic engineering may lead to the production of tailor-made oils at lower costs. Through PUFA pathway engineering, companies like DuPont or Microbia, Inc., among others, have developed optimized yeast and thraustochytrid strains for the production of those molecules (Kralovec et al., 2012). In addition, although some efforts are being made to manipulate the DNA of marine bacteria (Lauro et al., 2005; Stretton et al., 1998), research has been mainly focused in industrially appropriate well-known organisms like *E.coli*. The first report on the production of ω-3 LC-PUFAs in a genetically engineered *E.coli* was published by Yazawa in 1996, who cloned and expressed a 38 kbp DNA fragment from the genome of *Shewanella* sp strain SCRC-2378 and obtained a 4.5% of EPA within the total FA produced by the recombinant microorganism. Production of diverse ω-3 LC-PUFA in *E.coli* heterologously expressing *pfa* genes from different bacteria has been reported since then (see section I-1.1.1 for a detailed explanation on the role of *pfa* genes on PUFA biosynthesis).

Orikasa et al. (2006a) achieved a production of EPA of the 11.6% of the total FA by combining the *pfaA-D* gene cluster from the EPA-producing *Shewanella pneumatophori* SCRC-2738 and the *pfaE* from *M.marina* strain MP-1 and culturing the recombinant DH5α *E.coli* at 20°C for 36–48 hours. Later, Sugihara and colleages (2008) reported the obtaining of a 2% of DHA in DH5α *E.coli* cells co-expressing the *pfaA-D* gene cluster from *M.marina* MP-1and the PPTase from the EPA-producing bacterium *Photobacterium profundum* strain SS9 cultured at 15°C for 48 h.

A practical case of ω-3 LC-PUFA generation: Production of DHA in Escherichia coli.

Later, DHA was produced in recombinant DH5α *E.coli* cells co-expressing *pfaA-D* and *pfaE* genes from *M.marina* MP-1 (in different vectors) achieving a maximum of a 5.2% of the total FA in the bacteria when the cells were grown at 15°C for 96 hours (Orikasa et al., 2006b).

Finally a vector containing all *pfaA-E* genes from *M.marina* MP-1, genes required for DHA production, was created by Orikasa and co-workers (2009, see Fig I3.2).

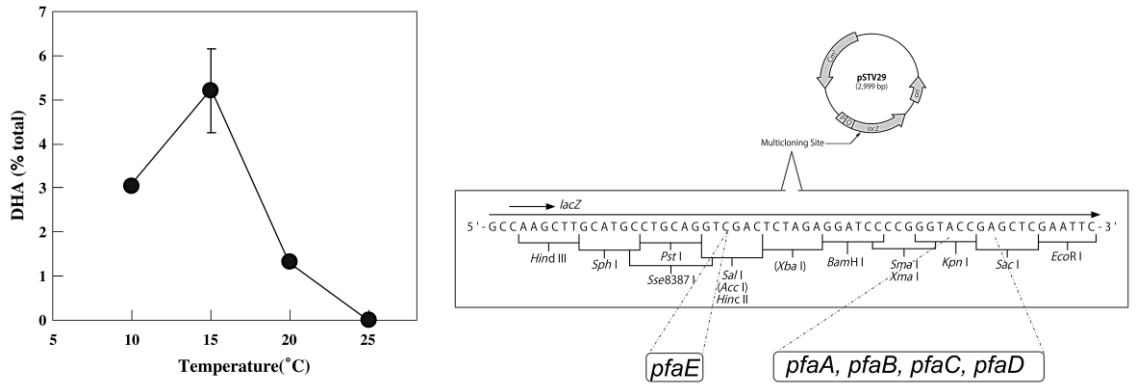

Figure I-34. A) Effects of growth temperature on the production of DHA in *E.coli* DH5a carrying a plasmid construction with the gene cluster *pfaA-E* from *M.marina* MP-1 and pET21a::*pfaE* with the DNA fragment for this gene from the same bacteria (Orikasa et al., 2006b). B) Outline of the plasmid pDHA4, a vector carrying all five *pfaA–E* genes responsible for DHA biosynthesis in *Moritella marina* MP-1 (Orikasa et al., 2009).

Gathering the current knowledge on bacterial lipid metabolism related to TAGs and LC-PUFA and taking into account this state of the art in the commercial production of value-added oils, in this thesis work we decided to study neutral lipids as well as Pfa for the bacterial production of TAGs with or without LC-PUFA.

AIMS AND SCOPE

2. Aims and Scope

TAG demand for diverse applications is continuously growing in our society. However, its current obtention from either fossil, animal or vegetal resources is not sustainable. Thus, the establishment of alternative sustainable processes for biodiesel production and for the generation of specific TAGs essential for human health, is urgently required. This situation motivated our research on metabolic pathways leading to TAG accumulation in microorganisms, from naturally TAG-producing to genetically engineered bacteria.

With the general purpose of widening the scientific knowledge on the reaction catalysed by the bifunctional enzymes WS/DGAT, reported to be the responsible of the last step in the TAG biosynthetic pathway in bacteria, in the present work we focused on two specific objectives:

1) Study the process carried out in genetically engineered *E.coli* bacteria expressing WS/DGAT enzymes. We are mainly interested in the effects of heterologous expression of the protein tDGAT (WS/DGAT from *T.curvata*) paying special attention to the FA composition of the compounds produced by the recombinant strain. Moreover, we intend to characterize and improve the production rate of the TAG biosynthetic process.

2) Improvement of the production of PUFA in a bacteria suitable for industrial purposes such as *E.coli* by means of the overexpression of different desaturase enzymes in this bacteria or the combination of the biosynthetic pathways for TAG and DHA (a ω-3 PUFA) in the same strain.

MATERIALS AND METHODS

"We must have perseverance and above all confidence in ourselves."

Maria Salomea Skłodowska-Curie

3. Materials and methods

3.1. Bacterial strains

The strains employed in this work are summarized in Table M-1. *Escherichia coli* MG1652, DH5α and BW28733 are derivatives of *E.coli* K-12. *E.coli* C41(DE3) is a derivative of *E.coli* BL21(DE3).

Table M-1. Bacterial strains used in this work

Strain	Genotype	Reference
***Rhodococcus opacus* PD630**	Wild type	DSM 44193 (Alvarez et al., 1996)
***Escherichia coli* MG1655**	F-, lambda-, rph-1	ATCC 47076 (Guyer et al., 1981)
***E.coli* DH5α**	Nx^R; F^-, endA1, glnV44 thi-1, recA1, relA1, gyrA96, deoR nupG Φ80dlacZΔM15, Δ(*lacZYA-argF*)U169, hsdR17(r_K^- m_K^+), λ–	(Grant et al., 1990)
***E.coli* BL21 (DE3) pLysS**	F^-, *ompT, hsdS*$^-$, gal, pLysS(cm^R)	(Studier and Moffatt, 1986)
***E.coli* C41 (DE3)**	$F^–$, *ompT, galλ, dcm,* $hsdS_B$(r_B-m_B-) (DE3)	(Miroux and Walker, 1996)
***E.coli* BW28733**	$lacI^q$, rrnB3, ΔlacZ4787, hsdR514, Δ(araBAD)567, Δ(*rhaBAD*)568 Δ(*araFGH*), Φ(*ΔaraEp* P_{CP8}-araE)	(Khlebnikov et al., 2001)
***E.coli* Keio Collection**	Km^R, set of single-gene knockout mutants of *E.coli* K-12	(Baba et al., 2006)
***Moritella marina* strain MP-1**	Wild type	ATCC 15381 (Felter et al., 1969)

3.2. Plasmids

Table M-2. Vectors and plasmid constructions used in this work

Plasmid	Description	Phenotype	Reference
pET29c	Expression vector.	Km^R	(Novagen)
pET3a	Expression vector.	Ap^R	(Rosenberg et al., 1987; Novagen)
pBAD33	Expression vector.	Cm^R	(Guzman et al., 1995)
pSU711	IncW R388 deletion-derivated plasmid without *oriT.*	Tc^R	(Francia et al., 1993)
pDHA	Plasmid pSTV29 carrying *pfaA, B, C, D, E* from *Moritella marina* for DHA production.	Cm^R	(Orikasa et al., 2009); Provided by Dr. Okuyama
pB*tDGAT*	Plasmid pBAD33 carrying the arabinose BAD promoter and the gen for the WS/DGAT from *Thermomonospora curvata.*	Cm^R	(Villa Torrecilla, 2012, PhD Thesis)
pBoR*tDGAT*	Plasmid pBAD33 carrying the arabinose BAD promoter, the *oriT* of the plasmid R388 and the gen for the WS/DGAT from *T.curvata.*	Cm^R	This work
pE*mbDGAT2*	Plasmid pET29c carrying the T7 promoter and the gen for the WS/DGAT from *Marinobacter hydrocarbonoclasticus* VT8.	Km^R	(Villa Torrecilla, 2012, PhD Thesis)
pE*abDGAT1*	Plasmid pET29c carrying the T7 promoter and the gen for the WS/DGAT from *Alcanivorax borkumensis.*	Km^R	(Villa Torrecilla, 2012, PhD Thesis)
pE*tDGAT*	Plasmid pET29c carrying the T7 promoter and the gen for the WS/DGAT from *T.curvata.*	Km^R	(Villa Torrecilla, 2012, PhD Thesis)
pEΔ9des	Plasmid pET3a carrying the T7 promoter and the gen for the Δ9desaturase from *Anabaena variabilis*	Ap^R	This work
pEΔ12des	Plasmid pET3a carrying the T7 promoter and the gen for the Δ12desaturase from from *A.variabilis.*	Ap^R	This work
pEΔ15des	Plasmid pET3a carrying the T7 promoter and the gen for the Δ15desaturase from *A.variabilis.*	Ap^R	This work

3.3. Oligonucleotides

Table M-3. Nucleotide sequences of some of the primers used in this work

Primer name	Nucleotide sequence (5' -->3')	Target DNA fragment
T7 universal primer	TAATACGACTCACTATAGGG	DNA inserts between T7 primers in pET plasmid constructions.
pT7 universal primer	GCTAGTTATTGCTCAGCGG	
pBAD_mcs1	CTGTTTCTCCATACCCGTT	DNA inserts in the multi-cloning site of pBAD33 plasmid constructions.
pBAD_mcs2	CTCATCCGCCAAAACAC	
16S universal primer 337F	GACTCCTACGGGAGGCWGCAG	16S ribosomal RNA
16S universal primer 1100R	GGGTTGCGCTCGTTG	
16S universal primer 805R	GACTACCAGGGTATCTAATC	
*tDGAT*_fragment_f	CATGCACCGCTGCTACGTGC	Fragment of the *tDGAT* gene from *T.curvata*
*tDGAT*_fragment_r	GCATTTGGCGAACTGCCGC	
mm_*pfaE*_f	GATAGCGAATCCCCCACTCC	Fragment of the *pfaE* gene from *M.marina*
mm_*pfaE*_r	ACAGCCAATGACGCCAAATG	

3.4. Microbiology techniques

3.4.1. Growth conditions and selection media

Rhodococcus opacus.

Rhodococcus opacus was grown in rich medium (RM) such as Luria-Bertani broth medium (LB, 1% BactoTryptone, 0.5% yeast extract, 0.5% NaCl; Pronadisa, Spain) or Streptomyces media (Fluka, Germany) in aerobic conditions at 30°C with shaking for 48-72 hours to obtain cells in stationary phase. In order to induce lipid production by controlling Nitrogen availability (Alvarez et al., 1996; Villa Torrecilla, 2012) minimal media (MM: M9 salts without Nitrogen source, $MgSO_4$ 2mM and $CaCl_2$ 0.1mM and carbon source 30 g/l -generally sodium gluconate-) with a reduced amount of Nitrogen source (NH_4Cl 0.1 g/L) was employed.

E. coli *and derivatives*

Liquid cultures of this model microorganism were prepared in flasks containing ¼ volume LB medium (Pronadisa, Spain). For solid media culture LA was employed (LB medium supplemented with 1.5 % (w/v) agar (Pronadisa, Spain). To test lipid production, a minimal medium was used in some experiments, containing M9 salts ($MgSO_4$ 2mM and $CaCl_2$ 0.1mM with D-glucose, sodium gluconate or arabinose 1%) supplemented with defined concentrations of NH_4Cl as source of Nitrogen (0.05 g/L and 1 g/L). All media was sterilized by autoclaving at 120°C for 20 minutes. The different components of the minimal media were sterilized separately through either autoclaving or membrane-filtering to avoid precipitation.

Selective media included antibiotics at the following concentrations:

- Ampicillin (Ap; Apollo Scientific, USA), 100 µg/mL;
- Chloramphenicol (Cm; Sigma Aldrich, USA), 25 µg/mL;
- Kanamycin sulphate (Km; Sigma Aldrich, USA), 50 µg/mL;
- Nalidixic acid (Nx; Sigma Aldrich, USA), 20 µg/mL;
- Tetracycline (Tc; Apollo Scientific, USA), 10 µg/mL;
- Trimethoprim (Tp, Apollo Scientific, USA),20 µg/mL.;
- Streptomycin sulphate (Sm; Apollo Scientific, USA), 300 µg/mL;
- Spectinomycin (Sp; Apollo Scientific, USA), 10 µg/mL;
- Erythromycin (Em; Apollo Scientific, USA), 200 µg/mL;
- Rifampicin (Rf; Apollo Scientific, USA), 100 µg/mL.

All antibiotic stocks were prepared at a concentration 1000-fold higher than the indicated final concentration. Trimethoprim and rifampicin stocks solutions were dissolved in DMSO, chloramphenicol in ethanol, tetracycline in ethanol/water 50 % v/v and the rest in sterile distilled water.

When needed, media was supplemented with glucose, arabinose, IPTG or Red Nile as described in the results section.

To preserve *E.coli* strains, stationary phase cultures were centrifuged and resuspended in peptone-glycerol [peptone 1.5 % (w/v), glycerol 50% (v/v)]. Strains were stored at -20 and -70°C. To confirm the antibiotic resistance patterns, the agar disk diffusion method was performed in LA media to carry out susceptibility testing for resistance against panels of 7 antibiotics, including representatives of the most common antibiotic resistance traits shown. The antibiotics disks were supplied by the company Bio-Rad (USA).

Marine bacteria

Moritella marina MP1 was grown in Marine Medium 2216 (Difco) at 12°C with shaking. For growing on solid media, 15g/L of agar (Pronadisa) was added to the Marine Medium before autoclaving. Duplicates of the strain were kept at -20 and -70°C.

3.4.2. Growth curves.

For estimation of cell density a Shimadzu UV-1630 spectrophotometer was employed to read the OD_{600nm} of 1mL sample.

For growing strains from the Keio collection, microtiter plates (Deltalab) with 1:100 dilutions were made in 200 µl/well fresh LB with the corresponding antibiotic. The 96-well plate was incubated overnight in an automatic fluorimeter (Victor3, PerkinElmer) with shaking at 30 or 37°C and automatic addition of distilled water to maintain a constant volume despite evaporation. OD_{600nm} reads were made every 20 minutes. 8-12 wells, each containing 200 µl fresh LB, were used as control in every experiment.

Similar experiments were carried out with strains from the Keio collection carrying the pBoRtDGAT plasmid construction in microtiter plates, but 1:40 dilutions were made in minimal media with 0.4% glycerol and 1 g/l NH_4Cl. At an OD_{600nm} of approximately 0.3, a stock solution of arabinose was manually added to every well to a final concentration of 0.001%. Simultaneously Red Nile stock solution was added to specific wells to a final concentration of 0.5 µg/mL and both the OD_{600nm} and the fluorescence were measured every 20 minutes. 8 wells were employed as control by using fresh minimal media.

3.4.3. Transformation

In this work, electroporation was the method most often employed to introduce plasmid DNA in *E.coli*.

Preparation of *E. coli* competent cells and electroporation.

For preparation of electro-competent cells, saturated, overnight cultures of the required *E.coli* strain were diluted 20-fold in LB medium, grown to an OD_{600nm} of 0.6 and chilled on ice for 30 min. Cells were then centrifuged at 4,000 rpm for 10 min at 4°C and washed with 1 volume pre-cooled sterile distilled water (Millipore Corporation). This was repeated twice. After the third centrifugation in the same conditions, the pellet was resuspended in ice-cold 10% glycerol and centrifuged again (4,000 rpm, 4°C, 10 min). Aliquots of 60 µl were frozen in a dry ice-ethanol bath and stored at -70 °C until usage.

The DNA to be transformed by electroporation has to be desalted to prevent electrical arcing. Samples were dialyzed in 0.05 µm pore-size nitrocellulose filters (Millipore GS) in a Petri dish filled with MilliQ distilled water for 25 minutes. DNA was then recovered from this filter and 1-10 ng were added to one previously thawed on ice aliquot of electroporation-competent cells. The mixture was transferred to an ice-cold 0.2-cm electroporation cuvette (Gene Pulser, Bio-Rad, USA) and subjected to an electric pulse (2.5 kV/cm 25µF and 200 Ω) in a MicropulserTMgene pulser (Bio-Rad, USA). Sterile fresh LB medium (1 mL) was added immediately after electroporation. Cells were incubated at 37°C for 2 hours with shaking to allow antibiotic resistance gene expression, and 100 µl were plated on antibiotic containing solid media.

For the transformation of *E.coli* with two plasmids, two subsequent transformations were performed, starting with the larger DNA plasmid.

3.4.4. Conjugation procedures

A method for bacterial transformation of large numbers of samples simultaneously was employed to facilitate a subsequent high-throughput analysis.

High-throughput conjugation (HTC) procedure

This method, which allows to analyse many samples at once, was performed adapting the protocol described by Fernandez-Lopez and co-workers (2005). Matings were performed in liquid media. *E.coli* DH5α carrying the conjugative but not transmissible plasmid pSU711 (Francia et al., 1993) and the mobilizable pBoRtDGAT was used as donor strain and 75 selected *E.coli* strains from the Keio collection were employed as recipient strains in order to identify genes that are critical to lipid accumulation.

Bacterial liquid cultures of both the donor (in flasks with LB supplemented with tetracycline and chloramphenicol) and the recipient strains (in 96-well microtiter plates, Deltalab, with 200 µl LB medium supplemented with kanamycin in each well) were grown to stationary phase. Then 150 µl of the donor culture were added to each well of the microtiter plate, and the plate was incubated at 37°C with slight shaking for 1 hour to leave conjugation to proceed. Then, microtiter cultures were centrifuged at 10°C and 3000rpm for 6 min and the supernatants were discarded to eliminate the antibiotics. 40 µl of sterile fresh LB were added to every well to resuspend the pellets and the conjugation mixtures were added to its corresponding well in a previously prepared selective solid media microtiter plate (with 250 µl LA supplemented with kanamycin and chloramphenicol -for selecting transconjugants-).

Each transconjugant was stored at -70°C after culturing in a microtiter plate with LB supplemented with chloramphenicol until stationary phase and then adding 20 % glycerol to each well.

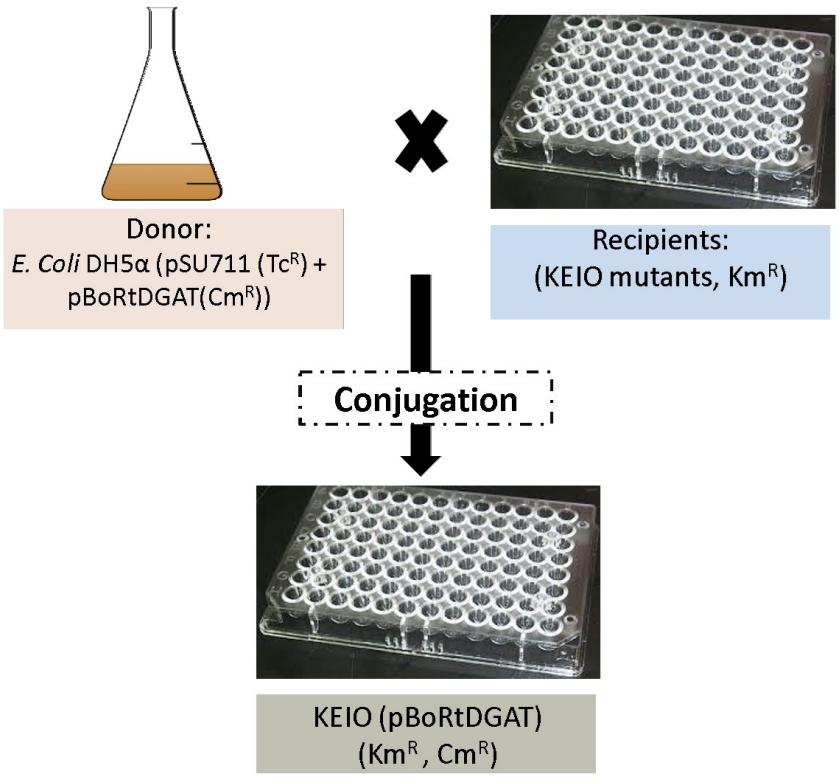

Figure M-1. HTC method.

3.5. Molecular biology techniques

General procedures for molecular biology were performed as described in Sambrook and Russell (2001).

3.5.1. DNA manipulation

Extraction and purification.

Different kits were used depending on the starting material and the applications of the purified product, following manufactures's recommendations.

Plasmid DNA was extracted using Gene JET Plasmid Miniprep Kit (Thermo Scientific) and genomic DNA was isolated with Instagene matrix (Bio-Rad, USA). PCR products were purified with the kit GenElute PCR Clean-Up (Sigma-Aldrich, USA) or extracted from electrophoretic gels by employing the kit GenElute Gel Extraction (Sigma-Aldrich, USA).

The DNA concentration was determined by measuring the absorbance at 260 nm in a Nano-Drop ND-1000 spectrophotometer.

Amplification: polymerase chain reaction (PCR)

For the amplification of DNA fragments subsequently used for cloning, the high fidelity enzymes Vent DNA polymerase (BioLabs, UK) or Phusion pol enzyme (ThermoScientific, USA) were employed and PCR reactions were set up to final volumes of 50 µl. For other amplification reactions, such as colony analysis, the Biotaq polymerase (Bioline, USA) was used, with final volumes of 25 µl. In every case PCR

mixtures contained both primers at a final concentration of 10 pmol/µl, 1 to 10 pg of template DNA, 200 µM of the deoxinucleotide (dNTPs) mixture and 1X of the commercial polymerase buffer that included $MgSO_4$ 20 mM, 1U of DNA polymerase and distilled water. All oligonucleotides were purchased from Sigma-Genosys (Sigma-Aldrich, USA). The following program was set in the thermocycler: 5-10 min of initial denaturation at 95°C; 25 cycles of amplification, including steps of denaturalization for 30 seconds at 94°C, annealing for 30 seconds at the corresponding annealing temperature (depending on the primers) and elongation for the appropriate time (1 minute for each Kb of target DNA to be amplified) at 72°C; and a last step of 10 min of final elongation at 72°C. After completion of the reaction, samples were maintained at 4°C for short-term conservation.

Enzyme digestion

Restriction enzymes were purchased from different suppliers such as Fermentas (Canada), NEB (USA) or Takara (Japan). Reactions were performed following the manufacturer's indications, generally in 20 µl as final volume and incubation at 37°C for 2 hours. Inactivation was carried out according to the specific recommendations of each enzyme, usually by incubation at 65 or 80°C during 10 minutes.

When several enzymes were required for the same DNA, either the double digestion instructions from the manufacturer were followed or both digestions were carried out with DNA purification in between.

Dephosphorylation

In order to improve efficiency in cloning procedures by decreasing the appearance of false positives, vectors were dephosphorylated to avoid vector religation. According to manufacturer's instructions, 1 U of Shrimp Alkaline Phosphatase (Thermo Scientific) was added to purified vector DNA after vector restriction digestion together with commercial buffer 2X and MiliQ water to reach a volume of 100 µl. Samples were incubated for 1 hour at 37°C. Inactivation was carried out by incubation at 65°C during 10 min.

Ligation

Insert fragments were obtained by restriction digestion of PCR amplification products obtained with primers incorporating the adequate restriction sites for ligation into the same sites of the (previously digested and dephosphorylated) plasmid vector. A minimum of 5:1 (insert/vector) molar ratio was used. Ligation reaction was generally performed with 0.5-10 ng of DNA and 2.5 U of T4 DNA ligase (Fermentas) in a final volume of 20 µl. It was incubated overnight at 22°C. For each ligation, the same reaction without insert DNA was used as negative control, adding water to reach the final volume. Inactivation was carried out by incubation at 65°C during 10 minutes.

Electrophoresis

DNA was analysed through agarose gel electrophoresis. Agarose was dissolved in TBE (Tris-HCl 45 mM, boric acid 45 mM, EDTA 0.5 mM and pH 8.2) to a final concentration of 0.7-1% (w/v), depending on the size of the DNA fragments to be resolved. For staining, 0.05 mg/mL SYBR Safe (Invitrogene, Life Technologies, USA) were added to the agarose solution before preparing the gel. Loading buffer (bromophenol blue 0.25 % (w/v), glycerol 30 % (w/v) in TBE 0.5x] was added to DNA samples in a 5:1 ratio: blue dye. Hyperladder I (Bio-labs, UK) or o 100 bp (Amersham), was used as molecular weight marker. A horizontal electrophoretic running system (Bio-Rad, USA) with TBE buffer 0.5 X was employed, with a constant voltage of 80-120V. Finally, a Quantity One software (BioRad, USA) served to visualize and analyse images taken by a Gel Doc 2000 (BioRad, USA) UV system.

Sequencing

The DNA sequence of all cloned PCR fragments was determined by MACROGEN Inc. "DNA Sequencing Service" (Amsterdam, The Netherlands). Samples consisted of 500 ng template DNA, 25 pmol polynucleotides and MiliQ water to a final volume of 10 µl.

High-throughput sequencing

Plasmid pDHA4 provided by Dr. Okuyama (Hokkaido University, Japan) was sequenced using high-throughput techniques. The library was prepared for 100 pb paired-end sequencing in the IBBTEC massive sequencing facility and sequenced in a HiSeq2000 sequencer (Illumina) in Health in Code (La Coruña, Spain).

3.5.2. Protein manipulation

Electrophoresis

Sodium dodecyl sulphate polyacrylamide gel electrophoresis (SDS-PAGE) were used for separation and visualisation of proteins (Sambrook and Russell, 2001). 8, 10 or 12 % polyacrylamide gels containing 0.1% SDS were made with acrylamide : bisacrylamide 29:1 purchased from Bio-Rad (USA). Samples for whole cell extract protein analysis were prepared by adding 150 µL of loading buffer (Tris-Cl 50 mM pH 6.8; SDS 2% (w/v); bromophenol blue 0.1% (w/v); glycerol 10% (v/v) and 100 mM β-mercaptoethanol) to 1 mL-culture-pellets. After 5 minutes of incubation at 100°C, 10 or 15 µl of every sample were loaded onto the gel. Either Low Range Protein Marker (Bio-Rad, USA) or SigmaMarker Low Range (Sigma-Aldrich, USA) were also loaded as molecular weight markers. Electrophoresis was carried out using a protein electrophoresis system from Bio-Rad (USA). The electrophoretic run was performed at 170 V and 330 mA for 50 minutes in SDS-PAGE running buffer (Tris 25 mM, glycine 192 mM, SDS 0.1 % (w/v). After the run, gels were stained by incubation in staining solution (Coomassie Brilliant Blue R-250 0.1% (Merck, Germany) in methanol/acetic acid (5:1, v/v) for 20 min at room temperature with slight shaking. For destaining, the gel was incubated for at least 3 hours in a solution of methanol/acetic acid/deionized water (4:1:5, v/v/v).

Protein quantification

Determination of protein concentration was carried out through different spectroscopic methods depending of the accuracy of the measurement needed.

Bradford method

The Bradford dye assay (Bradford, 1976) was the most accurate method used to determine protein concentration. This method is based on the equilibrium between two forms of Coomassie Brilliant Blue G dye in phosphoric acid and methanol (Protein assay, Bio-Rad, USA). Under strong acidic conditions, the dye is most stable as a doubly-protonated red form. Upon binding to protein it is most stable as an unprotonated, blue form. This effect can be detected by changes in the absorbance at 595 nm. The response is dependent on the protein concentration and is linear, so a convenient standard curve can be made using bovine serum albumin (BSA, Sigma-Aldrich) solutions of known concentration. 100 µl of sample were added to 900 µl of a 1:3.5 dilution of the reactive in distilled water. After 10 minutes, the absorbance at 595 nm was measured on a Shimadzu UV-1630 spectrophotometer, and its value plotted against the standard curve.

Absorbance at 280 nm

When a less precise quantification was required, absorbance at 280 nm was measured either with a Nano-drop or a conventional spectrophotometer. The extinction coefficient of the protein was used to calculate the concentration.

Western-blot

In order to confirm the over-expression of the His-tagged WS/DGAT protein (Ma2) for the realization of subsequent experiments, a western blot analysis was carried out. With that aim, *E.coli* C41 cells carrying the plasmid construction pEmbDGAT were grown overnight. A 1:20 dilution was made in fresh LB and IPTG 0.4 M was added for induction at OD_{600nm}=0.6. After 3 hours two samples of 1.5 mL of culture each were collected, centrifuged, and the pellets were frozen at -20°C to analyse the total protein extracts.

With this purpose two identical SDS-PAGE were made as previously described: one of them was immediately revealed and the other was used to continue with the protocol of protein detection by western blot (Towbin et al., 1979).

Transference of protein from the second SDS-PAGE gel to nitrocellulose filters (Whatman) was performed o/n at 4°C with slight agitation in a Bio-Rad system at 40V with Transference Buffer (Tris 20 mM, glycine 15 mM, methanol 20 % (v/v), pH 9.2). To confirm the transfer and locate and mark protein bands of the Molecular Weight Marker, gels were stained with Punceau S staining solution. Then, filters were washed three (3 times x 1 minute in agitation) with TBST buffer (Tris HCl 50mM, NaCl 150mM, Tween-20 0.05 % (v/v), pH 7.4). The filters were then incubated in blocking buffer (nonfat dry milk 6 % (w/v) in TBST) for 2 hours at 4°C and slight agitation. Then, filters were washed three times in TBST during 5 minutes at room temperature. Incubation with primary antibody (anti-polyHistidine-Alkaline Phosphatase from mouse, Sigma-Aldrich, diluted 1:10000 in a solution of nonfat dry milk 3 % (w/v) in TBST) was carried out during 2 h at 4°C with slight agitation. After the incubation, filters were washed another three times in TBST during 5 min at room temperature. Finally, the membrane filter was incubated in a Revelation Buffer (NBT and BCIP, Sigma-Aldrich, in H_2CO_3 buffer pH 9.5) and the reaction was stopped with distilled water.

3.6. Biochemistry.

3.6.1. Proteins

Recombinant protein production

A starter culture of *E.coli* C41 (DE3) carrying each genetic construction was grown overnight at 37°C in LB medium containing the appropriate antibiotics. A 20-fold dilution was prepared in 2L flasks containing 20% volume fresh LB selective medium in order to carry out the induction of the genes by the addition of 0.1-0.4 µM (final concentration) of isopropyl b-D-thiogalactoside (IPTG) at a DO_{600nm}=0.6.

For testing over-expression, aliquots of 1 mL cell cultures were harvested at different times by centrifugation at 13,200 rpm for 2.5 min and the pellets were frozen at -20°C for posterior analysis.

For protein purification, cells were collected 3 hours after induction by centrifugation at 5,000 rpm at 12°C for 20 minutes in a JA10 rotor (Beckman Coulter, USA). The supernatants were discarded and the pellets were frozen at -80°C.

Protein purification

Pellets corresponding to 1 L of culture of the recombinant *E.coli* strain expressing the protein of interest (previously confirmed by SDS-PAGE and western blot when required) were thawed in ice and resuspended in 20 mL of Lysis buffer (NaCl 1 M, TrisHCl 50 mM pH 7.5 and PMSF 100 µl), sonicated (40%, 3 times 90 seconds with 1 minute break in-between) and clarified by ultracentrifugation at 14,000 rpm for 20 minutes at 4°C. Additionally, supernatants were filtered through a piece of cotton.

Affinity chromatography column

Clean solutions containing the protein were loaded into a Níquel HisTrap HP column (GE Healthcare, 1 mL; Sigma-Aldrich, USA) previously equilibrated with buffer A (NaCl 1 M, TrisHCl 50 mM pH 7.5). The His-tagged bound proteins were eluted with a gradient of buffer B (500 mM of imidazole -Sigma, USA-, NaCl 1 M, TrisHCl 50 mM pH 7.5). All buffers were filtered with a 0.2 µm-pore size membrane. The flow through the column was always kept under 1 mL/min. All the procedure was performed at 4°C adapting the protocol described by Villa and co-corkers in 2014.

Ion-exchange chromatography column

In order to improve the purification, 2 mL of the solution containing the protein was loaded into a 20 mL ion-exchange chromatography column (DEAE-Tris-Acryl resin) equilibrated with 5mM sodium phosphate buffer pH 6.8. After applying the sample containing the Ma2 protein, fractions of 2.5 mL each were collected while loading the same buffer, till no absorbance at 280 nm were detected (the measurements were made in a spectrophotometer). Under these conditions Ma2 (with a basic isoelectric point of 8.97) does not bind to the column and is obtained with a higher purity in the flow through. The flow was kept under 0.4 mL/min. All the procedure was carried out at 4°C.

3.6.2. Lipids

Induction of lipid accumulation.

Different approaches were employed to enhance lipid production and accumulation depending on the microorganism and the promoters of the enzymes required for that metabolic change.

Inductor molecules like IPTG and arabinose were employed to provoke the expression of heterologous proteins under the corresponding promoters. Thus, cultures of *E.coli* C41 (DE3) or BW27783 with the corresponding DNA constructions were grown to an OD_{600nm} value of 0.5-0.6 and the expression of the enzyme was induced with either IPTG 100 μM or 0.05% arabinose, depending on the promoter of the protein. Cells were collected at different times after induction by centrifuging at 4000 rpm for 12 minutes at 4°C, placed in 2 mL *Eppendorf* tubes and stored frozen at -20°C until analysed.

Analysis of lipid fraction

a) ***in situ***

Analysis of the lipid fraction is considered *in situ* when lipid accumulation in different recombinant *E.coli* strains expressing the tDGAT is analysed or monitored without destroying the bacterial sample. The different techniques used for this analysis *in situ* could be useful for an iterative evolution of the best accumulating cells.

Cellular buoyancy.

Cell buoyancy, which might be associated to the lipid content of a microorganism, can be determined through cell sedimentation experiments. In an attempt based on the experiments described by Benoit and Klaus in 2005, 1:20 dilutions from starter cultures of *E.coli* C41 and *E.coli* DH5α with and without the *tDGAT* gene were made in fresh LB medium supplemented with the corresponding antibiotics and incubated at 37°C with shaking until OD_{600nm}=0.5-0.6 was reached. Then arabinose was added to DH5α cells to a final concentration of 0.05 % and IPTG was added to a final concentration of 0.05 mM. After 24 hours of over expression, dilutions 1:1, 1:4 and 1:8 of each culture were made in fresh LB and identical volumes were placed in assay tubes in vertical position on a horizontal surface at room temperature for a whole week. Periodically the turbid volume on each sample was measured as previously explained in Benoit and Klaus in 2005.

Fluorescence staining techniques.

The lipophilic dyes Red Nile (9-diethylamino-5-benzo[α]phenoxazinone; Sigma-Aldrich) and Bodipy (4,4-Difluoro-1,3,5,7-Tetramethyl-4-Bora-3a,4a-Diaza-s-Indacene; Thermo Scientific) were employed to stain the different bacterial strains. Samples of *E.coli* C41 (DE3) cells with/without plasmid pEtDGAT and *E.coli* BW27783 cells with/without pBtDGAT were prepared either by growing the bacterial cultures with either of those dyes or by incubation of the cultures previously grown without any staining molecule for 30 minutes at 4°C, centrifugation and resuspension in a volume of phosphate buffered saline (PBS) containing the dye. For Red Nile, the final concentration was usually 0.5 μg/mL (stock solution

prepared at 0.5 mg/mL in DMSO, Sigma, USA) whereas diverse concentrations from 0.1 to 10 µg/mL where tested with Bodipy (stock solution prepared at 5 mg/mL in DMSO, Sigma, USA).

Fluorescence microscopy imaging. Nile Red or Bodipy treated cells were mounted on microscope preparations with glycerol and examined under the inverted fluorescence microscope Leica AF6500 with a 63X oil immersion lens and an Andor iXon885 camera. All settings of the microscope, such as an exposure time of 0.5 s, a physical size per unit of 0.12698017 x 0.12697994 µm and a refractive index of 1.518, were identical for every image acquisition. Samples were excited with wavelengths of 482/18 and 562/40 nm and images were acquired with emission filters of 520-540 nm and 614-642 nm.

Time-lapse fluorescence microscopy monitoring of lipid accumulation. Cultures of C41 expressing or not tDGAT were treated either with Red Nile or Bodipy and agarose pads previously prepared adapting the protocol described by Skinner and co-workers (2013) to capture videos of the cultures. Previously sterilized warm agarose to a final concentration of 1.5%, together with $MgSO_4$ 2 mM, $CaCl_2$ 0.1 mM $MgCl_2$, M9 medium 1x, glycerol 0.1% and casamino acids were mixed and applied to the microscope slide. After waiting 15-20 minutes for the mixture to solidify, and removing with a fine razor blade the exceeding gel, 2 µl of every sample were placed on the center of the pad. Then they were pre-warmed at 37°C before placing in the 37°C-warm chamber of the inverted fluorescence microscope Leica AF6500 with a 63X oil immersion lens and an Andor iXon885 camera. Microscopy images were automatically taken every 20 minutes following further growth of the cells.

Flow cytometry analysis. The percentage of fluorescent cells in the different cultures was detected by a BD FACSCanto™ II flow cytometer (BD Biosciences, USA) using FACSDiva software (BD Biosciences, USA). A 1:40 dilution of each saturated *E.coli* culture, grown with the corresponding dye (Red Nile or Bodipy) was prepared with PBS. The same dilution of a bacterial culture without staining was made in every experiment as a control to calibrate the measurements.

Samples were excited with a 488 nm laser and emission was detected at 530 nm for green fluorescence or 695 nm for red fluorescence. A total of 30.000 events were acquired for every sample.

Fluorimetric analysis. A screening procedure for selecting *E.coli* strains with a better lipid production was developed based on the employment of a lipophilic dye. A fluorimeter (Victor3, Perkin Elmer, USA) was employed to measure the arbitrary fluorescence units emitted by every transconjugant obtained from the high-throughput conjugation experiment in 96-well microtiter plates (Deltalab).

Excitation laser wavelengths of 485, 490 and 560 nm were used to stimulate samples and filters of 535 and 620 nm were employed to detect the fluorescence emitted. 0.10 mm-linear shaking was automatized between measurements. A stabilized lamp energy of 30.000 units and emission aperture "above" and "small" were set for all measurements displayed in this Thesis work.

b) **analysis of isolated lipids**

The lipid species produced by the different bacterial strains used in this work were also analyzed through several invasive methods, requiring the isolation of these compounds for their study.

Lipid extraction

The lipid fraction of every cell culture was extracted using an adapted solvent-based method described by Hara and Radin (1978).

In general, for lipid extraction the following protocol was used: 1-2 ml of a solution of hexane / 2-isopropanol (3:2, v/v) (both were purchased from Sigma-Aldrich, USA) was added to every 10-25 ml cell pellet previously thawed at room temperature. After vigorously vortexing, microfuge tubes were left for 3 hours in a waving platform shaker (Polymax 1040, Heidolph). Then samples were centrifuged for 7 min at 13,200rpm and 8°C, the upper organic phase containing the neutral lipids was collected and placed into new 2 mL microfuge tubes and the solvent was evaporated in a rotational vacuum concentrator (Christ RVC2-18, Germany) with a vacuum bomb (Vacuubrand, Germany) at 40°C.

To extract lipids for NMR analysis 40-100 ml of the same extracting solution (hexane / 2-isopropanol (3:2, v/v) (Sigma-Aldrich, USA) was added to every 500-1000 ml cell pellet previously thawed at room temperature. The mixture of solvents and biomass was then loaded onto a separation funnel and shaked for a minute (holding the funnel upside down and opening the bottom valve frequently to reduce the build up pressure). The process was repeated three times, adding some fresh solvent mixture and collecting all the biomass retained in the storage tube. The upper organic phase, collected after every shaking in an erlenmeyer flask, was dried with anhydrous $MgSO_4$, and the resulting solution (with white solid debris) was filtered directly into a previously weighted erlenmeyer bulb. Solvent was evaporated in a Rotavapor (Büchi) connected to a Vacuum Bomb, setting the water bath at 42°C and the vacuum pressure at 360 mbar. The lipid extract weight was calculated by weighting the erlenmeyer bulb again with a digital analytical balance.

Analytic techniques

Analytic Thin Layer Chromatography (TLC). A solution consisting of hexane/diethyl ether acid/acetic acid (80:20:1, v/v/v) was employed as mobile phase while commercially coated Polygram Sílica Gel (Macherey-Nagel, Germany) was used as stationary phase to carry out the separation of lipid species. Every lipid extraction was resuspended in 14 µl of hexane / 2-isopropanol (3:2) and loaded by 1.5-2 µl-drops or through a Pasteur pipette (by capillarity) onto the Silica Gel. A mixture of FAAEs (0.5%), TAGs (0.5 %) and FFA (0.5%) was loaded for reference. The TLC plate was placed in the TLC cuvette 5-10 minutes after pouring the mobile phase (leaving enough time for vapour equilibration). Staining of the samples was performed either incubating 10-20 minutes in iodine vapour to visualize different lipid species or using UV light at 365 nm to detect compounds with aromatic groups. A densitometric analysis of scanned images of the TLC plates revealed with iodine vapour was carried out through the software Fiji (ImageJ).

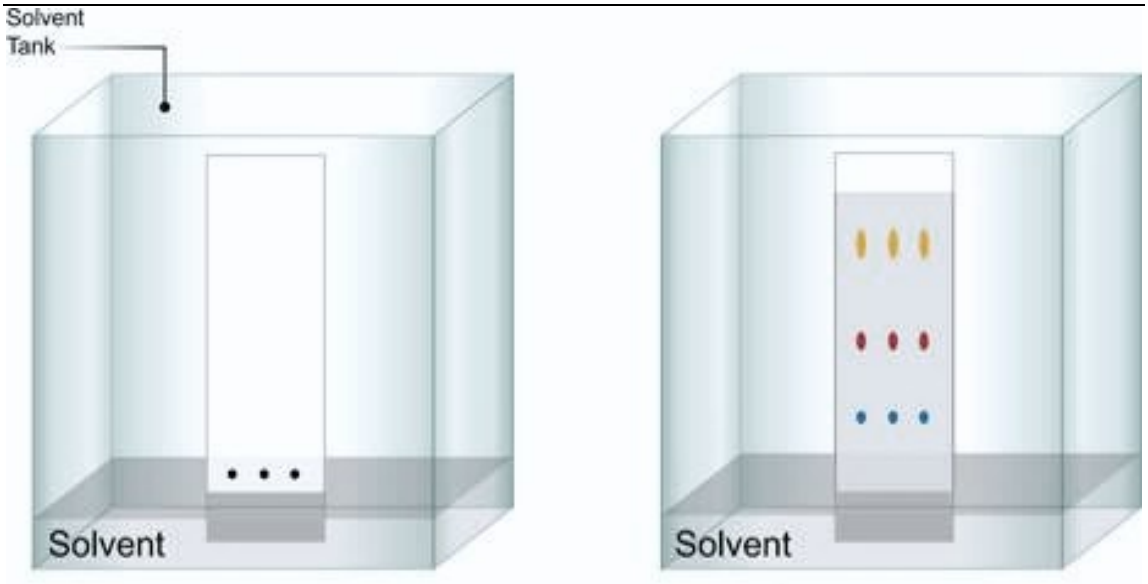

Figure M-2. Schematic representation of the TLC method.

Fatty Acid Methyl Esters (FAME) conversion and gas chromatography (GC). Different spots corresponding to both the recombinant strain *E.coli* C41 (DE3) carrying the DNA construction pEtDGAT and the wild type strain were carefully scraped off the TLC plate with a sharp scalpel and put into 2 mL microfuge tubes. The resulting mixtures of lipids-silica gel as well as the cell pellet of a whole culture of the wild type strain *E.coli* C41 (DE3), were converted into Fatty Acid Methyl Esters (FAMEs) through a protocol adapted from Miller and Berger (1985). Saponification was performed by adding 1.25 mL solution 15% NaOH (w/v) in methanol/deionized water (1:1, v/v) to each sample in glass tubes (Quality PYREX®, 16x100 glass test tubes with screw cap), the mixture was incubated at 100°C for 5 minutes, vortexed and incubated at 100°C for 25 more minutes. Methylation was carried out by adding 2.5 mL HCl 3N in methanol/water (13:11, v/v) and incubating at 80°C for 10 minutes. Lipids were extracted with 1.25 mL of hexane/ ethylic ether (1:1, v/v)

and shaking for 20 minutes. The 1 mL upper solution obtained after decanting was washed with a solution of 1.2% NaOH in deionized water, vortexed, briefly centrifuged for decanting and the 0.5 ml upper phase was transferred to a new vial.

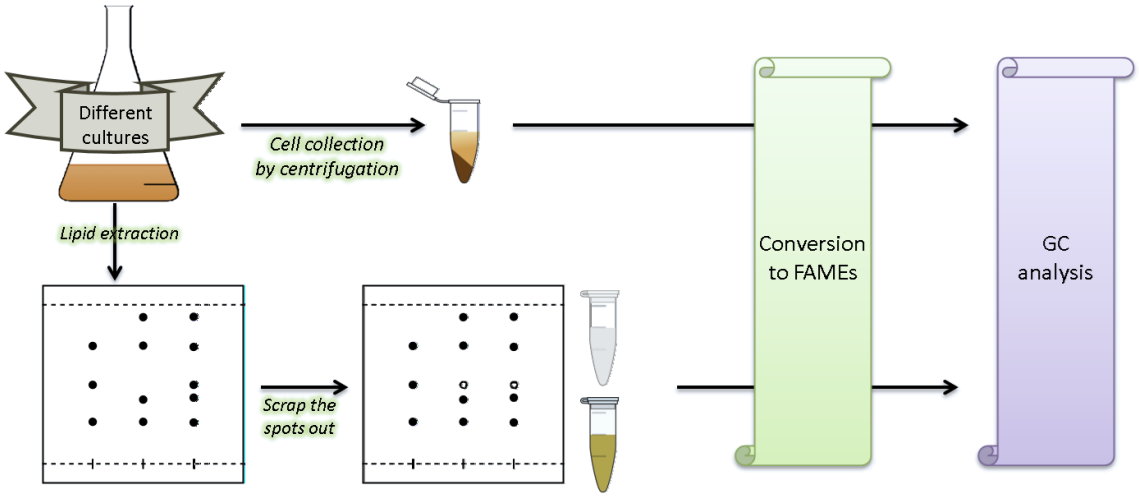

Figure M-3. Schematic representation of the process.

The FA profile was determined through the analysis of the FAMEs with a gas chromatograph (Model 7890A, Agilent, EEUU) at the company Biomar, Microbial Technologies (Spain). Analytes were separated on a column model DB-23 (60m, 0.25mm, 0.25 µm, Agilent, EEUU) using a temperature program of 130°C for 1 min followed by a temperature rise of 2.75°C per minute, 12 minutes at 215°C followed by a temperature ramp of 40°C per minute, 3 minutes at 230°C and finally 130°C for 1 min. Constant velocity of helium as a carrier gas was set at 20 ml/min in velocity mode. The flux of H_2 was 30 ml/min and N_2 at 22.508 ml/min was employed as auxiliary gas. Sample sizes of 2 µL were injected. The FID detector was set at 280°C.

FA identification was carried out from linear-chain FA equivalents and through comparison to standards in retention time. FAs with retention times ranging from methyl hexanoate to methyl tetracosanate were calculated according to Miller and Berger (1985). Standards were purchased from Sigma-Aldrich (USA).

Table M-4. List of the FA standards employed for GC analysis. Experimental retention time (RT, minutes) using the exact same conditions in the GC column used for all experiments are indicated.

FA common name	FA systematic name	Lipid number (nº carbon atoms : nº unsaturations)	RT
Caproic acid	Hexanoic acid	C6:0	2.9
Enantic acid	Heptanoic acid	C7:0	3.2
Caprilic acid	Octanoic acid	C8:0	3.6
Pelargonic acid	Nonanoic acid	C9:0	4.3
Capric acid	Decanoic acid	C10:0	5.2
Undecilic acid	Undecanoic acid	C11:0	6.4

Lauric acid	Dodecanoic acid	C12:0	7.9
Tridecilic acid	Tridecanoic acid	C13:0	9.9
MA, Miristic acid	Tetradecanoic acid	C14:0	12.1
Pentadecilic acid	Pentadecanoic acid	C15:0	14.5
PA, Palmitic acid	Hexadecanoic acid	C16:0	17.1
PO, Palmitoleic acid	(9Z)-hexadec-9-enoic acid	C16:1n7	17.9
Margaric acid	Heptadecanoico acid	C17:0	19.67
Cyclopropyl FA C17	9,10-Methylenehexadecanoic	C17:0cycle	20.43
SA, Stearic acid	Octadecanoic acid	C18:0	22.3
OA, Oleic acid	(9Z)-Octadec-9-enoic acid	C18:1n9	22.9
VC, *cis*-Vaccenic acid	(Z)-11-octadecenoic acid	C18:1n7	23.1
LA, Linoleic acid	(9Z,12Z)-9,12-octadecadienoic acid	C18:2n6	24.1
ALA, α-Linolenic acid	all-*cis*-9,12,15-octadecatrienoic acid	C18:3n3	25.8
SDA, Stearidonic acid	all-*cis*-6,9,12,15,-octadecatetraenoic acid	C18:4n3	26.5
Nonadecilic acid	Nonadecanoic acid	C19:0	24.8
Arachidic acid	Eicosanoic acid	C20:0	27.3
Gondoic acid	(Z)-Eicos-11-enoic acid	C20:1n9	27.8
AA, Arachidonic acid	(5Z,8Z,11Z,14Z)-Icosa-5,8,11,14-tetraenoic acid	C20:4n6	30.3
Eicosatetraenoic acid	Eicosa-(8,11,14,17)-tetraenoic acid	C20:4n3	31.4
EPA, timnodonic acid	(5Z,8Z,11Z,14Z,17Z)-5,8,11,14,17-icosapentaenoic acid	C20:5n3	32.1
Heneicosilic acid	Henicosanoic acid	C21:0	29.7
Behenic acid	Docosanoic acid	C22:0	31.5
Tricosilic acid	Tricosanoic acid	C23:0	34.6
Lignoceric acid	Tetracosanoic acid	C24:0	37.4
Docosapentaenoic acid (DPA, Clupanodonic acid)	all-*cis*-7,10,13,16,19-docosapentaenoic acid	C22:5n3	37.8
DHA, cervonic acid	all-*cis*-docosa-4,7,10,13,16,19-hexa-enoic acid	C22:6n3	38.6

***Ultra Pressure Liquid Chromatography/Mass Spectrometry (UPLC/MS*).** TAGs extracted from preparative TLC spots corresponding both to the recombinant strain *E.coli* C41 (DE3) carrying pEtDGAT and to the wild type strain were further separated by UPLC. With that purpose, a column Acquity UPLC BEH HSS T3 (100 × 2.1 mm, 1,7 µm p.s) and a Pre-column Vanguard (100 × 2.1 mm) were employed through the equipment Acquity UPLC System (Waters, USA) with a sample manager and a binary solvent manager. Solvents employed were methanol/acetonitrile/2-isopropanol (3:3:4, v/v/v; solvent A) and acetonitrile/2-isopropanol (3:7, v/v; solvent B), both with 0.1% NH_4OH (25%). Elution was carried out from a simple gradient with the following steps: initial, 100% A; 3 min, 100% A; 6 min, 98% A; 8 min, 98% A; 9.5 min, 95% A; 11 min, 95% A; 16 min, 100% A. Between samples, methanol was injected twice to wash and avoid the carry over.

MS analysis was performed in order to identify the lipid species present in each sample in a SYNAPT G2 HDMS (Waters, USA) equipment, with quadrupole time of flying (QToF) and electrospray ionization (ESI), the optimum method of ionization/vaporization for the widest range of polar biomolecules according to Griffiths and colleagues (2001). The capillary was set at 0.8 kV; sampling cone, 15 V; temperature, 90°C; desolvation temperature, 280°C; cone gas, 40 L/h; and desolvation gas, 700 L/h. Data was acquired from 5 scans/s in the range 0-18 min and 100-1200 Da for low energy function and 100-900 for the high energy function (MSE, base pick fragmentation, collision energy 30 V), with positive ionization (ESI^+). Mass signatures (m/z ratios) of parent and daughter fragment ions (those formed from the ionization of the molecule) were determined experimentally under direct injection using glyceryl tripalmitate (16:0/16:0/16:0), glyceryl triestearato (18:0/18:0/18:0), glyceryl trioleato (18:1/18:1/18:1), glyceryl trilinolenato (18:3/18:3/18:3) and glyceryl trilinoleato (18:2/18:2/18:2) as representative standards. The observed mass of the parent ion matched the mass of the triglyceride plus NH_4^+, a component of the mobile phase solvent. Both the UPLC lipid purification and the MS analysis were carried out in *Centro para el Desarrollo de la Biotecnología*, CDB, Bohecillo, Valladolid, Spain).

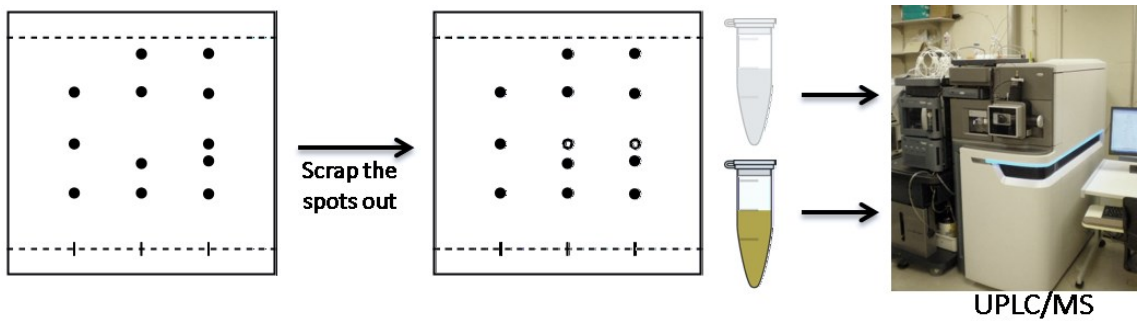

Figure M-4. Schematic representation of the process.

1D and 2D Nuclear Magnetic Resonance (NMR). NMR analysis of mixtures of lipids or pure lipids was performed in a FOURIER-300 MHz spectrometer (B_0 = 7.05 T, Bruker, Germany) at 23°C and 300.19 MHz using deuterated chloroform ($CDCl_3$, Sigma-Aldrich, USA) as solvent. ^1H NMR spectra were acquired of all the lipids, while 2-D H-H COSY experiments were carried out when further analysis was required. For all the pulse sequences, packages from Bruker were used. 700 µl of sample solutions containing 2-8 mg of purified lipids were placed in a 5 mm-diameter NMR tube (in such a way the length of the tube filled with the liquid sample occupied approximately 4.5 cm long). All spectra were recorded with sample rotation and the chemical shifts are expressed in δ scale (ppm), referenced to the residual signal of chloroform (7.26 ppm) (Hoffman, 2006). Signals were characterized as singlet (s), doublet (d), doublet of doublets (dd), triplet (t) or multiplet (m). The software TopSpin was employed to acquire the spectra and all data were analysed thought the software *MestreNova*. The assignments were performed mainly according to Alonso-Salces et al. (2012), Marcel et al. (1995), Silverstein et al. (2005) and Vlahov (1999).

The peaks corresponding to solvent non-deuterated (>1%) and trace impurities were identified following the method of Gottlieb et al. (1997). Spectra were referenced to the residual solvent peak (7.26 ppm for deuterated chloroform, 2.5 ppm for deuterated DMSO and 4.79 ppm for D_2O) as described by Hoffman in 2006. 2D H-H COSY spectra were symmetrised and the diagonal was suppressed before analysing the peaks.

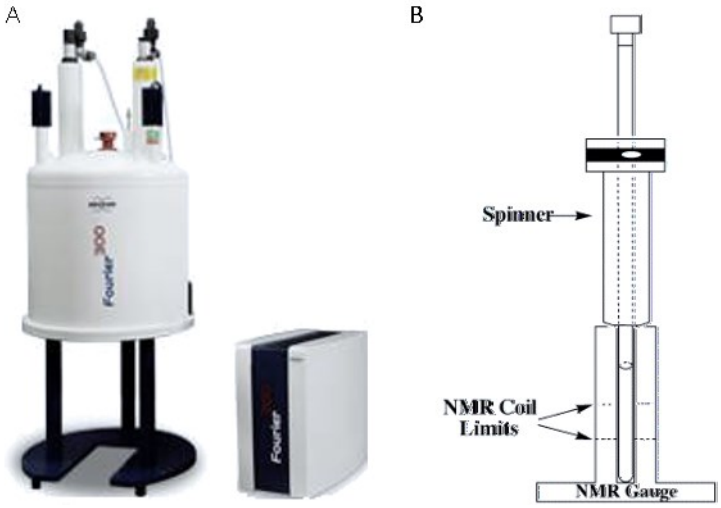

Figure M-5. Devices for NMR experiments. A) FOURIER-300 MHz spectrometer (Bruker, Germany) used for lipid analysis. B) Spinner to place the sample inside the magnet and gauge to measure the correct colocation of the tube.

Lipid purification

Preparative Thin Layer Chromatography (TLC). In order to mount the preparative TLC plates, a mixture of Silica and distilled water (14g and 28 mL for each plate) was shaked in a covered erlenmeyer flask and was poured on 20 x 20 cm glass plates previously placed in a perfectly horizontal surface. Immediately the silica mixture above the plate was smoothed with an applicator filled with distilled water and leaved a few hours to dry. Finally, the preparative TLC plate was activated by placing the plate overnight in a heater at 100°C.

Approximately 50 µg of each sample (solution of lipid extract resuspended in a small amount of hexane / 2-isopropanol (3:2) were completely loaded, with a capillary tube on the thinner side of a Pasteur pipette, along 5 cm on a previously pencil-marked horizontal application line. 150 mL of a solution of hexane/diethyl ether acid/acetic acid (80:20:1, v/v/v) was employed as mobile phase. Once the vapours on the TLC cuvette were equilibrated (about 20 minutes after pouring the mobile phase onto the covered cuvette), the TLC plate already containing the lipid mixture was carefully placed inside the cuvette. After TLC separation, staining was carried out by incubating 20-25 minutes in iodine vapour, and the separated lipid spots were marked with a pencil.

Aluminium foil sheets were used to collect the mixture of silica and lipids carefully scrapped out from each spot of the preparative TLC. Spots were primarily identified by its Rx value (that is the relation between the distance travelled by certain compound c and the migration distance of the standard x). The material corresponding to each spot was placed in a different erlenmeyer flask, where 4 mL of solution of hexane / 2-isopropanol (3:2) was added in order to extract the lipids present in the sample. After shaking for 1-2 minutes, the resulting solution was filtered directly into previously weighted erlenmeyer bulbs (with the aim of eliminating the silica). Solvent was evaporated from each sample in a Rotavapor (Büchi) connected to a vacuum pump, setting the water bath at 42°C and the vacuum pressure at 360 mbar. The weight of the purified lipids was calculated by weighting the erlenmeyer bulbs again with a digital analytical balance.

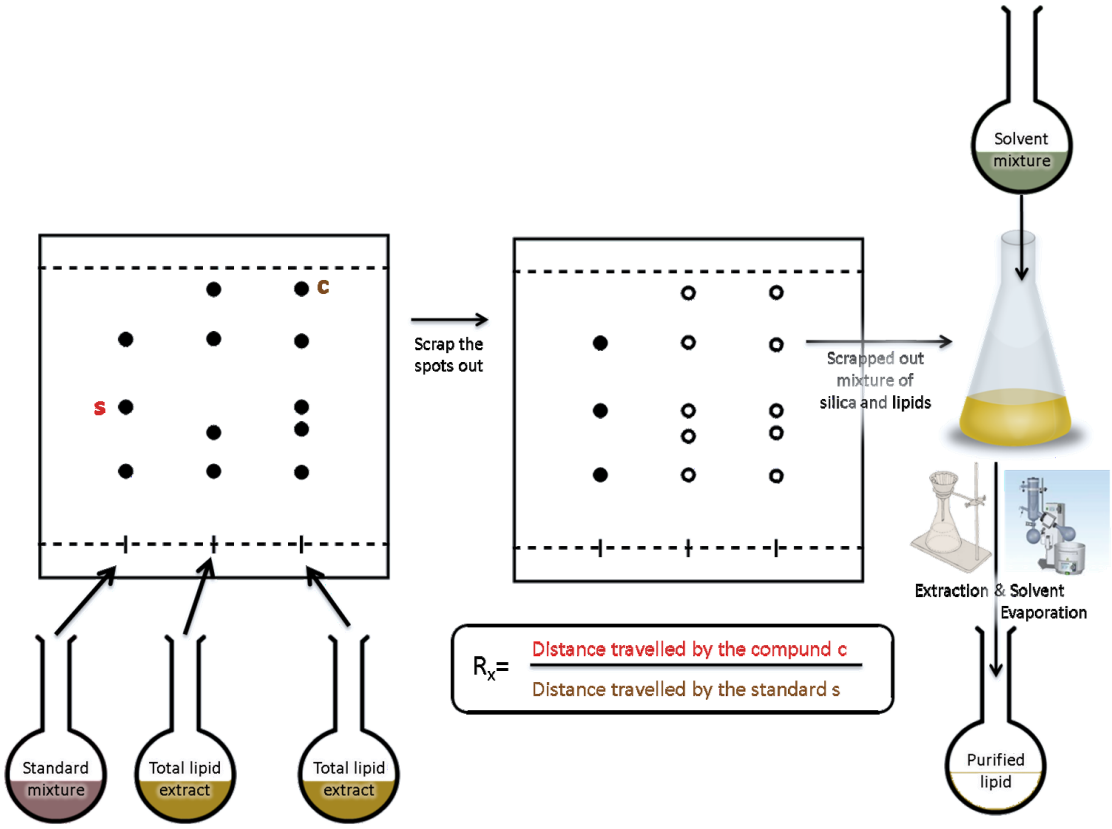

Figure M-6. Schematic representation of the lipid purification procedure through preparative TLC.

Dry-Column Flash Chromatography (DCC). The laboratory glassware was chosen and the protocol defined according to Leonard et al. (2013). As the lipid mixture to separate was in all cases less than 500mg, a Buchner funnel of 30 mm diameter was picked, together with a 125mL Kitasato flask and an elastomer adapter. 15 g of TLC grade silica (200-400 mesh) were weighed in a small beaker. For getting the sample adsorbed to the silica, a tiny quantity was added to the erlenmeyer bulb containing the lipid mixture together with some hexane. After shaking, the solvent was evaporated in a Rotavapor (Büchi) connected to a Vacuum pump, setting the water bath at 42°C and the vacuum pressure at 360 mbar, remaining a yellow dust.

To pack the column, the Buchner funnel, placed in a perfectly vertical position, was filled with the rest of the silica while tapping gently, pressing the silica down starting at the circumference and working towards the centre, until a firm bed was obtained, and a circle of filter paper was put on the top. Then the chromatography was carried out under vacuum: a pre-elution was made with 20 mL hexane to check the solvent run down the column with a horizontal front, meaning the column was perfectly packed. Finally, the sample was applied above the filter paper in the funnel and a new filter paper circle was placed on top. Connecting again the kitasato to the vacuum system, solutions of organic solvents were loaded sequentially (building a gradient of growing polarity -50 mL of hexane 100%, and 10 mL ethyl acetate in hexane 10, 20, 30, 40, 50, 60, 70, 80, 90 and 100%-), collecting at the same time 10 mL fractions and sucking the silica dry in between each fraction. Analytical TLCs were performed to determine the composition of each sample.

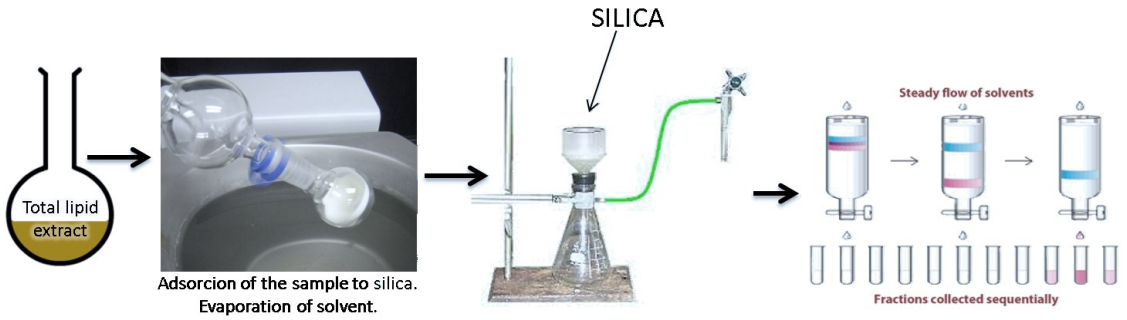

Figura M-7. DCC procedure

3.7. Protein-ligand interaction analysis

Saturated Transfer Difference - Nuclear Magnetic Resonance (STD-NMR experiments).

The method developed and first described by Mayer and Meyer in 1999 was employed to assess the *in vitro* interaction between a protein belonging to the WS/DGAT family and different lipid molecular compounds naturally occurring in *E.coli* C41. STD-NMR represents one of the most sensitive methods for screening of binding ligands of an enzyme. This technique consists in analysing small changes in NOE upon binding to pre-saturated macromolecules (i.e. selectively saturated or irradiated at a region of the spectrum that contains only resonances of large molecules) without labelling requirements. Magnetization transferred from the receptor to its bound ligand is measured by directly observing NMR signals from the ligand itself in the processed STD-NMR spectra. The difference in intensity due to saturation transfer can be quantified ($I_{STD} = I_0 - I_{SAT}$, see Fig M-8) and constitutes an indication of binding. For that method, different analysis were performed depending on the irradiation pulse:

- *Off-resonance* analysis was made with the irradiation pulse placed outside the spectral region of protein and ligand, which give rise to a normal ^{1}H spectrum of the whole mixture.
- *On-resonance* analysis was carried out when low-power irradiation was applied to a ^{1}H NMR spectral region containing protein signals but no ligand signals. This irradiation spreads quickly throughout the protein by the process of spin diffusion and saturates all protein ^{1}H NMR signals (i.e. the molecule is pre-saturated), provoking ^{1}H NMR signals from a ligand bound transiently to the protein become saturated and, upon dissociation, serve to decrease the intensity of the ^{1}H NMR signals measured from the pool of free ligand.
- The two resulting spectra are subtracted to yield the difference spectrum, in which the signals will be more intense depending on the proximity of each proton to the protein. All molecules without binding activity are cancelled out.

The maximum net effect of saturation on ligand protons occurs if a large excess of ligand is used because it is very unlikely that a ligand in a ligand-saturated solution re-enters the binding site. Hence, an approximately 100-fold molar excess of ligand over the protein is normally employed, allowing low µg protein concentrations to be used (Meyer and Peters, 2003; Milagre et al., 2012; Venkitakrishnan et al., 2012; Viegas et al., 2011). A schematic representation of the process can be observed in Fig M-8.

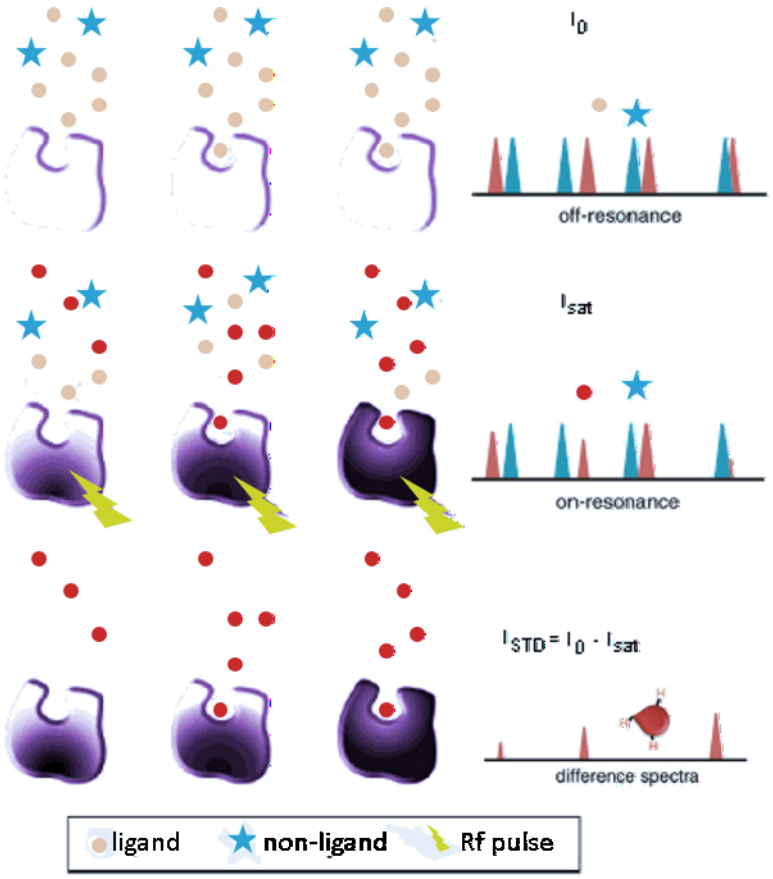

Figure M-8. Schematic representation of the STD-NMR experiments: A) *off resonance* experiment: control radiofrequency (rf) pulse, normal ^{1}H spectrum of the mixture, the intensity of the peaks is considered as I_0; B) *on resonance* experiment: selective rf pulse saturates the receptor, ligands that are in exchange between a bound and free form become saturated when bound to the protein and by exchange that saturation is carried into solution where it is detected; C) STD spectra: the subtraction of the spectra above ($I_{STD}=I_0-I_{SAT}$) yield only the signals corresponding to the binding ligand. Adapted from Figueiredo (2006) and Viegas et al. (2011).

To compare the normal ^{1}H NMR signals from the purified protein to those from the mixture of lipids and protein, three different NMR sample tubes were prepared in 5 mm-diameter NMR tubes to be analyzed in the conditions kept for the STD-NMR experiment.

- One with the enzyme of interest alone to check its normal ^{1}H NMR spectrum. Since the protein was in aqueous solution in all cases a 10% of deuterium oxide (D_2O, Sigma-Aldrich, USA) was added to the tube containing only the protein since this is the minimal percentage of deuterated solvent required to carry out the locking of the sample.
- Another with a mixture of possible substrates (without protein), using a solution of D_2O : deuterated-DMSO 5:1 (DMSO-d_6 , Sigma-Aldrich, USA) with the same purpose as the preceding sample. This mixture of substrates was in all cases a whole lipid extraction from the wt strain of *E.coli* C41.
- The mixture of both, protein and possible substrates, which would be dissolve in H_2O : DMSO-d_6 (5:1) due to the aqueous solution containing the enzyme and the necessity of solubilising the hydrophobic possible substrates (lipid extraction from *E.coli* C41 wt).

The proper STD - NMR experiment (acquirement of *on* and *off-resonance* spectra) was carried out with the third sample employed before (mixture of both the protein and the possible substrates).

The relation between the distance ligand-protein to NOE and the subsequent intensity observed in every signal of the final processed STD-NMR spectra also applies to the atomic level. For a molecule that binds to the receptor, only the signals of the hydrogens that are in close contact to the protein and receive magnetization transfer will appear in the difference spectrum and from those, the ones that are closer to the protein will have more intense I_{STD} signals, owing to a more efficient saturation transfer (see Fig M-9). Consequently, the epitope mapping can be realized by correlating STD-NMR and *off resonance* spectrum.

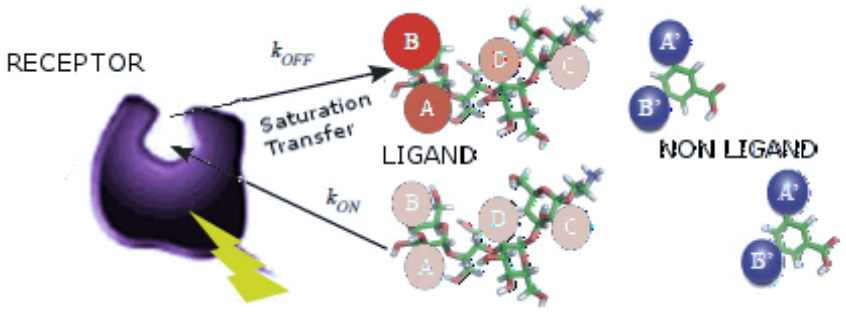

Figure M-9. Schematic representation of the employment of the STD spectrum data to carry out the epitope mapping of the binding ligand. Molecules specifically interacting with the protein will get either all or some of its ^{1}H nucleus saturated. Magnetization transfers from the saturated receptor when the distances ^{1}H-^{1}H are small enough (d < 4-5 Å), through NOE. Adapted from Angulo and Nieto (2011).

With the purpose of better identifying the compound interacting with the protein, some selective 1D ^{1}H TOCSY experiments were carried out with the same samples (mixture of both the protein and the possible substrates).

The software programs TopSpin and MestreNova were employed to acquire all the spectra, process the data, perform the assignments and realize the epitope mapping calculations of the STD spectra according to Viegas et al., 2011.

All ^{1}H NMR analysis related to this experiment were carried out in a spectrometer ASCEND-600 MHz (B_0= 14 T, Bruker, Germany) set at 15°C as temperature of the sample and the equipment, observing ^{1}H at 600.13 MHz. For all the analysis of pulse sequences, software packages from Bruker were used.

3.8. Bioinformatic tools

3.8.1. Sequence analysis software and public gene expression data sets

NCBI (www.ncbi.nlm.nih.gov)
All protein and nucleic acid sequences were obtained from the public databases at the National Center for Biotechnology Information.

Vector NTI (*Invitrogen*; http://www.thermofisher.com/es/en/home/life-science/cloning/vector-nti-software/vector-nti-advance-software/vector-nti-advance-downloads.html)
DNA sequences of every plasmid construction, oligonucleotide or codifying gene employed in this work were analysed through this software, which allows map visualization, sequence search and alignment, PCR primers or cloning strategies design.

BLAST (http://blast.ncbi.nlm.nih.gov/Blast.cgi; Altschul et al., 1997)
The Basic Local Alignment Tool (BLAST) was employed to find DNA and protein local similarity database searches through Nucleotide BLAST and Protein BLAST, respectively. Available on the website of the NCBI.

T-coffee (Notredame et al., 2000; http://www.ebi.ac.uk/Tools/msa/tcoffee/)
Multiple sequence alignments were made using the software program T-coffee (Tree based Consistency Objective Function For AlignmEnt Evaluation).

Primer3 (Untergasser et al., 2012; http://bioinfo.ut.ee/primer3-0.4.0/)
This program was employed for designing PCR and sequencing primers. It has the possibility to set several thermodynamic properties.

Expasy web tools (http://www.expasy.org/)
Further parameters of different amino acid sequences such as molecular weight, number of amino acids, composition, pI or molecular extinction coefficient were calculated through the Expasy web tools.

PDB (http://www.rcsb.org/pdb/home/home.do)
Protein Data Bank supplies information about the 3D shapes of proteins, nucleic acids, and complex assemblies. The availability of the 3D structure of every protein can be checked here.

3.8.2. Biomolecule structural modelling

Phyre2 (Kelley and Sternberg, 2009; http://www.sbg.bio.ic.ac.uk/phyre2/html/page.cgi?id=index)
The Protein Homology/analogY Recognition Engine V 2.0 uses advanced remote homology detection methods to build 3D models, predict ligand binding sites and analyze the effect of amino acid variants for a protein sequence. The tDGAT 3D structure was predicted by homology modeling using the Phyre2 server. The crystal structure of surfactin A synthetase c (SRFA-C), a nonribosomal peptide synthetase termination module [PDB: 2VSQ] was used as the template.

Pymol (The PyMOL Molecular Graphics System, Version 1.3 Schrödinger, LLC; http://pymol.org/dsc/)
PyMOL is a molecular graphics system designed for real-time visualization and rapid generation of high-quality molecular graphics images and animations. It was employed for editing PDB files and displaying maps. The three-dimensional model of the tDGAT was edited, analysed and structurally aligned with the 3D model of Ma2 (previously described by Villa et al., 2014). The electrostatic surface representation was also displayed for both models using PyMol.

ESPript3 (Robert and Gouet, 2014, http://espript.ibcp.fr/ESPript/ESPript/)
Easy Sequencing in PostScript is a program that permits to display on a figure multiple sequence alignments adorned with secondary structure elements. Multiple sequence alignments of the amino acid sequences of the representative proteins belonging to the family WS/DGAT were formatted with the structural modelling of the tDGAT using this program.

3.8.3. Experimental data processing and analysis

Quantity One 1-D Analysis Software *(Biorad)*
This software provided by Bio-Rad (USA) was used to acquire and process the images taken through a Gel Doc 2000 UV system.

Victor3 (*PerkinElmer*)
Software provided by PerkinElmer to acquire and process data measurements of OD_{600nm} or arbitrary units of fluorescence (with different excitation and emission filters) along the time, permitting liquid dispensing and control of the temperature, shaking, area scanning, measuring height, below fluorescence reading, dual label/ratio reading and kinetics.

ImageJ (Schneider et al., 2012; http://rsb.info.nih.gov/ij/download.html)
This open source image processing program designed for scientific multidimensional images was employed to analyse microscopy acquisitions and perform multiple imaging comparisons. Moreover, the estimated

quantification of lipid species through the images of the TLCs was carried out by means of this Java-based software.

Top Spin (*Bruker*)
Software provided by Bruker (Germany) to facilitate the acquisition and processing of NMR spectra.

Mestre Nova (*Mestrelab*; http://mestrelab.com/software/mnova/download/)
Multiplatform software for visualization, processing analysis and reporting NMR data.

ChemDraw (*PerkinElmer*; https://www.cambridgesoft.com/software/overview.aspx?cid=3984&gclid=CPauqNzs1scCFQmdGwodVCMBpQ)
This molecule editor was used for drawing chemical structures or finding compounds of interest through their systematic name and perform NMR spectrum simulations that help in the NMR analysis.

RESULTS AND DISCUSSION

"Se podes olhar, vê.
Se podes ver, repara."

José de Sousa Saramago.

4. Results and discussion

4.1. Optimization of TAG production by the heterologous expression of the WS/DGAT enzyme tDGAT

Heterologous expression of different proteins belonging to the family WS/DGAT has been reported to change the lipid profile of bacteria. Since Kalscheuer and Steinbüchel described for first time in 2003 an enzyme belonging to this family and showed its functionality in *E.coli*, several attempts have been made to improve the TAG production yield obtained through this model bacterium. The heterologous expression of the WS/DGAT from the thermophilic actinomycete *T.curvata* (tDGAT) in *E. coli* was reported to produce the accumulation of neutral lipids by Villa Torrecilla in his PhD Thesis (2012). This protein [Uniprot: D1AD40] is predicted to be coded by the genome of an actinobacteria with an optimal growing temperature of 50°C (Chertkov et al., 2011). Through TLC analysis he proved that spots corresponding to TAGs and certain kind of WE are only present in the TLC lanes coming from cultures of *E.coli* expressing tDGAT. Further analysis of TAG accumulation was performed varying culture conditions such as the carbon source (Moncalián et al., 2014; Villa Torrecilla, 2012).

tDGAT is the first thermophilic enzyme of the family WS/DGAT whose heterologous expression in a mesophilic organism like *E.coli* give rise to TAG production and accumulation. Proteins from organisms growing at high temperatures are usually robust and stable enzymes. Consequently, its importance in industrial large-scale processes relies on its capacity to act in the range of conditions suitable for industrial biocatalysis (Atomi, 2005; Coleman and Sharp, 2010).

The present work takes a closer look into the enzymatic activity of tDGAT in genetically engineered *E.coli* strains with diverse phenotypic characteristics, studying potential strategies for the optimization of TAG production and focusing on the quantification of the production rate achieved by those bacteria as well as in the characterization of the TAGs accumulated.

The main complication for the study of TAG accumulation arose in the difficulty of quantifying TAG at low concentrations. Thus, together with the description of the obtained results, insets in this section describe the optimization of diverse techniques for a better characterization and measurement of the changes in the bacterial lipid profile.

Fast TAG accumulation in *E.coli* with *tDGAT* induction

Although several reports can be found in the literature about TAG production in recombinant *E.coli* strains, little attention has been paid to culture times required for TAG production through these processes.

Different fractions of a recombinant bacterial culture of *E.coli* C41 strain containing a pET-derived plasmid able to express tDGAT (pEtDGAT) were collected at different times after the induction of the expression of tDGAT with 100 mM IPTG at OD_{600nm} = 0.5 (reached 1 hour 45 minutes after 1:20 dilution of an overnight starter culture). Neutral lipid extractions of 6.5 mg dry biomass aliquots were carried out as explained in section M-3.6.2, and loaded in a TLC plate together with serial known quantities of commercial TAGs: 4.5; 18; 36 and 72 µg of triolein were used as standard in order to estimate lipid production in each case (see Inset I). In Fig R-1.A an image of the TLC plate is shown. Densitometry analysis of TLC plates (shown in Fig R-1.B) showed the ability of the engineered strain for accumulating more than 30% of its neutral lipids as TAGs after 1.5 hours of over-expression of the heterologous protein, which could be translated into 4.8 mg TAG/L. Hence, this bacteria carrying the tDGAT is capable of accumulating 1.25 % of its dry biomass as TAGs (w/w) in a remarkably little over-expression time.

INSET I: Technique 1. Thin layer chromatography (TLC)

TLC is a chromatography method employed to separate the components of a mixture using a thin stationary phase supported by an inert backing (TLC plate) and a solution of adequate solvents placed in a developing chamber (see Fig M-2). The gas phase filling this chamber contains components of evaporated solvent molecules. As a matter of time and geometry, and as long as the chamber is tightly closed, saturation is eventually established. Different species migrate along the TLC plate at different speeds according to its affinity for the mobile stationary phases, while the mobile phase moves through the stationary phase by capillary forces. Distances (measured to the center of the spot) can be measured relative to the position of the standard substances (Rx). Therefore, similar compounds show a similar Rx value respect to a certain standard compound (see Fig M-6). By comparing the position of the spots from unknown samples to known standard compounds, we can identify the compounds present in every sample (Ahuja and Jespersen, 2006; Heftmann, 2004; Hines and Frazier, 1993; Touchstone, 1992)

In order to improve the reproducibility of the TLC experiments, filter paper can be placed inside the chamber to guarantee saturation of the gas phase. Although saturated chambers tend to give lower Rx values for the same separation than unsaturated chambers and the zones in saturated chambers are somewhat more diffuse, reproducibility of the result is much higher than in unsaturated chambers. Activation of the TLC plate (e.g. by air-drying) is also essential for a good chromatography performance (Fried and Sherma, 1999; Fuchs et al., 2011; Reich and Schibli, 2004).

Densitometric analysis

TLC plates were firstly digitalized with a high-resolution scanner (600 ppp). Estimation of the quantity of the different lipid species separated on the TLC plate was performed through the analysis software ImageJ. After converting the scanned picture into an 8-bit grayscale image, the threshold of the image was adjusted for visually improving the contrast and converting the background to white. Then identical areas were picked for every compound (elliptical selections for TAG measurements or rectangular ones for quantifying all neutral lipids present along each lane) and the *Integrated density* (i.e. the product of *Area* and *Mean gray value* - the sum of the gray values of all the pixels in the selection divided by the number of pixels -) was measured. Data from every selection was copied to a spreadsheet program such as Microsoft Excel.

For quantifying the lipids present in experimental lanes, a calibration curve needs to be calculated. With that purpose, several known quantities of commercial TAGs were also loaded side by side with the experimental lipid extractions from bacteria onto TLC plates (see an example in Fig i). Finally, experimental values of TAG concentrations can be inferred from the algebraic formula obtained from the linear regression.

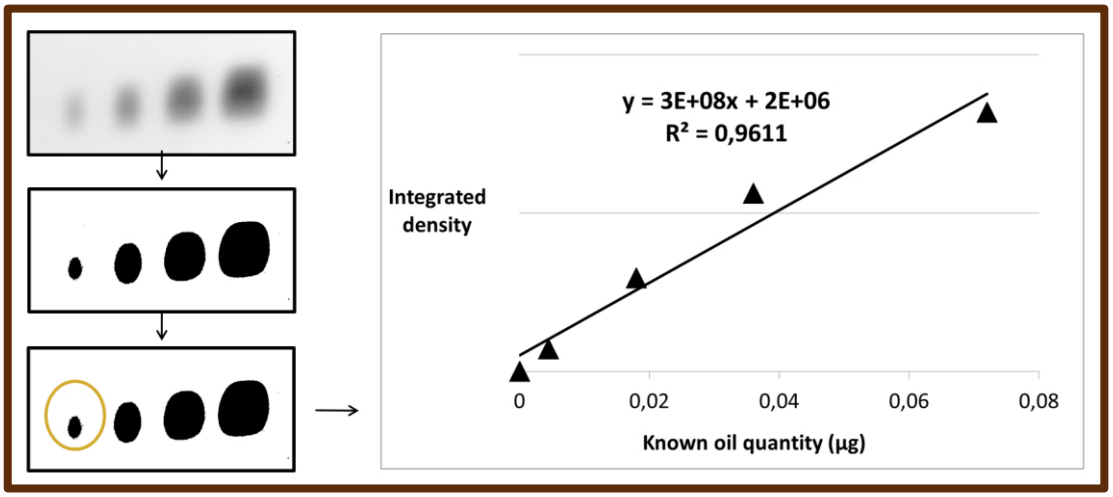

Figure i. Illustrated example of the procedure followed to construct the pattern curve and calculate the equation that will be used to estimate similar lipid species.

Moreover, this accumulation of TAGs in the recombinant strain was directly dependent on the expression of tDGAT, confirming data from previous studies, as 90 minutes of growing after induction are enough for a considerable production of tDGAT.

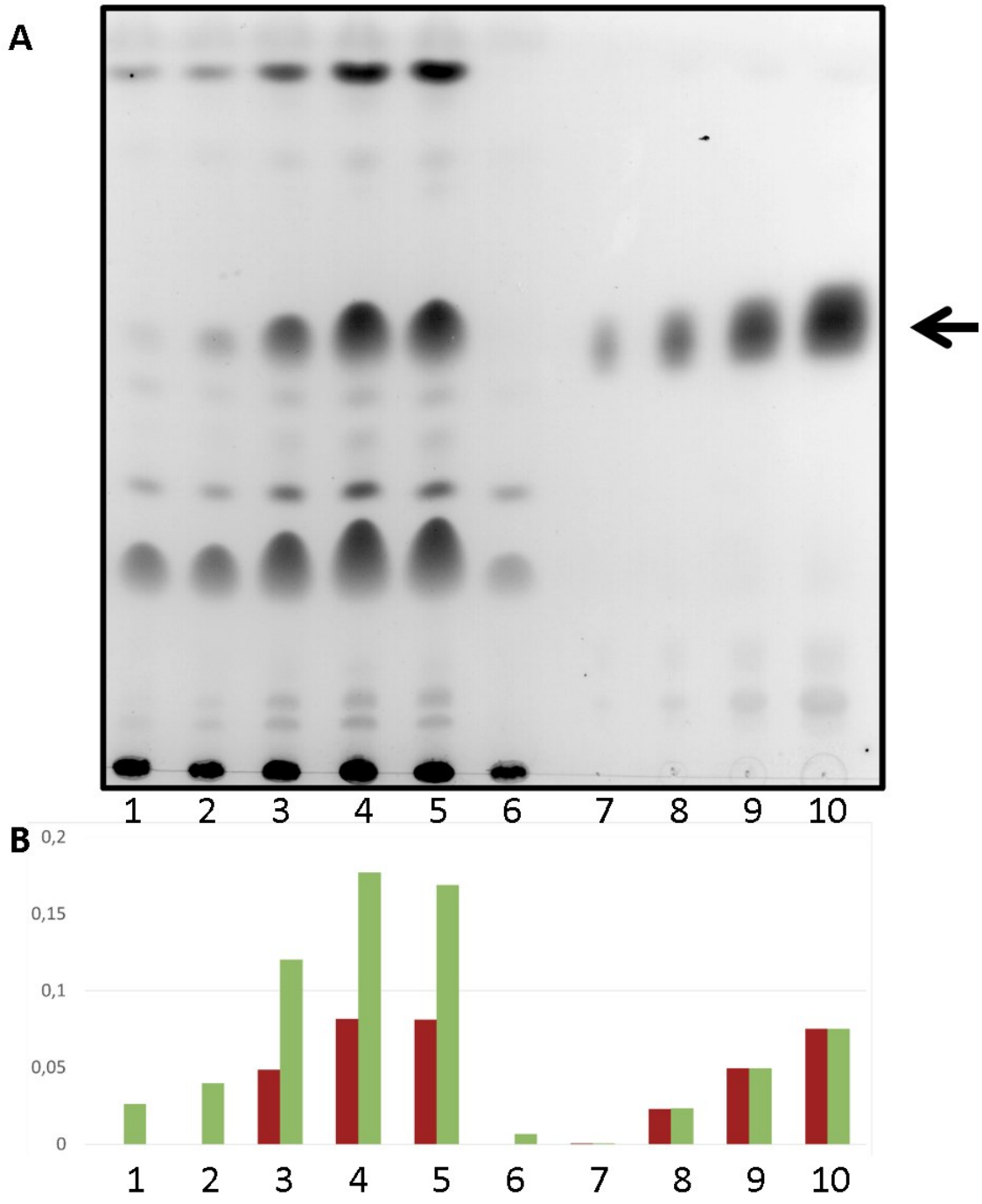

Figure R-1. A) TLC plate showing TAG production in the engineered *E.coli* strain along time after induction. Lipid extractions from cultures collected 0, 30, 60, 90 and 120 minutes after induction were loaded in lanes 1-5. A similar lipid extraction from wild type *E.coli* MG1655 was loaded in lane 6. Different amounts of purified TAGs (4.5; 18; 36 and 72 µg) were loaded in lanes 7-10 in order to estimate the TAG production by densitometric analysis. The black arrow shows the position of TAGs. B) Below the TLC, the bar graph shows the densitometric analysis of TAGs (red bars) and total lipids (green bars).

TAG production occurs in *E.coli* when tDGAT overexpression is induced independently of stressing conditions such as nitrogen starvation.

As detailed in section I-1.2.1., one of the main interests in using *E.coli* for TAG production is the wide substrate range of these bacteria. Previous work has shown that TAG accumulated in *E.coli* C41 upon expression of the tDGAT independently of the carbon source or the host strain (Moncalián et al., 2014; Villa Torrecilla, 2012). In this work we have determined if neutral lipid accumulation in the recombinant *E.coli* varies depending of the nitrogen concentration, a stressing condition widely reported to enhance TAG accumulation in naturally oleogenic microorganisms like actinomycetes (Alvarez et al., 2000). With that purpose, whole lipid extracts of *E.coli* C41 (pEtDGAT) cultures were loaded in TLC plates as described in section M-3.6.2 for analyzing TAG production with different nutrient availability. As shown in Fig R-2, TAG accumulation in *E.coli* expressing tDGAT is independent of the assayed nitrogen concentrations (0.05 g/l NH_4Cl and 1 g/l NH_4Cl) using glucose, gluconate or arabinose as carbon sources. The interest of those substrates relies on its common use for industrial processes. The recombinant strain *E.coli* (pEtDGAT) produces and accumulates neutral lipids when expressing the heterologous protein tDGAT. This heterologous enzyme is produced when the corresponding inductor for this genetic expression system (IPTG) is added, independently of environmental conditions commonly affecting this phenotypic trait in nature. This independence of TAG production on stressing conditions suggests that the regulation of the catalytic activity of tDGAT in recombinant *E.coli* cells totally differs from the situation in its natural hosts but relies on the expression system.

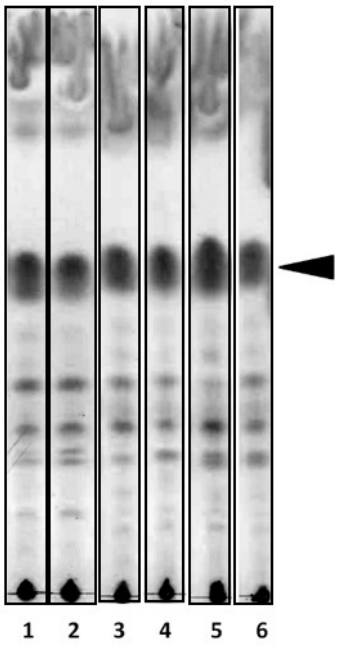

Figure R-2. TLC plates showing tDGAT *in situ* functionality in *E.coli* grown under diverse conditions of nitrogen availability and carbon source. Lipid extractions loaded onto lanes 1, 3, 5 correspond to cultures made on minimal media supplemented with 1 g/l NH_4Cl, while those on lanes 2, 4, 6 come from cultures grown on minimal media with 0.05 g/l NH_4Cl. All cultures contain 1% of carbon source: glucose (1, 2), gluconate (3, 4) or arabinose (5, 6). The black arrow points to the migration distance of the TAGs.

Dependence of neutral lipid accumulation in *E.coli* on temperature

Provided that one interesting characteristic of an enzyme for an industrial use is a wide temperature range of activity, lipid composition of *E.coli* C41 (pEtDGAT) cultures grown at different temperatures was tested by analytic TLC of the lipid extractions, as described in section M-3.6.2. In Fig R-3.A we can observe that similar TAG production was detected in lipid extracts from cultures grown at 25, 30 or 37°C. However, TAG was not detected at 15°C. These data match with the results of *in vitro* tests previously presented by Stöveken and co-workers (2005, see Fig R-3.B). This range of temperatures could

be suitable for an efficient process without excessive energy costs (Cote, 2013; Gupta et al., 2013), which reinforce the interest of this enzyme for biotechnological applications.

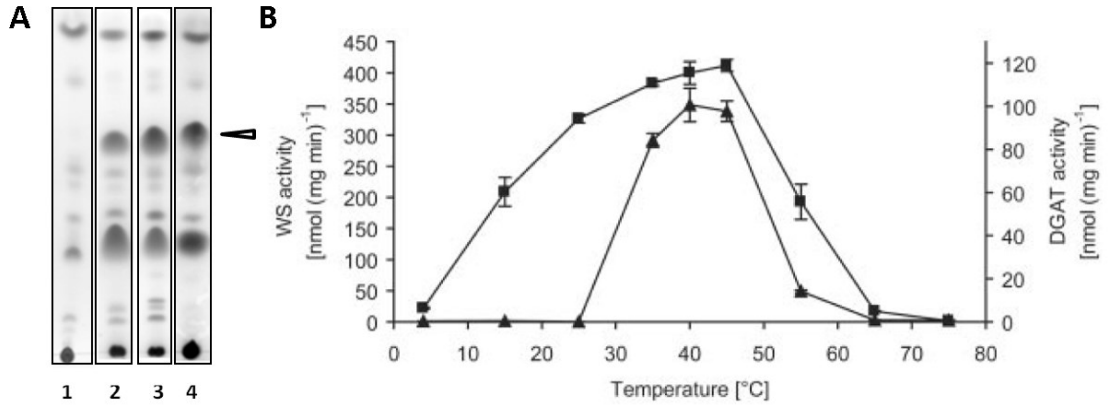

Figure R-3. A) Temperature dependency of tDGAT in *E.coli* cultures. Lipid extracts of cultures of *E.coli* C41 (pEtDGAT) grown in RM (LB) at different temperatures (15°C in lane 1; 25°C in lane 2; 30°C in lane 3; 37°C in lane 4). The white arrow point to the migration distance of the TAGs. B) *In vitro* temperature dependency of the activity of the WS/DGAT of *Acinetobacter* sp. strain ADP1 according to Stöveken et al. (2005). The two lines represent measurements of WS activity (filled squares) and DGAT activity (filled triangles) from two independent experiments.

Over-expression of the WS/DGAT proteins tDGAT and Ma2 changes the lipid profile of its host bacteria

The employment of different techniques to evaluate the alteration of the bacterial lipid profile in response to the heterologous expression of an enzyme belonging to the WS/DGAT family can complement previous analysis and provide new interesting data. Morover, since the properties of the commercial products derived from SCO depend on the chemical characteristics of these lipids, a detailed description of the oils produced in bacteria expressing WS/DGAT proteins is required. With this purpose, in this work we acquired ^{1}H NMR spectra (see section M-3.6.2 and Inset II) from whole lipid extracts from 37°C-cultures of *E.coli* expressing different proteins belonging to this family, such as tDGAT or Ma2.

INSET II: Technique 2. Proton Nuclear Magnetic Resonance (NMR) spectroscopy.

NMR uses a component of electromagnetic radiation (i.e. radio frequency waves) to promote transitions between nuclear energy levels (i.e. resonance). Magnetic nuclei absorb radio frequency energy when placed in a magnetic field of a specific strength and begin to resonate. The energy emitted when the nuclei return to their thermodynamically stable states is detected and the NMR data converted in an intensity vs. frequency plot through a Fourier Transformation (Mazzola et al., 2003)

In a ^{1}H NMR spectra, all hydrogen atoms having the same environment (so called "chemically equivalent protons", that is, with equal surrounding electron density) produce signals at the same position. Hence, different ^{1}H NMR signals indicates the presence of different set of chemically equivalent protons. However, each signal does not necessarily correspond to an individual set of protons, since sometimes the signals are not sufficiently separated and overlap each other (Bruice, 2004).

The position of a resonance signal in the spectrum, called the chemical shift, is defined as a measure of the distance to the signal of a reference compound (traditionally tetramethylsilane -TMS-) and denoted as δ symbol. Although deuterated solvents are used to prepare liquid samples to avoid too intense signals of its protons (that would make much more difficult the interpretation of the spectrum) at least a small amount of non-deuterated compound is always present in the sample. Therefore, according to Hoffman (2006) the addition of TMS to the sample is not mandatory since the solvent residual peak can be used to standardize. Furthermore, the deuterated solvent NMR signal is employed as well to ensure that the magnetic field does not change during the NMR experiment (locking). At the same time, good shimming (achieving an optimal, homogeneous magnetic field properly adjusting the currents) is one of the keys to get a good, high-resolution NMR spectrum (with sharp, symmetric peak lineshapes). The chemical shifts are obtained in parts per million (ppm) by dividing the frequency difference between the sample signal and the TMS signal, in hertz (Hz), by the TMS frequency in megahertz (MHz). For this reason, the chemical shift, in ppm, is independent of the measuring field strength, but the separation in Hz of two signals with a certain chemical shift difference increases linearly with field strength (Silverstein et al., 2005).

While the chemical shift give information about the minimum number of different sets of chemically equivalent protons present in the sample, and give a quite reliable notion about its identity, the intensity (or area under the peak, which is given by the integral) is proportional to the number of protons that make the signal, and the multiplicity (splitting on a NMR peak) suggest connectivity between individual sets of nuclei in a certain molecule, since is due to bound connections (Bruice, 2004).

In complex lipid mixtures like the samples here analyzed, the chemical shift of each signal allows the discrimination of structural groups and the proportionality of the intensity of every peak with the species causing them permits the obtaining of quantitative results (Almoselhy et al., 2014; Petrakis and Fraissard, 2012). In this way, it is possible to calculate the variation in the abundance of each kind of functional group between the samples.

Fig R-4 shows a comparison among the spectrum from the three lipid extracts assayed (*E.coli* wt or expressing tDGAT or Ma2). For more clarity, the spectrum is zoomed and only the region where all signals appear is shown. The only signal outside this region is the $CDCl_3$ solvent residual peak (7.26 ppm, data not shown).

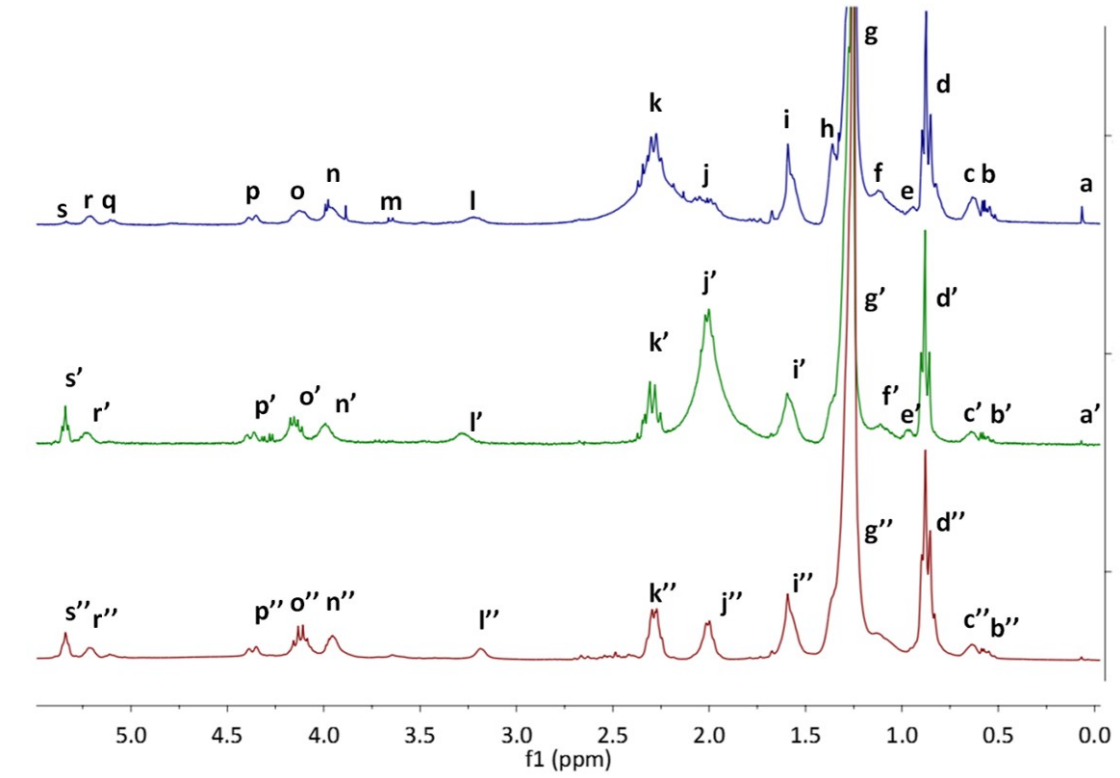

Figure R-4. Comparison of the 0.0-5.5 ppm regions of the ^{1}H NMR spectra ($CDCl_3$, 300.19 MHz) from the whole lipid extract of *E.coli* without any heterologous protein (upper blue spectrum), the whole lipid extract of the same bacteria expressing the tDGAT (middle green spectrum) and Ma2 (lower red spectrum).

Assuming that the perfect triplet at 0.88 ppm is due only to -C*H*$_3$ terminal methyl protons (peak d, d' and d''), and therefore normalizing the integrals of these signals as multiples of 3, variations in the abundance of certain species were calculated. The identification of the majority of the signal peaks was performed according to the literature (see Table R-1).

The most significant difference found in this comparison was the signal at 5.29 ppm (peaks s'', s' and s; Fig R-4). This signal, typical of the olefinic protons, increased 22-fold when tDGAT was expressed (middle green spectrum), and 17-fold with Ma2 (lower red spectrum) over the lipid extraction of the wt bacteria (upper blue spectrum). The signal at 2.01 ppm, typical of allylic protons, was also enhanced in the sample corresponding to *E.coli* expressing tDGAT (peak j') where it increased 6-fold with respect to the wt bacteria (peak j). On the other hand, there was a 2 and 4-fold decrease in the signal at 2.29 ppm (peak k) in the samples from the bacteria expressing the tDGAT or Ma2, respectively. According to the literature (Alonso-Salces et al., 2012; Vlahov, 1999) this peak corresponds either to methylene protons adjacent to a carboxylic group or to H-2 protons of acyl moieties in acylglyceric or ester compounds.

The observed differences suggest an accumulation of compounds with double bounds related to the activity of a WS/DGAT protein, mainly tDGAT. These data confirmed certain differences in the lipid profiles caused by the heterologous expression of a WS/DGAT enzyme, as other techniques have also shown, giving new evidence on the type of changes in the lipid profiles from these recombinant strains.

Table R-1. Chemical shift assignments of ^{1}H NMR signals indicated in the Fig R-10. Abbreviations: s, singlet; d, doublet; t, triplet; m, multiplet.

Peak	Chemical shift, δ (ppm)	Multiplicity	Proton/ Functional group	Attribution	Reference
a, a'	0.07	s	$CH_3[Si(CH_3)_2O]_nSi(CH_3)_3$	Silicone grease: Polydimethylsiloxane (PDMS)	Gottlieb et al., 1997
b, b', b''	0.50-0.60	m			
C, c', c''	0.60-0.69	Broad signal			
D, d', d''	0.88	t	-C*H*$_3$	Terminal methyl protons in every acyl chain	Vlahov 1999
E, e'	0.92-0.99	Broad signal	-*CH*$_3$	^{13}C satellite of signal at 0.88 ppm	Alonso-Salces et al., 2012
F, f'	1.00-1.16	Broad signal			
G, g', g''	1.25		-C*H*$_2$-	Methylene envelop of various compounds	Vlahov 1999
h	1.36				
i, i', i''	1.59		-OCO-CH$_2$-C*H*$_2$-	H-3 protons of acyl moieties in acylglyceric or ester compounds	Vlahov 1999
j, j', j''	2.01	Broad signal	=CH-C*H*$_2$-	Allylic methylenes	Vlahov 1999
k, k', k''	2.29	m	i) HOOC-C*H*$_2$-	i) Methylene protons adjacent to a carboxylic group	Alonso-Salces et al., 2012
			ii) -CO-C*H*$_2$-	ii) H-2 protons of acyl moieties in acylglyceric or ester compounds	Vlahov 1999

Peak	Chemical shift, δ (ppm)	Multiplicity	Proton/ Functional group	Attribution	Reference
l/l'/l''	3.22/3.28/3.18	Broad signal			
m	3.65	d	-C*H*$_2$OH	Glyceryl group in DAGs	Alonso-Salces et al., 2012
n, n', n''	3.90-4.04	Broad signal			
o, o', o''	4.05-4.23	m	C*H*-OH	Glycerol group in DAGs	Almoselhy 2014
			-C*H*$_2$-OR	H-1/H-3 proton of glycerol group TAG	Vlahov 1999
p, p', p''	4.30-4.44	d	-C*H*$_2$-OR	H-1/H-3 proton of glycerol group TAG	Vlahov 1999
q	5.10	m			
r, r', r''	5.16-5.26	Broad signal	>C*H*-OR	H-2 proton in TAGs	Vlahov 1999
s, s', s''	5.29	t	=C*H*-	All UFA	Vlahov 1999
t, t', t''	7.26 (not shown)			$CDCl_3$ solvent residual peak	Gottlieb et al., 1997

Over-expression of tDGAT increases MUFA content in *E.coli*.

As detailed in the section I-1.2.1, it is known that not all FA are similar for biodiesel production, being MUFA better than PUFA or SFA (Cao et al., 2014; Knothe, 2005). Thus, for a future possible application of *E.coli* TAGs for the production of biodiesel as well as any other commodity, we were interested in the study of the FA composition of *E.coli* TAGs.

For the analysis of TAGs, cultures of *E.coli* expressing tDGAT were grown at 37°C and collected in stationary phase. The diverse compounds in the extracted lipid fractions were first separated by TLC. Then, the spot corresponding to the TAGs (according to the migration distance) in the lane corresponding to the recombinant *E.coli* C41 (pEtDGAT) was scraped out of the TLC plate. A similar silica gel area from the wild type strain was also scraped out in order to be used as a control. After extraction (to clean the silica gel particles out) both samples, together with the whole cell pellet of cultures of both the recombinant and the wild type strain, were converted into FAMEs and analyzed by GC (see section M-3.6.2 and Inset III) to identify the FA profile.

INSET III: Technique 3. Gas chromatography (GC) analysis

A wide variety of compounds can be analyzed by GC. However, many unmodified molecules cannot be identified by gas chromatography and must be converted into stable and volatile derivatives to achieve successful GC elution and separation with a good sensitivity, selectivity, and specificity (Ahuja, 1976). By converting to FAMEs diverse lipid extracts from different *E.coli* strains and contrasting the resulting GC profiles we examined their FA pattern. Moreover, by comparing the retention time (RT) peaks in the chromatograms of the samples with those obtained from known standards we can be able to identify variations in the FA profile (see procedure and list of the FA standards employed in section M-3.6.2 and Table M-4).

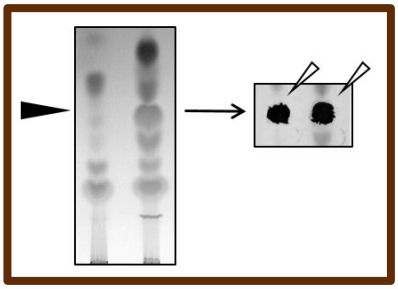

Figure ii. Preparative TLC plate showing the separations of the whole lipid extractions of *E.coli* C41 wt (left lane) and *E.coli* C41 (pEtDGAT) (right lane). The black arrow head points to the TAG compounds. Silica is scrapped out of the corresponding place in both lanes (resulting in the spaces indicated by white arrows in the right inset) even if nothing is revealed in the TLC.

Fig R-5 shows three of the GC chromatograms analyzed to visualize examples of the main samples analysed. The relative amount of palmitoleic (PO, 16:1n7) and *cis* vaccenic (VC, 18:1n7) acids is visibly increased in tDGAT expressing cells. Strikingly, the proportion of these MUFAs is even higher in the TAG fraction of the tDGAT expressing cells (Fig R-5). As expected, no FAME molecules were detected in the control TLC-spot sample (data not shown).

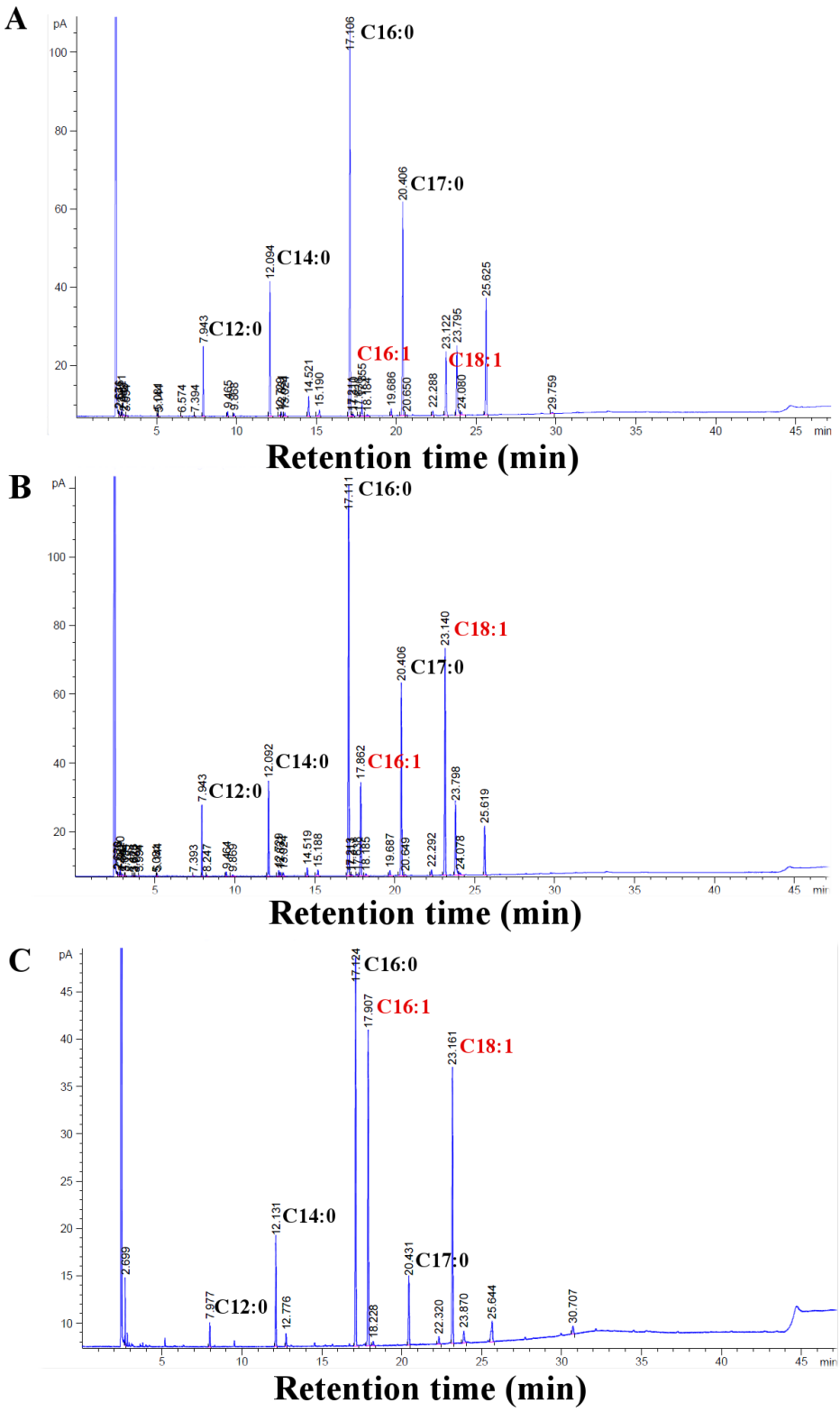

Figure R-5. Gas chromatograms obtained from the analysis of the FAMEs from the whole cell culture of both the wild type *E.coli* C41 (pET29c) (A) and the recombinant strain *E.coli* C41 (pEtDGAT) (B) as well as from the extracted TLC spots corresponding to TAGs (C) of the engineered strain. The main FA occurring in different percentages in the samples are labeled in red [the MUFA palmitoleic acid (C16:1n7) and *cis* vaccenic acid (C18:1n7)] or black [the SFA dodecanoic acid (C12:0), tetradecanoic acid (C14:0) and palmitic acid (C16:0) and the cyclopropane FA 9, 10-methylenehexadecanoic acid (C17:0cycle)].

A whole summary of the GC data is presented in Table R-2 and illustrated as a bar graph in Fig R-6. A relative increase of MUFA in *E.coli* C41 expressing the tDGAT protein with respect to the wild type strain can be observed. *E.coli* C41 wt is mainly composed of saturated palmitic acid (PA, C16:0, 30.64%) and cyclopropane FA methylene hexadecanoic acid (C17:0cycle, 17.75 %). However, our data indicate that monounsaturated PO and VC acids occurred in an outstandingly higher proportion in the whole FA pool in *E.coli* C41 (pEtDGAT) than in the wild type strain. This way, MUFA increased 2.7-fold in *E.coli* C41 (pEtDGAT) (from 10.6 to 28.5%, as indicated in Table R-2 and Fig R-7).

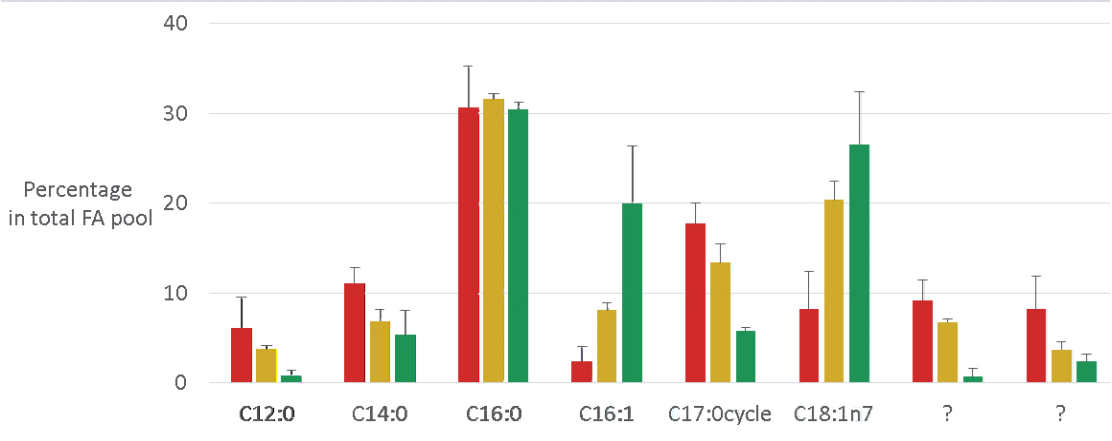

Figure R-6. Bar chart representing the shift in the FA profile. In red and yellow, FA content of the whole lipid extract of *E.coli* C41 wt and *E.coli* C41 (pEtDGAT); in green, FA composition of the TAGs produced by the engineered strain. Error bars indicate the standard deviation among three independent experiments.

Furthermore, the TAGs accumulated by *E.coli* C41 (pEtDGAT) were mainly constituted by those two MUFA (whose proportion remained between 25-31% in all cases, see Table R-1) together with a SFA, PA. Strickingly, while the proportion of PA is similar in TAGs and in total FAs, MUFA represents 46% of FA in the TAGs of *E.coli* (pEtDGAT), a 4.39-fold increase over the content of total FA in wt *E.coli* C41 as shown in Fig R-7.

Table R-2. Summary of GC results. Average percentage of the main FA occurring in each sample, calculated from three independent experiments.

Retention time (min)	FA name	Whole lipid *E.coli* C41	Whole lipid *E.coli* C41(pEtDGAT)	TAG *E.coli* C41 (pEtDGAT)
7.981	Lauric	6,14%	3,75%	0,87%
12.120	Miristic	11,15%	6,90%	5,34%
17.096	Palmitic	30,64%	31,58%	30,45%
17.871	Palmitoleic	2,39%	8,11%	20,01%
20.402	Cyclopropyl FA C17	17,75%	13,39%	5,77%
23.112	*cis* vaccenic	8,22%	20,38%	26,58%
23.870	Unknown	9,16%	6,76%	0,68%
25.586	Unknown	8,20%	3,72%	2,39%

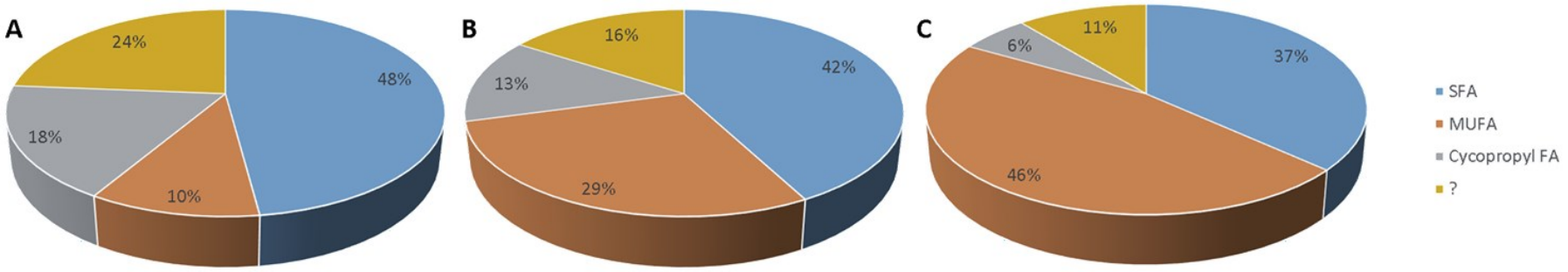

Figure R-7. Circular graphs showing the increment in MUFAs (in dark orange) in the TAGs from the recombinant strain. A) Whole lipid extraction from *E.coli* C41; B) Whole lipid extraction from *E.coli* C41 (pEtDGAT); C) TAG-TLC spot from *E.coli* C41 (pEtDGAT).

To confirm that the observed MUFA accumulation was due to the tDGAT expression, the FA composition of other engineered *E.coli* strains expressing tDGAT was analyzed. With this purpose, the expression system of the pBAD vectors (Guzman et al., 1995) was employed. The FA profile of the engineered bacteria *E.coli* BW27783 (pBtDGAT) was compared with that of the wt BW27783 strain, showing that the increment in MUFA over the total FA pool was independent of the expression system. In the left section of Fig R-8 we can observe that the content in MUFA increases 4-fold in the strain expressing the enzyme in comparison with the wt bacteria. TAG accumulation in this system was also checked by TLC analysis. In the right side of Fig R-8 we observe that although TAG production was lower in the pBAD system (as described by Villa Torrecilla in 2012), there is some TAG production of the same cultures showing a increment in MUFA upon expression of tDGAT.

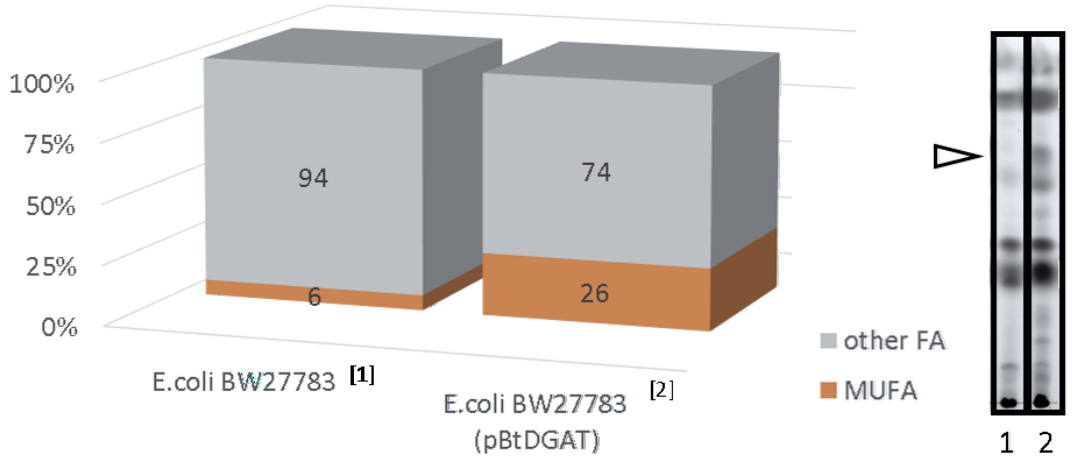

Figure R-8. Comparison between the FA profile of the wt *E.coli* BW27783 and the corresponding recombinant strain expressing tDGAT illustrated in bar graphs showing the MUFA percentage (dark orange) among the whole FA pool in different strains (left) and TLC analysis of both strains (right). The white arrow points to the migration distance of the TAGs in the TLC plates.

Similar analysis were performed with some members of the Keio collection, a set of mutant *E.coli* strains lacking different non-essential genes (Baba et al., 2006). In order to facilitate the transformation of several different strains with the tDGAT expressing plasmid by conjugation, a vector containing the $oriT_{R388}$ in addition to the gen for the protein tDGAT under the arabinose-inducible BAD promoter, was assembled (see Fig R-9.A). The plasmid construction, named pBoRtDGAT, was conjugated through the pSU711 plasmid (see Fig R-9.B) to different keio strains.

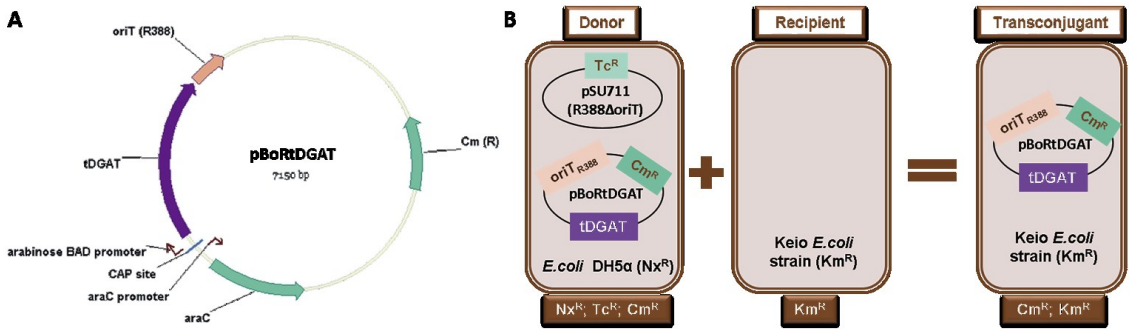

Figure R-9. A) Schematic map of the plasmid construction pBoRtDGAT showing the main features. The gene for the protein tDGAT is colored in purple, the origin of transfer from R388 in orange and the original genes from the pBAD33 vector for the regulator protein AraC and for the resistance to Cm are presented in green. The promoters and the catabolite activator protein (CAP, also known as cAMP receptor protein) site are signaled as well. B) Representation of the conjugation process carried out in every case to introduce the gene for the tDGAT protein into the different Keio mutant strains. Abbreviations: Tc^R, resistance to tetracycline; Cm^R, resistance to chloramphenicol; Km^R; resistance to kanamycin.

Among the transconjugants obtained, the FA composition of *E.coli ΔfadR (*pBoRtDGAT*),* a strain lacking a relevant transcriptional regulator that mediates in lipid metabolism; *E.coli ΔfadE* (pBoRtDGAT), a strain with a deletion over the gene responsible for the first step in β-oxidation and *E.coli ΔuvrA* (pBoRtDGAT), a strain lacking a gene non-related with lipid metabolism, was analysed through GC and compared to the native *E.coli* strain, MG1655. Fig R-10 presents a bar graph with this comparison, showing that the MUFA content can increase up to 12-fold when expressing tDGAT. Like in the above explained experiment, TAG accumulation was evaluated by TLC analysis. In Fig R-10 (right), we observe TAG presence upon expression of the protein tDGAT in the assayed strains cultured in similar conditions.

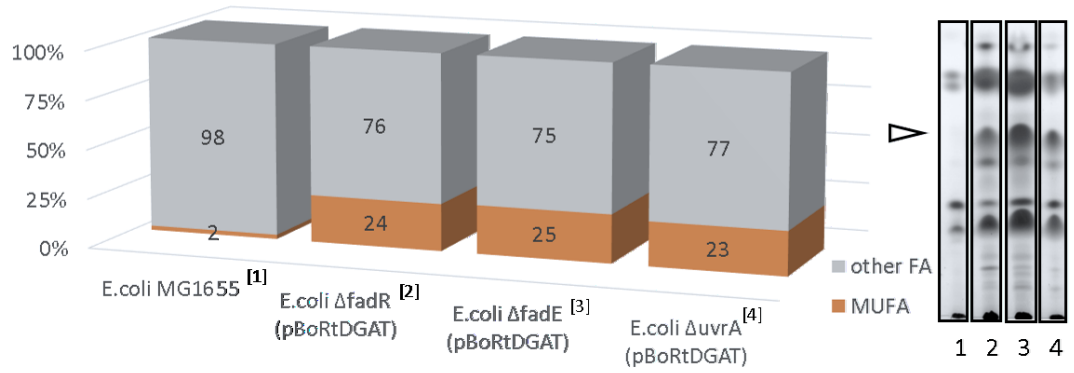

Figure R-10. Bar graphs showing the MUFA percentage (dark orange) among the whole FA pool in several Keio strains expressing the heterologous enzyme tDGAT compared to the native *E.coli* strain MG1655 (left) and TLC analysis the four strains (right). The white arrow points to the migration distance of the TAGs in the TLC plates.

At the same time, the particular behavior of the expression of tDGAT in the strain *E.coli* Δ*dgkA* was assessed. That way, we focused in the basal expression occurring under the arabinose-inducible BAD promoter (see Inset IV), considering the previous observations by Guzman and colleagues (1995).

INSET IV: Glucose repression of basal expression

Generally, the overexpression of heterologous proteins in bacterial cells is performed when cultures have achieved at least a mid-log phase. tDGAT overexpression in strains carrying its codifying gene were induced using this procedure and significative functionality was observed. Nonetheless, in the case of the Keio strain *E.coli* Δ*dgkA,* the protein tDGAT appears to prevent cell growth when the OD_{600nm} of the culture is very low. In contrast to the normal growth of this strain without any plasmid, the strain *E.coli* Δ*dgkA* (pBoRtDGAT) is not capable of proliferating even without induction (so it does not achieve a mid-log phase of growth). According to Guzman and coworkers (1995), this effect was erased by supplementing the growth media with D-glucose and preventing that way basal expression of the heterologous protein. Interestingly, the protein tDGAT was seen to be functional after induction with arabinose at a more advanced growth phase of this growing culture.

This initial repression of the basal production of tDGAT by supplementation of the growth media with D-glucose was assessed in other strains carrying the protein under the promoter $P_{BAD.}$ As illustrated in Fig iii, later induction with identical concentrations of arabinose of strains carrying this plasmid construction leaded to a higher tDGAT activity in the cultures where basal expression of the heterologous protein had been repressed.

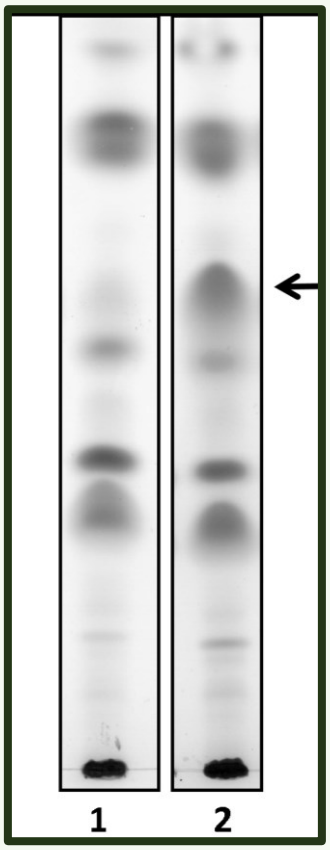

Figure iii. TLC plate showing the analysis from lipid extracts from *E.coli* BW27783 (pBtDGAT) cultured without (1) and with (2) supplemental glucose (at a final concentration of 0.2%) before induction, to prevent basal expression of the heterologous protein tDGAT under the promoter P_{BAD}. Cultures were collected 20 hours after induction with arabinose at mid-log growth phase.

This MUFA accumulation seems to be independent of the growth temperature of the host bacteria as well, as shown in Fig R-11. The increment in these FA occurs even when DGAT functionality is not detected in TLC analysis of the lipid extractions (Fig R-3.A shows a TLC analysis of an *E.coli* (pEtDGAT) culture grown at 15°C).

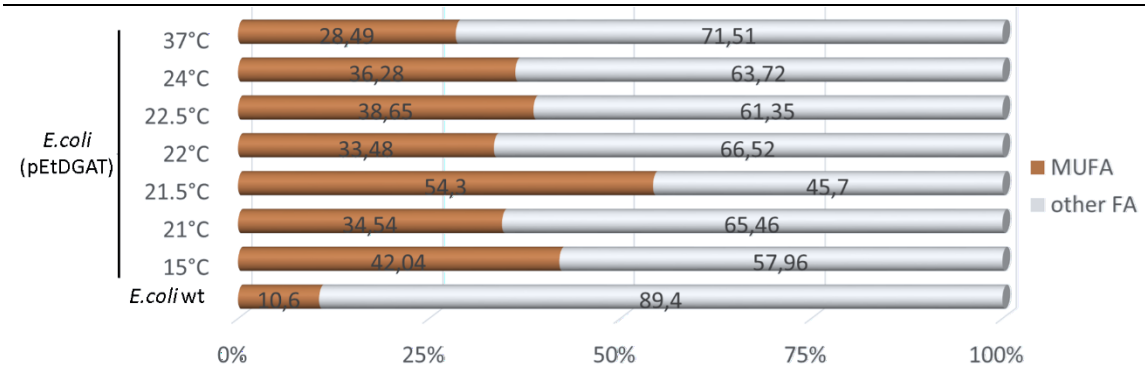

Figure R-11. Bar graph showing the MUFA percentage (dark orange) among the whole FA pool in *E.coli* C41 (pEtDGAT) grown at different temperatures ranging from 15 to 37°C. The lower column corresponds to wt *E.coli* C41.

As described in section I-1.1.1, the FA composition of *E.coli* varies with the bacterial strain and growth conditions. An increase in MUFAs generally correlates with lower growth temperatures (Heath, Richard J. et al., 2002; Mansilla et al., 2004). Likewise, the proportion of cyclopropane FAs depends on the bacterial growth phase: cyclopropane FAs proportion is larger when cells are collected in stationary phase (Magnuson et al., 1993). On the other hand, shifts in the FA profiles towards an increment in the proportion of MUFAs due to the heterologous expression of different genes have been reported both in plants (Vanhercke et al., 2013) and bacteria (Kerviel et al., 2014). For example, Rucker and co-workers studied TAGs produced in a recombinant *E.coli* strain in 2013. They reported a significant proportion of MUFA among the FA forming part of the TAGs produced by the engineered bacteria (see Fig R-12.A).

A

Fatty acid	% Total triglyceride fatty acids
16:0	53.3 %
18:1	22.8 %
16:1	22.7 %
14:0	1.2 %

B

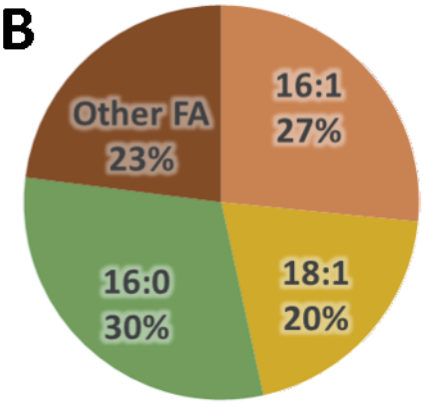

Figure R-12. A) FA composition of TAGs in *E.coli* EDE3 (pJR1). Plasmid pJR1 expresses both a PAP (phosphatidic acid phosphatase, native from *E.coli*) and a WS/DGAT (wax ester synthase/diacylglycerol : CoA acyltransferase, from *A.calcoaceticus* ADP1). Source: Rucker et al. (2013). Almost half of the FA of these TAG compounds are MUFA, similarly to our results from the analysis of the TAG fraction from *E.coli* C41 (pEtDGAT) (B).

Although they did not employ neither the same host strain, WS/DGAT protein or culture conditions used in our work, their results are coherent with the data here presented (Fig R-12.B or Fig R-7.C). According to our results, a recombinant bacteria expressing tDGAT significantly increases its content in MUFA at least to a quarter of the total bacterial FA pool. MUFA increase seems to be independent of

other phenotypic characteristics of the microorganism and of growth temperature, and occurs even when DGAT activity is not detectable through TLC analysis. This indicates that a relevant part of the double bonds observed by ^{1}H NMR were related to the FA profile, especially to the FA accumulating in the TAG compounds. Lin and co-workers also reported in 2013 an increment in MUFA in an *E.coli* strain expressing an enzyme belonging to the WS/DGAT family. However, the precise explanation to this metabolic response is not clear yet. Our hypothesis relies in the possible spontaneous degradation that MUFA might develop through β-oxidation. MUFA becoming part of the TAGs in the recombinant strain are probably chemically protected from this degradation. Therefore, the percentage of MUFA in the total FA pool of the strain expressing tDGAT increases. That would also explain the percentages found in the analyzed TAG fractions. Another possible explanation is an effect of the overexpression of the protein tDGAT that mimics the decrease in temperature. For instance, a higher selectivity of this enzyme for MUFA could produce a bias in its biosynthesis. This way, the activation of the biosynthesis of MUFA could be provoked by the reduction of its concentration in the cytosol and membranes while these FA are diverted to TAGs. The high percentage of C17:0cycle is probably obtained because all samples have been harvested at stationary phase, although a slight decrease can be observed in the profile of the whole lipid extract of the recombinant strain.

A significant proportion of the TAGs in *E.coli* (pEtDGAT) contains one MUFA

Lipid fractions purified from both the engineered *E.coli* C41 (pEtDGAT) and the wild type strain *E.coli* C41 were analyzed through ^{1}H NMR. Analysis of the acquired spectra showed that ^{1}H NMR profiles typical of TAG compounds were only detected among the samples from engineered bacteria.

A pure commercial TAG compound such as the saturated tributirine [TAG (4:0/4:0/4:0), PubChem: 6050] was firstly analyzed in order to obtain an experimental model spectra of a TAG compound acquired in the same conditions used for the samples from the bacterial extracts (see Fig R-13).

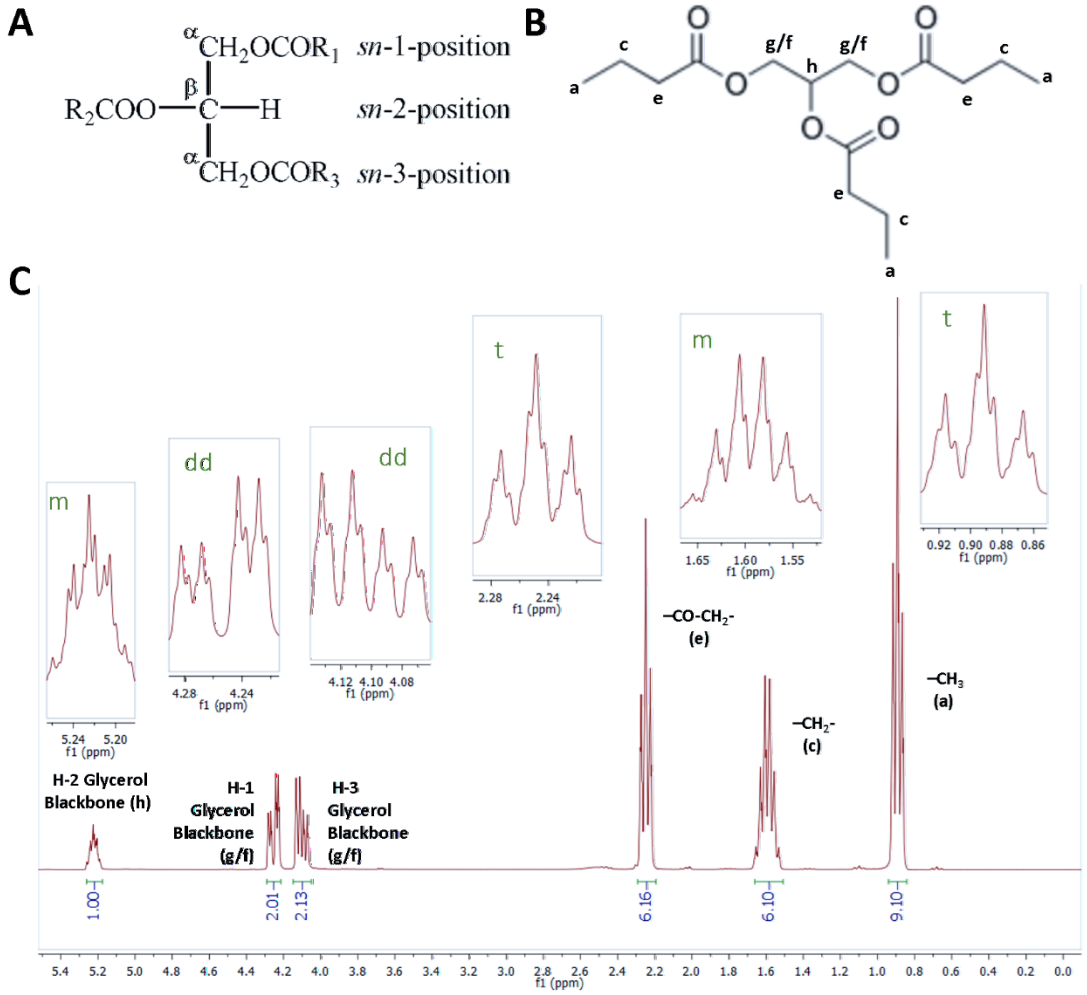

Figure R-13. A) Basic structure of TAGs by Fisher projection. R_1CO, R_2CO and R_3CO are the acyl groups whose position on the glycerol backbone is designated either by the Greek symbols α, β, α' or by the stereospecific numbering 1, 2, 3. Image from Vlahov, 1999. B) Tributirine structural formula with peak assignments corresponding the spectra below. C) ^{1}H NMR spectrum of tributirine. Every signal is amplified to better visualize multiplicity (in green), while the assignments (notes in black) and the integral values (blue numbers under each peak) are indicated on the main spectra. Assignments and multiplicity of this compound are also detailed in Fig R-12 and Table R-3 (with the same nomenclature). Abbreviations: dd, doublet of doublets; t, triplet; m, multiplet.

The detailed comparison between the experimental spectrum of the commercial tributirine and a sample purified from *E.coli* expressing tDGAT is shown in Fig R-14. For clarity, only the zoomed region between 5 and 5.5 ppm is shown, since this region where most of signals appear. The only signal outside this region is the $CDCl_3$ solvent residual peak (7.26 ppm, data not shown). Regarding the chemical shifts of the different peaks, its multiplicity and the literature data (Lie Ken Jie and Lam, 1995; Vlahov, 1999) signals were assigned to the most probable set of protons and attributed to the probable functional group (Table R-3). The protons of the glycerol backbone are responsible for the multiplet at 5.26 ppm and the doublet of doublets at 4.14 and 4.29 ppm. The triplet at 5.35 indicates some double bound present in the purified molecule. The rest of the signals are due to other protons in the acyl moieties. The peak at 1.57 ppm is probably the sum of two signals that overlap: the H-3 protons of acyl moieties in TAGs and residual molecules of H_2O in the sample. The absence of peaks around 0.98 ppm confirms the absence of ω-3 acyl moieties. The number of protons was attributed to each signal in accordance to the integration of the peaks and the functional groups assignment (Silverstein et al., 2005).

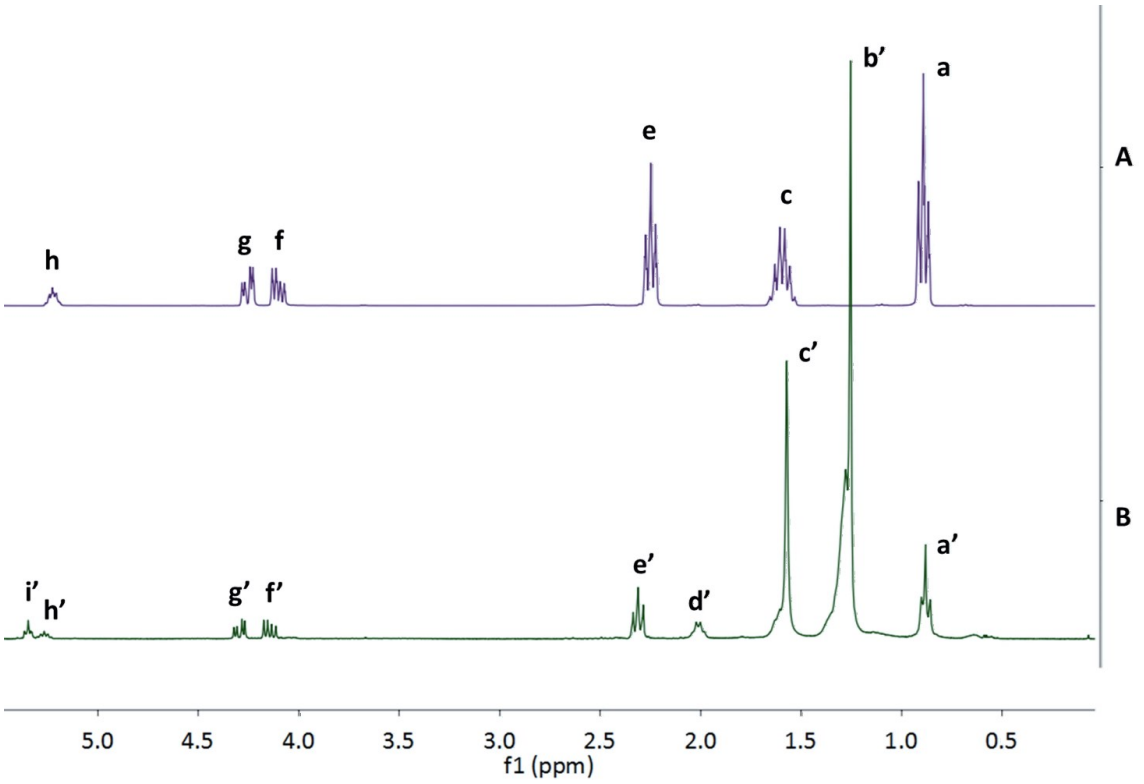

Figure R-14. Comparison of the 0.0-5.5 ppm region of the ^{1}H NMR spectra ($CDCl_3$, 300.19 MHz) from the commercial TAG tributirine (4:0/4:0/4:0) (purple upper spectrum) and a lipid compound purified from the recombinant microorganism *E.coli* C41 (pEtDGAT) (green low spectrum).

Table R-3. Assignments of the different peaks of the ^{1}H NMR spectra displayed in Fig R-12. Abbreviations: s, singlet; d, doublet; dd, doublet of doublets; t, triplet; m, multiplet.

Peak Name (agree with figure)	Chemical Shift, δ (ppm)	Peak multiplicity	Assigned number of H's	Proton-Functional group
a/a'	0.89/0.88	t	9	-C*H*$_3$ → (terminal methyl protons of saturated and unsaturated chains)
b'	1.25	Broad signal	~70	-C*H*$_2$- →(Protons of methylene envelop)
c/c'	1.59/1.57	m	6	-COO-CH$_2$-C*H*$_2$- → (H-3 protons of acyl moieties in triacylglycerols) H$_2$O → (residual molecules)
d'	2.01	m	4	=C- C*H*$_2$- → (allylic methylenes)
e/e'	2.25/2.31	t	6	COO- C*H*$_2$- → (H-2 protons of acyl moieties in triacylglycerols)
f/f'	4.10/4.14	dd	2	-C*H*$_2$-OR → (H-1 and H-3 protons of glycerol, the assignments are interchangeable)
g/g'	4.25/4.29	dd	2	
h/h'	5.23/5.26	m	1	>CH-OR → (H-2 of the glycerol backbone)
i'	5.35	t	2	=C*H*– → (olefinic protons of unsaturated FA)

With the aim of performing a deeper analysis and being able to more reliably identify the compound a two-dimensional homonuclear H correlation spectroscopy (2D H-H COSY) experiment was carried out with the same sample from *E.coli* C41 (pEtDGAT).

Two-dimensional (2D) NMR techniques can be used to simplify the complexity and solve structural problems such as those arising from overlapping of peaks. While 1D spectra are plots of intensity vs frequency (chemical shift), in 2D spectra, made of various 1D experiments, the intensity is plotted as a function of two frequencies, f1 and f2.

The most usual way of representing a 2D spectrum on paper is a contour plot, like the one shown in Fig R-15, in which the intensity of the peaks consists in contour lines drawn at suitable intervals, in the same way as a topographical map. These spectra are always arranged in a way the f2 co-ordinates of the peaks correspond to those found in the normal 1D spectrum, relation that is emphasized by plotting the 1D spectrum alongside the f2 axis.

2D H-H COSY experiments provide information concerning coupled systems. The chemical shift range of each peak is plotted on both axes, corresponding to coupled sets of protons. All off-diagonal peaks indicate magnetization through bound connectivity and that way the coupling network in the molecule can be traced. Coupling between protons that are even three chemical bonds apart can be seen through this technique. Moreover, since diagonal peaks provide no useful information beyond the 1D spectrum they may be removed to clarify the spectra (Keeler, 2011; Silverstein et al., 2005).

Spectra of the 2D H-H COSY experiment carried out with the sample purified form *E.coli* C41 (pEtDGAT) was diagonalized (i.e. the diagonal peaks were removed to clear up the spectra) and made symmetrical. Fig R-15 shows the processed contour plot. Most frequencies were linked, if possible, with those found in the ^{1}H NMR spectra (green low spectra in Fig R-14). The f2 frequencies were then matched to the corresponding f1 frequencies according to the 2D H-H COSY spectra. That way f2 and f1 coordinates are detailed in Table R-4. Those data confirm the correspondence of the spectra with a TAG containing a MUFA. As expected from the assignments indicated in Table R-3, the olefinic protons (peak i') were coupled with the allylic methylenes (peak d'), which simultaneously were coupled with protons of the methylene envelop of the acyl chains (peak b'). Moreover, the H-2 of the glycerol backbone showed significative coupling only with the other protons corresponding to the peaks f' and g'.

This result confirmed the production of TAGs in the model bacteria cell heterologously expressing this enzyme, its dependence on the *in vivo* functionality of the latter and indicated a relevant content in MUFA in the TAG compounds accumulated by the tDGAT-expressing strain, suggesting a predominant ratio of one doble bond (i.e. 2 olefinic protons) per TAG. This proportion is in accordance with the high MUFA proportion previously detected through GC analysis in the same purified fraction.

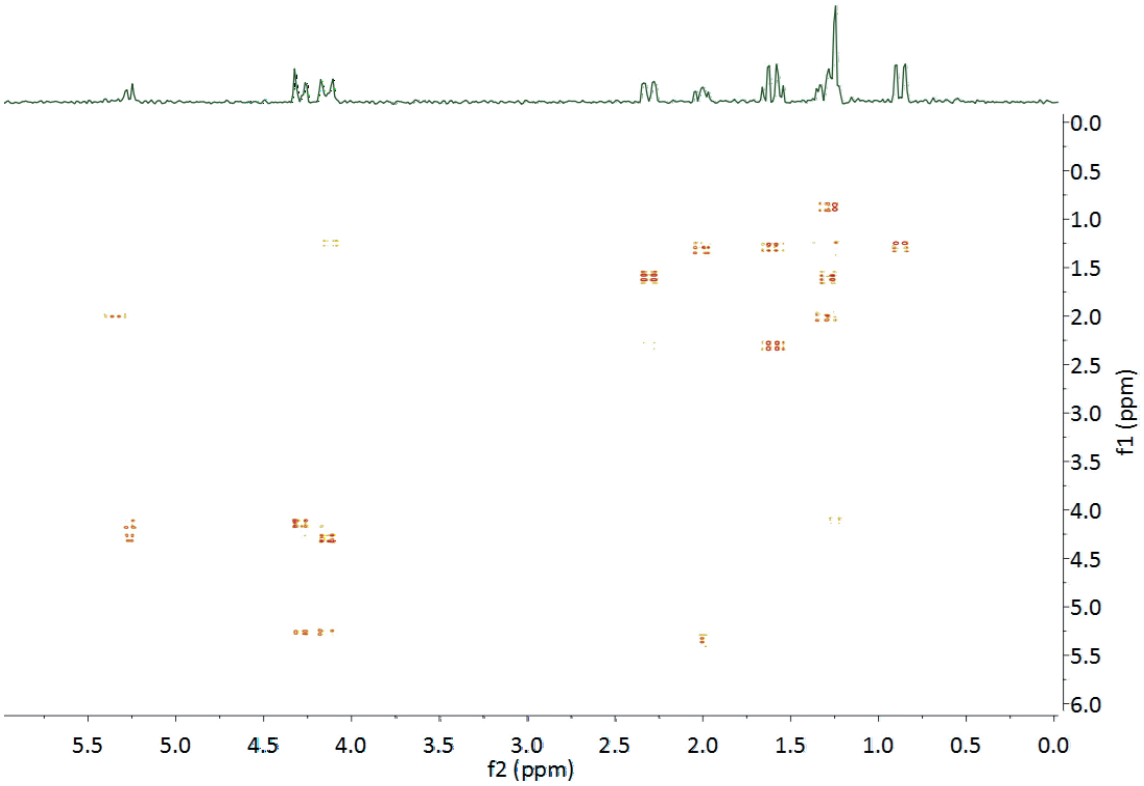

Figure R-15. Contour plot representations of the 0-6 ppm region of the 2D H-H COSY spectrum of the TAG of the 1D ^{1}H NMR ($CDCl_3$, 300.19 MHz) analysis displayed above.

Table R-4. Cross-peaks of the 2D H-H COSY experiment.

Peak Name (agree with figures)	f2	f1	Coupled with:	Normalized integral
a	0.48	-0.37		2.10
b	1.20	0.85	a	4.57
c	1.55	1.27	b	48.04
d	1.97	1.30	b	15.53
e	2.30	1.62	c	269.26
f	4.06	1.28	(b)	1.00
g	4.28	4.12	f	26.13
h	5.24	4.26	g	21.04
h	5.25	4.18	f	23.16
i	5.29	2.00	d	11.58

The vast majority of the TAGs produced by *E.coli* C41 (pEtDGAT) are composed of 1 MUFA and 2 SFAs

TAG production and accumulation has been widely described in *R.opacus* when grown in precise conditions (Alvarez et al., 1996, 2000). In this work, we analized TAG accumulated both by an oleogenic bacteria in stressing conditions and by *E.coli* C41 (pEtDGAT).

INSET V: Technique 4. Ultra Pressure Liquid Chromatography/Mass Spectrometry (UPLC/MS) analysis.

MS has contributed to the solution of many structural problems over the last 60 years using various ionization methods. To analyse a sample by MS we measure the *m/z* ratio of gas-phase ions. Thus, the sample must first be ionized and vaporized. 'Soft ionization' methods such as electrospray (ESI) permit the ionization and vaporization of large, polar, and thermally labile biomolecules, giving rise to beams of ions as a result, which are sampled by the mass spectrometer. Importantly, ESI depends on concentration rather than on mass (Griffiths et al, 2001; Griffiths, 2003).

The TAG fractions from cultures of *R.opacus* grown in RM (without producing TAGs) and grown in MM-gluconate (TAG-producing culture) were extracted from a TLC plate. Both samples were then analyzed by an UPLC/MS coupled system. The base peak ion (BPI) chromatograms confirmed the presence of those molecules only in the second culture (grown under TAG-production conditions, see Fig iv.D). The most abundant species were identified according to the LipidMaps Web Database (Structure Database, LMSD) and are presented here as a bar chart (Fig iv.F).

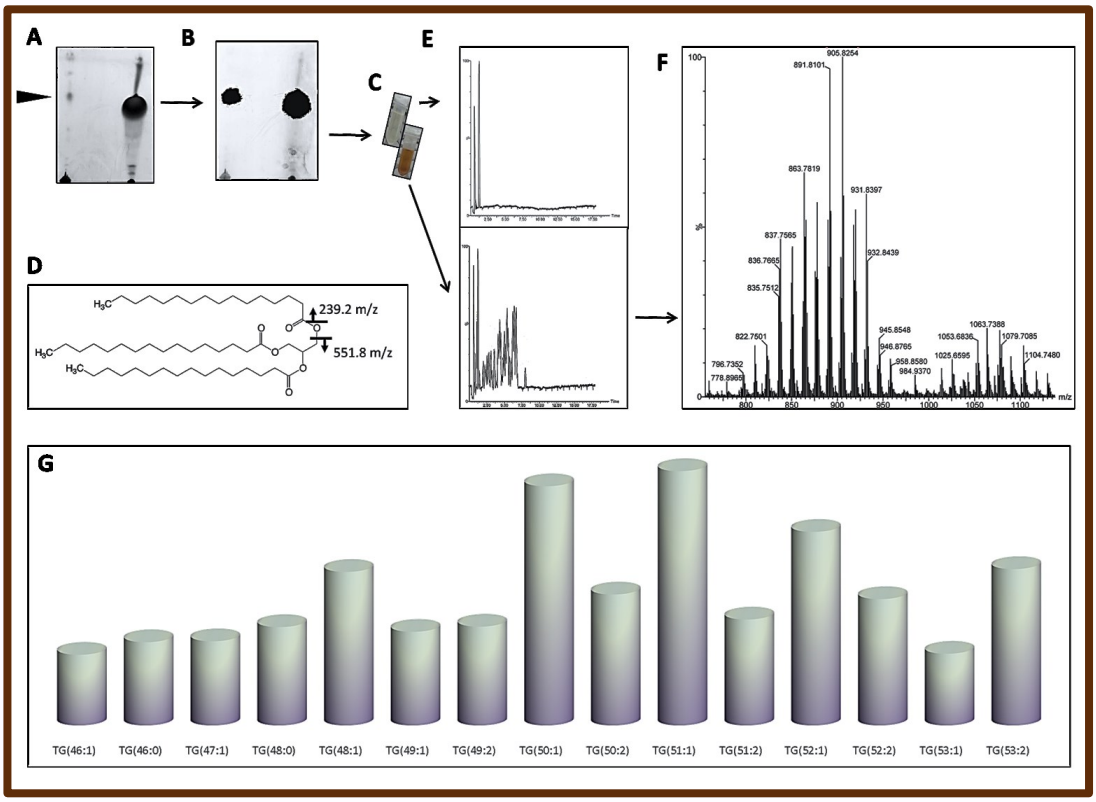

Figure iv. A) Preparative TLC plate showing the separations of the whole lipid extractions of *R.opacus* grown in RM (left) and MM-gluconate (right). The black arrow points to the TAG compounds. B) Silica was scrapped out of the corresponding place in both lanes. C) Lipid compounds were extracted from silica gel. D) BPI chromatograms from UPLC analysis, corresponding to *R.opacus* grown in RM (up) and MM-gluconate (down). E) Extracted ion chromatogram (EIC) of the sample from the TAG-producing culture of *R.opacus*. F) Bar graph showing the main TAGs found in the MM-gluconate culture of *R.opacus*. G) Example of the fragmentation of the TAG tripalmitate during mass spectrometry. Image from Rucker et al., 2013.

Once we tested the method with an oleogenic microorganism (see Fig iv in Inset V), the process was repeated with both the engineered *E.coli* C41 strain carrying tDGAT and the wt bacteria. The analysis by UPLC/MS confirmed the presence of TAG only in the engineered strain (see Fig R-16.A). The EIC of the TAGs present in the extract from the bacteria expressing the tDGAT enzyme showed their diverse nature (Fig R-16.B) whereas a bar chart illustrated the most abundant species found (R-16.C). Outstandingly, a significant quantity seemed to consist of one MUFA and two SFA (see Fig R-16.D).

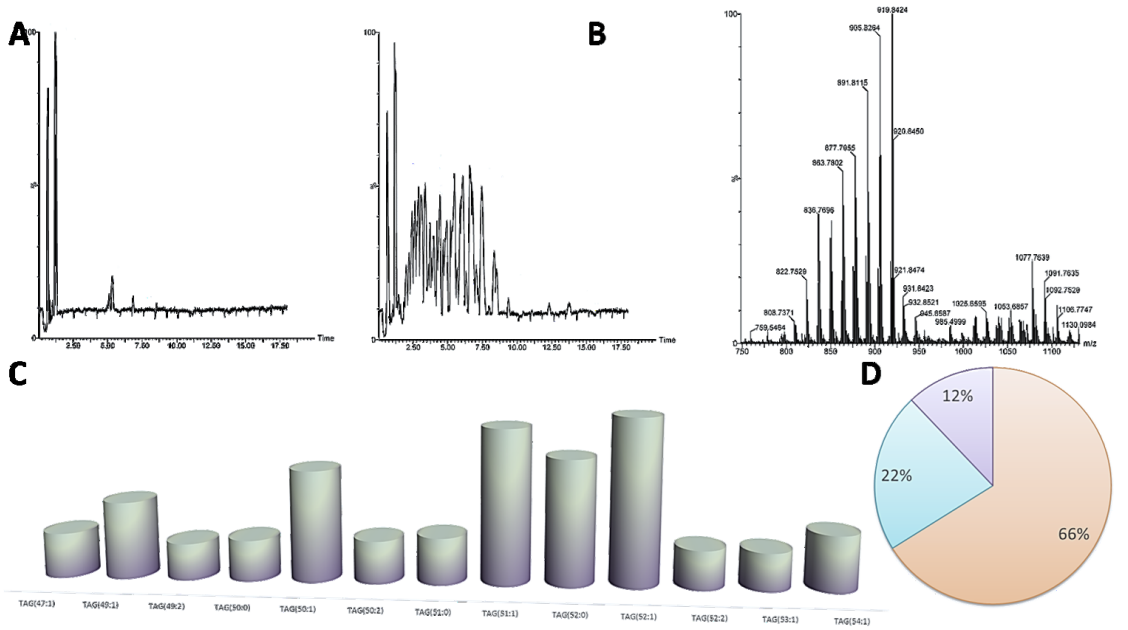

Figure R-16. The accumulation of TAGs in the recombinant strain was confirmed by UPLC/MS analysis. A) BPI chromatogram of extracted TLC-TAG spot of *E.coli* C41 (left) and *E.coli* C41 (pEtDGAT) (right). B) EIC of extracted TLC-TAG spot of *E.coli* C41 (pEtDGAT). C) Main TAGs found in recombinant strain. D) Proportion of TAGs constituted by only 1 MUFA and 2 SFAs (in orange), by 2 MUFAs and 1 SFA (in purple) or by 3 SFAs (in blue) among the preponderant TAG especies found in the engineered strain.

This result correlates well with data obtained from GC analysis, where we observed an important proportion of MUFA among the FA of the TAG purified from *E.coli* C41 (pEtDGAT) (see Fig R-7.C). Data obtained from NMR analysis also suggested this profile of TAGs (containing one double bond per TAG, which can be translated in 1 MUFA and 2 SFA) as predominant in the engineered bacteria.

4.1.1. Improvement of TAG accumulation by positive selection

It is known that natural selection leads to the fixation of advantageous mutations, leading to diverse evolutionary innovations and species differences (Lefébure and Stanhope, 2009). Additionally, directed evolution in the laboratory (adaptative or positive artificial selection) has been proved as a highly effective framework for optimizing or altering the activities of precise individual genes and gene products (Packer and Liu, 2015). Nevertheless, the success of this technique mainly relies on the genetic component of a phenotypic trait (Golding and Dean, 1998). The production of bacterial TAGs has shown to be strongly dependent on the genetic background of the microorganism, both on the ability for keeping the pertinent balance of precursors and specially on the activity of an acyltransferase enzyme (Alvarez, 2016). This high genetic constituent makes of positive selection a possible mechanism to optimize lipid production in bacteria. However, positive selection requires of a high throughput selection method that has not been developed yet for TAG accumulation in bacteria. Thus, we have analyzed the differential behaviour of native and tDGAT *E.coli* cells under different conditions and analytical techniques to find an optimal method for positive selection.

Cell sedimentation

In first place we analysed the different flotability associated to the lipid accumulation. The average buoyancy of a bacterial strain increases with its content in lipids (Devries and Eastman, 1978; Lee et al., 2006). In oleogenic bacteria such as *Rhocococcus* sp., the difference in buoyancy between cultures grown in RM and those grown in lipid-accumulating conditions is easily observed (Wältermann et al., 2000). With the aim of checking wheter the lipid accumulation observed in *E.coli* when expressing the tDGAT was detectable at a first glance, an experiment to test cell sedimentation speed was performed as described in section M-3.6.2. This method might lead to a different strategy for direct evolution (i.e. imposing a selection pressure and select improved variants according to a precise phenotypic trait). However, no significant difference in buoyancy was observed between the engineered bacteria grown in maximum lipid accumulation conditions and the wild type. That was probably due to the very low TAG production yield in the recombinant *E.coli,* still far from the high lipid contents observed in oleogenic microorganisms.

Fluorescence techniques.

Optimization of single-gene products by positive selection requires genetic diversity and carefully designed strategies for selecting functional variants among large numbers of candidates. With respect to the second requirement, high-throughput screenings rely on the rapid assessment of optical features such as colour, fluorescence or turbidity. Thus, the chosen methods should avoid an infrastructure-intensive or a time-consuming nature (Packer and Liu, 2015). Hence, with the purpose of developing a screening method to detect recombinant strains able to produce and accumulate high lipid contents, we first assayed and described the behavior of different tDGAT recombinant strains previously shown to be producing TAG compounds upon staining with fluorescent lipophilic dyes. Then, we optimize a process based on fluorescence measurements for carrying out high-throughput screening of TAG-producing *E.coli* strains in order to identify improved cultures.

One of the most commonly employed selective lipophilic dyes is Nile Red. It binds to intracellular lipids and emits fluorescent light when surrounded by hydrophobic environments. Its excitation and emission spectra varies with solvent polarity, being quenched in aqueous medium. According to Greenspan and coworkers (1985), yellow-gold fluorescence (with an emission maximum at 528 nm) rather than red fluorescence (emission wavelenleghts longer than 590 nm) should be employed for obtaining the best selectivity for cytoplasmic lipid droplets, although the analysis could be performed with either fluorescence. Posterior reports about the Red Nile stained lipid-accumulating cells fluorescence has been detected through filters with longer wavelengths (e.g. Pinzon et al., 2011; Spiekermann et al., 1999). For that reason, this parameter was studied for the experiments presented in this work, considering the detailed preparation protocol in every measurement. In any case, different techniques based on fluorescence *in situ* measurements of Nile Red give us valuable information about the lipid content in both the engineered bacteria and the wild type microorganism (Greenspan and Fowler, 1985; Greenspan et al., 1985).

Bodipy$^{505/515}$ has been proposed as an alternative lipophilic dye to Nile Red. Bodipy$^{505/515}$ was reported to monitor oil storage within live algal cells. This stain, with better permeation abilities, shows a narrower emission spectrum and improved photostability properties (Brennan et al., 2012; Cooper et al., 2010; Govender et al., 2012).

Fluorescence microscopy images show neutral lipid accumulation in *E.coli* strains expressing tDGAT.

TAGs accumulation in the tDGAT recombinant *E.coli* strains tested reminds lipid accumulation in naturally oleogenic bacteria. We have analyzed by fluorescence microscopy the localization of the Nile Red fluorescence in the tDGAT strains to observe the lipid accumulation pattern. The appearance of Red Nile stained *E.coli* cells expressing the enzyme tDGAT through the expression system of the pET vectors have been previously described by Villa Torrecilla (2012). In this work we compared the behavior of this recombinant strain to a different *E.coli* strain carrying the tDGAT gene under a distinct expression system. With that aim, *E.coli* C41 (pEtDGAT) and BW27783 (pBtDGAT*)* were collected 6 hours after over-expression of tDGAT in presence of the dye Nile Red together with the corresponding wild type bacteria as control and microscope slides were mounted and analyzed as described in section M-3.6.2. Fig R-17 shows several

microscopy images of those bacteria. Round inclusions with high fluorescence can only be observed in cells expressing tDGAT (marked with red arrows in Figs R-17.B and R-17.D). As previously presented in this work both recombinant strains are able to accumulate neutral lipids when cultured under similar conditions (see Figs R-1 and R.8). These observations suggest intracellular lipid droplets could be binding most of the dye in these cases, giving rise to a high fluorescence in precise points. In contrast, the fluorescence observed in microscopy images of the corresponding wild type strains (Figs R-17.A and R-17.C) show an homogeneous signal along every bacteria.

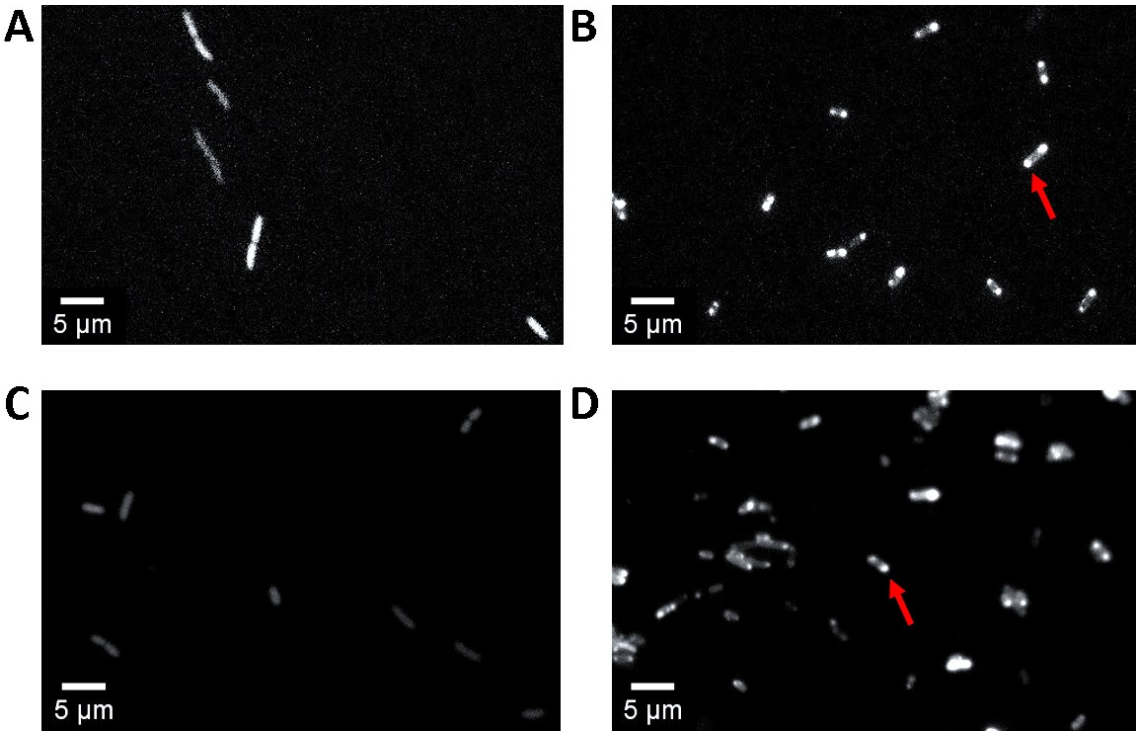

Figure R-17. Fluorescence microscopy images of *E.coli* C41 (A), *E.coli* C41 (pEtDGAT) (B), *E.coli* BW27783 (C) and *E.coli* BW27783 (pBtDGAT) (D), all grown with Red Nile from the induction of the heterologous proteins (and similar timing for the controls). Merged images of all the fluorescence scans acquired are displayed. Red arrows point to round inclusions with high fluorescence in the engineered strains.

Besides, in order to visualize the growth of tDGAT recombinant bacteria, agarose pads were prepared as detailed in section M-3.6.2 with cultures of *E.coli* (pEtDGAT) previously grown with Nile Red (which was added as well at the induction time) and the same culture without dye. The cells were analysed 20 hours after the addition of the inductor (arabinose). Fig R-18 shows some of the microscope images acquired every 20 minutes while bacterial cells were growing on the microscope preparation. It is important to take into consideration that the growth medium employed in the time-lapse experiment here presented is MM, which makes *E.coli* metabolism slower respect to most of the other experiments (performed with LB as culture medium). In the images in Fig R-18 different bacteria seem to be present in the sample, since different shapes can be observed among the Red Nile stained *E.coli* (pEtDGAT) cells. Some bacteria only show the low homogeneous fluorescence typical of *E.coli* C41 wild type cells (see Fig R-17.A) and show cell division along the time of the assay (for instance, those highlighted with a light orange circle). However, other bacteria exhibit round forms with high fluorescence (marked with red arrows) showing the same pattern observed in Fig R-17.B, which suggest that they are accumulating neutral lipids. Nonetheless, we cannot observe any cell division within this group of bacteria. Since the visualization was performed 20 hours after overexpression, a fraction of the bacterial population might have lost the gene codifying for the tDGAT protein, which represents a burden for the cell. In this way, the non-lipid-producing *E.coli* cells behave in the same way than the wt bacteria. In contrast, in the images of the recombinant bacteria without stain (see Fig R-19), very low homogeneous fluorescence was observed. Nonetheless, a slow cell division was noticed in all the bacteria in these images (some example is rounded by a light orange circle).

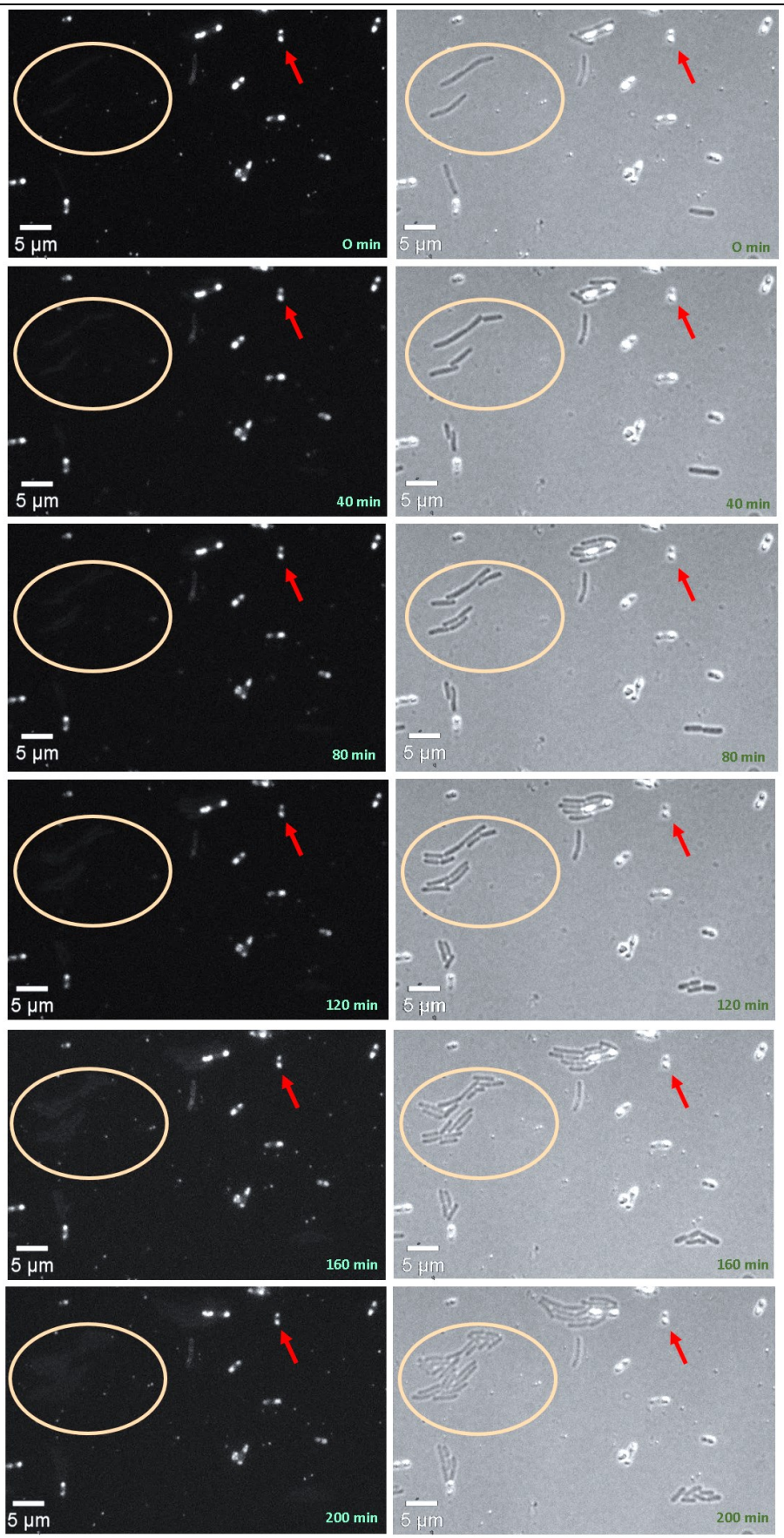

Figure R-18. Time-lapse sequence from Nile Red stained *E.coli* (pEtDGAT) cells. Merged images of all the fluorescence scans (left) and these together with phase-contrast microscopy (right) are displayed at different times. Growing cells are highlighted with a circle and round inclusions with an arrow.

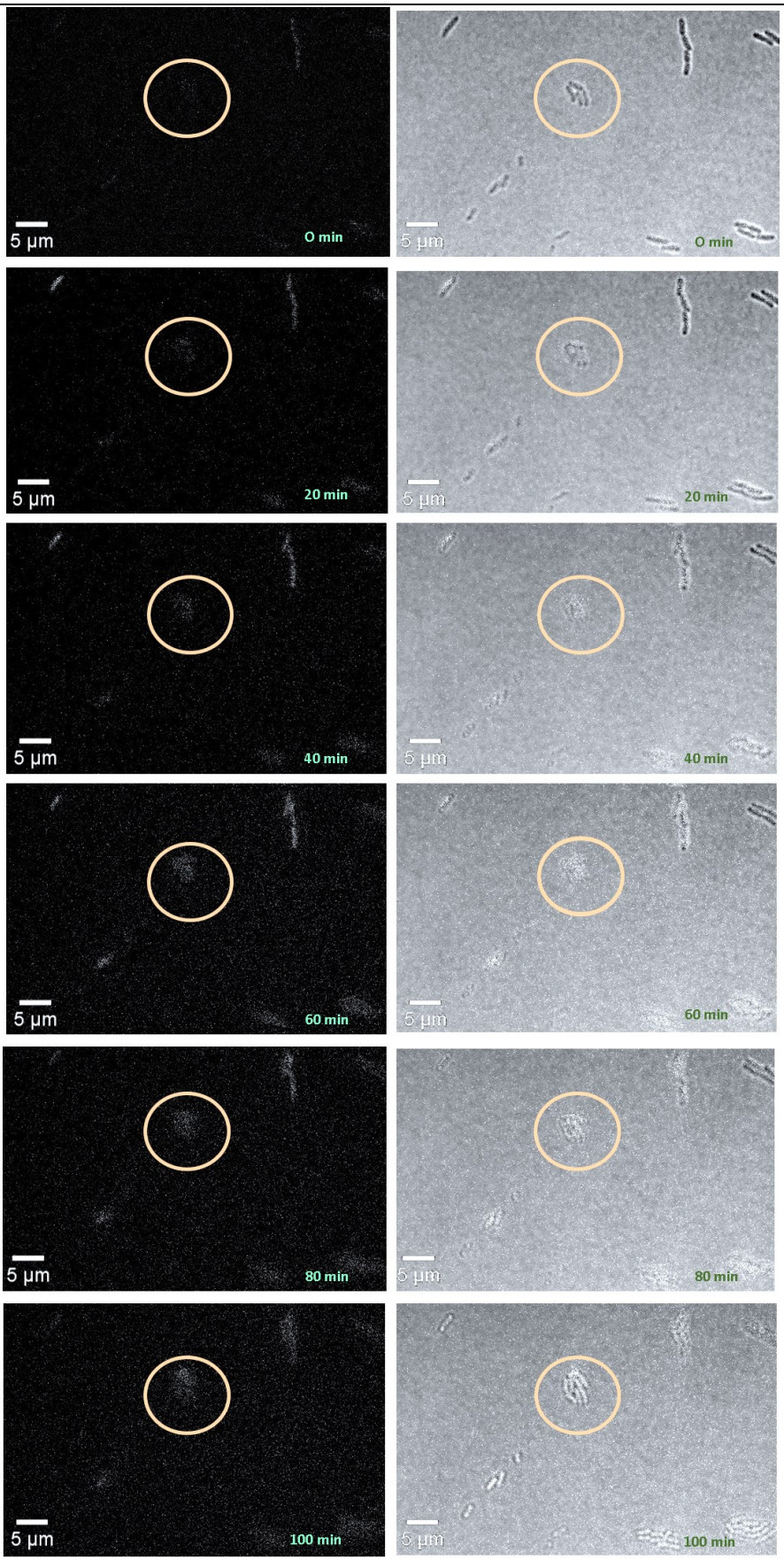

Figure R-19. Time-lapse sequence from *E.coli* (pEtDGAT) cells without stain. Merged images of all the fluorescence scans (left) and these together with phase-contrast microscopy (right) are displayed at different times. Growing cells are highlighted with a circle and round inclusions with an arrow.

Flow cytometry might be employed to detect lipid accumulation in *E.coli* strains expressing a tDGAT.

With the aim of assessing the employment of flow cytometry to measure the fluorescence in bacteria stained with lipophilic dyes, we tested some strains whose lipid content had been evaluated through other techniques (e.g. see Fig R-1). Fig R-20 shows a significant increment in the fluorescence detected by flow cytometry in *E.coli* C41 (pEtDGAT) over the *wt* strain. Red fluorescence (measured at an emission wavelength of 695 nm) detected in bacteria stained with Red Nile increases from 1.1% of the events measured in the sample corresponding to the wt strain to 34.5% in the engineered strain (Fig R-20 left). Green fluorescence (emission detected at 530 nm) quantified in bacteria stained with Bodipy$^{505/515}$ augments from 23.8% to 75.3% (Fig R-20 right). The increase in the events detected as fluorescent in the recombinant strain accumulating TAGs was, therefore, higher than 30% in both analysis, which roughly matches with the TAG increment estimated by densitometric evaluation of TLC analysis (see section R-4.1.1).

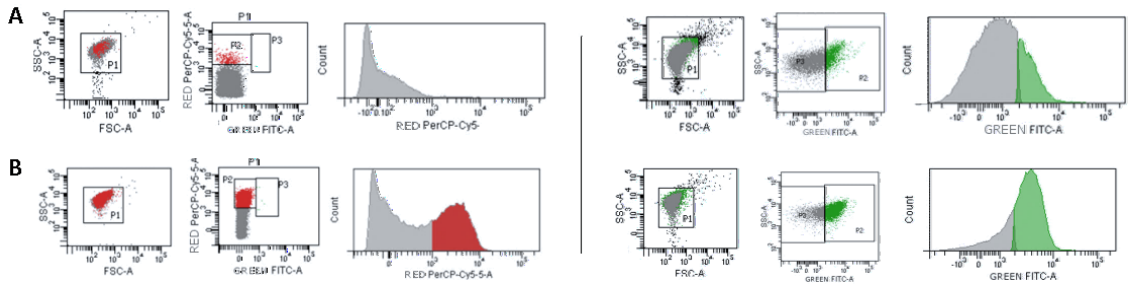

Figure R-20. Fluorescence emitted by stained bacteria treated with a lipophilic dye correlates with the expression of tDGAT in bacteria. Images of cytometry analysis of *E.coli* C41 wt (A) and *E.coli* C41 (pEtDGAT) cultures (B) grown with the dyes Nile Red (left) or Bodipy (right) for 20 h after induction of the cells with IPTG.

Monitoring of the lipid production in the engineered *E.coli* strain through fluorescence spectroscopy

For evaluation in continuous of TAG accumulation in *E.coli* strains expressing the enzyme tDGAT we used Nile red fluorescence spectroscopy. Taking advantage of the photostability of the dye (Greenspan et al., 1985), we have observed that lipid production and accumulation in *E.coli* strains expressing the enzyme tDGAT can be observed along the time through Nile Red staining. Fig R-21.A shows the overlapping of the fluorescence measurements obtained every 20 minutes from different *E.coli* cultures. The lipophilic dye was added to half of those cultures 5 hours and 30 minutes after the beginning of the experiment (black arrow indicates this time point in the graph), and the plate was further incubated in the fluorimeter for almost 20 more hours (see sections M-3.4.2 and M-3.6.2). The model strain *E.coli* MG1655 was employed as control strain while the TAG-accumulating engineered strain *E.coli ΔfadE* (pBoRtDGAT) showed the effect provoked by the overexpression of the tDGAT enzyme. According to the data obtained, the induction of the overexpression of tDGAT (with the addition of arabinose also at 5 hours and 30 minutes) sparked the fluorescence detected at 620 nm in the latter culture. This analysis correlates with the result obtained from TLC densitometric analysis of a tDGAT expressing strain showing a rapid production of neutral lipids within a short overexpression time (see section R-4.1). The neutral lipid content stabilizes around 10 hours in this case. However, as pointed out in the previous monitoring experiment (time-lapse fluorescence microscopy), it is important to remark the timing is not comparable with other results since this experiment was carried out in MM, which implies a slower bacterial metabolism. In Fig 21.B we can observe by TLC analysis of the two strains employed, cultured in the same media, that MG1655 did not produce TAG while *E.coli ΔfadE* (pBoRtDGAT) accumulated these neutral lipids.

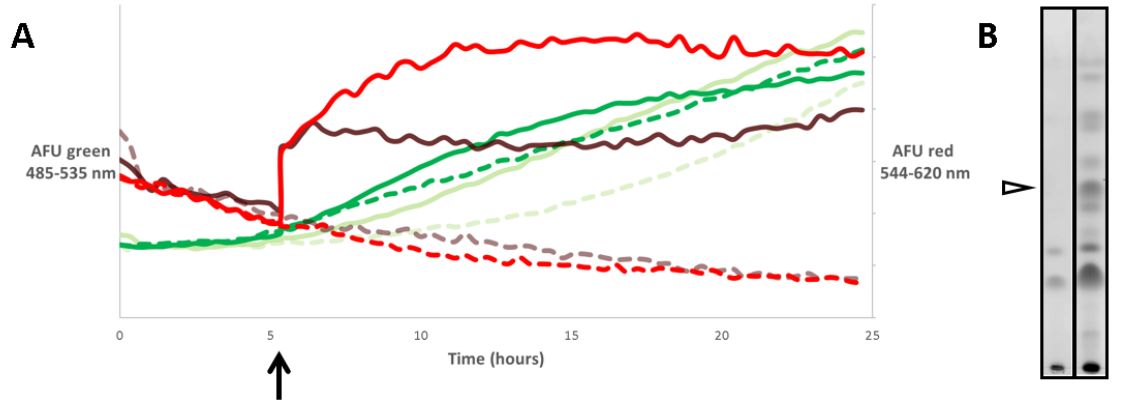

Figure R-21. A) Monitorization of lipid production in the TAG-accumulating engineered strain *E.coli ΔfadE* (pBoRtDGAT). Solid lines correspond to measures from cultures where Red Nile was added at the time indicated with the black arrow, while dashed lines represent the measures from the cultures without the lipophilic dye. The black arrow points as well at the time when the overexpression of the protein tDGAT was induced in the corresponding cultures. Red and dark green lines correspond to cultures of *E.coli ΔfadE* (pBoRtDGAT) whereas brown and light green lines correlates to values from *E.coli* MG1655. Thus, "green" (485-535 nm) and "red" (560-620 nm) fluorescence measures are coloured in green and red tones, respectively. Abbreviations: AFU, Arbitrary fluorescence units. Average of four experiments were taken into account for every data line. B) TLC analysis of the negative control *E.coli* MG1655 (left) and the TAG-producing *E.coli ΔfadE* (pBoRtDGAT) (right). The white arrow point to the migration distance of the TAGs.

Optimization of a fluorescence technique for the detection of *in vivo* TAG accumulation in *E.coli*: tDGAT expression in Keio collection.

Detection methods following lipid extraction such as TLC, GC or NMR are slow. Besides, the employment of microscopy techniques for observing neutral lipid accumulation in bacteria is also time-consuming. However, the observed correspondence between fluorescence and accumulation of neutral lipids when treating cultures with lipophilic stains such as Red Nile set the basis for the development of a high throughput analysis method that might allow an efficient optimization of the oil production in bacteria and exceed the yields obtained to the moment. Moreover, punctual measurements of the fluorescence emitted by different cultures avoid any bias related to the photostability of the dye. Based in protocols already developed with neutral lipid-producing algae (Cagnon et al., 2013; Chen et al., 2009), several experiments were performed with the aim to optimize this technique for the engineered bacteria.

On one hand, a small number of *E.coli* cultures expressing or not tDGAT were employed to set the main parameters for posterior fluorescence measurement in the fluorimeter where larger numbers of samples would be tested. This preliminar lower amount of cultures was grown in Erlenmeyer flasks or falcon tubes, allowing the performance of a parallel analysis through traditional methods such as TLC to validate the results obtained. This way, Red Nile was chosen as the most appropriate dye for rapidly distinguishing stained strains with high neutral lipid content, rather that Bodipy, since the range of fluorescence values between positive and negative controls was wider with Red Nile, as Fig R-22 illustrates. Within Red Nile experiments, the preferred light filter to detect fluorescence was 560-620 nm (red fluorescence, see Fig R-22.A).

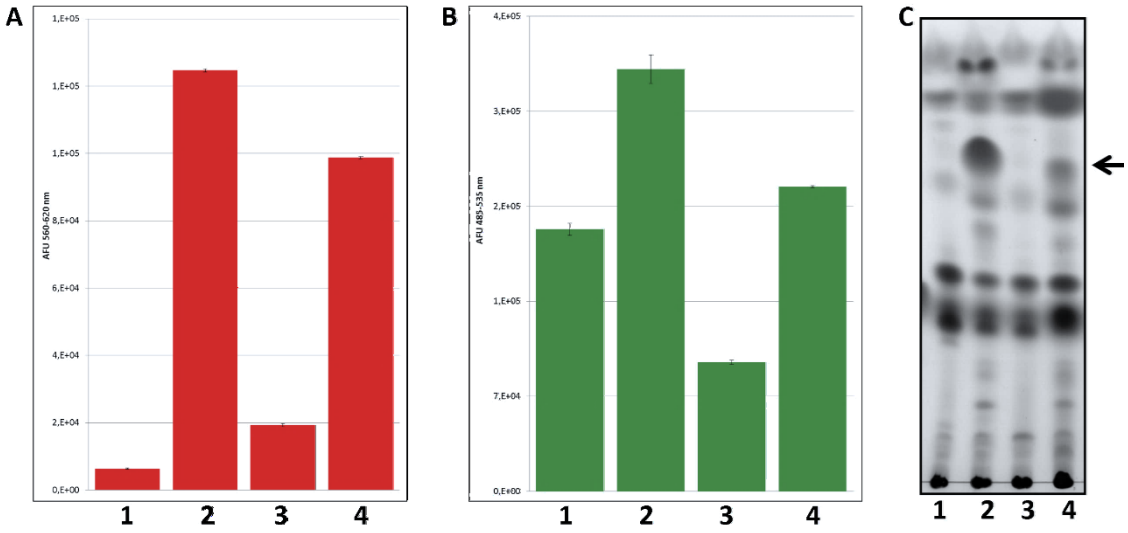

Figure R-22. Bar charts showing red fluorescence (560-620 nm) average measurements from cultures stained with 0.5 µg/ml of Red Nile (A) and green fluorescence (486-535 nm) from cultures stained with Bodipy (B). Columns correspond to the strains *E.coli* C41 (1), *E.coli* C41 (pEtDGAT) (2), *E.coli* BW27783 (3) and *E.coli* BW27783 (pBtDGAT) (4) induced as convenient for each strain. Error bars correspond to three experiments. AFU: Arbitrary Fluorescence Units. C) TLC plate showing the neutral lipid profile of the lipid extracts from the cultures used for the fluorescence spectroscopy experiments. Black arrow points to the TAGs. AFU: Arbitrary fluorescent units.

The protocol for staining the samples was then tested. Staining just before measuring fluorescence was seen to be more appropriate than growing the cultures with the dye. Moreover, the best staining procedure consisted of pelleting the sample and resuspension in a solution of 25% DMSO in PBS containing 0.5 µg/ml of Red Nile- After 20 minutes incubation at room temperature with shaking and centrifugation, the stained pelleted sample was resuspended in the same solution without dye. In Fig R-23 we can observe the wide range between the fluorescence values obtained after this last wash step.

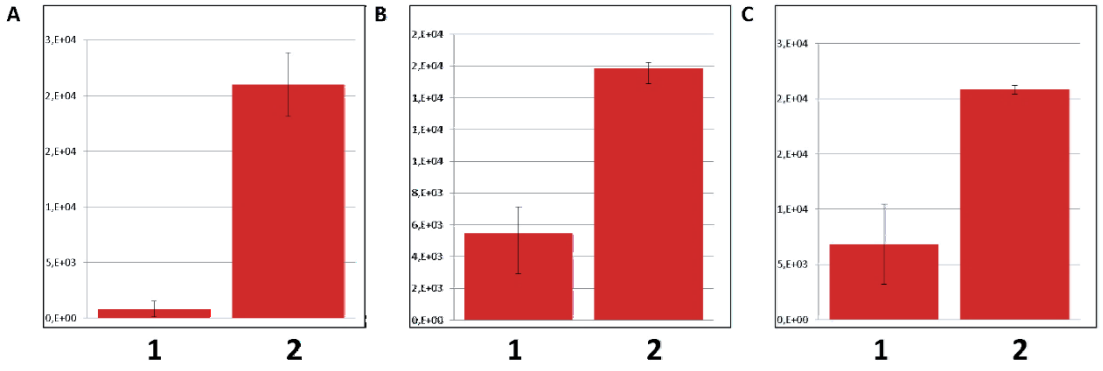

Figure R-23. *E.coli* BW27783 (1) and *E.coli* BW27783 (pBtDGAT) (2) stained with Red Nile in a solution of 25% DMSO in PBS and finally resuspended in the same solution without dye (A), stained with Red Nile in a solution of 25% DMSO in PBS and resuspended in a solution of 50% DMSO : PBS (B) and stained with Red Nile in PBS and resuspended in PBS (C). Bar errors correspond to two independent experiments.

Interestingly, the increase in the fluorescence detected in the strains *E.coli* C41 (pEtDGAT) and *E.coli* BW27783 (pBtDGAT) respect to their respective wt bacteria is higher than 30%, which supports the results obtained by flow cytometry and TLC densitometry.

Finally, 96-well microtiter plates were employed to carry out large-scale experiments in similar conditions. In Fig R-24 an example of the processed data of a high-throughput experiment performed as explained can be observed. With the objective of detecting gene deletions affecting tDGAT functionality, TAG production was assessed in a collection of *E.coli* strains with different single-gene deletions (the Keio collection) carrying the WS/DGAT enzyme. For constructing these strains, the plasmid pBoRtDGAT (a plasmid containing the gene for the protein tDGAT and the *oriT* of R388) was conjugated to different strains from the Keio collection through the plasmid pSU711 (an *oriT*-deficient derivative of the conjugative plasmid R388 able to mobilize plasmids with this *oriT;* see Fig R-9). Subsequently, the cultures were incubated in covered microtiter plates at 37°C with 80 rpm-shaking and the expression of the heterologous protein was induced with arabinose. The red fluorescence emitted by each culture was measured through fluorescence spectroscopy after staining with Red Nile. *E.coli* BW27783 and *E.coli* BW27783 (pBtDGAT) were employed as control strains for all experiments with Keio strains due to the more similar genetic background and tDGAT overexpression system compared to the more efficient TAG producer *E.coli* C41 (pEtDGAT). According to the bar graph displayed in Fig R-24 as example of the results of this experiment, the fluorescence values obtained from the recombinant strains assayed were similar or lower than the TAG-producing strain used as positive control, *E.coli* BW27783 (pBtDGAT). This indicates that a gene deletion related to an enhancement of TAG production was not found among the tested candidates. Nevertheless, the utility of this method for detecting a recombinant strain with improved production of TAG production among genetically diverse bacteria is proved in this work. Hence, this might strongly facilitate further research on the optimization of this process by means of large-scale experiments.

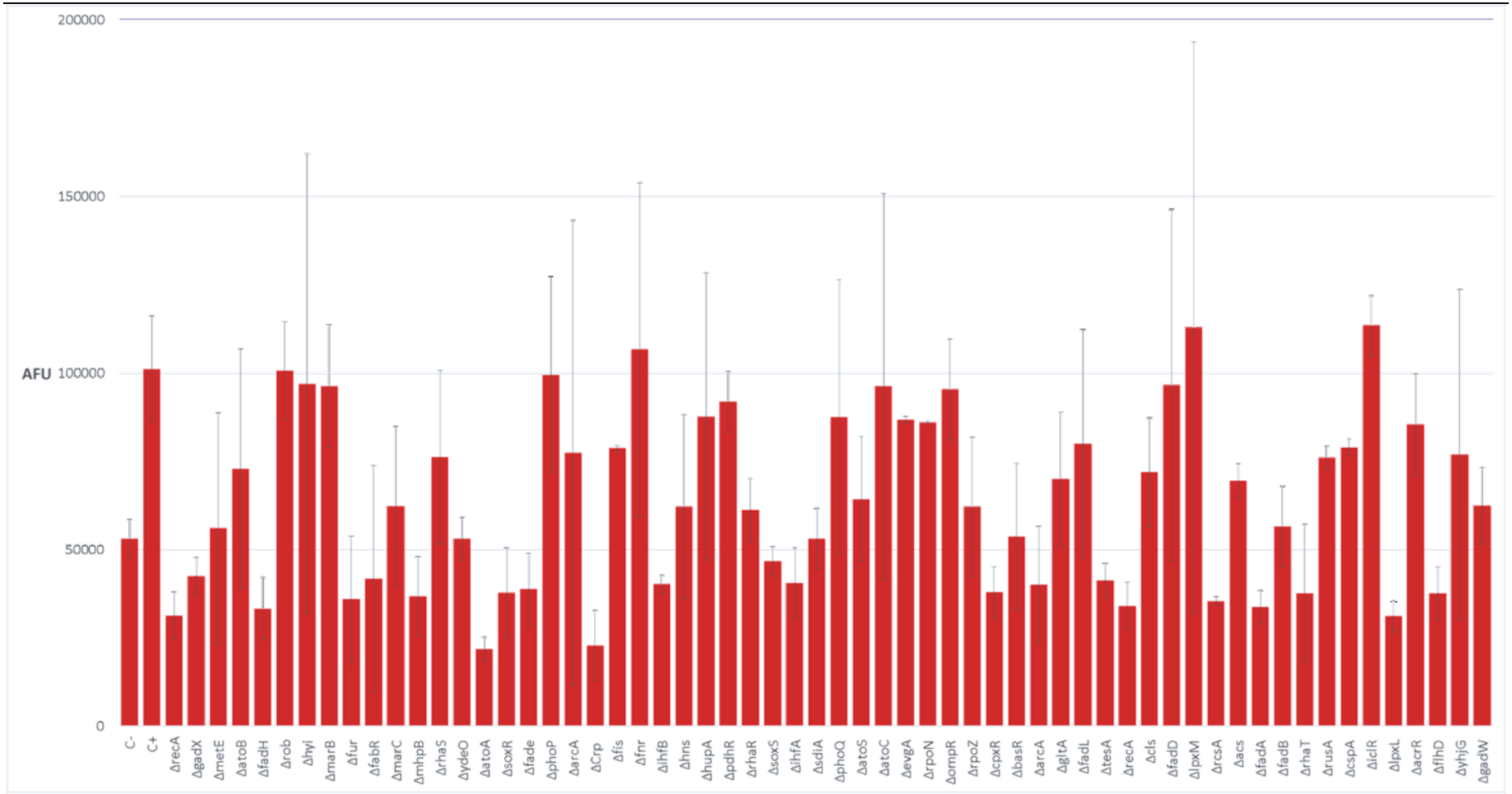

Figure R-24. Bar graph with the processed data from red fluorescence measurements of a set of Keio strains carrying the enzyme tDGAT after their culturing and staining with Red Nile. C+ and C- correspond to positive and negative controls, respectively. In the rest of the samples, only the gene deletion is indicated, since all of them are *E.coli* bacteria belonging to the Keio collection carrying the plasmid construction pBoRtDGAT. AFU: Arbitrary fluorescent units.

4.2. PUFA production in *E.coli*.

The importance of the identification and development of new processes for the production of PUFA was discussed in section I-1.2.2. Besides, the proteobacteria *E.coli* is generally seriously considered for the production of any commercially interesting compound, due to its extensively documented metabolism, its simplicity to be genetically manipulated and its suitability for industry. Hence, the production of these PUFA by using this model bacteria as biofactory is an attractive and promising target that requires important research efforts.

As explained in section I-1.1.1, it is known that *E.coli* is naturally capable of producing ω-7 FA such as PO and VC through an anaerobic pathway (Heath, Richard J. et al., 2002). However, the production of PUFA requires more complex processes using precise enzymes that this bacteria lacks.

In the present work, genetic engineering tools are employed to include these new genetic abilities into *E.coli* from two different approaches covering the two pathways for PUFA biosynthesis described in the introduction (section I-1.1.1).

4.2.1. Heterologous expression of desaturases Δ9, Δ12 and Δ15 in *E.coli* .

The aerobic pathway for the biosynthesis of PUFA employs a series or desaturases and elongases for the production of PUFA using the UFA products of FAS as substrates. The first UFAs in this pathway are OA, LA and ALA, three FA with 18 carbons in length and subsequent 1, 2 or 3 unsaturations (see Figs I-8 and I-31). The enzymes responsible for the catalysis of these unsaturations are the Δ9 desaturase and the methyl-end desaturases Δ12 and Δ15, respectively.

With the aim of providing *E.coli* with the ability for producing EFAs, the bacteria was transformed with pET-derived plasmids containing the genes coding for these enzymes in the cyanobacteria *Anabaena variabilis* ATCC 29413 (the main characteristics of these genes and the enzymes they codify are detailed in Table R-5).

Table R-5. Length of desaturases genes in *Anabaena variabilis* and length and molecular weight of the codified proteins.

Enzyme	Gene DNA length	Number of amino acids	Protein MW	GI (NCBI)
Δ9 desaturase	819 pb	272	31,35 kDa	75910410
Δ12 desaturase	1053 pb	350	41,37 kDa	75910409
Δ15 desaturase	1080 pb	359	41,99 kDa	75910408

The presence of the constructed plasmids from *A.variabilis* in the recombinant *E.coli* strains was confirmed by PCR (see in Fig R-25).

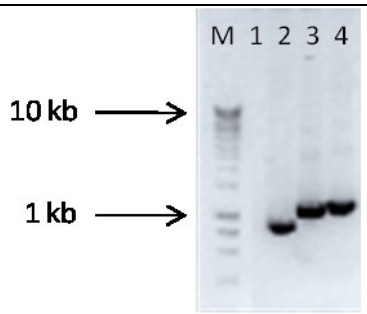

Figure R-25. DNA electrophoresis gel showing the results of the PCR testing of the recombinant *E.coli* strains carrying desaturases genes from *A.variabilis*. PCR was performed with the universal primers T7/pT7. Lane M shows Hyper Ladder DNA Marker (Bioline) and 1 the negative control of the PCR reaction (sterile distilled H_2O). Lanes 2-4 show PCR bands corresponding to the gene fragments flanked by those primers in the pET3a vector: 2, *E.coli* C41 (pEΔ9des); 3, *E.coli* C41 (pEΔ12des) and 4, *E.coli* C41 (pEΔ15des).

The FA content of every culture was then checked though GC analysis. However, no differences were found among the chromatograms. Since *E.coli* is not able to synthesize OA spontaneously, we tested the lipid composition after culturing bacteria with exogenous addition of this FA. As observed in Fig R-26, the lipid profile in the three recombinant strains remained similar. The main FA exogenously added (OA and LA, marked with arrows in the images) appear in all chromatograms in a similar proportions (46% and 9%, respectively), while PA (approximately 12% in all the three samples) and other FA typically occurring in wt *E.coli* FA profiles appeared in similar proportions in all the samples tested. This data indicates that none of the heterologous desaturase protein was properly functioning in this conditions.

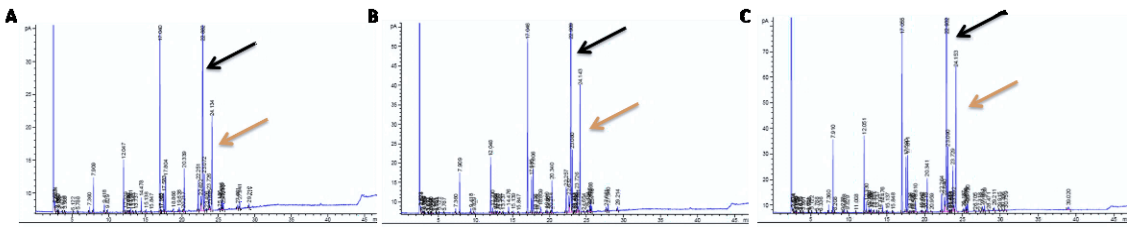

Figure R-26. GC chromatograms of the recombinant *E.coli* strains carrying desaturases genes from *A.variabilis*. A) *E.coli* C41 (pEΔ9des); B) *E.coli* C41 (pEΔ12des) and C) *E.coli* C41 (pEΔ15des). Black arrow points to OA and orange arrow to LA, both due to external supplementation.

4.2.2. Heterologous expression of the DHA-producing cluster Pfa and the enzyme tDGAT in *E.coli*

The alternative pathway that allows the formation of LC-PUFA implying less chemical reactions and energy relies on a multienzymatic complex codified by a large gene cluster. As explained in section I-1.2.2, the production of LC-PUFA such as DHA has already been achieved in *E.coli* through its transformation by means of genetic engineering tools with the genes for the *Pfa* synthase from the marine proteobacteria *M.marina* MP-1. This way, a maximum DHA production yield was obtained in cultures grown at 15°C but no DHA was detected in recombinant *E.coli* cultures grown above 25°C (Orikasa et al., 2006b). Moreover, Orikasa and co-workers constructed in 2009 the plasmid pDHA4, carrying the five genes responsible for the production of the LC-PUFA in one genetic construction, by employing the previous constructions pDHA3 (carrying the four pfaA-D genes from *M.marina*, Orikasa et al., 2006b) and pET21a::*pfaE* (also carrying a gene from *M.marina* Orikasa et al., 2006a).

Since the complete sequence of the vector pDHA4 has not been published, we decided to sequence the plasmid pDHA4 kindly provided by Dr. Okuyama (Hokkaido University, Japan). As illustrated

in Fig R-27, the high-throughput procedure revealed a 27,336 bp length DNA plasmid construction carrying both the 864 bp DNA gene *pfaE* from *M.marina* MP-1 [Genbank: AB262366.1] under the T7 promoter and terminator from the expression vector pET21a [GenBank: EF456737.1] and a 22,471 pb DNA fragment from the gene cluster [Genbank: AB025342.2] containing the four genes *pfaA-D* from the same bacteria.

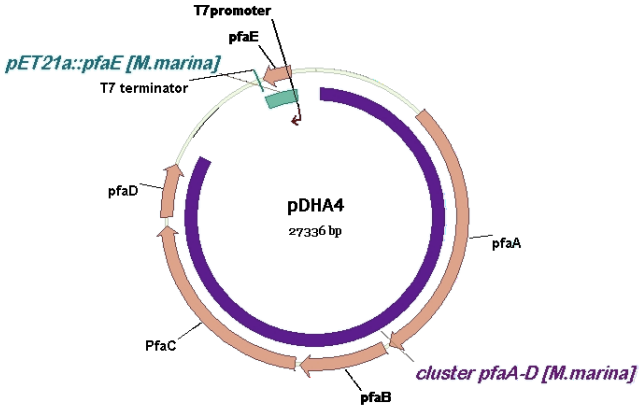

Figure R-27. Map of the plasmid pDHA4 that contains a fragment of the expression vector pET21a with the gene *pfaE* from *M.marina* MP-1 (in green) and the fragment with 100% homology with the *pfaA*-D cluster from the same bacteria (in purple). The five genes responsible for the production of DHA are colored in orange.

Other microorganisms such as certain thraustochytrids naturally produce a great proportion of TAGs enriched in DHA at higher temperatures (25-30ºC; Raghukumar, 2008). Thus, a possible strategy for developing an easily culturable microorganism with elevated yields of DHA production consists of combining its DHA biosynthesis with TAG accumulation. That way, DHA molecules could remain protected from divert into membrane phospholipids, while neutral lipids could act as a sink, enhancing DHA biosynthesis. Therefore, with this aim, in this work *E.coli* was co-transformed with both the plasmid pEtDGAT (carrying the gene responsible for the formation of neutral lipids such as TAGs in bacteria) and pDHA4. The presence of both genetic constructions was confirmed through visualization of bands in electrophoretic gels showing PCR products in the expected position. In Fig R-28 we can observe the expected PCR product sizes for *tDGAT* or *pfaE* fragments in the corresponding strains or purified DNA.

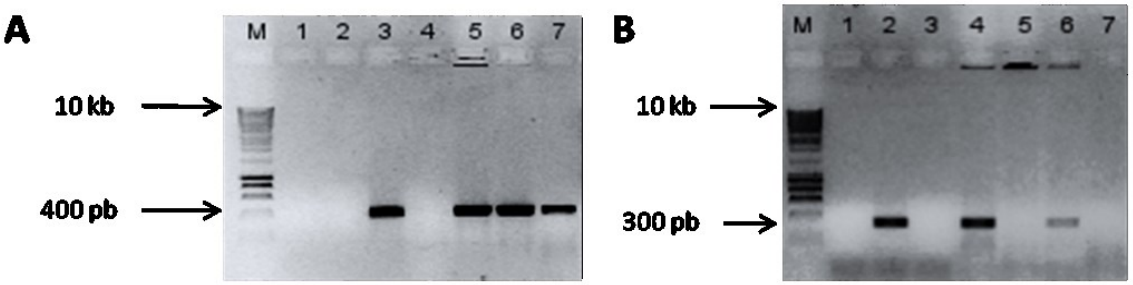

Figure R-28. DNA electrophoresis gels showing the results of the PCR testing of the recombinant *E.coli* strains carrying the gene for the synthesis of TAGs and/or the gene cluster for the synthesis of DHA. A) Products of the PCR performed with the primers mm_*pfaE* (against the 425 bp *pfaE* gene from *M.marina* carried by the plasmid pDHA4. B) Products of the PCR carried out with the primers *tDGAT*_fragment (against a 326 bp DNA fragment of the gene *tDGAT*). In both images: lane M shows Hyper Ladder DNA Marker (Bioline) and 1 the negative control of the PDR reaction (sterile distilled H_2O). Lanes 2-7 show bands corresponding to: 2, positive control I (purified pEtDGAT); 3, positive control II (purified pDHA4); 4, *E.coli* C41 (pEtDGAT); 5, *E.coli* C41 (pDHA4); 6, *E.coli* C41 (pEtDGAT + pDHA4) and 7, purified genomic DNA from *M.marina* MP-1.

SDS-PAGE gels exhibit the over-expression of tDGAT depending on the induction conditions in every culture grown above 21.5°C (see Fig R-29). As expected, a higher temperature such as 37°C seems better for a fast over-expression of this enzyme, independently of the presence of the Pfa gene cluster. However, the over-expression of the five proteins codified by the Pfa gene cluster was not visually clear in the gel images. Probably that was due to the large size, some of them could have been fragmented by proteolysis during the analysis.

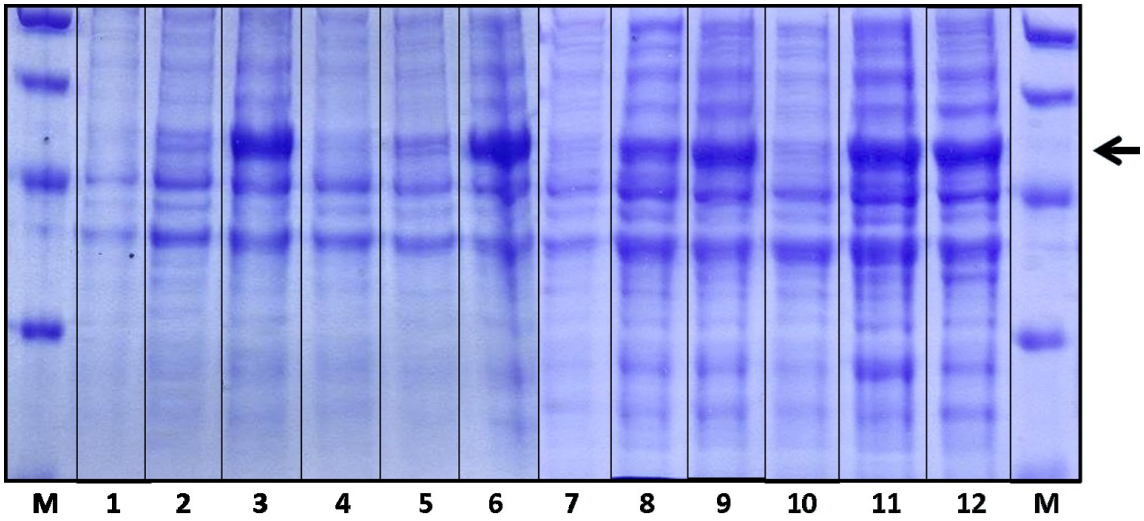

Figure R-29. SDS-PAGE gel showing the whole cellular lysates of different cultures of *E.coli* C41 (pEtDGAT + pDHA4) collected 1.5 hours (lanes 1-3), 3.5 hours (lanes 4-6), 5 hours (lanes 7-9) and 23 hours (lanes 10-12) after addition of the inductor IPTG. Lanes 1, 4, 7 and 10 correspond to cultures grown at 15°C; lanes 2, 5, 8 and 11 to cultures grown at 21.5°C and lanes 3, 6, 9 and 12 to cultures grown at 37°C. The Low Range Protein Marker was loaded on the first and final lanes (M). Black arrow points to the predicted molecular weight of the protein tDGAT (approximately 52 kDa).

Both the functionality of the tDGAT (Moncalián et al., 2014; Villa Torrecilla, 2012) and the effects of the Pfa genes from *M.marina* (see section I-1.2.2 for a list of these genes; (Orikasa et al., 2006b) have been separately reported in *E.coli*. Hence, we first confirmed that *E.coli* C41 (pEtDGAT + pDHA4) was producing either TAG or DHA in the optimal growth conditions for each proccess in spite of carrying the additional plasmid construction. In Fig R-30.A we can observe the TAG production of the engineered strain at 37°C, and in Fig R-30.B we see *E.coli* C41 (pEtDGAT + pDHA4) produces DHA at 15°C.

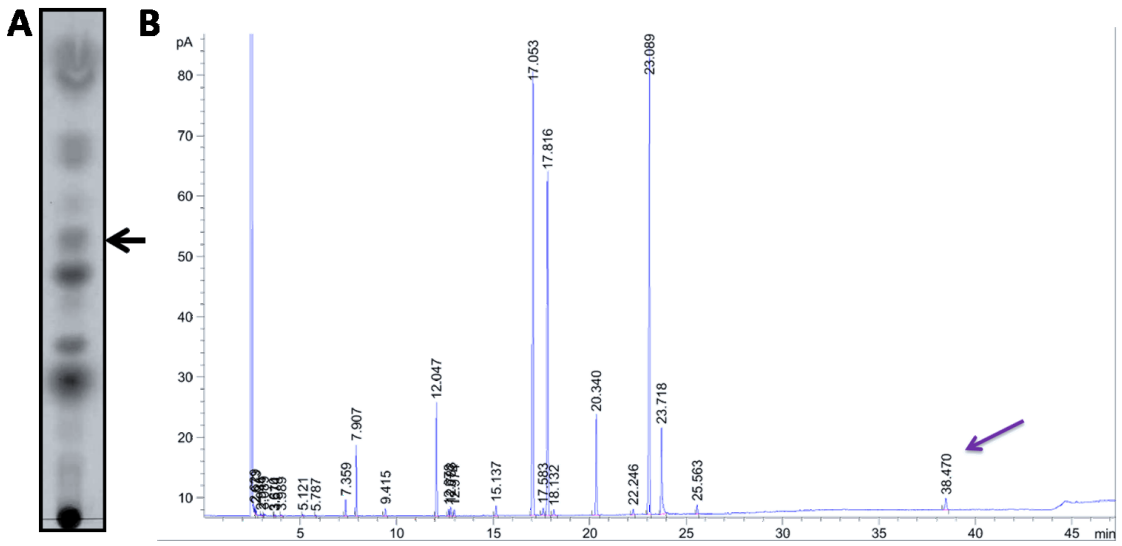

Figure R-30. A) TLC plate showing the lipid profile of the *E.coli* C41 (pEtDGAT + pDHA4) cultured at 37°C. B) GC chromatogram from the same strain grown at 15°C. The purple arrow points at the signal corresponding to DHA, representing a 1.14%.

Thus, in an attempt to find common conditions for the production of both lipid compounds simultaneously, the engineered strain *E.coli* C41 (pEtDGAT + pDHA4) was cultured at several temperatures. Nonetheless, neither DHA was detected with growth temperatures above 21.5°C nor TAG production was observed below this temperature. Fig R-31 presents analysis for both compounds in *E.coli* C41 (pEtDGAT + pDHA4) cultured at this temperature. Fig R-31.A shows TAG compounds can be found in the engineered strain, while Fig R-31.B shows a GC chromatogram of its lipid extract where a low concentration of DHA (0.36% of the whole FA pool) is observed. Moreover, a comparison of neutral lipid production in *E.coli* C41, in *E.coli* C41 (pEtDGAT) and in *E.coli* C41 (pEtDGAT + pDHA4), all cultured at 21.5°C, was carried out through both Nile Red and Bodipy$^{505/515}$ staining and flow cytometry. As we can observe in Fig R-31.C, red fluorescence detected in bacteria stained with Red Nile increased from 1.5 % in the wt strain to 26 % in the *E.coli* C41 (pEtDGAT), but only to 7.4 % in *E.coli* C41 (pEtDGAT + pDHA4). In Fig R-31.D green fluorescence quantified in bacteria stained with Bodipy$^{505/515}$ is shown. From a 12 % of the events detected as fluorescent in the wt bacteria, an augment to 48.2 % was measured in bacteria over-expressing only the tDGAT protein. However, only a 33.6 % of the events were quantified as fluorescent in the engineered bacteria expressing the enzymes of both biosynthesis pathways). This suggests that the activity of the tDGAT is lowered by the reduced expression of the Pfa gene cluster. Finally, no DHA was detected in the GC analysis of the TAG-TLC spots from the engineered strain, which could be due to the low DHA concentrations obtained, due to a no-incorporation of DHA into the TAG present in the strain or due to the DHA degradation possibly suffered during a long analysis procedure implying lipid extraction. Due to the high number of double bonds of this FA, it might be easily oxidized, which implies a more difficult manipulation.

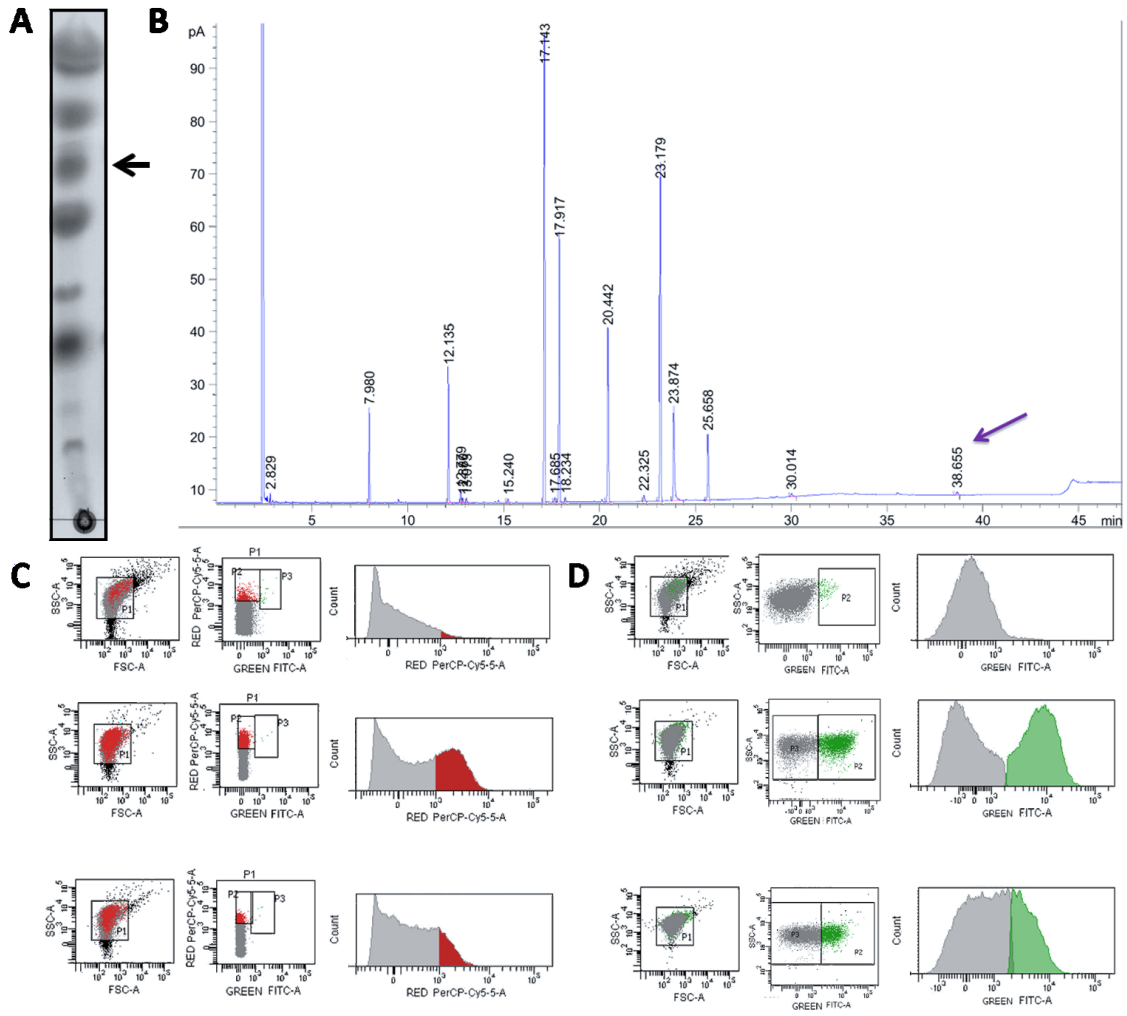

Figure R-31. TLC plate (A) and GC chromatogram (B) of the lipid extract of *E.coli* C41 (pEtDGAT + pDHA4) cultured at 21.5°C. The purple arrow points at the signal corresponding to DHA, representing a 0.36%. Flow cytometry analysis were also performed at this temperature throw Red Nile (C) and Bodipy staining (D) and comparisons of the results obtained with cultures of *E.coli* C41 (upper line), *E.coli* C41 (pEtDGAT) (middle line) and *E.coli* C41 (pEtDGAT + pDHA4) (lower line) are presented here.

4.3. New insights on WS/DGAT characterization

As explained in the section I-1.1.3, proteins belonging to the WS/DGAT family have been shown to be distributed along the different kingdoms, from prokaryota to protists, plants and animals (Röttig and Steinbüchel, 2013). However, the current knowledge about their structure and catalytic mechanism is still limited. The great biotechnological potential of these proteins makes a deeper research on them of major importance to contribute to the development of improved enzymes through protein engineering.

4.3.1. Structural model of the bifunctional enzyme tDGAT.

The three-dimensional (3D) model of the tDGAT protein was predicted through the PHYRE Web server (Kelley and Sternberg, 2009). Like all members of this acyl-CoA-dependent acyltransferase family, tDGAT is predicted to be a monomer with a two-domain structure (Nt domain and Ct domain) connected by an helical linker consisting of helixes α7 and α8 (see Fig R-32). The core of the Nt domain contains a four-stranded mixed sheet (β2, β5, β6 and β7) surrounded by three alpha-helices (α2, α4 and α5). The core of the Ct domain consists of a five-stranded mixed sheet (β8, β9, β10, β11 and β12) and five alpha-helices (α9, α10, α11, α13 and α14) covering the external face of the sheet. Again similarly with other acyl-coA dependent acyltransferases, the catalytic center ^{140}HHxxxDG^{147}, which emerge in the Nt domain of the polypeptidic chain, appears in the hydrophobic pocket or channel that restricts the accessibility of hydrophilic substrates. The conserved motif II arises in one extreme of the central tunnel, which suggest a crucial role interacting with the substrate accessing the catalytic site. Differently to the main residues responsible for the reactions catalyzed by this enzyme, the ^{281}ND^{282} residues of this motif II belong to the Ct domain and are located at the end of α11. Comparison with previously solved structures, as observed by Villa and co-workers in 2014, leaded to think that these residues might be interacting with the phosphate groups of the acyl-CoA. Besides, the ^{118}PLW^{120} amino acids forming motif I appear in the Nt domain, spatially close to the catalytic center located in a connecting loop between the helix α4 and the sheet-strand β6. As previously suggested, this motif could have an important role in the proper folding of the catalytic center.

Moreover, the 482-amino acid sequence of the enzyme tDGAT, a protein with a molecular mass of approximately 52 kDa, was aligned with representative members of the WS/DGAT family (listed in Table R-6) through the software T-Coffee. As shown in Fig R-33, tDGAT contains all the conserved motifs characteristic of WS/DGAT already described in the literature (Röttig and Steinbüchel, 2013). Furthermore, the theoretical pI and the GRAVY coefficient (Grand average of hydropathy; Kyte and Doolittle, 1982) of all the aligned proteins were calculated through Expasy bioinformatical tools in order to compare the enzymes. Table R-6 shows that the only protein among the most representative WS/DGAT with positive GRAVY (i.e. a hydrophobic average charge) was tDGAT. Besides, according to the theoretical isoelectric point (pI) of 6.44 this thermophilic protein would be negatively charged in an environment with a neutral pH, like the rest of the proteins from actinomycetes, microorganisms accumulating mainly TAGs as storage compound.

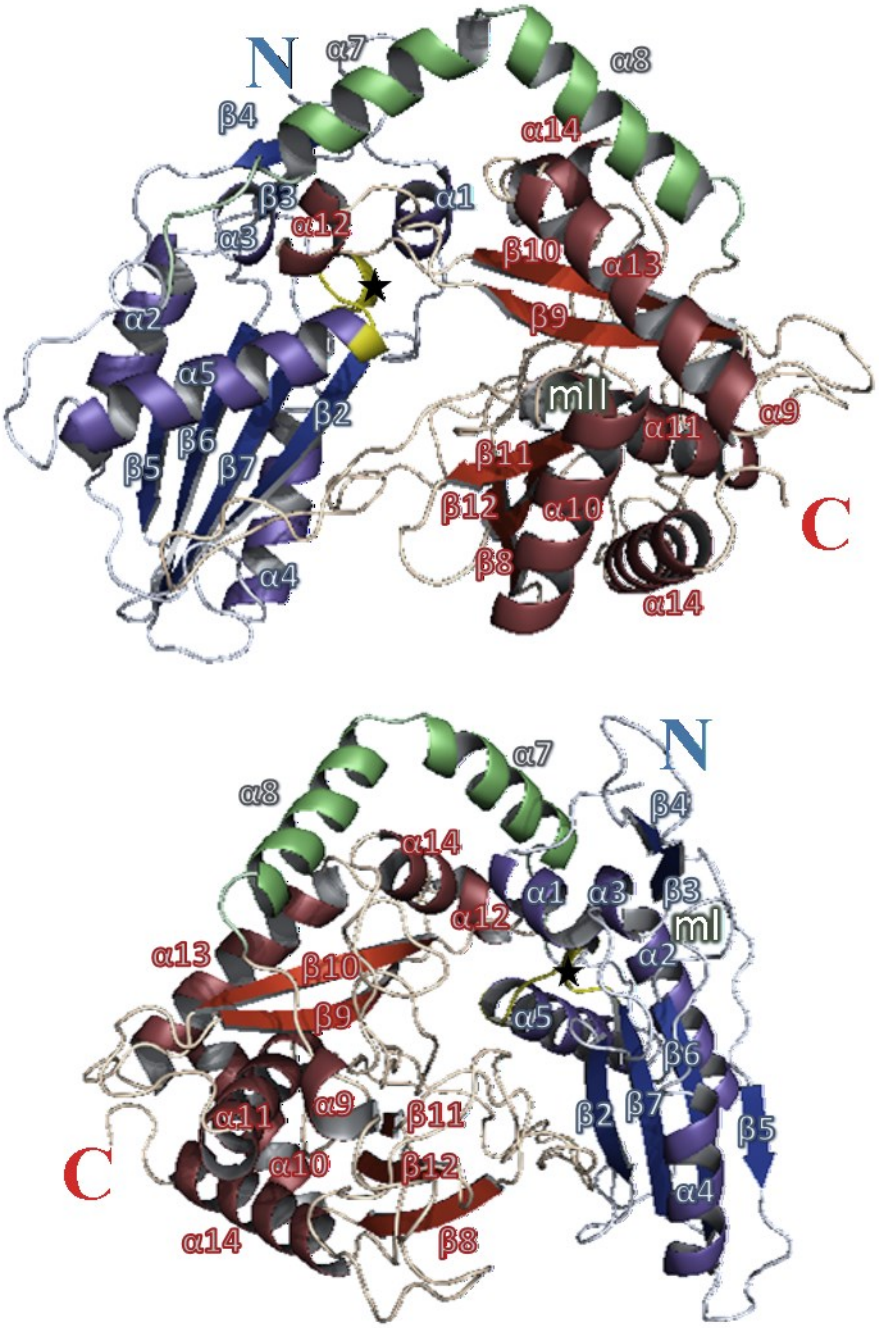

Figure R-32. Structural prediction analysis of the tDGAT protein revealed a monomer with a two-domain structure: Nt domain is colored in blue, Ct domain in red and the connecting loops in green. Beta sheets and alpha helices are shown in darker colors and labeled with the same notation used in the alignment. The active site HHxxxDG is also marked with a black star and colored in yellow. Other important conserved motifs are labeled (mI and mII).

Table R-6. Representative proteins of the WS/DGAT family. Actinomycetes are highlighted with bold typography.

Protein name	Organism	Database accession number	Size (amino acids)	Hydrophobic amino acids (AFLIVPG)	Polar amino acids (QNHSTYCMW)	Negatively charged residues (ED)	Positively charged residues (RK)	Theoretical pI	GRAVY value
tDGAT	*Thermomonospora curvata* DSM 43183	[NCBI: YP_003301387.1]	482	289	86	55	52	6.44	0.043
Ma2	*Marinobacter hydrocarbonoclasticus* VT8	[NCBI: YP_960328]	473	223	148	48	54	8.97	-0.285
Av1	*Alcanivorax* sp. 97CO-5	[GenBank: EUC69427.1]	451	215	141	44	51	9.12	-0.194
Ma1	*Marinobacter hydrocarbonoclasticus* VT8	[NCBI: YP_957462]	455	207	148	53	47	6.32	-0.295
Ac1	*Acinetobacter* sp. ADP1	[NCBI: YP_045555]	458	213	142	48	55	9.05	-0.203
Ps1	*Psychrobacter cryohalolentis* K5	[NCBI: YP_579515]	479	222	146	51	60	9.23	-0.187
Rh1	*Rhodococcus jostii* RHA1	[NCBI: YP_701572]	420	214	124	45	37	5.85	-0.126
Ms1	*Mycobacterium* sp.	[NCBI: YP_001073143]	454	238	120	51	45	6.08	-0.108
Nf1	*Nocardia farcinica*	[NCBI: YP_117375]	448	232	118	51	47	6.32	-0.109
At1	*Arabidopsis thaliana*	[NCBI: NP_568547]	481	219	148	54	60	8.81	-0.039

In Fig R-33 we can observe a graphical representation with the secondary structure elements of the modeled tDGAT protein above the MSA previously performed. Remarkably, a mismatch appears in the residues corresponding to the helix α8 of tDGAT (below a green representation of the secondary structure in the image) respect to this region in other WS/DGAT proteins. This secondary structure is part of the loop connecting the two domains of the enzyme. The amino acids in the protein region corresponding to the helical linker are poorly conserved among the WS/DGAT members, nevertheless that sequence seems to be longer in tDGAT.

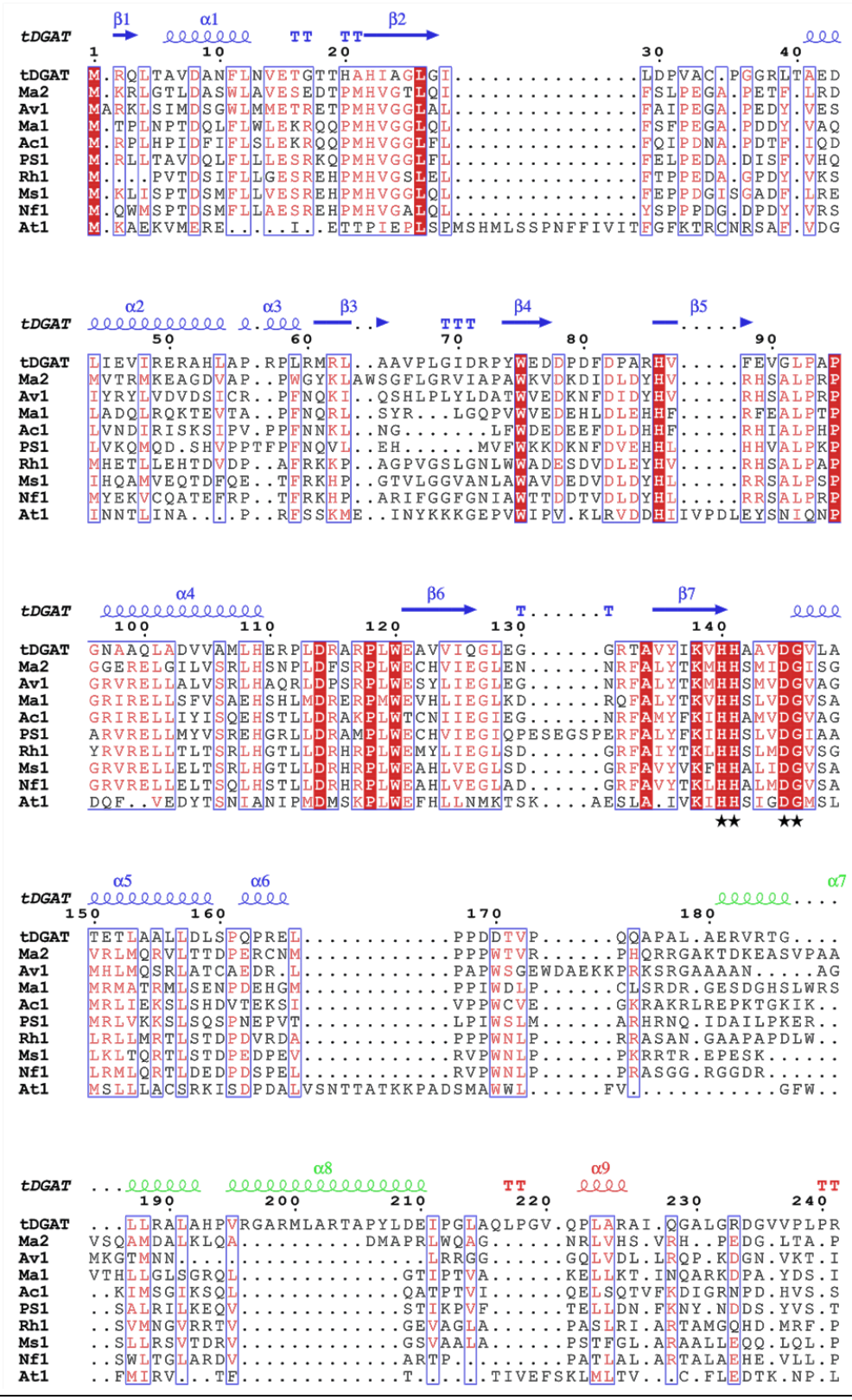

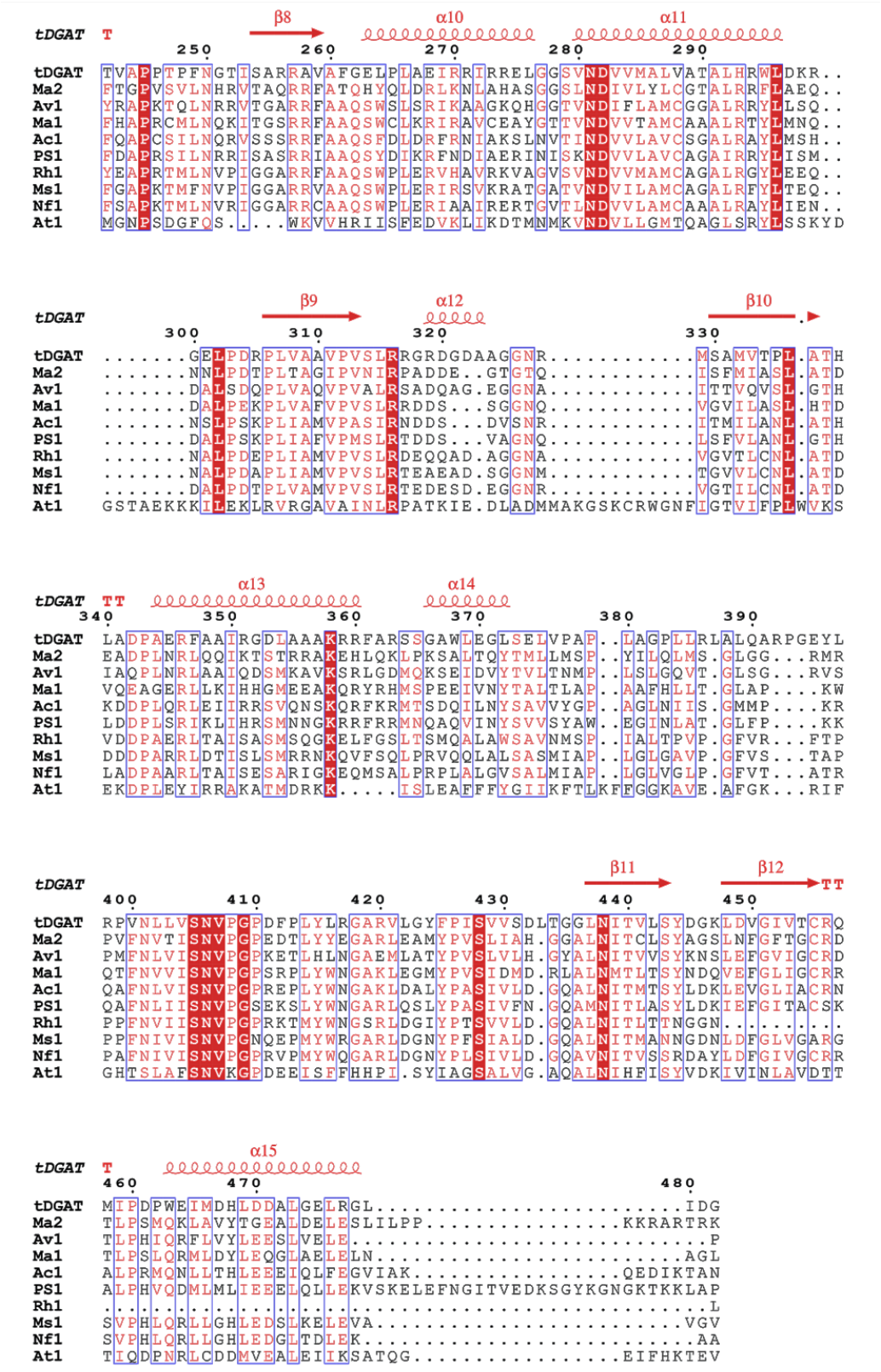

Figure R-33. Multiple sequence alignment of representative enzymes belonging to the WS/DGAT family. The coding sequences for the proteins were obtained from annotated protein data bases and are listed in Table R-6. Identical residues are shown in white on a red background, while similar residues are shown in red. The secondary structure elements of the modeled tDGAT protein are shown above the alignment. Secondary structure representation is colored blue for the N-terminal domain, red for the C-terminal domain, and green for the connecting helices. The active site motif HHxxxDG is remarked with black stars.

Additionally, the predicted 3D structure of tDGAT was compared with this of its homolog Ma2, which was employed in this work for *in vitro* experiments due to its better solubility (Villa Torrecilla, 2012). The structural alignment was generated through Pymol, giving rise to the images shown in Fig R-34. Both proteins showed an identical predicted 3D structure, sharing conserved motifs.

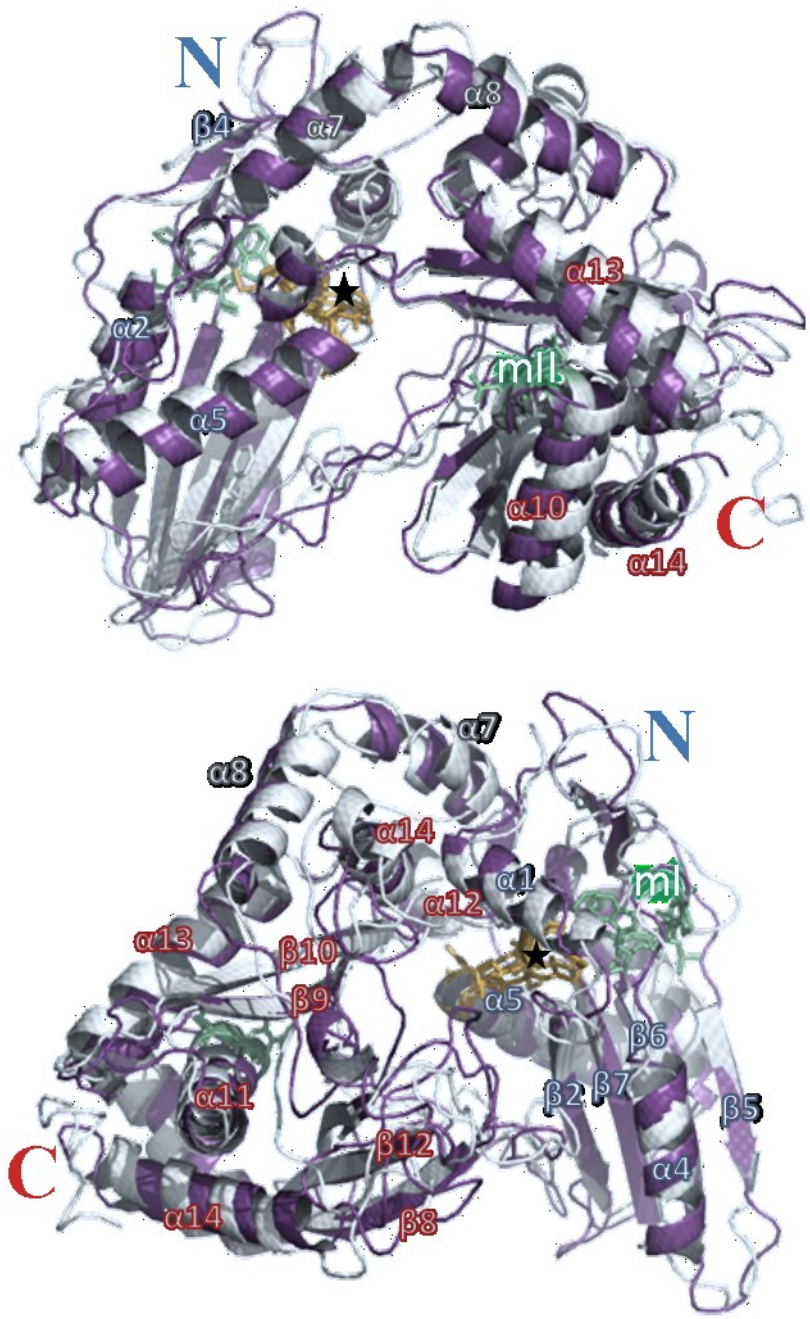

Figure R-34. Structural alignment of 3D prediction analysis of tDGAT (purple) and Ma2 (white). Residues corresponding to the active site motif characteristic of the WS/DGAT family are highlighted in orange and marked with a black star. The main other conserved motifs also responsible for the activity of these proteins are colored in green and labeled as mI and mII. Secondary structures of tDGAT are labeled in red (for those belonging to the Ct domain) or blue (those from Nt domain).

Taking into account that the hydrophobicity of the environment surrounding the enzymes of this family has been suggested to significantly influence the activity and/or substrate specificity of WS/DGAT proteins (Kalscheuer and Steinbüchel, 2003; Wältermann et al., 2005) we decided to analyze the vacuum electrostatics prediction of both structurally aligned proteins. Fig R-35 shows the different disposition of the hydrophobic residues. As we can observe, the amphiphilic trait seems to be more pronounced in tDGAT, in spite of the higher average hydrophobicity observed in Table R-6. This might be related with the poor solubility of the tDGAT previously described (Villa Torrecilla, 2012).

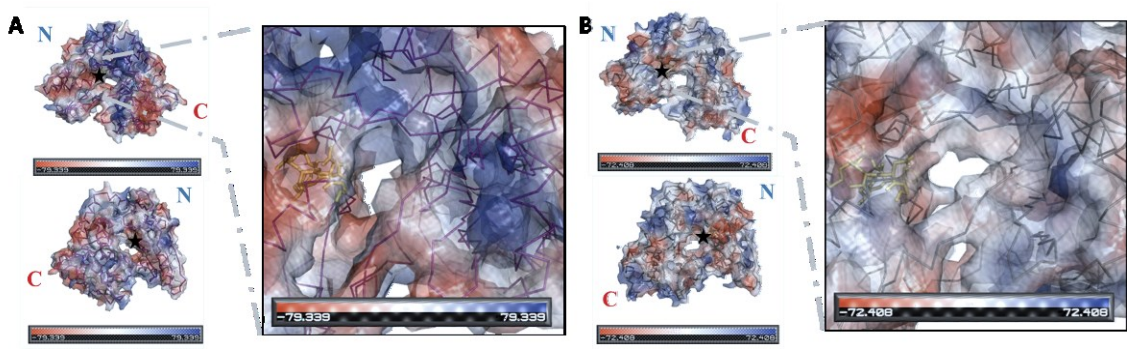

Figure R-35. Predicted electrostatic surface of both proteins (A: tDGAT; B: Ma2) overlapped onto the ribbon representation of the skeleton. Both sides of the proteins are shown. The active site is again marked with a black star. Zoomed views of the catalytic motif (in the hydrophobic tunnel) are also shown in both enzymes.

4.3.2. Small molecules naturally occurring in *E.coli* interact with the Ma2 protein.

The study of the requirements of the reactions catalyzed by the enzymes of the WS/DGAT family, its specificity and the catalytic process at molecular level would allow the optimization of a process to obtain the desired products.

Many strategies have been developed to analyze protein-ligand interactions due to its essentiality for all life processes, from conventional methods based on the measurement of the physicochemical properties of the macromolecule when bound to the ligand to more powerful and sophisticated techniques that observe physical parameters in both structures (Harding and Chowdhry, 2001). Among the latter, high resolution NMR focuses on isotopic label-free signals of the ligand and utilizes Nuclear Overhauser effect (NOE) between protein and ligand (Meyer and Peters, 2003; Takeuchi and Wagner, 2006).

INSET VI: Nuclear Overhauser effect and Saturation Transfer Difference-NMR experiment.

The NOE is observed as a change in intensity of one resonance when the intensity of a neighboring resonance is perturbed and its rate of transmission is proportional to the internuclear distance. The relation of this measurable effect with spatial distances explains its wide use both in biology for the structure determination of biomolecules, and as a routine method for conformational analysis in chemistry. Generally, homonuclear NOE is positive for small molecules and negative for big molecules. Moreover, the effect can propagate throughout the molecule in a process known as spin diffusion. The introduction of new methodology has extended its use for analysis or intermolecular interactions and analysis of ligand binding (Williamson, 2008).

When a small molecule (ligand) is bound to a large-molecular-weight-protein (the protein receptor molecule) it behaves as a part of the large molecule and adopts the corresponding NOE behaviour, that is, it shows strong negative NOEs, so-called transferred NOEs (trNOEs). Hence, by looking at its size, binding of a ligand to a receptor protein can be characterized. Furthermore, the orientation of bound ligands in protein binding pocket s can be determined by observing intermolecular trNOE (Meyer and Peters, 2003). Saturation Transfer Difference-NMR (STD-NMR) is a technique that can be employed for carrying out a screening of ligands (detecting which substrates are interacting with the enzyme tested among a mixture of molecules) and determining the epitope mapping of those molecules, as explained in section M-3.7.

STD-NMR with known enzyme-substract

Viegas et al (2011) and Figueiredo and Marsaioli (2007) were used to familiarize with the method and optimize the protocol in the available equipent for doing the assays related to this work by using BSA with a known ligand such as salicilic acid and a non-binding molecule such as D-glucose. As illustrated in Fig v.A, only the signals due to protons from the salicylic acid arised in the spectra resulting from the STD-NMR experiment. Hence, we can say this is the only binding ligand to BSA in this mixture. Aditionally, the attributed signals of the salicylic acid (see Fig v.B) were integrated in both spectra to calculate the position of the ligand during the interaction (i.e. epitope mapping).

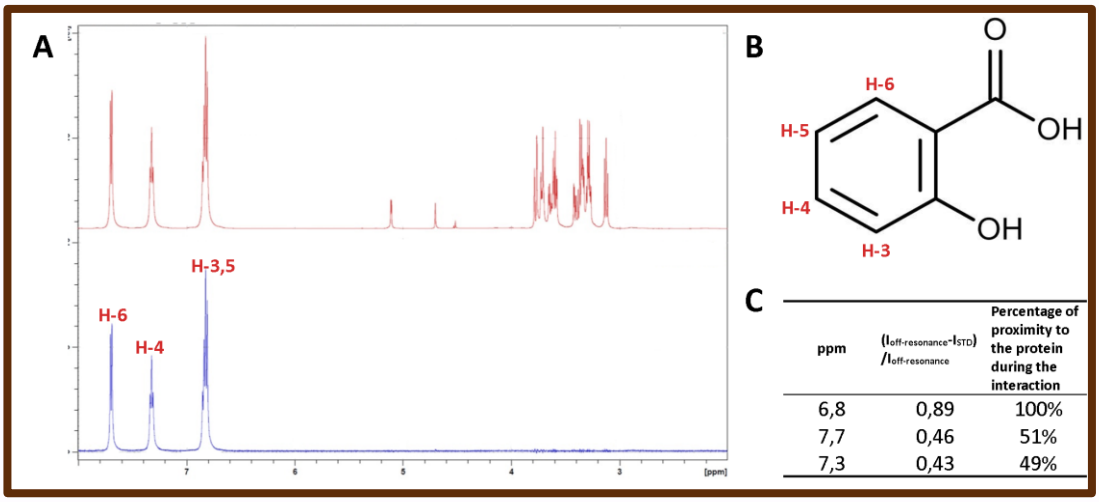

ppm	$(I_{off-resonance}-I_{STD})/I_{off-resonance}$	Percentage of proximity to the protein during the interaction
6,8	0,89	100%
7,7	0,46	51%
7,3	0,43	49%

Figure v. A) Comparison between the processed STD (75 mM SPB, 600.13 MHz) spectra (in blue) and the off resonance (i.e. normal ^{1}H spectra; in red) obtained from a mixture containing BSA protein and the possible ligands D-glucose (whose sets of protons give rise to the signals are known to appear from 3 to 5.5 ppm) and salicylic acid (responsible for the signals appearing from 6.5 to 8 ppm). B) Structural formula of salicylic acid with peak assignments corresponding with the spectrum in the left. C) Assignments for the signals appearing in the processed STD-NMR spectrum and epitope mapping showing the orientation of the molecule binding to BSA. Abbreviations: SPB , Sorensen's Phosphate Buffer; BSA, Bovine Serum Albumin.

In this work, high resolution NMR Spectroscopy studies were performed in order to better understand the molecular recognition events between enzymes belonging to the WS/DGAT protein family and different lipid compounds occurring naturally in the wt host cell.

Different attempts were made in order to detect the binding ligands interacting with proteins among a mixture of possible substrates by employing whole cell lysates containing a high concentration of the overexpressed protein. In order to confirm the overexpression of the His-tagged proteins tDGAT and Ma2 in the corresponding recombinant *E.coli* cells, a SDS-PAGE electrophoretic gel and a western blot of the protein extracts were simultaneously performed and compared. In Fig R-36.A we can observe the overexpression of both heterologous proteins in the recombinant bacteria. However, in Fig R-36.B we can observe that the anti-his antibody only binds to Ma2, while binding to the His-tagged tDGAT cannot be seen. At first glance this seem to be related to the difficulty to be purified showed by the protein tDGAT (Villa Torrecilla, 2012). Nonetheless, the variability in the inmunodetection associated with the use of His-tagged antibodies has been previously described (Wilken et al., 1999) and its independence of the ability of the His-tagged protein to be purified through Ni affinity columns still lacks an explanation (Debeljak et al., 2006). Thus, our result does not the low solubility previously observed in tDGAT. In this way, both proteins were properly overexpress, but the sensibility of this particular antibody against a 6-his epitope differs in both proteins, in spite of the similarity of this amino acid sequence in both cases (since this fragment was codified from a DNA sequence from the same plasmid vector, pET29c).

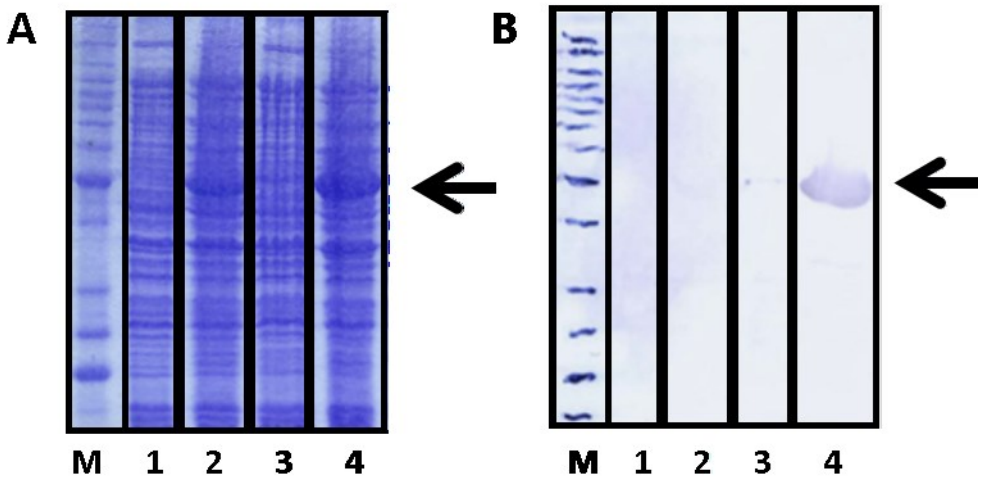

Figure R-36. SDS-PAGE gel (A) and western blot membrane (B) showing the whole cellular lysates of different cultures of *E.coli* C41 (pEtDGAT) [lanes 1 and 2] and *E.coli* C41 (pEmbDGAT) [lanes 3 and 4] collected 0 hours [lanes 1 and 3] and 2.5 hours [lanes 2 and 4] after addition of the inductor IPTG. The SigmaMarker Low Range was loaded on the first lanes (M). Black arrows point to the predicted molecular weight of both WS/DGAT proteins (approximately 52-53 kDa).

Since unspecific interactions and overlapping signals prevented the arise of clear results by NMR analysis employing whole cell extracts (data not shown), a purified WS/DGAT protein was required. Among WS/DGAT proteins, a better purification yield can be achieved with Ma2 tDGAT (Villa Torrecilla, 2012). Hence, the 473 amino acid Ma2, with a molecular mass of approximately 53 kDa and a theoretical pI of 8.97, was employed to perform further STD-RMN experiments (see section M-3.7 and Inset VI).

All STD-NMR experiments were carried out with the whole lipid extract of *E.coli* C41 (compounds naturally occurring in the bacteria) as mixture of possible substrates. The temperature of the analysis was set to 15°C to fit equilibrium between the stability of the protein and the enough viscosity of the amphipathic deuterated solvent required to solubilize the hydrophobic substrates in the aqueous solution containing the enzyme (a solution of D_2O:DMSO-d_6 5:1, i.e. deuterated water : deuterated dimethyl sulfoxide, was used for this purpose).

With the aim of elucidating interactions at molecular level, the STD-NMR experiment was carried out as explained in section M-3.7 with the WS/DGAT protein Ma2 against the whole lipid pool naturally present in the wt *E.coli* C41. Fig R-37 shows the processed STD-NMR spectra obtained, were some interaction between the protein and some molecules can be observed (see Table R-7 for assignments of every signal).

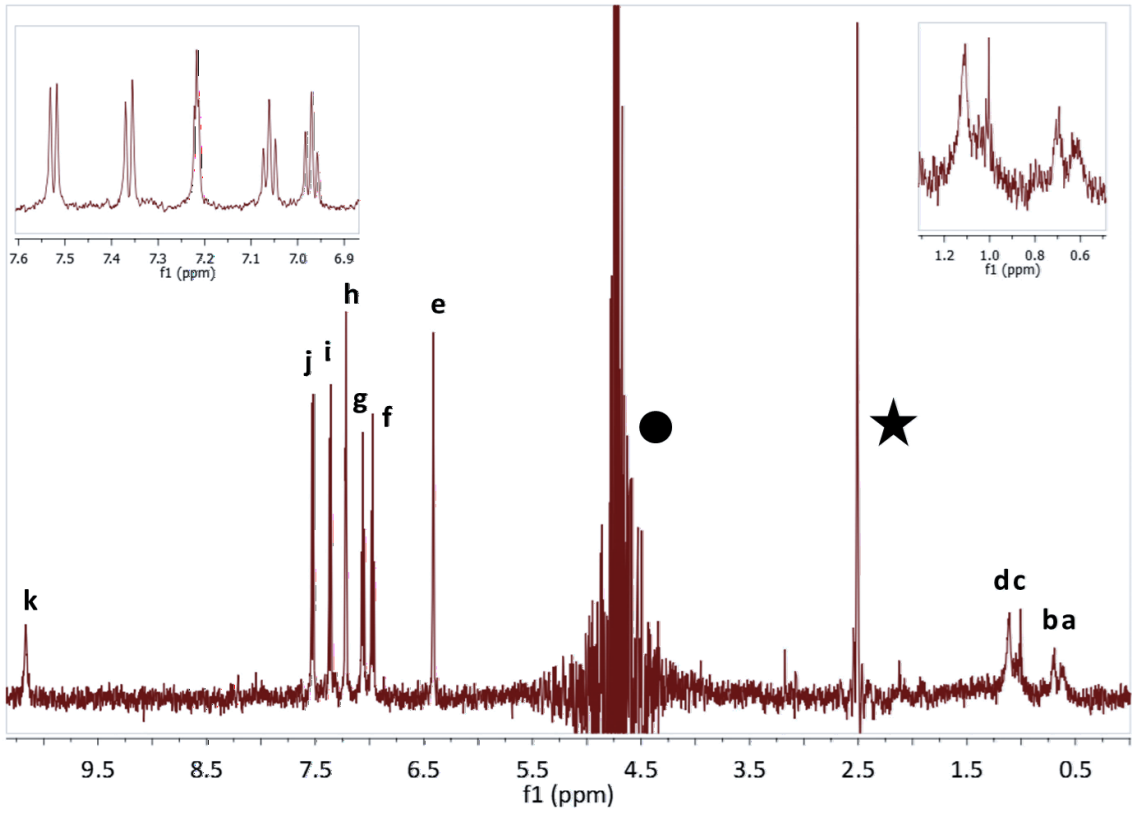

Figure R-37. Detailed analysis of the obtained STD (**H_2O:DMSO-d_6 5:1,** 600.13 MHz) spectrum. The signals from the binding compound are named from right to left. The residual peaks of the solvents are marked with a circle (D_2O at 4.7 ppm) and a star (DMSO-d_6 at 2.5 ppm).

Comparison of the ^1H spectrums from the protein Ma2, from the whole lipid extraction from the wt C41 *E.coli* and from the mixture of both, together with the processed STD spectrum obtained from the STD-NMR experiment performed as explained in section M-3.7, showed that the molecule the protein is interacting with was also present in the lipid pool (Fig R-38).

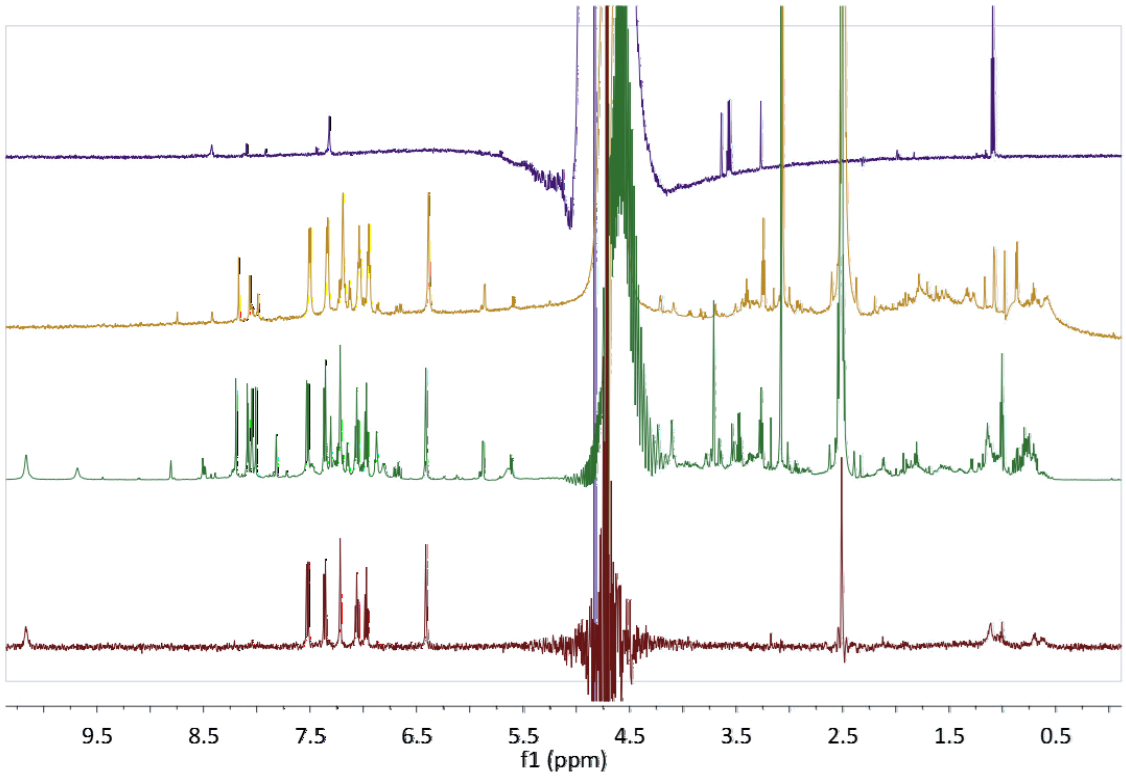

Figure R-38. Comparison of the 0-10.5 ppm regions of the ^{1}H NMR spectra (600.13 MHz) of the Ma2 (purple spectrum, H_2O:D_2O 9:1), the whole lipid extract from the wt *E.coli* C41 (golden spectrum, **D_2O:DMSO-d_6 5:1**), the mixture of both (green spectrum, **H_2O:DMSO-d_6 5:1**) and the processed STD spectrum (red spectrum, **H_2O:DMSO-d_6 5:1**).

In the same way, the STD-NMR spectrum was correlated with the *off resonance* spectrum from the mixture (i.e., the normal ^{1}H spectra of the mixture, acquired with the irradiation frequency set at a value that is far from any signal, ligand or protein; see Fig R-39). By integrating every signal corresponding to the binding ligand revealed by the STD experiment in both spectra (signals appearing in both the STD-NMR spectrum and the *off resonance* spectrum), and estimating in that manner the magnetization of every group of protons, with correlates with the affinity of the correspondent set of protons with the enzyme and therefore with the distance to the protein during the binding process, epitope mapping was calculated (see Table R-7).

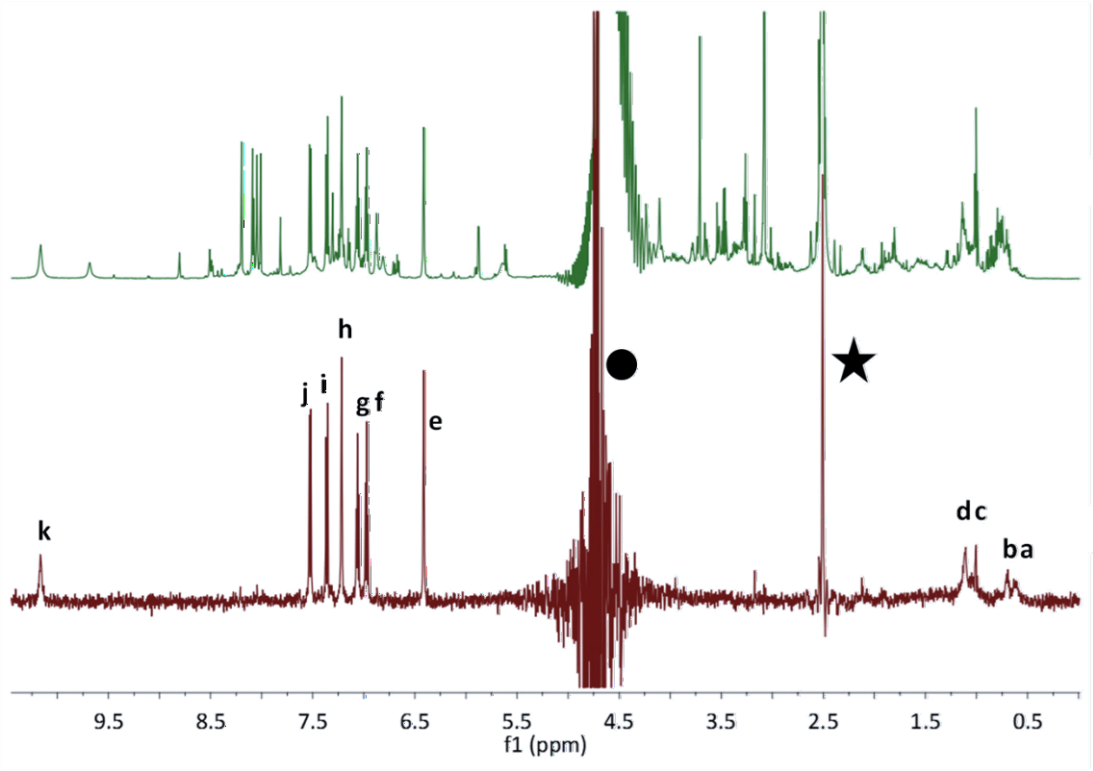

Figure R-39. Comparison of ^{1}H NMR spectra (**H_2O:DMSO-d_6 5:1,** 600.13 MHz) from the NMR tube containing the mixture of the purified Ma2 together with the lipid extract from the wt host bacteria. The upper green spectrum A corresponds to *off-reference* spectrum, the normal ^{1}H spectrum of the whole mixture. The lower red spectrum B corresponds to the processed STD-NMR spectrum, which shows signals only from compounds binding to the enzyme (named a-k). The signals of the solvents are marked with a circle (D_2O at 4.7 ppm) and a star (DMSO-d_6 at 2.5 ppm).

Table R-7. Assignments for the signals appearing in the processed STD-NMR spectrum and epitope mapping showing the orientation of the molecule binding to Ma2. Identical regions were integrated and analyzed in both off and STD spectra for performing calculations. The multiplicity and the attribution of number of protons was performed from the normal ^{1}H spectrum of the mixture. The orientation of the molecule was calculated according to the magnetization received from each proton. Abbreviations: s, singlet; d, doublet; t, triplet; m, multiplet.

Peak name	(chemical shift, ppm)	Functional group	Peak multiplicity	Assigned number of H's	$(I_{off\text{-}resonance}-I_{STD})/I_{off\text{-}resonance}$	Percentage of proximity to the protein during the interaction
a	0.61		m	1	0,066	83%
b	0.70		m	1.97	0,033	42%
c	1.00		t	1.42-2	0,025	31%
d	1.11		m	3.65	0,038	49%
e	6.41		s	2.37	0,079	100%
h	7.22		m	2.96	0,062	79%
f	6.97	Aromatic ring	t	2.67	0,065	82%
g	7.06		t	3.19	0,059	75%
i	7.36		t	2.99	0,060	77%
j	7.52		d	2.61	0,070	88%
k	10.17	-COO*H* (carboxylic group)	s	1.42	0,061	78%

With the aim of better identifying this molecule, several selective one-dimensional total correlation spectroscopy (1D TOCSY) experiments were carried out with the same NMR sample tube used for the STD-NMR experiment (i.e. the sample containing the mixture of the protein Ma2 with the lipid extracted from *E.coli* C41). In this method a certain proton is chosen by a frequency-selective pulse, so that the measurement reveals all resonances of the spin system, giving rise to spectra showing only signals of protons belonging to the same coupling network (Facke and Berger, 1995; see golden and green spectra in Fig R-40). The presence of the singlet in 6.41 ppm in both TOCSY spectra here displayed, with the rest of the signals appearing distributed among them indicates the main ligand shown in the STD-NMR experiment is a unique molecule with two different spin systems. Furthermore, the presence of two doublets and two triplets in the region of 6.5 to 8.0 ppm indicates that the unknown interacting compound has an aromatic group.

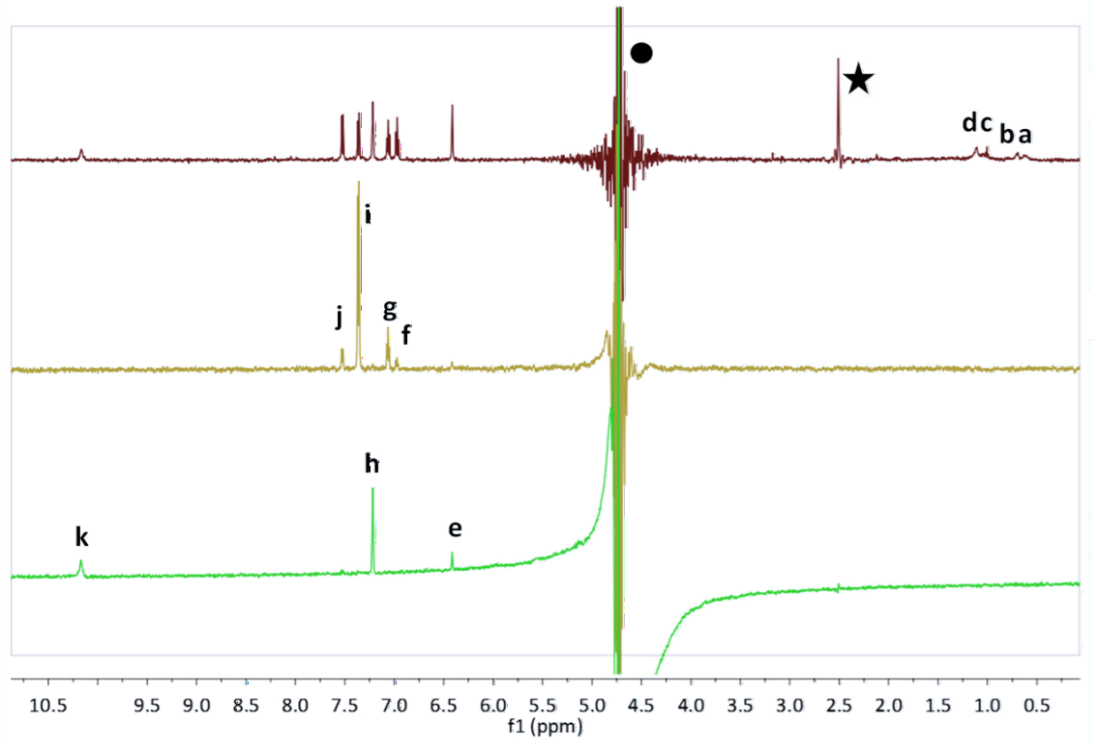

Figure R-40. TOCSY experiments (H_2O:DMSO-d_6 5:1, 600.13 MHz) realized with the same mixture used for the STD-NMR experiment of the fig R-3.2 (red spectrum in this image). The signals of the solvents are marked with a circle (D_2O at 4.7 ppm) and a star (DMSO-d_6 at 2.5 ppm).

An analytical TLC plate of the sample was run and one spot on the bottom line was revelled with 365nm UV light, which supports the hypothesis of the binding compound containing an aromatic ring (data not shown).

Ma2 had previously been purified and showed *in vitro* activity in precise laboratory conditions (Holtzapple and Schmidt-Dannert, 2007; Villa et al., 2014). However, *in situ* DGAT activity was not detected with the heterologous expression of this enzyme in *E.coli* (unpublished data). These small compounds with affinity for the protein occur naturally in *E.coli* and have a high hydrophobicity, since were extracted from its biomass together with the lipid fraction.

Thus, the results presented here increment the biochemical and structural knowledge of the family of proteins WS/DGAT, the nature of the substrates used *in vivo* by these proteins and the production of lipid molecules related to its overexpression. This helps to clarify the pathway for the possible biotechnological applications of this lipid synthesizing system.

4.4. General discussion

The increasing demand in recent years for new alternative sources of oil for diverse commercial purposes has strongly enhanced research on the development of sustainable processes leading to the biosynthesis of lipid compounds. Specifically, among the most interesting possible applications of TAG compounds are their use as a renewable alternative for biodiesel production or as source of valuable FA (see section I-1.2).

The unsustainability of traditional oil sources leaded to research in SCO. Nevertheless, microorganisms naturally producing and accumulating neutral lipids are generally not easy to culture, lack tools to be efficiently genetically engineered and result unappropriated for industrial use. For that reason, scientific efforts have focused in more suitable organisms such as microalgae or *E.coli*. The production of neutral lipids in the latter has been reported to depend on the heterologous expression of an enzyme belonging to the family WS/DGAT. These enzymes play an essential role, since they are responsible for the last esterification step in the production of neutral lipids in bacteria, whether it is TAGs or WEs (Arabolaza et al., 2008; Kalscheuer and Steinbüchel, 2003; Rucker et al., 2013). The results described in this work intend to contribute to the general knowledge on the production of TAGs in such bacteria while paving the way for the optimization of efficient processes for its use in biotechnological industry for the obtainment of both generic and specific oils.

4.4.1. Methods for quantifying and improving the TAG production yield in *E.coli* when expressing tDGAT.

The production and accumulation of TAG compounds in *E.coli* cells expressing the thermophilic protein tDGAT was recently reported in our research group (Moncalián et al., 2014; Villa Torrecilla, 2012). The catalytic ability within a wide range of reaction conditions of stable enzymes coded by thermophilic organisms might be essential for industrial processes, which explains its huge biotechnological potential (Coleman and Sharp, 2010). In this work different techniques are employed to quantify and characterize TAG production in different *E.coli* strains while employing metabolic and genetic strategies with the intention to optimize TAG generation in the recombinant strain. Simultaneously, a high-throughput method for detecting improved TAG-producers based on fluorescent lipophilic dyes was developed.

On one hand, lipid extracts of diverse *E.coli* cultures together with standard samples, consisting of known oil quantities, were analysed through traditional TLC. Densitometric evaluation of the digitalized TLC plates revealed a remarkable capacity of the bacteria expressing tDGAT of producing TAGs in a short time after induction of overexpression of the heterologous protein. Actually, *E.coli* C41 (pEtDGAT) accumulated more than 30% of its neutral lipids as TAGs in 1.5 hours of over-expression when cultured at 37°C. As explained in section I-1.2.1, during the development of this Thesis the production and accumulation of TAGs has been reported in different engineered *E.coli* strains through the expression of diverse enzymes belonging to the WS/DGAT family. This process has been achieved both in engineered *E.coli* strains with some deleted gene (Arabolaza et al., 2008; Comba et al., 2014; Janßen and Steinbüchel, 2014b; Lin et al., 2013) and in wt *E.coli* strains overexpressing some additional proteins (Comba et al., 2013; Janßen and Steinbüchel, 2014b; Röttig et al., 2015; Rucker et al., 2013). Interestingly, the process here studied takes place in a wt *E.coli* strain without further modification. In addition, little attention has been paid in the literature to the culture time, which represents a crucial bottleneck for industrial processes. In this work we prove that the strain developed in our group achieves in a very short time TAG production never reported in similar culture conditions with this genetic background. Moreover, we also prove the functionality of this enzyme to be independent of stressing conditions such as nitrogen starvation (a typical inductor for lipid production in naturally oleogenic microorganisms). This suggests that the regulation of the catalytic activity of the enzyme heterologously expressed in recombinant cells totally differs from the situation in its natural hosts. Thus, a careful design of the expression system for this protein might be the main requirement for lipid production in *E.coli*. Additionally, TAG production in *E.coli* was detected at different culture temperatures from 25 to 37°C, although no TAGs were visualized in the TLC analysis at 15°C. This range of temperatures could be suitable for an efficient process without excessive energy costs

(Cote, 2013; Gupta et al., 2013). This TAG production at feasible industrial temperatures confirms the ample biotechnological potential of the enzyme tDGAT over other described members of the WS/DGAT family. Further metabolic and genetic improvement of bacterial strains expressing this protein and subsequent optimization of the fed-batch fermentation process might lead to yields higher than those obtained to the moment.

On the other hand, the strong genetic component observed in the production of bacterial TAGs makes of positive selection a possible mechanism to optimize lipid production in bacteria. However, this strategy requires of a high throughput selection method that has not been developed yet for TAG accumulation in these microorganisms. Thus, we have analyzed the differential behaviour of native and tDGAT *E.coli* cells under different conditions and analytical techniques to find an optimal method for positive selection.

We first analysed the different flotability associated to the lipid accumulation. The average buoyancy of a bacterial strain increases with its content in lipids and can be easily observed in oleogenic bacteria. Nevertheless, no significant difference in buoyancy was detected between the engineered bacteria grown in maximum lipid accumulation conditions and the wild type, probably due to the still very low TAG production yield of the recombinant *E.coli*.

Since techniques based in lipophilic dyes reveal the neutral lipid content without requirement of lipid extraction, several fluorescence techniques were assessed with the purpose of describing the behaviour of different strains already analysed through traditional methods such as TLC. Microscopy images acquired from two *E.coli* strains expressing tDGAT stained with Red Nile, showed a marked fluorescence concentrated in round inclusions that were absent in the corresponding wild type strains analysed in the same conditions. Two different tDGAT expression systems (pET and pBAD) showed similar inclusions. At the same time, wt bacteria showed homogeneous fluorescence along the whole cells, probably due to the interaction of the dye with lipid compounds naturally occurring in *E.coli*. The fluorescence profile of the recombinant bacteria resembled the situation in oleogenic microorganisms (Alvarez et al., 1996), suggesting an accumulation of the neutral lipids in lipid droplets in the engineered *E.coli* bacteria. Besides, lipid accumulation was monitored by fluorescence spectroscopy and by fluorescence microscopy. The results obtained by fluorescence spectroscopy show an increment in the fluorescence detected at 620 nm in every culture stained with Red Nile compared to non-stained cultures. As expected, only the red fluorescence from the TAG-producing strain continued rapidly increasing immediately after the induction of the overexpression of the enzyme tDGAT. Nonetheless, the augment in the fluorescence detected in the recombinant strain stopped before the cells entered the stationary growth phase, resulting in a higher stable fluorescence value in this bacteria than in the wild type strain. These data support the previous result from TLC densitometric analysis of a rapid production of neutral lipids within a short overexpression time. Furthermore, *E.coli* (pEtDGAT) cells were monitored 20 hours after induction of the hetelologous protein and Red Nile-staining through time-lapse fluorescence microscopy. Visualization of the bacterial cells along the time showed different shapes in a recombinant culture of this proteobacteria expressing tDGAT. The images displayed bacteria presenting the same profile observed beforehand for recombinant bacteria, in marked round inclusions, which suggest that they were accumulating neutral lipids, and bacteria showing only homogeneous fluorescence that seemed to divide (with a fluorescence profile similar to that seen in wt *E.coli* cells). Since the growing of the bacteria on the agarose pads was monitored 20 hours after adding the inductor and the Red Nile dye to the recombinant culture (previously grown in covered erlenmeyer flasks), we hypothesize a fraction of the bacterial population could have lost the gene codifying for the tDGAT protein, which represents a burden for the cell. In this way, the non-lipid-producing *E.coli* cells behave in the same way than the *wt* bacteria.

Likewise, cytometric analysis of *E.coli* (pEtDGAT) and its control strain was in agreement with the previous analysis performed by TLC densitometry: an increase higher than 30% in the events detected as fluorescent cells was observed in the engineered strain with Red Nile (i.e. they had a significant amount of dye in its cytoplasm –which implies the presence of neutral lipid compounds-). This increment reached more than 50% with Bodipy, which could be due to differences in the affinity for some or all neutral lipids of each particular dye. Finally, fluorescence spectroscopy measurements of cells stained after growing were acquired from samples of *E.coli* cultures, expressing or not the enzyme. This way, fluorescence spectroscopy measurements revealed a significant increment on the engineered strain with both dyes

tested, all far exceeding this 30%. This higher increase could be explained by the affinity of lipophilic dyes for any kind of neutral lipid, while TLC differentiates specific compounds such as TAGs.

Provided the close relation among neutral lipid accumulation and fluorescence in cultures stained with lipophilic colorants togueter with the acquired knowledge about the different methods to evaluate fluorescence measurements, a method was developed to rapidly asses a great amount of genetically engineered *E.coli* strains. With this purpose we based on the report published by Chen and co-workers in 2009, who employed 96-well plates to identify high neutral lipid-producing microalgae through Red Nile staining and fluorescence spectroscopy. This way, the measurement conditions in a fluorimeter were optimized (see section R-4.1.2) to visualize improved neutral lipid-producing strains. After this high-throughput approach by means of Red Nile staining, the detected mutants with higher TAG production could be further characterized by more time-consuming traditional methods implying lipid extraction. A summary of this procedure is schematized in Fig D-1. A similar approach was recently published for detecting high oil-accumulating green microalgae from cytometric analysis of Red Nile stained strains (Cagnon et al., 2013). Besides, a pattern curve was performed with commercial oil in order to quantify the lipid content while carrying out this experiment (data not shown). However, the range of proportionality of the standard did not match with the values obtained from the still low TAG-producing *E.coli* cells. The method here described permits the assessment of high amounts of samples, allowing the identification of improved TAG-producing strains among large collections.

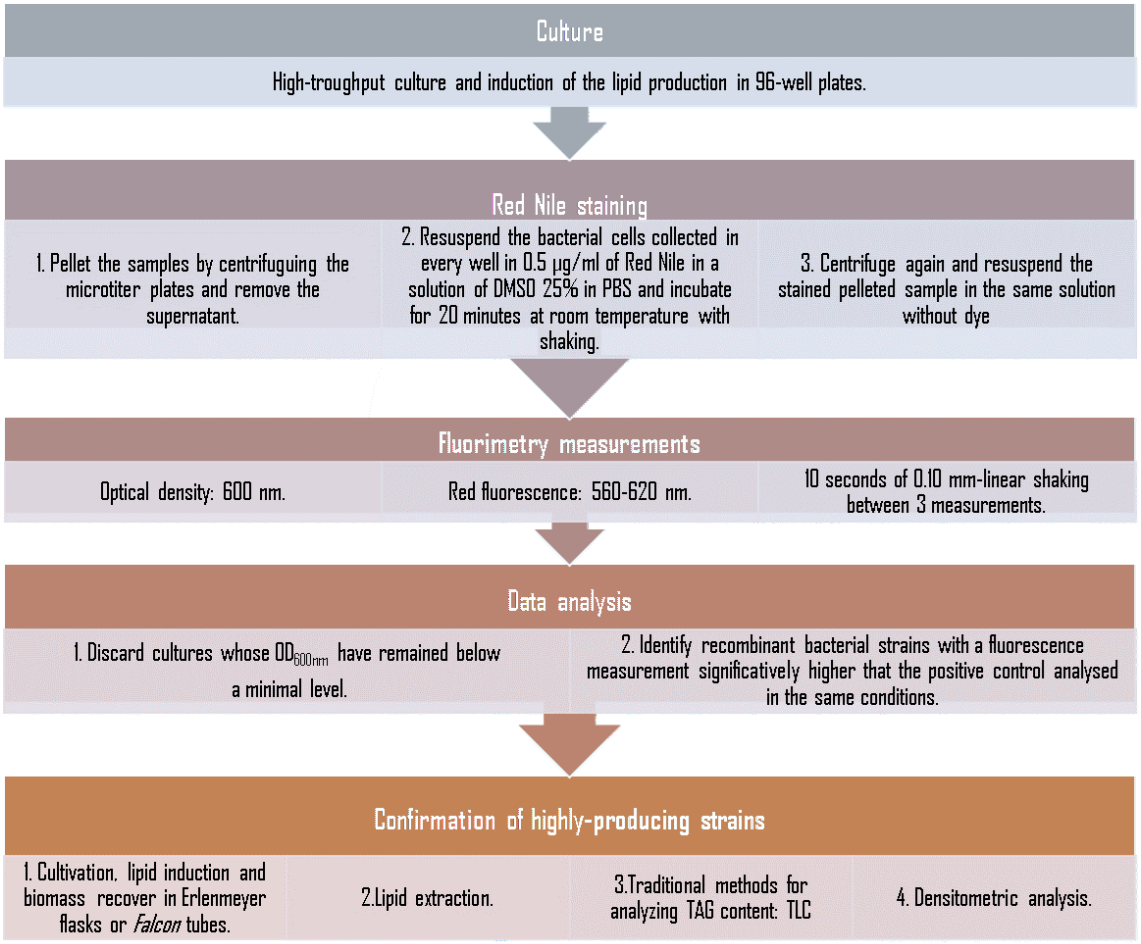

Figure D-1. Outline of the process developed for selection of high TAG producing strains.

With the aim of identifying genes whose absence was related to neutral lipid biosynthesis and accumulation, the tDGAT enzyme was heterologously expressed in a set of mutant *E.coli* strains lacking different non-essential genes (belonging to the Keio Collection, Baba et al., 2006). A vector containing the $oriT_{R388}$ together with the gen for the protein tDGAT was constructed to facilitate the transformation of the

Keio strains, while the helper plasmid pSU711 (Francia et al., 1993) was introduced in in the donor strain to mobilize the vector of interest to the collection of mutants. The previously developed selection method was then carried out with the resulting transconjugants employing *E.coli* BW27783 and *E.coli* BW27783 (pBtDGAT) as control strains. None of the evaluated Keio transconjugants emitted a fluorescence value higher that the one measured in the positive control, which would have implied a higher neutral lipid content. Nonetheless, the suitability of this procedure for detecting efficient TAG-accumulating *E.coli* strains among large numbers of samples was proved with this attempt.

During the development of this method diverse metabolic strategies were also employed for optimizing the growing conditions for TAG production, such as varying the composition of the growth media (especially nitrogen concentration and salinity), growth temperatures and oxygenation of the culture, induction times and concentrations or over-expression times. Although no relevant data aroused from these attempts, we provide new methods for identifying improved TAG-producing cultures and ideas for diversifying the variability, both from genetic and metabolic approaches. Further research through the techniques here described could lead to novel interesting findings.

All in all, TLC and subsequent densitometry analysis, overcoming its difficulties in reproducibility and taking detection limits into account, might be considered as the most reliable semi-quantitative technique to analyse changes in the general neutral lipid profile and measuring the bacterial content in certain lipid specie. Nevertheless, it is a time-consuming method implying lipid extraction that prevents a study with a high number of samples. Alternative techniques, especially those based on fluorescent dyes, allow the drawing of a more general picture while permitting larger studies by following the previously explained steps.

4.4.2. Characterization of the change in the lipid profile produced by the expression of tDGAT and description of the produced TAGs.

The properties of the commercial products derived from SCO depend on the characteristics of its FA composition. In particular, biodiesel quality has been widely reported to be related to the type of acyl chains forming the FAAEs (Cao et al., 2014; Knothe, 2005). The interest on this potential application for the employment of TAGs produced by genetically engineered bacteria justifies our interest in the elucidation of the FA constitution.

^{1}H NMR analysis of lipid extracts from diverse *E.coli* strains carrying the genes for the acyltransferases tDGAT or Ma2 cultured at 37°C pointed to an outstanding increment in double bonds in the samples from the engineered strains expressing WS/DGAT proteins over the corresponding wild type strain. GC analysis of similar lipid extracts of phenotypically diverse *E.coli* strains expressing the protein tDGAT through different expression systems and their corresponding controls (without the heterologous protein) revealed a bias towards the MUFAs palmitoleic and *cis*-vaccenic acids in the recombinant strains. While MUFA proportion in the wt *E.coli* strain was below 11% of the total FA in the bacteria, at least 25% of MUFA are detected in strains expressing the enzyme tDGAT, independently of the phenotypic traits of the host strain, the protein expression system or the culture growth temperature. As a matter of fact, even the recombinant bacteria whose TAG production could not be visualized through TLC analysis showed an important increment in the MUFA proportion, like happened when culturing *E.coli* C41 (pEtDGAT) at 15°C. This indicates that a relevant part of the double bonds observed by ^{1}H NMR were related to the FA profile. Furthermore, according to GC analysis MUFA were observed to accumulate in the TAG compounds, achieving a 46% of its FA. The other FA present in all samples in a significant proportion were the saturated PA, representing around 25-31% in all cases.

The FA profile in *E.coli* varies with the strain and growth conditions. It was described that MUFA proportion increases while culture temperature decreases (Heath and Jackowski, 2002; Mansilla et al. 2004). Besides, augments in the MUFA cellular content have been previously described in literature in response to the heterologous expression of different proteins such as an ester hydrolase in *E.coli* (Kerviel et al., 2014) or an eukaryotic transcription factor together with a diacylglycerol acyltransferase in plants (Vanhercke et al., 2013). Among WS/DGAT enzymes, Lin and co-workers reported in 2013 a 3-3.7- fold

increase in the UFA fraction for different *E.coli* strains containing the *dgkA* deletion (lacking the gene responsible for the diversion of DAG to PL biosynthesis) and expressing WS/DGAT enzymes from different microorganisms over de FA composition of the wild type strain. Besides, Röttig and colleagues (2015) also described a bias toward MUFA (especially *cis* vaccenic acid) in an engineered *E.coli* strain overexpressing several proteins (including a bacterial WS/DGAT) and producing TAGs. Hence, this effect is not particular of the WS/DGAT enzymes employed in this work. Likewise, Rucker and co-workers (2013) observed that almost half of the FA in the TAG produced by another engineered *E.coli* strain were MUFA, which matches with our results. However, the explanation to this metabolic response is yet unclear. Our hypothesis relies either in the chemical protection FA acquire when becoming part of the TAG compounds (e.g. from β-oxidation) or in a higher selectivity of the WS/DGAT enzymes for MUFA, which could produce an increment of the biosynthesis of these FA (by decreasing its concentration in the cytosol). Both possible interpretations would explain the increase in MUFA in the whole bacterial FA pool as well as the high MUFA content of the TAGs produced by the recombinant strain. The similarity of this bias in the FA content could also be related to the important function of TAG compounds in the cells as "sink" for unnecessary FA, which converts those neutral lipids in membrane fluidity regulators according to growth temperature (Alvarez and Steinbüchel, 2002; Wältermann and Steinbüchel, 2005).

Moreover, the ^{1}H NMR spectra from purified TAGs from *E.coli* C41 (pEtDGAT) showed the typical profile of a TAG compound. Additionally, the analysis of the signals suggested a ratio of 2 olefinic protons in every TAG, which can be translated in a FA composition of 1 MUFA and 2 SFA per TAG, suggesting a predominant profile for TAGs in this strain. According to the UPLC/MS analysis an ample proportion of the TAG in the engineered bacteria showed that composition, supporting this statement. The high MUFA proportion previously detected in TAGs through GC analysis of the same purified fraction also supports these results.

To sum it up, a general picture of the lipid profile of different bacteria can be obtained by TLC analysis and methods based on fluorescence dyes, and might be supported by GC or ^{1}H NMR analysis of whole lipid extracts. The last methods, although time consuming, give rise to more detailed characterizations. UPLC/MS analysis is also another technique that should be taken into consideration for the analysis of the relative FA composition within the TAG molecules.

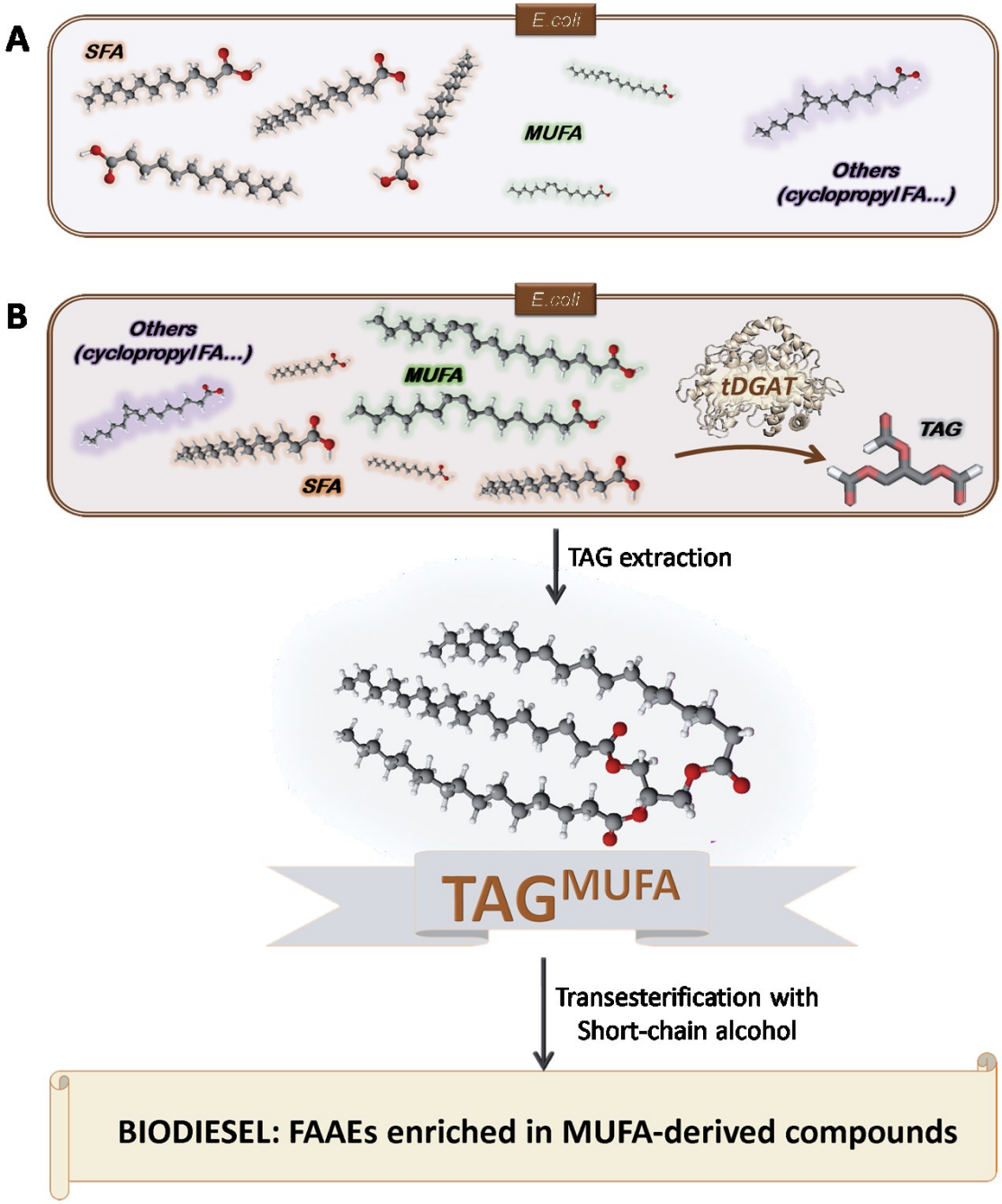

Figure D-2. A) Schematic representation of a wild type *E.coli* bacteria with some naturally occurring FA. B) Genetically engineered *E.coli* bacteria expressing a WS/DGAT enzyme. Abbreviations: SFA, saturated fatty acids; MUFA, monounsaturated fatty acids; TAG, triacylglyceride; TAG^{MUFA}, TAG enriched in MUFA.

4.4.3. Generation of LC-PUFA in *E.coli*

The requirement of alternative methods for the production of LC-PUFA has provoked wide research on its biosynthesis metabolism in bacteria. As explained in the section I-1.1.1, the biosynthesis of these secondary metabolites in bacteria can occur through two different pathways: the aerobic pathway and the anaerobic pathway. Thus, we have introduced in *E.coli* each of these pathways for the production of ω-3 PUFAS.

On one hand, we focused in the most common PUFA biosynthetic pathway: the aerobic pathway. Through this pathway, the production of the simpler EFAs (LA, C18:2, and ALA, C18:3) require few reactions to convert the final products of FAS (see Fig I-31). Starting from SA, only a sequence of reactions catalysed by the desaturases Δ9, Δ12 and Δ15 are required to synthetize OA, LA and ALA, respectively. From these PUFA the human organism is able to synthesize any other EFA. The three putative desaturases, from *A.variabilis*, were overexpressed in *E.coli* in this work (see section R-4.2.1). However, no EFAs were detected in the lipid extracts of any of the bacterial cultures probably because *E.coli* is not able to efficiently express these heterologous genes.

On the other hand, we address the anaerobic PUFA biosynthetic pathway, in particular the production of the ω-3 LC-PUFA DHA. The biosynthesis of this valuable molecule in genetically engineered *E.coli* bacteria carrying the PKS genetic cluster from *M.marina* have already been reported in very precise conditions by Orikasa and co-workers (2006). They observed DHA production only below 25°C, while the maximum yield (a 5% of the total FA) was achieved at 15°C. Thus, the feasibility of TAG and DHA biosynthesis has been separately proved in the same bacteria. Besides, other microorganisms with higher DHA production yield incorporate the ω-3 PUFA into TAG compounds, while growing at higher temperatures (normally among 25–30°C) more suitable for industrial purposes (Raghukumar, 2008). Thus, with the aim of increasing the DHA yield by its esterification into bacterial TAGs, which incidentally represent the most common way to carry lipids into the diet, in this work we constructed an *E.coli* strain with the required metabolic pathways for both DHA and TAG (i.e. tDGAT and the *Pfa* synthase from *M.marina*). By carrying out the corresponding TLC and GC analysis, we proved the simultaneous activity of both pathways in precise conditions (21.5°C). However, the yield obtained is just a proof-of concept that needs to be seriously improved. Probably for this reason, DHA was not detected in the purified TAGs from a culture of *E.coli* expressing the required enzymes for both metabolic pathways through GC analysis. Together with using different strains, distinct expression systems for the heterologous proteins and overexpression of other acyltransferases involved in the biosynthesis of DAG, the use of a different WS/DGAT for neutral lipid production could be an interesting strategy for obtaining TAGs enriched in PUFA, since tDGAT is an optimum protein to work at high temperatures, but not as much at the low temperatures required for DHA production. The assessment of the FA composition of all lipid species produced in genetically engineered bacteria through the available techniques also might provide crucial data leading to correctly focus further genetic modifications towards this goal.

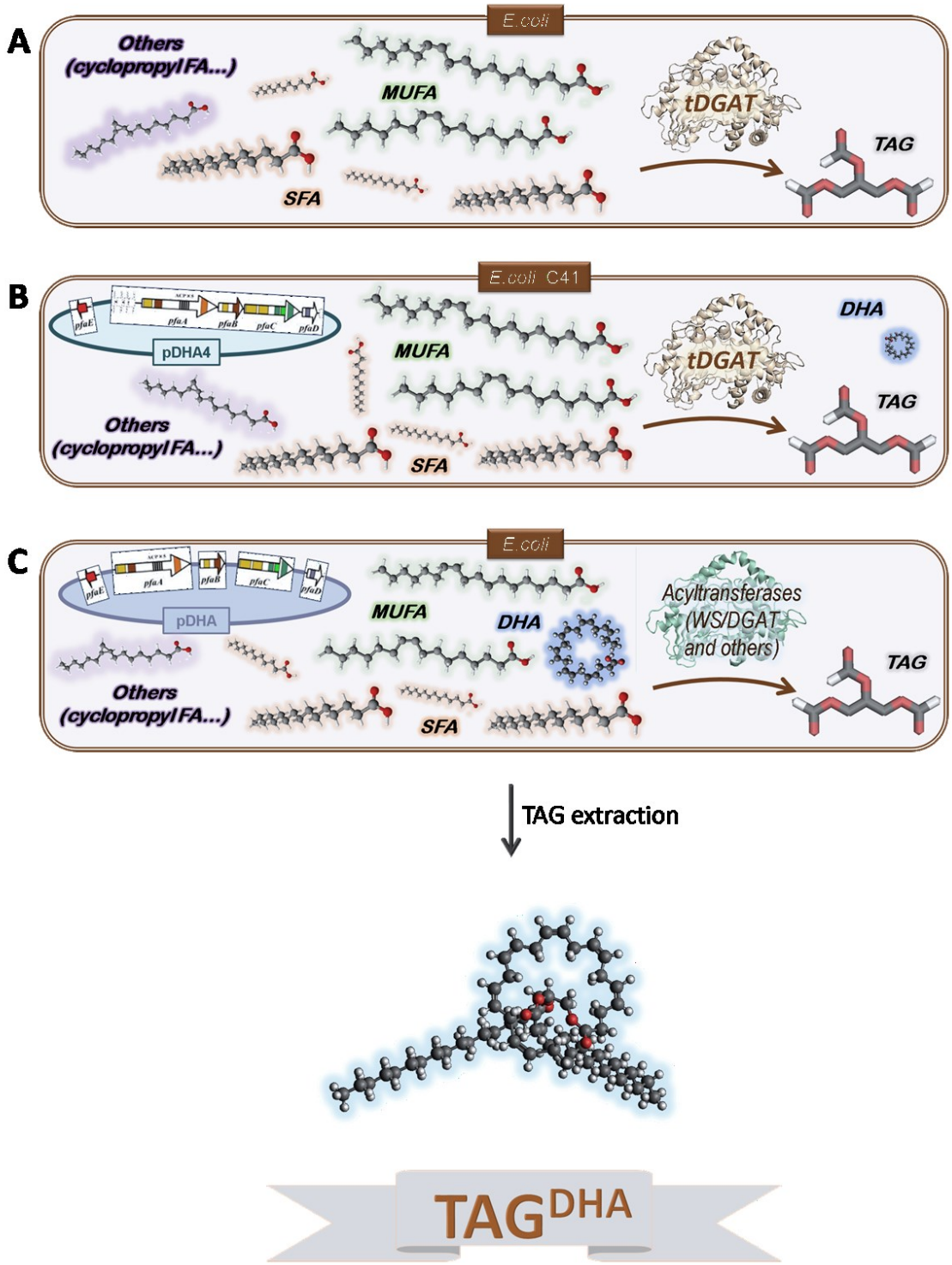

Figure D-3. Scheme illustrating the production of TAGs enriched in ω-3 PUFA in genetically engineered *E.coli* bacteria. A) *E.coli* bacteria modified to produce neutral lipids such as TAGs through the enzyme tDGAT; B) *E.coli* C41 bacteria engineered to produce neutral lipids such as TAGs through the enzyme tDGAT, and DHA through the PKS form *M.marina*; C) Different *E.coli* strain engineered to produce TAGs enriched in DHA through specific acyltransferases able to introduce LC-PUFA to DAG, another WS/DGAT enzyme and a slightly modified vector pDHA carrying the 5 Pfa genes responsible for DHA production in *M.marina* under distinct expression systems. The image of the PKS gene cluster of *M.marina* was taken from Orikasa et al., 2009. Abbreviations: SFA, saturated fatty acids; MUFA, monounsaturated fatty acids; DHA, docosahexaenoic acid; TAG, triacylglyceride; TAG^{DHA}, TAG enriched in DHA.

4.4.4. 3D structure and catalytic mechanism of the enzymes belonging to the WS/DGAT family.

Despite the enzymes WS/DGAT have been widely studied (Röttig and Steinbüchel, 2013), up to the moment there is no report available in the literature on the crystal structure of any enzyme of this family. Stöveken and co-workers described in 2009 the catalytic mechanism, which relies in the highly conserved motif HHxxxDG (see section I-1.1.3). Later, two more conserved motifs were identified by our research group, one of them discussed to be involved in the interaction with the activated FA and the other, with a structural role, also determinant for the catalytic activity (Villa et al., 2014). Nevertheless, the great biotechnological potential of the enzymes belonging to the WS/DGAT family strongly motivates a more detailed understanding of the 3D structure, the reaction mechanism, and the substrate specificity in order to optimize all process they are involved in.

With the purpose of widening our knowledge on the 3D structure of the WS/DGAT proteins, in this work the 3D structure of the protein tDGAT was modelled, showing a conformation of the enzyme in a monomer composed of two domains connected by an helical linker (as occurs in other acyltransferases) and confirming the presence of all the previously described conserved domains. An alignment of the amino acid sequence with representative members of the WS/DGAT family supported this conservation and revealed a longer sequence within the connecting loop in the protein tDGAT. Besides, the comparison of the prediction of some physico-chemical parameters revealed that tDGAT was the only enzyme with a positive GRAVY. Moreover tDGAT has a pI lower than 7, like WS/DGAT proteins from other actinomycetes also producing TAG compounds. On the contrary, all WS/DGAT proteins studied in this work from WE-producing bacteria had a pI value above 7. The prediction of the electrostatic surface of the proteins tDGAT and Ma2 showed a more intense amphipathic trait of the first enzyme, although the spatial conformation of both proteins showed great similarity according to the structural alignment of the 3D models. These data could be related to the insolubility of the protein tDGAT, which motivated the use of a homolog know to be able to solubilize in aqueous solutions for *in vitr*o experiments.

Besides, the specificity of WS/DGAT enzymes has been reported to be quite low. The elucidation and subsequent modification of the catalytic mechanisms as well as the recognition processes at molecular level are required to redefine the synthesis reaction towards the desired product and achieve an improved yield of the reaction. With this purpose STD-NMR experiments were performed to detect protein-ligand interactions among the purified Ma2 enzyme and a great mixture of potential binding molecules (the whole lipid extract from a wild type *E.coli* strain). This way, some small molecule naturally occurring in *E.coli* was observed to interact with the protein Ma2. This molecule was not identified, but was placed among the compounds with an aromatic group. Our results suggest that, in spite of the broad spectrum of the WS/DGAT enzymes, they seem to have some predilection for certain type of molecules.

This work shows a new approach to study the specificity of the WS/DGAT enzymes and set the basis for further research on this line, which is certainly essential for the modification of this proteins (i.e. rational design) with high biotechnological potential and the achievement of improved reaction yields on the desired outputs (i.e. TAG compounds enriched in the pertinent FAs for the corresponding application).

CONCLUSIONS AND FUTURE PERSPECTIVES

“If you can't explain it simply,
you don't understand it well enough"

Albert Einstein

5. Conclusions and future perspectives

In this work we have further described and widen our knowledge on the effects of the heterologous expression of WS/DGAT enzymes in *E.coli.* In addition to the confirmation of the previously reported production of neutral lipids under different conditions, we have characterized the nature of the esterified FA. Interestingly, an increase in the production of palmitoleic and *cis* vaccenic acids in the bacterial strains expressing an enzyme from this family was detected. Moreover, we have observed that those MUFA (the only UFA synthesized by proteobacteria) constitute a significant part of the TAGs produced by the recombinant strain expressing the protein tDGAT. Furthermore, a relevant proportion of those TAG seem to be constituted by 1 MUFA and 2 SFA according to UPLC/MS and ^{1}H NMR analysis. This fact highlights the great biotechnological potential of the tDGAT enzyme for synthesizing appropriate neutral lipids for the production of biodiesel, provided the dependence of the physico-chemical properties of this biofuel on its acyl chain composition.

At the same time we have estimated the TAG-production rate of the recombinant *E.coli* strain expressing the protein tDGAT. The production yields reported in this work are still far from the profitable employment of this process for any industrial purpose. Nevertheless, to our knowledge this is the first time this yield is achieved in this conditions. Therefore, this thermophilic enzyme has a huge potential to develop efficient processes of TAG production upon further improvement. Moreover, we have developed a high-throughput method that allows the detection of strains with greater TAG production rates than those obtained to the moment. Supported by other traditional laboratory techniques, this method facilitates the optimization of the process here studied. For instance, extending the analysed genetic diversity through mutagenesis of the protein tDGAT could lead to the discovery of improved proteins.

We have also constructed an *E.coli* strain capable of simultaneously synthesizing TAGs and PUFAs in precise conditions. This proof-of-concept work proves the feasibility of synthesizing high-value oils in bacteria as suitable for industrial culture as *E.coli*. Future optimization of this process could lead to a sustainable production of TAGs enriched in ω-3 LC-PUFA in the form of TAG. The employment of a different WS/DGAT enzymes, the detailed analysis of the expression systems of all heterologous genes or the study of the substrate specificity of the acyltransferases implied in DAG biosynthesis would be interesting strategies.

With the aim of optimizing both processes related to the enzyme tDGAT (the biosynthesis of both generic and specific TAGs) we have studied the 3D structure as well as the substrate specificity of the WS/DGAT proteins. This way, we have gone in depth in the scientific knowledge on the structure and the metabolic reaction catalysed by those enzymes. In spite of the promiscuity attributed to the WS/DGAT we have seen a preference for certain substrates. Additional investigations towards a complete elucidation of the characteristics of these enzymes, the specificity, the reaction requirements and the protein-substrate interactions at molecular level could lead to a total understanding of the reaction mechanism. This knowledge is crucial for the employment of WS/DGAT enzymes in the above mentioned processes, allowing rational design of the protein and different modifications leading to the desired products. An interesting approach would consist on an exhaustive study on the protein-substrate interactions among different WS/DGAT enzymes and commercial molecules. Thus, although we did not obtain an efficient *E.coli* strain for TAG production, our studies paved the road for a future achievement of this goal.

RESUMEN EN CASTELLANO

“la luna me ilumina…
entra la claridad”

6. Resumen en castellano

6.1. Introducción y Objetivos

Hoy en día, importantes bienes comerciales tienen su origen en los triacilglicéridos (también conocidos como triglicéridos, trigliceroles o TAGs). Además de las aplicaciónes directas de los TAG como grasas y aceites para uso culinario, estos lípidos neutros tienen un elevado interés debido a dos aplicaciones principales:

a) Representan la principal materia prima para la *producción de biodiesel*, un sustituto al actual modelo energético dependiente de petróleo y fósiles. El biodiesel, que se constituye de ésteres de ácidos grasos de cadena media/larga y alcoholes de cadena corta (FAAEs, Fatty Acid Alkyl Esters), se puede obtener de la transesterificación química o enzimática de TAGs con metanol o etanol (Kalscheuer et al., 2006a). Las propiedades del biocombustible (poder calorífico, flujo a baja temperatura, estabilidad a la oxidación y emisiones de óxidos de nitrógeno) dependen de la longitud y el grado de insaturación de los ácidos grasos que forman sus moléculas (Duan et al., 2011; Knothe, 2005).

b) Pueden ser una importante *fuente de ácidos graso esencialess*. Actualmente la proporción de ácidos grasos esenciales ω-3/ω-6 ingeridos en las dietas occidentales están descompensadas. Por ello, un incremento adecuado en la ingesta de ácidos grasos poli-insaturados (PUFA, Poly-unsaturated Fatty Acids) *ω-3* ha sido relacionado con diversos beneficios para la salud humana (Das, 2006; Huang et al., 2004; Simopoulos, 2002a). Además de su utilidad en el campo de la medicina, incluyendo desde los suplementos dietéticos hasta su uso para diferentes propósitos terapéuticos y farmacéuticos, las propiedades antioxidantes e hidratantes para la piel de los aceites ricos en ácidos grasos ω-3 (como el ácido docosahexanoico, DHA) han sido descritos en diversos estudios (Rucker et al., 2013; Viola and Viola, 2009). Estos ácidos grasos ω-3 son también necesarios para el crecimiento de los peces en piscifactorías.

Sin embargo, el modelo tradicional de obtención de este recurso biológico, basado en un origen animal y/o vegetal, no es sostenible. Para la obtención de biodiesel se utilizan desde aceites vegetales aptos para alimentación humana hasta grasas animales de deshecho, pasando por aceite procedente de vegetales no comestibles cultivados con este fin (Atabani et al., 2012; Kegl et al., 2013; Uthoff et al., 2009). Por otro lado, la principal fuente de PUFA ω-3 es el aceite de pescado, aunque el consumo de algunos vegetales y ciertos animales también aporta, en menor medida, estas moléculas (Hoffmann et al., 2008; Meyer et al., 2003). Es importante destacar que en los peces, la mayoría de los PUFA procede de su dieta: su principal origen está en los microorganismos acuáticos (Food and Agriculture Organization of the United Nations, 2014). La creciente demanda tanto de aceites y grasas (cuyo pronóstico para los próximos años es un continuo aumento que puede llegar a superar la producción, según Alvarez ,2010) como de PUFA (Kautharapu et al., 2013), unidos al elevado coste y a la preocupación de la sociedad por el futuro agotamiento de los recursos, ha motivado la búsqueda de alternativas de producción basadas en recursos renovables. Una solución razonable a este problema consiste en el desarrollo de una eficiente plataforma microbiana de producción de TAGs con las características adecuadas, la cual proporcionaría una fuente inagotable para estos lípidos (Alvarez, 2010; Garay et al., 2014; Peralta-Yahya et al., 2012).

Los TAGs, junto con las ceras (WEs, por sus siglas en inglés) y los polihidroxialcanohatos (PHAs), son los principales componentes de las inclusiones lipídicas presentes en los diferentes organismos (Wältermann and Steinbüchel, 2006). La capacidad de almacenar energía mediante la síntesis de algún tipo de lípido neutro supone una gran ventaja adaptativa cuando los sustratos escasean (Röttig and Steinbüchel, 2013). Sin embargo, aunque los TAGs son la principal forma de almacenaje de energía y fuente de ácidos grasos (FA, fatty acids) de organismos eucariotas como levaduras, hongos, plantas y animales, sólo unas pocas especies de bacterias poseen esta propiedad (Alvarez and Steinbüchel, 2002). La capacidad de acumular grandes cantidades de lípidos, sobre todo de algunos actinomicetos oleaginosos Gram-positivos (como *Mycobacterium* sp., *Nocardia* sp., *Rhodococcus* sp., *Micromonospora* sp., *Dietzia* sp., *Gordonia* sp. y

Streptomycetes), normalmente en respuesta a la escasez de nitrógeno, ha sido descrita en diversos estudios (Murphy, 2012). Se definen como microorganismos oleoginosos aquellos que pueden acumular más del 20% de su peso seco como lípidos. Aunque en menores cantidades también se han encontrado acúmulos de TAGs en algunas proteobacterias Gram-negativas como *Alcanivorax* sp., *Marinobacter* sp. o *Acinetobacter* sp. (Alvarez and Steinbüchel, 2002; Wältermann and Steinbüchel, 2005).

El paso final de la ruta más común de biosíntesis de TAGs en bacterias está catalizado por una una aciltransferasa de la familia WS/DGAT (Wax ester Synthase/CoA : Diacylglycerol Aciltransferase. Estas enzimas bifuncionales son las responsables finales de la formación de dos tipos de lípidos neutros en bacterias: la esterificación de alcoholes grasos o diacilglicerol (DAG) a ácidos grasos da lugar a ceras o TAGs (Kalscheuer and Steinbüchel, 2003). Se trata de proteínas con cierto carácter anfipático, con regiones hidrofóbicas necesarias para su interacción con sustratos lipídicos pero cargadas en ambientes de pH neutro debido a su punto isoeléctrico, por lo que se ha especulado con la dependencia de su actividad y/o especificidad respecto del ambiente que las rodea (Röttig and Steinbüchel, 2013; Stöveken et al., 2005; Wältermann et al., 2005). Stöveken y colaboradores caracterizaron en 2005 la primera proteína de esta clase. Más adelante se demostró que el motivo altamente conservado HHxxxDG era el responsable de la catálisis (Stöveken et al., 2009). Recientemente se detectaron otros dos dominios conservados característicos de las enzimas WS/DGAT y se demostró su gran repercusión en la actividad catalítica. Además, se describió el modelo tridimensional de estas proteínas, formadas por dos dominios conectados por una secuencia de amino ácidos en forma helicoidal, de tal forma que el centro catalítico estaría localizado en un canal hidrofóbico (Villa et al., 2014). Las aciltransferasas WS/DGAT han sido descritas como enzimas de gran promiscuidad, siendo capaces de actuar sobre un elevado número de sustratos (Stöveken and Steinbüchel, 2008; Stöveken et al., 2005). Sin embargo, es importante destacar la gran variedad de homólogos que componen esta familia de proteínas, dispares en tamaño, secuencia o actividad específica en diferentes hospedadores naturales o artificiales. La gran mayoría de estas proteínas se han encontrado en procariotas (con un gran número de ortólogos entre las actinobacterias, aunque la relación filogenética entre miembros de proteobacterias era mayor), si bien también se han identificado miembros en plantas, protistas y animales (Röttig and Steinbüchel, 2013; Villa et al., 2014).

Por otro lado, la biosíntesis de PUFA se realiza por dos vías diferentes. La ruta más común, la denominada ruta aerobia, produce los PUFA procesando por elongación y desaturación aerobia (es decir, inserción de dobles enlaces a través de desaturasas específicas dependientes de oxígeno) de los FA producidos por la sintasa de ácidos grasos (FAS) (Russell and Nichols, 1999). De esta manera, la síntesis de DHA, 22:6n3 desde acetil-CoA requiere aproximadamente 30 actividades enzimáticas diferentes y cerca de 70 reacciones (Metz et al., 2001). En las Figuras I-8 e I-31 podemos observar esquemas de esta ruta biosintética. La ruta alternativa es conocida como ruta anaerobia (ya que no requiere oxígeno molecular para llevar a cabo la reacción). Esta vía consta de complejos multienzimáticos llamados poliquétido sintasas (PKS), codificados por 5 genes dispuestos en largos clústers de 20-30 kb, que producen los PUFA a partir de acetil-CoA y malonil-CoA (Hoffmann et al., 2008; Shulse and Allen, 2011). Dentro del grupo de organismos que llevan a cabo esta vía se ha estudiado en detalle la síntesis de ácido docosahexanoico (C22:6, DHA) en las bacterias marinas *Moritella marina* MP-1 (Orikasa et al., 2006rec;) y de ácido eicosapentaenoico (C20:5, EPA) en *Shewanella* sp.(Okuyama et al., 2007; Yazawa, 1996).

Debido a la dificultad y elevado coste del cultivo de microorganismos naturalmente productores de estos lípidos de interés comercial, sumado a la falta de herramientas para su modificación genética, y en algunos casos a las restricciones de seguridad, han llevado al empleo de herramientas genéticas para la introducción de la rutas de biosíntesis pertinentes en microorganismos más manipulables y apropiados para el cultivo a gran escala como la bacteria modelo *E.coli*. La capacidad de producir diferentes compuestos lípidicos en esta gamma-proteobacteria ha sido demostrada en diversos trabajos en los últimos años (Kalscheuer et al., 2006a, 2006b; Schirmer et al., 2010). Mediante la expresión heteróloga de una enzima de la familia WS/DGAT de un microorganismo naturalmente productor de lípidos neutros, la producción de TAGs también se ha conseguido en este microorganismo, aunque el rendimiento obtenido es aún bajo (Comba et al., 2014; Janßen and Steinbüchel, 2014b; Moncalián et al., 2014; Röttig et al., 2015; Rucker et al., 2013; Villa Torrecilla, 2012). Del mismo modo, la expresión de los genes responsables de la síntesis de PUFA ω-3 en *E.coli* ha dado lugar a la producción en *E.coli* de estos valiosos ácidos grasos (Sugihara et al., 2008; Yazawa, 1996). La introducción del clúster genético que codifica para la PKS de

M.marina MP-1 dio lugar a la producción de DHA en *E.coli* cuando este microorganismo mesófilo era cultivado a temperaturas en torno a los 15°C (Orikasa et al., 2006b).

Con el actual conocimiento sobre el metabolismo lipídico bacteriano relacionado con los TAGs y los PUFA y el estado de su producción con fines comerciales, en este trabajo nos proponemos profundizar en los procesos de biosíntesis de dichos lípidos de alto valor añadido añadido y desarrollar procesos para obtener mayor rendimiento en la producción de TAGs ricos en los ácidos grasos pertinentes según su futura aplicación, es decir, con o sin PUFA. Para ello nos centraremos en la reacción catalizada por las enzimas de la familia WS/DGAT.

De este modo, los objetivos concretos que nos planteamos en el presente trabajo de Tesis doctoral fueron:

1) Estudiar el proceso que se desarrolla en bacterias *E.coli* que expresan enzimas de la familia WS/DGAT. Nuestro principal interés radica en los efectos de la expresión heteróloga de la enzima tDGAT (WS/DGAT de *T.curvata*), prestando especial atención a la composición de FA de los compuestos producidos. Además, pretendemos caracterizar y mejorar la tasa de producción del proceso de biosíntesis de TAGs.

2) Mejorar la producción de PUFA en una bacteria adecuada para su empleo en procesos industriales como *E.coli*. Para ello, por un lado expresaremos diferentes desaturasas procedentes de otros microorganismos en esta bacteria y por otro combinaremos las rutas biosintéticas de TAG y DHA (un PUFA ω-3) en la misma cepa bacteriana.

6.2. Resultados y Discusión

6.2.1. Optimización de la producción de TAGs mediante la expresión heteróloga de enzimas de la familia WS/DGAT.

Se ha demostrado que la expresión de diferentes enzimas de la familia WS/DGAT en bacterias da lugar a la producción de lípidos neutros (Kalscheuer and Steinbüchel, 2003). Trabajo previo en nuestro laboratorio llevó a la identificación de la primera enzima WS/DGAT procedente de una actinobacteria termofílica (tDGAT, codificada por un gen de *Thermomonospora curvata*) que heterólogamente expresada en *E.coli* daba lugar a cambios en el perfil lipídico de la gamma-proteobacteria, siendo uno de ellos la producción de lípidos neutros (Moncalián et al., 2014; Villa Torrecilla, 2012). La gran importancia de las enzimas termofílas (con gran estabilidad térmica) en los procesos biotecnológicos radica en su capacidad catalítica en un amplio rango de condiciones de reacción, lo que puede resultar decisivo en procesos industriales a gran escala (Coleman and Sharp, 2010).

Con el objetivo de profundizar en la descripción de los efectos de la sobre-expresión de la proteína tDGAT en cepas de *E.coli* con distintos fenotipos, se exploraron diferentes técnicas de laboratorio, las cuales fueron optimizadas para la caracterización y cuantificación de los TAGs producidos en bacterias recombinantes.

En primer lugar se realizaron análisis por cromatografía en capa fina (TLC) de extractos lipídicos totales de cultivos de *E.coli* C41 expresando o no la proteína tDGAT a través de un vector pET (ver Tabla M-2) e incubados a 37°C (temperatura óptima para el crecimiento de la proteobacteria). El análisis densitométrico de las imágenes digitalizadas de las placas de TLC puso de manifiesto que la producción y acumulación de lípidos neutros ocurría de una manera especialmente rápida tras la inducción de la sobre-expresión de la aciltransferasa. Se observó que en 90 minutos de sobre-expresión de la enzima tDGAT, la cepa recombinante de *E.coli* era capaz de acumular 4,8 mg de TAGs por litro de cultivo, lo que representaba más de un 30% de los lípidos extraídos o un 1,25% de su peso seco (ver Figura R-1). Se demostró también que esta producción de TAGs es independiente del estrés producido por la falta de nitrógeno, factor del que depende la acumulación de lípidos neutros en la mayoría de microorganismos oleogénicos como los actinomicetos (Alvarez et al., 2000). Además, se probó la actividad enzimática de la proteína tDGAT en *E.coli* a diferentes temperaturas mayores a 25°C. Sin embargo, no se detectaron TAGs en los extractos lipídicos de cultivos incubados a 15°C.

Aunque durante el desarrollo de este trabajo de Tesis doctoral se ha descrito la producción y acumulación de TAGs en diversas cepas recombinantes de *E.coli* expresando enzimas WS/DGAT, apenas se ha prestado atención al tiempo de cultivo necesario para detectar una producción significativa de este lípido neutro. Sin embargo, este aspecto tiene gran relevancia para la producción comercial en industria ya que se traduce en términos económicos. Los rendimientos de producción de TAGs aquí descritos no habían sido observados en ninguna cepa salvaje de *E.coli* con estas características genéticas y cultivadas en condiciones similares en un tiempo tan corto. Estos datos sugieren, por tanto, que la optimización del cultivo de esta cepa recombinante junto con la investigación de modificaciones genéticas adicionales beneficiosas para la producción de TAGs pueden llevar a rendimientos que permitan la realización de este proceso a nivel industrial y a su introducción en el mercado. Por otro lado, la observación de actividad catalítica con independencia de condiciones estresantes como la escasez de nitrógeno lleva a pensar que la producción de tDGAT depende solamente de la expresión heteróloga de la proteína. Por ello, podríamos pensar que el mecanismo de acción de la enzima WS/DGAT expresada en cepas recombinantes difiere del que puede observarse en sus hospedadores naturales. Además, la enzima muestra actividad aciltransferasa en un rango de temperaturas adecuado para la producción a gran escala. Estos datos confirman el gran potencial de la sobre-expresión de la enzima termófila tDGAT en *E.coli* para el desarrollo de procesos biotecnológicos de producción de TAGs de alto rendimiento.

Con el fin de profundizar en los cambios en el perfil lipídico de las cepas que expresan las proteínas WS/DGAT, los espectros de resonancia magnética nuclear de protón (^{1}H RMN; $CDCl_3$, 300.19 MHz) de los extractos lipídicos totales de la cepa salvaje *E.coli* C41 y la misma bacteria expresando diferentes proteínas de la familia WS/DGAT como tDGAT o Ma2 se compararon entre sí. Se identificaron los cambios en el

espectro de acuerdo con la literatura y se realizaron los cálculos comparativos asumiendo que el triplete que aparece en 0.88 ppm en los 3 espectros corresponde solamente a protones de grupos metilo terminales $–CH_3$, y normalizando por tanto las integrales de estos picos como múltiplos de 3 (ver Figura R-4 y Tabla R-1).

La diferencia más significativa se observó en la señal en 5,29 ppm, típica de protones olefinicos (dobles enlaces), en que el pico era 22 o 17 veces mayor que el correspondiente a la cepa salvaje en los espectros de *E.coli* C41 expresando tDGAT o Ma2, respectivamente. La señal en 2,01 ppm, normalmente atribuida a protones alílicos (adyacentes a un doble enlace) también aumentaba 6 veces respecto al mismo pico en la cepa salvaje. Por el contrario, los picos en 2,29 ppm, correspondientes a los espectros de *E.coli* C41 expresando tDGAT o Ma2 eran 2 y 4 veces menores que el correspondiente a la cepa salvaje, respectivamente. Estos picos pueden atribuirse tanto a protones metilenicos adyacentes a un grupo carboxilo como a protones H-2 de cadenas acílicas de acilgliceroles o ésteres (Alonso-Salces et al., 2012; Vlahov 1999).

Estos datos indican una acumulación de compuestos con dobles enlaces en las bacterias recombinantes que expresan enzimas WS/DGAT, especialmente en la que expresa la enzima tDGAT.

Debido a que las propiedades del biodiesel dependen de las características de los FA que componen el aceite del que deriva (Knothe, 2005), decidimos que el análisis del perfil de FA de las cepas de *E.coli* productoras de TAGs, así como de estos lípidos neutros, era interesante para saber la idoneidad de este proceso para esta su aplicación en la producción de biocombustibles.

Los extractos lipídicos de diversos cultivos de *E.coli* C41 (pEtDGAT) y de sus respectivos controles (la cepa salvaje) cultivados a 37°C se analizaron por cromatografía de gases (GC). Los análisis indicaron que los FA presentes en una cepa salvaje de *E.coli* C41 en mayor proporción son el FA saturado ácido palmitico (PA, C16:0, cuya proporción frente al total de FA de la bacteria era del 30.64%) y el FA ciclo propano ácido metil hexadecanoico (C17:0cycle, con un 17.75 %). Sin embargo, la cepa de *E.coli* C41 productora de lípidos neutros posee una elevada proporción de los ácidos grasos monoinsaturados (MUFA) ácido palmitoleico (PO, 16:1n7) y ácido *cis* vaccénico (VC, 18:1n7), de manera que la proporción de MUFA es 2,7 veces mayor que en la cepa salvaje (de 10.6 a 28.5%, ver Tabla R-2 y Figura R-6).

Al mismo tiempo se analizó por GC el perfil de FA de los TAGs purificados mediante TLC (raspados de la placa de silica gel). En los TAGs producidos por la cepa recombinante los FA mayoritarios eran, además del PA (cuya proporción se mantiene en todas las muestras entre 25-31%), los dos MUFA PO y VC. Así, el porcentaje de MUFA en el total de FA de los TAGs de la cepa recombinante de *E.coli* es del 46%, lo que representa un aumento del 439% sobre el contenido de MUFA en la cepa salvaje (ver Figuras R-6 y R-7).

Para confirmar si este desequilibrio en el perfil de FA a favor de los MUFA estaba relacionado con la expresión de la enzima tDGAT, se usó un sistema de expresión diferente (vectores pBAD, Guzman et al. 1995) en cepas de *E.coli* con fenotipos distintos (BW27783 y algunos miembros de la colección Keio, ver Tabla M-1) y se realizaron cultivos a 37°C. La comparación de los cromatogramas obtenidos mostró un aumento de MUFA en estas cepas de *E.coli* productoras de lípidos neutros de unas 12 veces respecto a sus respectivos controles, como se puede observar en las Figuras R-8 y R-10). Además, según los análisis del perfil de FA de *E.coli* C41 (pEtDGAT) cultivada a diferentes temperaturas (entre 15 y 37°C) este aumento en la proporción de MUFA ocurre hasta en el caso en que la actividad aciltransferasa no es detectada en el análisis por TLC de las extracciones lipídicas (ver Figuras R-3 y R-11). Estos resultados sugieren que el aumento de MUFA es independiente de la cepa hospedadora, del sistema de expresión y de la temperatura a la que se cultiva la bacteria.

El perfil de FA de *E.coli* varia con la cepa y las condiciones de cultivo, de manera que normalmente la proporción de MUFA aumenta a medida que disminuye la temperatura de incubación del microorganismo (Heath, Richard J. et al., 2002; Mansilla et al., 2004). Del mismo modo, la proporción de FA ciclo propanos aumenta en fase estacionaria de crecimiento (Magnuson et al., 1993). Por otro lado, se han descrito aumentos de MUFA en respuesta a la expresión heteróloga de proteínas tanto en plantas (Vanhercke et al., 2013) como en bacterias (Kerviel et al., 2014). Lin y colaboradores observaron en 2013

un aumento de 3 - 3,7 veces respecto de la cepa salvaje en la proporción de MUFA en cultivos a 37°C de la cepa de *E.coli ΔdgkA* (con la deleción del gen responsable del desvío de DAG hacia la biosíntesis de fosfolípidos) expresando diversas enzimas de la familia WS/DGAT. Este incremento en MUFAs también se observaba cuando la producción de TAGs era indetectable. Por su lado, Rucker y colaboradores describieron en 2013 los principales FA que componían los TAGs producidos por otra cepa de *E.coli*, entre los cuales casi la mitad eran MUFA, lo que coincide con nuestros resultados (ver Figura R-12)..

De este modo, podemos decir que la expresión heteróloga de la proteína tDGAT en *E.coli* está relacionada con un incremento de los MUFA bacterianos, alcanzando al menos un cuarto del total de FA. Este incremento parece ser independiente tanto de las características fenotípicas del microorganismo hospedador (incluyendo la producción de TAGs) como de la temperatura de crecimiento del mismo (ver Figuras R-4 a R-11). Sin embargo, la explicación a esta respuesta metabólica está aún por clarificar. Nuestra hipótesis se basa en la posible degradación espontánea que todos los FA pueden experimentar a través de la ruta metabólica de la β-oxidación. Los FA que pasan a formar parte de lípidos neutros como los TAGs quedarían químicamente protegidos de esa degradación, lo que daría lugar a un aumento en el porcentaje de MUFA en los FA bacterianos totales. Esto también explicaría las elevadas proporciones de MUFA observadas en los propios TAGs.

La posible función de los TAGs como "depósito" de FA innecesarios ha sido presentada como una forma de adaptación de las bacterias productoras de estos lípidos neutros a los cambios en la temperatura de crecimiento, mediante la regulación de la composición de los lípidos de membrana (Alvarez and Steinbüchel, 2002; Wältermann and Steinbüchel, 2005). La sobre-expresión de la enzima tDGAT parece tener en *E.coli* un efecto similar a la disminución de la temperatura. Por ello, otra explicación posible al incremento en el porcentaje de MUFA sería una mayor selectividad de esta proteína por estos FA, lo que provocaría un incremento de la proporción de MUFA en los TAGs y una reducción de la concentración de MUFA en el citosol (causada por su "secuestro" por parte de la tDGAT). Esto provocaría un desequilibrio en la biosíntesis de estos FA: al detectarse menos MUFA en el citosol la biosíntesis se activaría.

Los resultados obtenidos de los análisis por GC sugieren además que una parte significativa de los dobles enlaces que aparecen en *E.coli* al expresar una enzima WS/DGAT (como observamos en los espectros ^{1}H RMN de extractos lipídicos totales) se encuentran en cadenas acílicas.

Entre las fracciones lipídicas purificadas por cromatografía de columna seca (DCC) de cepas de *E.coli* salvaje y recombinante cultivada a 37°C se observaron espectros ^{1}H RMN ($CDCl_3$, 300.19 MHz) típicos de TAGs sólo en la cepa de *E.coli* expresando la enzima tDGAT. Para mayor claridad, en este trabajo representamos en la Figura R-14 la comparación de espectros de un TAG comercial, tributirina, y una muestra procedente de *E.coli* C41 (pEtDGAT) y detallamos la atribución de los picos en la Tabla R-3. El triplete que aparece en esta última muestra en 5,35 ppm indica la presencia de dobles enlaces. Las integrales fueron normalizadas teniendo en cuenta que el pico en 0,88 ppm corresponde a 9 protones (de los 3 grupos metilo terminales $–CH_3$ de las cadenas acílicas de un TAG), de modo que calculamos que hay 2 protones olefínicos por cada molécula de TAG. Para comprobar dichos resultados realizamos con esta muestra el experimento RMN bidimensional 2D H-H COSY (2-Dimensional homonuclear H COrrelation SpectroscopY), que muestra qué grupos de protones están relacionados entre sí a través de enlaces químicos. Los cálculos realizados (ver Figura R-15 y Tabla R-4) corroboran que se trata de un TAG formado por 1 solo MUFA. Esto indica una proporción significativa de TAG constituidos por 1 MUFA y 2 ácidos grasos saturados (SFA).

Por otro lado, el análisis mediante cromatografía líquida de alta presión acoplada a espectrometría de masas (UPLC/MS) de las fracciones correspondientes a los TAGs producidos por *E.coli* C41 (pEtDGAT) cultivada a 37°C y purificadas por TLC, confirmó la presencia de estos lípidos neutros sólo en la cepa recombinante (como se puede observar en los cromatogramas en la sección A de la Figura R-16). Un análisis más detallado de los compuestos específicos presentes en esta muestra mostró las especies de TAGs más frecuentes. Como podemos observar en la Figura R-16.D más de la mitad de los TAGs analizados están compuestos por un MUFA y dos SFA, mientras el resto están formados por 2 MUFA y 1 SFA o por 3 SFA. De este modo, mostramos en este trabajo diferentes datos apuntando a la importante proporción de MUFA entre los TAGs producidos por *E.coli* C41 (pEtDGAT), así como al tipo de FA que mayoritariamente componen dichos lípidos neutros.

Una vez caracterizada la producción de TAGs en estas cepas recombinantes de *E.coli*, se estudiaron posibles estrategias para desarrollar un método de selección positiva que permitiese la mejora en el rendimiento.

En primer lugar se abordó una estrategia basada en la relación entre el contenido en lípidos de un organismo y su flotabilidad (Devries and Eastman, 1978; Lee et al., 2006) para seleccionar cepas recombinantes de *E.coli* con una producción de TAGs optimizada. Sin embargo, a diferencia de lo que ocurre bacterias oleogénicas en que los mayores productores de lípidos tienen menor densidad (Wältermann et al., 2000), la actual producción de TAGs en *E.coli* resultó ser insignificante como para provocar suficientes diferencias de densidad en la población. Según nuestros experimentos de sedimentación celular este método no es adecuado para *E.coli* con los rendimientos actuales.

A continuación nos centramos en técnicas de fluorescencia basadas en colorantes lipofílicos. Para ello, caracterizamos el comportamiento de cepas de *E.coli* en las que análisis tradicionales como la TLC han mostrado producción de TAG.

Imágenes de microscopía de fluorescencia de diferentes cepas de *E.coli* recombinantes, con distintos sistemas de expresión para la enzima tDGAT, muestran cierta semejanza en la acumulación de TAGs en estas bacterias con inclusiones previamente descritas en bacterias oleogénicas (Alvarez et al., 1996). Como podemos observar en la Figura 17, las imágenes de bacterias que expresan la enzima tDGAT presentan inclusiones redondeadas con mayor fluorescencia ausentes en los controles.

Por otra parte se cultivó *E.coli* C41 (pEtDGAT) con y sin Rojo Nilo, se prepararon pads de agarosa (portas para microscopio cubiertos de una capa de medio de cultivo definido solidificado con agarosa) y se monitorizó el crecimiento de las bacterias sobre dicho soporte colocado en una cámara a 37°C acoplada al microscopio de fluorescencia, obteniendo imágenes cada 20 minutos (en las Figuras R-18 y R-19 podemos observar una representación de estas imágenes). En los fotogramas correspondientes a las bacterias teñidas podemos observar dos morfologías diferentes, entre las cuales sólo las que no muestran inclusiones redondeadas con mayor fluorescencia y, presumiblemente, no acumulan lípidos neutros, muestran división celular. Por el contrario, entre las bacterias sin teñir sólo vemos bacterias en lento crecimiento. Las bacterias que muestran división celular presentan además un perfil de fluorescencia similar al observado anteriormente en la cepa salvaje *E.coli* C41 (aunque mucho menos intenso en la salvaje). En cambio, el perfil de fluorescencia de las bacterias en que no vemos división celular alguna recuerda al visto anteriormente en *E.coli* C41 (pEtDGAT) con Rojo Nilo.

Tanto el colorante Rojo Nilo como el alternativo Bodipy$^{505/515}$ se utilizaron para teñir diferentes cultivos de *E.coli* C41 (pEtDGAT) y la cepa salvaje incubados a 37°C y analizar dichas cepas mediante citometría de flujo. El incremento de los eventos detectados como fluorescentes entre los analizados en cada caso fue superior a un 30% con ambos colorantes (ver Figura R-20). Este cálculo coincide con el aumento de TAGs en la bacteria recombinante previamente obtenido por análisis densitométrico de las placas de TLC. Podemos decir por tanto que esta técnica también puede usadarse para detectar la producción de lípidos neutros en cepas de *E.coli* expresando la enzima tDGAT.

La acumulación de lípidos neutros también se monitorizó mediante la medida de la fluorescencia cada 20 minutos en el fluorímetro Victor donde se cultivaron las cepas (a 37°C con agitación) en una placa microtiter de 96 pocillos. Tanto el inductor (arabinosa) como el colorante (Rojo Nilo) se añadieron manualmente a los cultivos correspondientes cuando la DO_{600nm} alcanzó aproximadamente 0.3. Según los datos obtenidos, la inducción de la expresión heteróloga tDGAT provocaba un inmediato aumento de la fluorescencia en la cepa recombinante teñida, cuyo valor se estabilizaba unas horas después, aún en fase exponencial de crecimiento (el gráfico de la Figura R-21 muestra las medidas de fluorescencia).

La correspondencia observada entre la acumulación de TAGs y la fluorescencia en cultivos tratados con colorantes lipofílicos permite el desarrollo de un método de análisis de alto rendimiento que puede dar lugar a una eficiente optimización de la producción de TAGs en bacterias. Basándonos en protocolos ya existentes desarrollados con algas productoras de lípidos neutros (Cagnon et al., 2013; Chen et al., 2009), en este trabajo hemos puesto a punto un procedimiento basado en colorantes fluorescentes y en el cultivo

de diferentes cepas bacterianas en placas de 96 pocillos cuyas medidas serán obtenidas en un fluorímetro. Para ello, en primer lugar establecemos los principales parámetros de medida de fluorescencia, así como los pasos a seguir para teñir las muestras, a partir de un número reducido de cultivos de *E.coli* productores o no de TAGs, de manera que podemos llevar a cabo análisis por métodos tradicionales como TLC para confirmar los resultados. Es interesante destacar que, siguiendo el protocolo optimizado de tinción y medida de fluorescencia, los análisis fluorimétricos indicaron un incremento mayor al 30% en la fluorescencia detectada en *E.coli* C41 (pEtDGAT) y *E.coli* BW27783 (pBtDGAT) respecto de sus correspondientes cepas salvajes. Estos datos añadirían otra evidencia a los datos previamente obtenidos por citometría de flujo y análisis densitométrico de placas de TLC. Finalmente se realizaron estos experimentos en condiciones similares en placas de 96 pocillos. Con el fin de estudiar el efecto de la eliminación de diferentes genes en la síntesis de los lípidos neutros en bacterias, se transformó el gen de la enzima tDGAT en diferentes mutantes knockout de *E.coli* utilizando la colección Keio (construcción sistemática de mutantes knockout en cada uno de los genes/ORFs de *E.coli* ;Baba et al., 2006). Para ello utilizamos el plásmido pBoRtDGAT, que contiene tDGAT optimizado para *E.coli* bajo un promotor inducible por arabinosa y el origen de transferencia de R388 y el plásmido pSU711 como movilizador (Francia et al., 1993). De este modo facilitamos la transformación eficiente de diferentes cepas con este plásmido. Un ejemplo de este análisis puede observarse en la Figura R-24, donde vemos que no se detectó un nivel de fluorescencia significativamente mayor que el correspondiente al control positivo en ninguna de las cepas analizadas. No obstante, queda así demostrada la utilidad de este método para seleccionar cepas con mayor producción de TAGs que la observada hasta el momento.

6.2.2. Obtención de PUFAs en *E.coli*.

La gamma-proteobacteria *E.coli* es normalmente una alternativa óptima para la producción de cualquier compuesto de interés comercial, debido al gran conocimiento que tenemos sobre su metabolismo, a la existencia de múltiples herramientas que facilitan su manipulación genética y a su idoneidad para el cultivo industrial. La importancia de la identificación y desarrollo de nuevos procesos para la producción de PUFA ha motivado la investigación del empleo de este microorganismo como bio-factoría.

Se sabe que *E.coli* produce de forma natural FA ω-7 como PO y VC (Heath, Richard J. et al., 2002), pero la producción de PUFA implica procesos más complicados con enzimas de las que esta bacteria modelo carece. Por ello, en este trabajo utilizamos herramientas de ingeniería genética para aportar a *E.coli* la capacidad de sintetizar PUFA mediante cualquiera de las dos rutas biosintéticas existentes.

En primer lugar construimos diferentes cepas de *E.coli* C41 transformando la bacteria con diversos genes de desaturasas procedentes de la cianobacteria *Anabaena variabilis* ATCC (ver Tabla R-5) con el propósito de que el microorganismo sea capaz de convertir los productos finales de su FAS en los ácidos grasos esenciales (EFAs) más sencillos: los ácidos linoleico (ω-6 LA, C18:2n6) y α-linolénico (ω-3 ALA, C18:3n3). La presencia de los genes correspondientes a las desaturasas Δ9, Δ12 y Δ15 en la proteobacteria se comprobó mediante PCR. El contenido en FA se analizó mediante GC, sin embargo no se encontraron diferencias entre los cromatogramas. Como sabemos que *E.coli* no sintetiza de forma natural ácido oleico (OA, C18:1n9, sustrato para la formación de LA), por lo que decidimos cultivar las cepas con un suplemento comercial de OA en el medio (que, como posteriormente comprobamos, contenía LA). Observamos entonces que en todos los cromatogramas obtenidos aparecen los ácidos grasos OA y LA en proporciones similares, además de otros FA típicos de la proteobacteria, como PA (ver Figura R-26). Podemos decir por tanto que ninguna de las proteínas heterólogamente expresadas era funcional en las condiciones ensayadas.

Posteriormente abordamos la ruta anaerobia de biosíntesis de PUFA. Se ha comprobado que la producción heteróloga de DHA es posible en *E.coli* mediante la introducción en el microorganismo de la poliquétido sintasa de *M.marina* MP-1 y el cultivo de esta cepa a temperaturas menores a 25°C, preferiblemente a 15°C (Orikasa et al., 2006b). Por otro lado, se ha propuesto que una de las funciones clave de los TAGs consiste en actuar como "depósito" de ciertos FA, que quedan químicamente protegidos de su desvío hacia la síntesis de fosfolípidos, regulando de esta manera la fluidez de la membrana celular en respuesta a las variaciones de temperatura (Alvarez and Steinbüchel, 2002; Heath, Richard J. et al., 2002; Lin et al., 2013). Puesto que en el mismo organismo modelo se ha probado la producción de TAGs

(mediante la inducción de un gen que codifique para una WS/DGAT), en este trabajo combinamos ambas rutas anabólicas en dicha bacteria con el fin de obtener una eficiente producción de DHA a una temperatura más apropiada para su cultivo a nivel industrial. Esta estrategia gana fuerza al fijarse en otros microorganismos cuyo mayor rendimiento de producción de DHA en forma de TAGs ocurre a mayores temperaturas de crecimiento, 25–30°C (Raghukumar, 2008). Así, para modificar la composición de los TAGs presentes en una cepa bacteriana capaz de acumular lípidos neutros, inducimos la co-expresión de los genes del clúster que codifican para la síntesis de la PKS de *M.marina* MP-1 (de forma que variaremos el perfil de FA existentes en la misma) a través del plásmido pDHA4 (Orikasa et al., 2009) y el gen responsable de la biosíntesis de TAGs (utilizaremos el gen de la enzima tDGAT) en la misma cepa.

En primer lugar se confirmó la presencia de ambas construcciones genéticas en la cepa *E.coli* C41 (pEtDGAT + pDHA4), así como la sobre-expresión de las proteínas heterólogas a diferentes temperaturas de cultivo (ver Figuras R-28 y R-29). Observamos sobre-expresión de la enzima tDGAT a partir de 21.5°C, sin embargo, no podemos apreciar sobre-expresión de las 5 proteínas que forman la PKS, posiblemente debido a su gran tamaño, que facilita su fragmentación durante el análisis.

Seguidamente comprobamos la actividad de ambos procesos biosintéticos en las condiciones óptimas de crecimiento para cada uno de ellos. Así, independientemente de la carga genética adicional, observamos mediante análisis por TLC la producción de TAGs en *E.coli* C41 (pEtDGAT + pDHA4) cultivada a 37°C, y detectamos DHA en el cromatograma obtenido del análisis GC del cultivo de la misma cepa a 15°C (ver Figura R-30). Sin embargo, no detectamos nada en el análisis de cada uno de estos cultivos para el compuesto lipídico cuya producción no era óptima.

Con el propósito de encontrar condiciones de cultivo comunes para la producción simultánea de ambos compuestos lipídicos, se cultivó la cepa *E.coli* C41 (pEtDGAT + pDHA4) a diferentes temperaturas. Los TAGs fueron observados por TLC a temperaturas de cultivo mayores a 21.5°C, mientras que el DHA se detectaron por análisis GC por debajo de esta temperatura de cultivo. Los análisis por GC, TLC y citometría de flujo se muestran en la Figura R-31, donde podemos observar la producción simultánea de ambas moléculas. El cromatograma muestra que la producción de DHA es especialmente baja (0,36% del total de FA en la célula). Los dos colorantes lipofílicos previamente utilizados en este trabajo, Rojo Nilo y Bodipy$^{505/515}$, se usaron para comparar la producción de lípidos neutros a esta temperatura de *E.coli* C41, *E.coli* C41 (pEtDGAT) y *E.coli* C41 (pEtDGAT + pDHA4). En ambos casos el porcentaje de eventos detectados como fluorescentes en la cepa con ambas rutas biosintéticas fue mayor que en el control pero menor que en la cepa que sólo producía lípidos neutros. Esto sugiere que la actividad de la enzima tDGAT queda reducida por la expresión del clúster de la PKS.

Finalmente analizamos las fracciones de TAGs de esta cepa, purificadas por TLC. Sin embargo, no detectamos DHA en el análisis GC. Estos resultados podrían deberse a los bajos rendimientos obtenidos, a su localización en los fosfolípidos y no-incorporación a los TAGs presentes en la bacteria o a la degradación del DHA a lo largo del procedimiento de análisis (que incluyó extracción lipídica, TLC y análisis GC). A causa del gran número de dobles enlaces de este FA, pude ser fácilmente oxidado, lo que dificulta su manipulación.

6.2.3. Caracterización de las proteínas de la familia WS/DGAT

Las proteínas de la familia WS/DGAT, ampliamente distribuidas, tienen un gran potencial biotecnológico, como se explica en la introducción. Por ello es importante profundizar en el actual conocimiento sobre su estructura, su especificidad y su mecanismo catalítico.

Con el propósito de ampliar nuestro entendimiento acerca de la estructura tridimensional (3D) de las proteínas WS/DGAT, se empleó el software PHYRE Web para predecir el modelaje estructural de la enzima tDGAT. De esta manera se confirmó que esta aciltransferasa, como todos los miembros de esta familia, es un monómero formado por dos dominios estructurales unidos por una región helicoidal. Como podemos observar en la Figura R-32, el dominio Nt (N terminal) contiene 4 láminas β rodeadas por 3 hélices α mientras el Ct (C terminal) consiste en 5 láminas β y 5 hélices α. El centro catalítico ^{140}HHxxxDG^{147}, al igual que en otras aciltransferasas dependientes de acil-CoA, aparece en un canal hidrofóbico que restringe la

accesibilidad de sustratos hidrofílicos. En un extremo de este canal se observa el motivo II ^{281}ND^{282}, lo que sugiere un papel esencial de estos residuos en la interacción con el sustrato. De hecho, estudios previos en el laboratorio observaron su posible interacción con los grupos fosfato del acil-CoA, según comparaciones con estructuras resueltas anteriormente (Villa et al., 2014). Por otro lado, los aminoácidos ^{118}PLW^{120} del motivo I aparecen espacialmente cercanas al centro activo, lo que, como se ha sugerido anteriormente, puede indicar un papel estructural relacionado con el correcto plegamiento de la proteína.

Además, la secuencia de aminoácidos de la enzima tDGAT se alineó con las secuencias de miembros representativos de la familia WS/DGAT (ver Tabla R-6 y Figura R-33), demostrándose que contiene todos los motivos conservados en la familia descritos en la literatura (Röttig and Steinbüchel, 2013; Villa et al., 2014). Asimismo, se calcularon algunos parámetros físico-químicos de estas secuencias mediante herramientas bioinformáticas. Se observó que la única proteína entre las analizadas con un índice global de hidrofobicidad (GRAVY, *Grand average of hydropathy*) positivo era tDGAT, mientras según su punto isoeléctrico (6,44) estaría cargada negativamente en un ambiente neutro, al igual que ocurre con otras proteínas de actinomicetos oleogénicos, que acumulan TAGs como compuesto de reserva. Como podemos observar en la Figura R-33, los residuos correspondientes a parte de la región helicoidal conectora entre los dos dominios, la hélice α8, destacan en el alineamiento. Aunque esta región está poco conservada en todos los miembros de la familia WS/DGAT, parece ser más larga en tDGAT.

Por otro lado el modelo 3D aquí presentado de la enzima tDGAT se alineó estructuralmente mediante el software Pymol al modelo estructural de su homólogo Ma2 (WS/DGAT de *Marinobacter hydrocarbonoclasticus* VT8) presentado por Villa Torrecilla, 2012, mostrando una gran similitud y compartiendo localización espacial de los motivos conservados (ver Figura R-34). Igualmente, teniendo en cuenta la relevancia de la hicrofobicidad del ambiente para la actividad y/o la especificidad de las enzimas de esta familia (Kalscheuer and Steinbüchel, 2003; Wältermann et al., 2005), se predijo y se comparó la distribución de cargas superficiales en las proteínas alineadas. En la Figura R-35 podemos observar diferencias en la distribución de los residuos hidrofóbicos, que muestran un carácter anfipático más pronunciado en tDGAT. Se destaca también en ambas enzimas la disposición espacial de los residuos apolares en el canal hidrofóbico donde se encuentra el centro catalítico.

El estudio de las interacciones proteína-ligando entre una enzima de la familia WS/DGAT y sus sustratos puede darnos valiosa información acerca del mecanismo catalítico de estos biocatalizadores a nivel molecular y sobre su especificidad, conocimiento que permitiría una eficiente mejora de la enzima dirigida a la obtención de los productos deseados.

Diferentes estrategias pueden utilizarse para investigar este tipo de interacciones, entre las cuales en este trabajo hemos llevado a cabo técnicas de RMN de alta resolución. Concretamente utilizamos la técnica de espectroscopia RMN de Diferencia de transferencia de saturación (STD-NMR, *Saturation Transfer Difference-NMR*), basada en el análisis del Efecto Nuclear Overhausser (NOE) entre proteína y ligando con la gran ventaja de usar ligandos no marcados. De este modo podemos realizar un *screening* o cribado de potenciales ligandos, detectando los sustratos concretos que están interaccionando con la enzima. Podemos además determinar el mapa del epítopo, consistente en definir la orientación de la molécula de sustrato en la interacción o describir qué partes de la misma están más cercanas a la enzima durante la interacción (y por tanto tienen mayor afinidad).

Para realizar los experimentos STD-NMR, se estableció una temperatura de 15°C con el fin de alcanzar un equilibrio entre la estabilidad de la enzima y la baja viscosidad del solvente anfipático utilizado para solubilizar los sustratos hidrofóbicos en la solución acuosa en la que se encontraba la proteína, cuya estabilidad es mayor a menores temperaturas. Previamente a la realización del experimento STD se adquirieron espectros ^{1}H RMN (600,13 MHz) en las mismas condiciones tanto de cada una de las muestras por separado (proteína y solución apolar de sustratos) como de la mezcla de ambas (esta última, en que se uso como solvente para el experimento una solución de D_2O:DMSO-d_6 5:1, agua deuterada : dimetilsulfóxido deuterado, fue la muestra posteriormente empleada para realizar propiamente el experimento STD-NMR).

El experimento STD-NMR consiste en realidad en la realización de dos experimentos (y la consiguiente adquisición de dos espectros) y la posterior resta de los espectros obtenidos, de modo que

obtendremos un espectro "diferencia" (el espectro STD) que sólo contiene picos cuya intensidad ha cambiado (aquellos que corresponden a los ligantes). El experimento referencia coincide básicamente con un espectro ^{1}H RMN normal. El segundo experimento consiste en pre-saturar la proteína (es decir, aplicar una radiofrecuencia en la zona espectral que contiene sólo señales de la proteína) de modo que ésta transmitirá su magnetización sólo a las moléculas que interaccionen, o lo que es lo mismo, a los ligandos. La intensidad de esta transmisión nos da idea, además, de la afinidad con que interacciona cada grupo de protones de la molécula.

La Figura R-37 muestra el espectro STD obtenido con la proteína Ma2, previamente purificada de *E.coli* (pEmbDGAT), mezclada con el extracto lipídico total de *E.coli* C41. Podemos observar que hay moléculas que interaccionan con la proteína. Al comparar con los espectros ^{1}H RMN (600,13 MHz) previamente adquiridos de cada uno de los componentes y de la propia la mezcla, vemos que las moléculas que aparecen en el espectro STD están naturalmente presentes en la cepa salvaje (ver Figura R-38). Además, sabemos que dichas moléculas son apolares ya que fueron extraídas de *E.coli* C41 junto con los lípidos. Las atribuciones de cada grupo de protones y el cálculo del mapa del epítopo aparecen detalladas en la Tabla R-7.

Por otro lado, se intentó averiguar más información sobre los ligandos realizando con la misma muestra y en las mismas condiciones experimentos monodimensionales ^{1}H RMN TOCSY (*Total Correlation Spectroscopy*, técnica en que un grupo de protones concreto es irradiado mediante un pulso selectivo, de forma que vemos resonancia en todos aquellos grupos de protones que pertenezcan a la misma red de acoplamiento). Así, vemos que se trata de un solo tipo de molécula formada por dos sistemas de acoplamiento, uno de los cuales es un anillo aromático (debido a los 2 dobletes y 2 tripletes que aparecen en la región entre 6,5 y 8,0 ppm de un mismo espectro TOCSY), aunque no conseguimos identificar dicha molécula.

6.3. Conclusiones y perspectivas futuras

En este trabajo hemos ampliado nuestro conocimiento sobre los efectos de la expresión heteróloga de las enzimas WS/DGAT en *E.coli*. Además de confirmar la producción de lípidos neutros en estas bacterias recombinantes en diversas condiciones, hemos descrito la composición de las cadenas acílicas de los compuestos lipídicos producidos. Así, hemos detectado un incremento en la producción de los ácidos palmitoleico y *cis* vaccénico en las bacterias recombinantes que expresaban esta enzima. Del mismo modo observamos que estos MUFA (los únicos FA insaturados sintetizados por estos microorganismos) constituían una parte importante de los TAG producidos por la cepa recombinante que expresa la proteína tDGAT. Lo que es más, según análisis UPLC/MS y ^{1}H RMN una gran proporción de estos TAG parecen estar formados por 1 MUFA y 2 SFA. Estos resultados destacan y refuerzan el gran potencial biotecnológico de la enzima tDGAT para la síntesis de lípidos neutros adecuados para la producción de biodiesel, dada la dependencia de las propiedades físico-químicas de este biocombustible de su composición de cadenas acílicas.

Al mismo tiempo hemos estimado la tasa de producción de TAG de la cepa recombinante de *E.coli* que expresa la enzima tDGAT. Los niveles de producción descritos en este trabajo están aún lejos del desarrollo de un proceso rentable que pueda utilizarse en la industria. Sin embargo, esta es la primera vez que se consigue un rendimiento así en estas condiciones, lo que confirma el enorme potencial para el desarrollo de procesos eficientes de producción de TAG mediante esta enzima termofílica. Asimismo, hemos desarrollado un método de alto rendimiento basado en la fluorescencia producida por el colorante Rojo Nilo en presencia de TAGs o lípidos neutros que nos premitirá la identificación de sistemas más efectivos en la producción de TAGs. Una posible estrategia para optimizar este proceso consistiría en ampliar la diversidad genética mediante la mutagénesis del gen de la tDGAT. Mayor investigación en este sentido podría llevar a la detección de cepas recombinantes con mejores tasas de producción de TAG que las obtenidas hasta el momento y al desarrollo de un proceso altamente eficiente que tendría interesantes aplicaciones.

Hemos construido también una cepa de *E.coli* capaz de sintetizar al mismo tiempo TAG y PUFA en condiciones de cultivo concretas. Este trabajo demuestra la posibilidad de sintetizar ambos compuestos lipídicos de valor añadido en una misma bacteria tan adecuada para el cultivo a nivel industrial como *E.coli*. Aunque nuestros resultados son simbólicos sientan las bases para la obtención de microorganismos capaces de producir elevados rendimientos de TAGs ricos en DHA. El empleo de una enzima WS/DGAT diferente para la síntesis de lípidos neutros así como el análisis detallado de los sistemas de expresión de las proteínas heterólogas responsables de la biosíntesis de las moléculas deseadas y de la especificidad de la enzima tDGAT o de otras aciltransferasas que formen diácilglicéridos (intermediarios para la síntesis de TAG) podrían ser estrategias interesantes.

Con el propósito de optimizar ambos procesos relacionados con la enzima tDGAT (la biosíntesis de TAG genéricos y específicos) hemos estudiado tanto la estructura tridimensional como la especificidad de sustrato de las proteínas de la familia WS/DGAT. De esta manera hemos profundizado en el conocimiento científico sobre las características estructurales y la reacción metabólica catalizada por estas enzimas. A pesar de la gran promiscuidad atribuida a las enzimas WS/DGAT, hemos observado cierta preferencia por algunos sustratos. Una comprensión adecuada de las características de dichas enzimas, de los requerimientos de las reacciones que catalizan, su especificidad y el proceso catalítico a nivel molecular facilitaría el diseño racional y la selección u obtención de un miembro eficiente de esta familia, permitiendo así la optimización de diferentes procesos para obtener los productos deseados. Una estrategia interesante consistiría en la realización de un estudio más exhaustivo de la interacción proteína-sustrato con diferentes enzimas WS/DGAT y sustratos comerciales, el cual podría diseñarse a partir de los datos aportados en este trabajo. De esta forma, aunque no hemos obtenido una cepa de *E.coli* capaz de producir eficientemente TAG con las características deseadas, nuestro trabajo sienta las bases para la futura obtención de este objetivo.

REFERENCES

7. References

Ahmad, A.L., Yasin, N.H.M., Derek, C.J.C., and Lim, J.K. (2011). Microalgae as a sustainable energy source for biodiesel production: A review. Renew. Sustain. Energy Rev. *15*, 584–593.

Ahuja, S. (1976). Derivatization in gas chromatography. J. Pharm. Sci. *65*, 163–182.

Ahuja, S., and Jespersen, N. (2006). Modern Instrumental Analysis (Elsevier).

Allen, E.E., and Bartlett, D.H. (2002). Structure and regulation of the omega-3 polyunsaturated fatty acid synthase genes from the deep-sea bacterium Photobacterium profundum strain SS9. Microbiol. Read. Engl. *148*, 1903–1913.

Allen, E.E., Facciotti, D., and Bartlett, D.H. (1999). Monounsaturated but not polyunsaturated fatty acids are required for growth of the deep-sea bacterium Photobacterium profundum SS9 at high pressure and low temperature. Appl. Environ. Microbiol. *65*, 1710–1720.

Almoselhy, R.I.M., Allam, M.H., El-Kalyoubi, M.H., and El-Sharkawy, A.A. (2014). 1H NMR spectral analysis as a new aspect to evaluate the stability of some edible oils. Ann. Agric. Sci. *59*, 201–206.

Alonso-Salces, R.M., V., M., Guillou, C., and Hberger, K. (2012). Quality Assessment of Olive Oil by 1H-NMR Fingerprinting. In Olive Oil - Constituents, Quality, Health Properties and Bioconversions, D. Boskou, ed. (InTech),.

Altschul, S.F., Madden, T.L., SchÃ¤ffer, A.A., Zhang, J., Zhang, Z., Miller, W., and Lipman, D.J. (1997). Gapped BLAST and PSI-BLAST: a new generation of protein database search programs. Nucleic Acids Res. *25*, 3389–3402.

Alvarez, H.M. (2010). Biotechnological Production and Significance of Triacylglycerols and Wax Esters. In Handbook of Hydrocarbon and Lipid Microbiology, K.N. Timmis, ed. (Springer Berlin Heidelberg), pp. 2995–3002.

Alvarez, H.M. (2016). Triacylglycerol and wax ester-accumulating machinery in prokaryotes. Biochimie *120*, 28–39.

Alvarez, H., and Steinbüchel, A. (2002). Triacylglycerols in prokaryotic microorganisms. Appl. Microbiol. Biotechnol. *60*, 367–376.

Alvarez, H.M., Mayer, F., Fabritius, D., and Steinbüchel, A. (1996). Formation of intracytoplasmic lipid inclusions by Rhodococcus opacus strain PD630. Arch. Microbiol. *165*, 377–386.

Alvarez, H.M., Kalscheuer, R., and Steinbüchel, A. (2000). Accumulation and mobilization of storage lipids by Rhodococcus opacus PD630 and Rhodococcus ruber NCIMB 40126. Appl. Microbiol. Biotechnol. *54*, 218–223.

Al-Zuhair, S. (2007). Production of biodiesel: possibilities and challenges. Biofuels Bioprod. Biorefining *1*, 57–66.

Angulo, J., and Nieto, P.M. (2011). Espectroscopía RMN de Diferencia de Transferencia de Saturación (STD NMR). Aplicaciones en Química del Reconocimiento Molecular.

Antoni, D., Zverlov, V.V., and Schwarz, W.H. (2007). Biofuels from microbes. Appl. Microbiol. Biotechnol. *77*, 23–35.

Arabolaza, A., Rodriguez, E., Altabe, S., Alvarez, H., and Gramajo, H. (2008). Multiple Pathways for Triacylglycerol Biosynthesis in Streptomyces coelicolor. Appl. Environ. Microbiol. *74*, 2573–2582.

Arts, M.T., Ackman, R.G., and Holub, B.J. (2001). "Essential fatty acids" in aquatic ecosystems: a crucial link between diet and human health and evolution. Can. J. Fish. Aquat. Sci. *58*, 122–137.

Atabani, A.E., Silitonga, A.S., Badruddin, I.A., Mahlia, T.M.I., Masjuki, H.H., and Mekhilef, S. (2012). A comprehensive review on biodiesel as an alternative energy resource and its characteristics. Renew. Sustain. Energy Rev. *16*, 2070–2093.

Atomi, H. (2005). Recent progress towards the application of hyperthermophiles and their enzymes. Curr. Opin. Chem. Biol. *9*, 166–173.

Baba, T., Ara, T., Hasegawa, M., Takai, Y., Okumura, Y., Baba, M., Datsenko, K.A., Tomita, M., Wanner, B.L., and Mori, H. (2006). Construction of Escherichia coli K-12 in-frame, single-gene knockout mutants: the Keio collection. Mol. Syst. Biol. *2*.

Banković-Ilić, I.B., Stojković, I.J., Stamenković, O.S., Veljkovic, V.B., and Hung, Y.-T. (2014). Waste animal fats as feedstocks for biodiesel production. Renew. Sustain. Energy Rev. *32*, 238–254.

Benoit, M., and Klaus, D. (2005). Can genetically modified Escherichia coli with neutral buoyancy induced by gas vesicles be used as an alternative method to clinorotation for microgravity studies? Microbiol. Read. Engl. *151*, 69–74.

Bergé, J.-P., and Barnathan, G. (2005). Fatty acids from lipids of marine organisms: molecular biodiversity, roles as biomarkers, biologically active compounds, and economical aspects. Adv. Biochem. Eng. Biotechnol. *96*, 49–125.

Berg, JM, Tymoczko, JL, and Stryer, L (2002). Fatty Acids Are Key Constituents of Lipids - Biochemistry. In Biochemistry. 5th Edition., (New York: W H Freeman),.

Brennan, L., Blanco Fernández, A., Mostaert, A.S., and Owende, P. (2012). Enhancement of BODIPY505/515 lipid fluorescence method for applications in biofuel-directed microalgae production. J. Microbiol. Methods *90*, 137–143.

Brown, H.A., and Marnett, L.J. (2011). Introduction to Lipid Biochemistry, Metabolism, and Signaling. Chem. Rev. *111*, 5817–5820.

Brown, H.A., and Murphy, R.C. (2009). Working towards an exegesis for lipids in biology. Nat. Chem. Biol. *5*, 602–606.

Bruice, P.Y. (2004). Organic Chemistry 4th Edition (Pearson Prentice Hall).

Cagnon, C., Mirabella, B., Nguyen, H.M., Beyly-Adriano, A., Bouvet, S., Cuiné, S., Beisson, F., Peltier, G., and Li-Beisson, Y. (2013). Development of a forward genetic screen to isolate oil mutants in the green microalga Chlamydomonas reinhardtii. Biotechnol. Biofuels *6*, 178.

Cao, Y., Liu, W., Xu, X., Zhang, H., Wang, J., and Xian, M. (2014). Production of free monounsaturated fatty acids by metabolically engineered Escherichia coli. Biotechnol. Biofuels *7*, 59.

Chen, W., Zhang, C., Song, L., Sommerfeld, M., and Hu, Q. (2009). A high throughput Nile red method for quantitative measurement of neutral lipids in microalgae. J. Microbiol. Methods *77*, 41–47.

Chertkov, O., Sikorski, J., Nolan, M., Lapidus, A., Lucas, S., Del Rio, T.G., Tice, H., Cheng, J.F., Goodwin, L., Pitluck, S., et al. (2011). Complete genome sequence of Thermomonospora curvata type strain (B9). Stand. Genomic Sci. *4*, 13–22.

Chi, X., Yang, Q., Zhao, F., Qin, S., Yang, Y., Shen, J., and Lin, H. (2008). Comparative Analysis of Fatty Acid Desaturases in Cyanobacterial Genomes. Comp. Funct. Genomics *2008*.

Clomburg, J.M., and Gonzalez, R. (2010). Biofuel production in Escherichia coli: the role of metabolic engineering and synthetic biology. Appl. Microbiol. Biotechnol. *86*, 419–434.

Coleman, R.G., and Sharp, K.A. (2010). Shape and evolution of thermostable protein structure. Proteins *78*, 420–433.

Comba, S., Menendez-Bravo, S., Arabolaza, A., and Gramajo, H. (2013). Identification and physiological characterization of phosphatidic acid phosphatase enzymes involved in triacylglycerol biosynthesis in Streptomyces coelicolor. Microb. Cell Factories *12*, 9.

Comba, S., Sabatini, M., Menendez-Bravo, S., Arabolaza, A., and Gramajo, H. (2014). Engineering a Streptomyces coelicolor biosynthesis pathway into Escherichia coli for high yield triglyceride production. Biotechnol. Biofuels *7*, 172.

Cooper, M.S., Hardin, W.R., Petersen, T.W., and Cattolico, R.A. (2010). Visualizing "green oil" in live algal cells. J. Biosci. Bioeng. *109*, 198–201.

Cote, W. (2013). Biomass Utilization (Springer Science & Business Media).

Daniel, J., Deb, C., Dubey, V.S., Sirakova, T.D., Abomoelak, B., Morbidoni, H.R., and Kolattukudy, P.E. (2004). Induction of a novel class of diacylglycerol acyltransferases and triacylglycerol accumulation in Mycobacterium tuberculosis as it goes into a dormancy-like state in culture. J. Bacteriol. *186*, 5017–5030.

Das, U.N. (2006). Essential Fatty acids - a review. Curr. Pharm. Biotechnol. *7*, 467–482.

Debeljak, N., Feldman, L., Davis, K.L., Komel, R., and Sytkowski, A.J. (2006). Variability in the Immunodetection of His-tagged Recombinant Proteins. Anal. Biochem. *359*, 216–223.

Dellomonaco, C., Clomburg, J.M., Miller, E.N., and Gonzalez, R. (2011). Engineered reversal of the β-oxidation cycle for the synthesis of fuels and chemicals. Nature *476*, 355–359.

Desbois, A.P., and Smith, V.J. (2010). Antibacterial free fatty acids: activities, mechanisms of action and biotechnological potential. Appl. Microbiol. Biotechnol. *85*, 1629–1642.

Devries, A.L., and Eastman, J.T. (1978). Lipid sacs as a buoyancy adaptation in an Antarctic fish. Nature *271*, 352–353.

DiRusso, C.C., Heimert, T.L., and Metzger, A.K. (1992). Characterization of FadR, a global transcriptional regulator of fatty acid metabolism in Escherichia coli. Interaction with the fadB promoter is prevented by long chain fatty acyl coenzyme A. J. Biol. Chem. *267*, 8685–8691.

Duan, Y., Zhu, Z., Cai, K., Tan, X., and Lu, X. (2011). De novo biosynthesis of biodiesel by Escherichia coli in optimized fed-batch cultivation. PloS One *6*, e20265.

Elbahloul, Y., and Steinbüchel, A. (2010). Pilot-Scale Production of Fatty Acid Ethyl Esters by an Engineered Escherichia coli Strain Harboring the p(Microdiesel) Plasmid. Appl. Environ. Microbiol. *76*, 4560–4565.

Facke, T., and Berger, S. (1995). Application of Pulsed Field Gradients in an Improved Selective TOCSY Experiment. J. Magn. Reson. A *113*, 257–259.

Fahy, E., Subramaniam, S., Brown, H.A., Glass, C.K., Merrill, A.H., Murphy, R.C., Raetz, C.R.H., Russell, D.W., Seyama, Y., Shaw, W., et al. (2005). A comprehensive classification system for lipids. J. Lipid Res. *46*, 839–862.

FAO GLOBEFISH (2011). Demand and supply of feed ingredients for farmed fish and crustaceans: trends and prospects.

Felter, R.A., Colwell, R.R., and Chapman, G.B. (1969). Morphology and Round Body Formation in Vibrio marinus. J. Bacteriol. *99*, 326–335.

Fernandez, B.J. (2011). Genetic characterization of omega-3 polyunsaturated fatty acid synthesis in the psychrophilic bacterium Colwellia psychrerythraea. University of California.

Fernandez-Lopez, R. (2005). Unsaturated fatty acids are inhibitors of bacterial conjugation. Microbiology *151*, 3517–3526.

Figueiredo, I.M. (2006). RMN de 1H aplicada as Interações supramoleculares entre proteínas e cofatores ou inibidores. Universidade Estadual de Campinas.

Figueiredo, I.M., and Marsaioli, A.J. (2007). Screening protein-ligand interactions using ^{1}H NMR techniques for detecting the ligand. Quím. Nova *30*, 1597–1605.

Food and Agriculture Organization of the United Nations (2014). The State of World Fisheries and Aquaculture.

Francia, M.V., Cruz, F. de la, and Lobo, J.M.G. (1993). Secondary sites for integration mediated by the Tn21 integrase. Mol. Microbiol. *10*, 823–828.

Fried, B., and Sherma, J. (1999). Thin-Layer Chromatography, Revised And Expanded (CRC Press).

Fuchs, B., Süß, R., Teuber, K., Eibisch, M., and Schiller, J. (2011). Lipid analysis by thin-layer chromatography—A review of the current state. J. Chromatogr. A *1218*, 2754–2774.

Galano, J.-M., Lee, J.C.-Y., Gladine, C., Comte, B., Le Guennec, J.-Y., Oger, C., and Durand, T. (2015). Non-enzymatic cyclic oxygenated metabolites of adrenic, docosahexaenoic, eicosapentaenoic and α-linolenic acids; bioactivities and potential use as biomarkers. Biochim. Biophys. Acta BBA - Mol. Cell Biol. Lipids *1851*, 446–455.

Garay, L.A., Boundy-Mills, K.L., and German, J.B. (2014). Accumulation of high-value lipids in single-cell microorganisms: a mechanistic approach and future perspectives. J. Agric. Food Chem. *62*, 2709–2727.

Golding, G.B., and Dean, A.M. (1998). The structural basis of molecular adaptation. Mol. Biol. Evol. *15*, 355–369.

Gottlieb, H.E., Kotlyar, V., and Nudelman, A. (1997). NMR Chemical Shifts of Common Laboratory Solvents as Trace Impurities. J. Org. Chem. *62*, 7512–7515.

Govender, T., Ramanna, L., Rawat, I., and Bux, F. (2012). BODIPY staining, an alternative to the Nile Red fluorescence method for the evaluation of intracellular lipids in microalgae. Bioresour. Technol. *114*, 507–511.

Grant, S.G., Jessee, J., Bloom, F.R., and Hanahan, D. (1990). Differential plasmid rescue from transgenic mouse DNAs into Escherichia coli methylation-restriction mutants. Proc. Natl. Acad. Sci. U. S. A. *87*, 4645–4649.

Greenspan, P., and Fowler, S.D. (1985). Spectrofluorometric studies of the lipid probe, nile red. J. Lipid Res. *26*, 781–789.

Greenspan, P., Mayer, E.P., and Fowler, S.D. (1985). Nile red: a selective fluorescent stain for intracellular lipid droplets. J. Cell Biol. *100*, 965–973.

Griffiths, W.J. (2003). Tandem mass spectrometry in the study of fatty acids, bile acids, and steroids. Mass Spectrom. Rev. *22*, 81–152.

Griffiths, W.J., Jonsson, A.P., Liu, S., Rai, D.K., and Wang, Y. (2001). Electrospray and tandem mass spectrometry in biochemistry. Biochem. J. *355*, 545–561.

Guichardant, M., Calzada, C., Bernoud-Hubac, N., Lagarde, M., and Véricel, E. (2015). Omega-3 polyunsaturated fatty acids and oxygenated metabolism in atherothrombosis. Biochim. Biophys. Acta *1851*, 485–495.

Gunstone, F.D., Harwood, J.L., and Dijkstra, A.J. (2007). The Lipid Handbook with CD-ROM, Third Edition (CRC Press).

Gupta, V.K., Schmoll, M., Maki, M., Tuohy, M., and Mazutti, M.A. (2013). Applications of Microbial Engineering (CRC Press).

Gurr, M.I., and Harwood, J.L. (1991). The nature of lipids and their place in living things. In Lipid Biochemistry, (Springer US), pp. 1–9.

Gurr, M.I., Harwood, J.L., and Frayn, K.N. (2002). Lipids as Energy Stores. In Lipid Biochemistry, (Blackwell Science Ltd), pp. 93–126.

Guyer, M.S., Reed, R.R., Steitz, J.A., and Low, K.B. (1981). Identification of a sex-factor-affinity site in E. coli as gamma delta. Cold Spring Harb. Symp. Quant. Biol. *45 Pt 1*, 135–140.

Guzman, L.M., Belin, D., Carson, M.J., and Beckwith, J. (1995). Tight regulation, modulation, and high-level expression by vectors containing the arabinose PBAD promoter. J. Bacteriol. *177*, 4121–4130.

Handke, P., Lynch, S.A., and Gill, R.T. (2011). Application and engineering of fatty acid biosynthesis in Escherichia coli for advanced fuels and chemicals. Metab. Eng. *13*, 28–37.

Hara, A., and Radin, N.S. (1978). Lipid extraction of tissues with a low-toxicity solvent. Anal. Biochem. *90*, 420–426.

Harding, S.E., and Chowdhry, B.Z. (2001). Protein-ligand Interactions: Hydrodynamics and Calorimetry : a Practical Approach (Oxford University Press).

Hauvermale, A., Kuner, J., Rosenzweig, B., Guerra, D., Diltz, S., and Metz, J.G. (2006). Fatty acid production in Schizochytrium sp.: Involvement of a polyunsaturated fatty acid synthase and a type I fatty acid synthase. Lipids *41*, 739–747.

Heath, Richard J., Jackowski, Suzanne, and Rock, Charles O. (2002). Fatty acid and phospholipid metabolism in prokaryotes. In Biochemistry of Lipids, Lipoproteins and Membranes, (Elservier Science B.V.),.

Heftmann, E. (2004). Chromatography: Fundamentals and applications of chromatography and related differential migration methods - Part A: Fundamentals and techniques (Elsevier).

Hines, M.E., and Frazier, K.S. (1993). Differentiation of mycobacteria on the basis of chemotype profiles by using matrix solid-phase dispersion and thin-layer chromatography. J. Clin. Microbiol. *31*, 610–614.

Hoffman, R.E. (2006). Standardization of chemical shifts of TMS and solvent signals in NMR solvents. Magn. Reson. Chem. MRC *44*, 606–616.

Hoffmann, M., Wagner, M., Abbadi, A., Fulda, M., and Feussner, I. (2008). Metabolic engineering of omega3-very long chain polyunsaturated fatty acid production by an exclusively acyl-CoA-dependent pathway. J. Biol. Chem. *283*, 22352–22362.

Hofvander, P., Doan, T.T.P., and Hamberg, M. (2011). A prokaryotic acyl-CoA reductase performing reduction of fatty acyl-CoA to fatty alcohol. FEBS Lett. *585*, 3538–3543.

Holtzapple, E., and Schmidt-Dannert, C. (2007). Biosynthesis of isoprenoid wax ester in Marinobacter hydrocarbonoclasticus DSM 8798: identification and characterization of isoprenoid coenzyme A synthetase and wax ester synthases. J. Bacteriol. *189*, 3804–3812.

Horrocks, L.A., and Yeo, Y.K. (1999). Health benefits of docosahexaenoic acid (DHA). Pharmacol. Res. *40*, 211–225.

Huang, C., Chen, X., Xiong, L., Chen, X., Ma, L., and Chen, Y. (2013). Single cell oil production from low-cost substrates: The possibility and potential of its industrialization. Biotechnol. Adv. *31*, 129–139.

Huang, Y.-S., Pereira, S.L., and Leonard, A.E. (2004). Enzymes for transgenic biosynthesis of long-chain polyunsaturated fatty acids. Biochimie *86*, 793–798.

Icho, T., and Raetz, C.R. (1983). Multiple genes for membrane-bound phosphatases in Escherichia coli and their action on phospholipid precursors. J. Bacteriol. *153*, 722–730.

International Energy Agency (IEA) (2015). World Energy Outlook Special Report 2015: Energy and Climate Change.

Janßen, H.J., and Steinbüchel, A. (2014a). Fatty acid synthesis in Escherichia coli and its applications towards the production of fatty acid based biofuels. Biotechnol. Biofuels *7*, 7.

Janßen, H.J., and Steinbüchel, A. (2014b). Production of triacylglycerols in Escherichia coli by deletion of the diacylglycerol kinase gene and heterologous overexpression of atfA from Acinetobacter baylyi ADP1. Appl. Microbiol. Biotechnol. *98*, 1913–1924.

Jenke-Kodama, H., Sandmann, A., Müller, R., and Dittmann, E. (2005). Evolutionary implications of bacterial polyketide synthases. Mol. Biol. Evol. *22*, 2027–2039.

Ji, X.-J., Ren, L.-J., and Huang, H. (2015). Omega-3 Biotechnology: A Green and Sustainable Process for Omega-3 Fatty Acids Production. Front. Bioeng. Biotechnol. *3*.

Kaiser, B.K., Carleton, M., Hickman, J.W., Miller, C., Lawson, D., Budde, M., Warrener, P., Paredes, A., Mullapudi, S., Navarro, P., et al. (2013). Fatty Aldehydes in Cyanobacteria Are a Metabolically Flexible Precursor for a Diversity of Biofuel Products. PLoS ONE *8*, e58307.

Kalscheuer, R., and Steinbüchel, A. (2003). A novel bifunctional wax ester synthase/acyl-CoA:diacylglycerol acyltransferase mediates wax ester and triacylglycerol biosynthesis in Acinetobacter calcoaceticus ADP1. J. Biol. Chem. *278*, 8075–8082.

Kalscheuer, R., Stölting, T., and Steinbüchel, A. (2006a). Microdiesel: Escherichia coli engineered for fuel production. Microbiol. Read. Engl. *152*, 2529–2536.

Kalscheuer, R., Stöveken, T., Luftmann, H., Malkus, U., Reichelt, R., and Steinbüchel, A. (2006b). Neutral lipid biosynthesis in engineered Escherichia coli: jojoba oil-like wax esters and fatty acid butyl esters. Appl. Environ. Microbiol. *72*, 1373–1379.

Kalscheuer, R., Stöveken, T., Malkus, U., Reichelt, R., Golyshin, P.N., Sabirova, J.S., Ferrer, M., Timmis, K.N., and Steinbüchel, A. (2007). Analysis of Storage Lipid Accumulation in Alcanivorax borkumensis: Evidence for Alternative Triacylglycerol Biosynthesis Routes in Bacteria. J. Bacteriol. *189*, 918–928.

Kaneda, T. (1991). Iso- and anteiso-fatty acids in bacteria: biosynthesis, function, and taxonomic significance. Microbiol. Rev. *55*, 288–302.

Kautharapu, K.B., Rathmacher, J., and Jarboe, L.R. (2013). Growth condition optimization for docosahexaenoic acid (DHA) production by Moritella marina MP-1. Appl. Microbiol. Biotechnol. *97*, 2859–2866.

Keeler, J. (2011). Understanding NMR Spectroscopy (John Wiley & Sons).

Kegl, B., Kegl, M., and Pehan, S. (2013). Biodiesel as Diesel Engine Fuel. In Green Diesel Engines, (Springer London), pp. 95–125.

Kelley, L.A., and Sternberg, M.J.E. (2009). Protein structure prediction on the Web: a case study using the Phyre server. Nat. Protoc. *4*, 363–371.

Kerviel, V., Hérault, J., Dumur, J., Ergan, F., Poisson, L., and Loiseau, C. (2014). Cloning and expression of a gene from Isochrysis galbana modifying fatty acid profiles in Escherichia coli. J. Appl. Phycol. *26*, 2109–2115.

Khlebnikov, A., Datsenko, K.A., Skaug, T., Wanner, B.L., and Keasling, J.D. (2001). Homogeneous expression of the P(BAD) promoter in Escherichia coli by constitutive expression of the low-affinity high-capacity AraE transporter. Microbiol. Read. Engl. *147*, 3241–3247.

Knothe, G. (2005). Dependence of biodiesel fuel properties on the structure of fatty acid alkyl esters. Fuel Process. Technol. *86*, 1059–1070.

Knothe, G. (2006). Analyzing biodiesel: standards and other methods. J. Am. Oil Chem. Soc. *83*, 823–833.

Knothe, G., and Dunn, R.O. (2009). A Comprehensive Evaluation of the Melting Points of Fatty Acids and Esters Determined by Differential Scanning Calorimetry. J. Am. Oil Chem. Soc. *86*, 843–856.

Kralovec, J.A., Zhang, S., Zhang, W., and Barrow, C.J. (2012). A review of the progress in enzymatic concentration and microencapsulation of omega-3 rich oil from fish and microbial sources. Food Chem. *131*, 639–644.

Kyte, J., and Doolittle, R.F. (1982). A simple method for displaying the hydropathic character of a protein. J. Mol. Biol. *157*, 105–132.

Lanfranconi, M.P., Alvarez, A.F., and Alvarez, H.M. (2015). Identification of genes coding for putative wax ester synthase/diacylglycerol acyltransferase enzymes in terrestrial and marine environments. AMB Express *5*, 128.

Lauro, F.M., Eloe, E.A., Liverani, N., Bertoloni, G., and Bartlett, D.H. (2005). Conjugal vectors for cloning, expression, and insertional mutagenesis in gram-negative bacteria. BioTechniques *38*, 708, 710, 712.

Lee, R., Hagen, W., and Kattner, G. (2006). Lipid storage in marine zooplankton. Mar. Ecol. Prog. Ser. *307*, 273–306.

Lefébure, T., and Stanhope, M.J. (2009). Pervasive, genome-wide positive selection leading to functional divergence in the bacterial genus Campylobacter. Genome Res. *19*, 1224–1232.

Leonard, J., Lygo, B., and Procter, G. (2013). Advanced practical organic chemistry (CRC Press).

Li, Q., Du, W., and Liu, D. (2008). Perspectives of microbial oils for biodiesel production. Appl. Microbiol. Biotechnol. *80*, 749–756.

Lie Ken Jie, M.S.F., and Lam, C.C. (1995). 1H-Nuclear magnetic resonance spectroscopic studies of saturated, acetylenic and ethylenic triacylglycerols. Chem. Phys. Lipids *2*, 155–171.

Lin, F., Chen, Y., Levine, R., Lee, K., Yuan, Y., and Lin, X.N. (2013). Improving Fatty Acid Availability for Bio-Hydrocarbon Production in Escherichia coli by Metabolic Engineering. PLoS ONE *8*, e78595.

lipid LIPID MAPS Lipid Structure Database (LMSD) : LIPID MAPS Lipidomics Gateway.

Liu, Y., Zhang, C., Shen, X., Zhang, X., Cichello, S., Guan, H., and Liu, P. (2013). Microorganism lipid droplets and biofuel development. BMB Rep. *46*, 575–581.

Liu, Y., Xu, Y., Zhang, F., Yun, J., and Shen, Z. (2014). The impact of biofuel plantation on biodiversity: a review. Chin. Sci. Bull. *59*, 4639–4651.

Lu, C., Xin, Z., Ren, Z., Miquel, M., and Browse, J. (2009). An enzyme regulating triacylglycerol composition is encoded by the ROD1 gene of Arabidopsis. Proc. Natl. Acad. Sci. *106*, 18837–18842.

Lutterbach, M.T.S., and Galvão, M.M. (2010). Fuel for the Future: Biodiesel – A Case study. In Applied Microbiology and Molecular Biology in Oilfield Systems, C. Whitby, and T.L. Skovhus, eds. (Springer Netherlands), pp. 229–235.

Magnuson, K., Jackowski, S., Rock, C.O., and Cronan, J.E. (1993). Regulation of fatty acid biosynthesis in Escherichia coli. Microbiol. Rev. *57*, 522–542.

Mansilla, M.C., Cybulski, L.E., Albanesi, D., and Mendoza, D. de (2004). Control of Membrane Lipid Fluidity by Molecular Thermosensors. J. Bacteriol. *186*, 6681–6688.

Marcel, S.F.L.K.J., C, C.L., and Lie (1995). 1H-Nuclear magnetic resonance spectroscopic studies of saturated, acetylenic and ethylenic triacylglycerols. Chem. Phys. Lipids *2*, 155–171.

Mayer, M., and Meyer, B. (1999). Characterization of Ligand Binding by Saturation Transfer Difference NMR Spectroscopy. Angew. Chem. Int. Ed. *38*, 1784–1788.

Mazzola, E.P., Lambert, J.B., and Holland, L.N. (2003). Nuclear Magnetic Resonance Spectroscopy: An Introduction to Principles, Applications, and Experimental Methods (Upper Saddle River, N.J: Cisco Press).

Meesapyodsuk, D., and Qiu, X. (2012). The front-end desaturase: structure, function, evolution and biotechnological use. Lipids *47*, 227–237.

Metz, J.G., Roessler, P., Facciotti, D., Levering, C., Dittrich, F., Lassner, M., Valentine, R., Lardizabal, K., Domergue, F., Yamada, A., et al. (2001). Production of polyunsaturated fatty acids by polyketide synthases in both prokaryotes and eukaryotes. Science *293*, 290–293.

Meyer, B., and Peters, T. (2003). NMR Spectroscopy Techniques for Screening and Identifying Ligand Binding to Protein Receptors. Angew. Chem. Int. Ed. *42*, 864–890.

Meyer, B.J., Mann, N.J., Lewis, J.L., Milligan, G.C., Sinclair, A.J., and Howe, P.R.C. (2003). Dietary intakes and food sources of omega-6 and omega-3 polyunsaturated fatty acids. Lipids *38*, 391–398.

Milagre, C.D.F., Cabeça, L.F., Almeida, W.P., and Marsaioli, A.J. (2012). β-lactam antibiotics epitope mapping with STD NMR spectroscopy: a study of drug-human serum albumin interaction. J. Braz. Chem. Soc. *23*, 403–408.

Miller, L., and Berger, T. (1985). Bacteria identification by gas chromatography of whole cell fatty acids. Hewlett-Packard Appl. Note *228*, 241.

Miroux, B., and Walker, J.E. (1996). Over-production of Proteins inEscherichia coli: Mutant Hosts that Allow Synthesis of some Membrane Proteins and Globular Proteins at High Levels. J. Mol. Biol. *260*, 289–298.

Moncalián, G., de la Cruz, F., Villa, J.A., Lázaro, B., and Cabezas, M. (2014). Heat-stable triacylglycerol synthases and uses thereof.

Morita, N., Ichise, N., Yumoto, I., Yano, Y., Ohgiya, S., and Okuyama, H. (2005). Cultivation of microorganisms in the cultural medium made from squid internal organs and accumulation of polyunsaturated fatty acids in the cells. Biotechnol. Lett. *27*, 933–941.

Murphy, D.J. (2012). The dynamic roles of intracellular lipid droplets: from archaea to mammals. Protoplasma *249*, 541–585.

Notredame, C., Higgins, D.G., and Heringa, J. (2000). T-coffee: a novel method for fast and accurate multiple sequence alignment. J. Mol. Biol. *302*, 205–217.

Nwachukwu, R.E.S., Shahbazi, A., Wang, L., Worku, M., Ibrahim, S., and Schimmel, K. (2013). Optimization of cultural conditions for conversion of glycerol to ethanol by Enterobacter aerogenes S012. AMB Express *3*, 12.

Okuyama, H., Orikasa, Y., Nishida, T., Watanabe, K., and Morita, N. (2007). Bacterial Genes Responsible for the Biosynthesis of Eicosapentaenoic and Docosahexaenoic Acids and Their Heterologous Expression. Appl. Environ. Microbiol. *73*, 665–670.

Orikasa, Y., Nishida, T., Hase, A., Watanabe, K., Morita, N., and Okuyama, H. (2006a). A phosphopantetheinyl transferase gene essential for biosynthesis of n-3 polyunsaturated fatty acids from Moritella marina strain MP-1. FEBS Lett. *580*, 4423–4429.

Orikasa, Y., Nishida, T., Yamada, A., Yu, R., Watanabe, K., Hase, A., Morita, N., and Okuyama, H. (2006b). Recombinant production of docosahexaenoic acid in a polyketide biosynthesis mode in Escherichia coli. Biotechnol. Lett. *28*, 1841–1847.

Orikasa, Y., Tanaka, M., Sugihara, S., Hori, R., Nishida, T., Ueno, A., Morita, N., Yano, Y., Yamamoto, K., Shibahara, A., et al. (2009). pfaB products determine the molecular species produced in bacterial polyunsaturated fatty acid biosynthesis. FEMS Microbiol. Lett. *295*, 170–176.

Packaged Facts Global Market for EPA/DHA Omega-3 Products.

Packer, M.S., and Liu, D.R. (2015). Methods for the directed evolution of proteins. Nat. Rev. Genet. *16*, 379–394.

Peralta-Yahya, P.P., Zhang, F., del Cardayre, S.B., and Keasling, J.D. (2012). Microbial engineering for the production of advanced biofuels. Nature *488*, 320–328.

Petrakis, L., and Fraissard, J. (2012). Magnetic Resonance: Introduction, Advanced Topics and Applications to Fossil Energy (Springer Science & Business Media).

Pinzon, N.M., Aukema, K.G., Gralnick, J.A., and Wackett, L.P. (2011). Nile Red Detection of Bacterial Hydrocarbons and Ketones in a High-Throughput Format. mBio *2*, e00109–e00111.

Polyak, S.W., Abell, A.D., Wilce, M.C.J., Zhang, L., and Booker, G.W. (2011). Structure, function and selective inhibition of bacterial acetyl-CoA carboxylase. Appl. Microbiol. Biotechnol. *93*, 983–992.

Qiu, X. (2003). Biosynthesis of docosahexaenoic acid (DHA, 22:6-4, 7,10,13,16,19): two distinct pathways. Prostaglandins Leukot. Essent. Fatty Acids *68*, 181–186.

Qiul, J., Fan, X., and Zou, H. (2011). Development of biodiesel from inedible feedstock through various production processes. Review. Chem. Technol. Fuels Oils *47*, 102–111.

Quintana, N., Van der Kooy, F., Van de Rhee, M.D., Voshol, G.P., and Verpoorte, R. (2011). Renewable energy from Cyanobacteria: energy production optimization by metabolic pathway engineering. Appl. Microbiol. Biotechnol. *91*, 471–490.

Raghukumar, S. (2008). Thraustochytrid Marine Protists: production of PUFAs and Other Emerging Technologies. Mar. Biotechnol. N. Y. N *10*, 631–640.

Ramos, M.J., Fernández, C.M., Casas, A., Rodríguez, L., and Pérez, Á. (2009). Influence of fatty acid composition of raw materials on biodiesel properties. Bioresour. Technol. *100*, 261–268.

Reich, E., and Schibli, A. (2004). A standardized approach to modern high-performance thin-layer chromatography (HPTLC). JPC - J. Planar Chromatogr. - Mod. TLC *17*, 438–443.

Ridgway, N., and McLeod, R. (2015). Biochemistry of Lipids, Lipoproteins and Membranes (Elsevier).

Robert, X., and Gouet, P. (2014). Deciphering key features in protein structures with the new ENDscript server. Nucleic Acids Res. *42*, W320–W324.

Rosano, G.L., and Ceccarelli, E.A. (2014). Recombinant protein expression in Escherichia coli: advances and challenges. Front. Microbiol. *5*.

Rosenberg, A.H., Lade, B.N., Dao-shan, C., Lin, S.-W., Dunn, J.J., and Studier, F.W. (1987). Vectors for selective expression of cloned DNAs by T7 RNA polymerase. Gene *56*, 125–135.

Rossi, D.M., da Costa, J.B., de Souza, E.A., Peralba, M. do C.R., and Ayub, M.A.Z. (2012). Bioconversion of residual glycerol from biodiesel synthesis into 1,3-propanediol and ethanol by isolated bacteria from environmental consortia. Renew. Energy *39*, 223–227.

Rossi, M., Amaretti, A., Raimondi, S., and Leonardi, A. (2011). Getting Lipids for Biodiesel Production from Oleaginous Fungi. In Biodiesel - Feedstocks and Processing Technologies, M. Stoytcheva, ed. (InTech),.

Röttig, A., and Steinbüchel, A. (2013). Acyltransferases in bacteria. Microbiol. Mol. Biol. Rev. MMBR *77*, 277–321.

Röttig, A., Zurek, P.J., and Steinbüchel, A. (2015). Assessment of bacterial acyltransferases for an efficient lipid production in metabolically engineered strains of E. coli. Metab. Eng. *32*, 195–206.

Rucker, J., Paul, J., Pfeifer, B.A., and Lee, K. (2013). Engineering E. coli for triglyceride accumulation through native and heterologous metabolic reactions. Appl. Microbiol. Biotechnol. *97*, 2753–2759.

Russell, N.J., and Nichols, D.S. (1999). Polyunsaturated fatty acids in marine bacteria--a dogma rewritten. Microbiol. Read. Engl. *145 (Pt 4)*, 767–779.

Sakuradani, E., Ando, A., Ogawa, J., and Shimizu, S. (2009). Improved production of various polyunsaturated fatty acids through filamentous fungus Mortierella alpina breeding. Appl. Microbiol. Biotechnol. *84*, 1–10.

Sambrook, J., and Russell, D.W. (2001). Molecular cloning, vol. 1-3 (Cold Spring Harbor Laboratory Press, Cold Spring Harbor, NY).

Schirmer, A., Rude, M.A., Li, X., Popova, E., and Cardayre, S.B. del (2010). Microbial Biosynthesis of Alkanes. Science *329*, 559–562.

Schneider, C.A., Rasband, W.S., and Eliceiri, K.W. (2012). NIH Image to ImageJ: 25 years of image analysis. Nat. Methods *9*, 671–675.

Schweizer, E., and Hofmann, J. (2004). Microbial Type I Fatty Acid Synthases (FAS): Major Players in a Network of Cellular FAS Systems. Microbiol. Mol. Biol. Rev. *68*, 501–517.

Shi, S., Valle-Rodríguez, J.O., Khoomrung, S., Siewers, V., and Nielsen, J. (2012). Functional expression and characterization of five wax ester synthases in Saccharomyces cerevisiae and their utility for biodiesel production. Biotechnol. Biofuels *5*, 7.

Shulse, C.N., and Allen, E.E. (2011). Widespread Occurrence of Secondary Lipid Biosynthesis Potential in Microbial Lineages. PLoS ONE *6*, e20146.

Sijtsma, L., and de Swaaf, M.E. (2004). Biotechnological production and applications of the omega-3 polyunsaturated fatty acid docosahexaenoic acid. Appl. Microbiol. Biotechnol. *64*, 146–153.

Silverstein, R.M., Webster, F.X., and Kiemle, D. (2005). Spectrometric Identification of Organic Compounds (Hoboken, NJ: John Wiley & Sons).

Simopoulos, A.P. (2002a). The importance of the ratio of omega-6/omega-3 essential fatty acids. Biomed. Pharmacother. Bioméd. Pharmacothérapie *56*, 365–379.

Simopoulos, A.P. (2002b). Omega-3 fatty acids in inflammation and autoimmune diseases. J. Am. Coll. Nutr. *21*, 495–505.

Skinner, S.O., Sepúlveda, L.A., Xu, H., and Golding, I. (2013). Measuring mRNA copy number in individual Escherichia coli cells using single-molecule fluorescent in situ hybridization. Nat. Protoc. *8*, 1100–1113.

Spiekermann, P., Rehm, B.H., Kalscheuer, R., Baumeister, D., and Steinbüchel, A. (1999). A sensitive, viable-colony staining method using Nile red for direct screening of bacteria that accumulate polyhydroxyalkanoic acids and other lipid storage compounds. Arch. Microbiol. *171*, 73–80.

Sprecher, H., Luthria, D.L., Mohammed, B.S., and Baykousheva, S.P. (1995). Reevaluation of the pathways for the biosynthesis of polyunsaturated fatty acids. J. Lipid Res. *36*, 2471–2477.

Stachelhaus, T., Mootz, H.D., Bergendahl, V., and Marahiel, M.A. (1998). Peptide bond formation in nonribosomal peptide biosynthesis. Catalytic role of the condensation domain. J. Biol. Chem. *273*, 22773–22781.

Steen, E.J., Kang, Y., Bokinsky, G., Hu, Z., Schirmer, A., McClure, A., del Cardayre, S.B., and Keasling, J.D. (2010). Microbial production of fatty-acid-derived fuels and chemicals from plant biomass. Nature *463*, 559–562.

Stöveken, T., and Steinbüchel, A. (2008). Bacterial acyltransferases as an alternative for lipase-catalyzed acylation for the production of oleochemicals and fuels. Angew. Chem. Int. Ed Engl. *47*, 3688–3694.

Stöveken, T., Kalscheuer, R., Malkus, U., Reichelt, R., and Steinbüchel, A. (2005). The Wax Ester Synthase/Acyl Coenzyme A:Diacylglycerol Acyltransferase from Acinetobacter sp. Strain ADP1: Characterization of a Novel Type of Acyltransferase. J. Bacteriol. *187*, 1369–1376.

Stöveken, T., Kalscheuer, R., and Steinbüchel, A. (2009). Both histidine residues of the conserved HHXXXDG motif are essential for wax ester synthase/acyl-CoA:diacylglycerol acyltransferase catalysis. Eur. J. Lipid Sci. Technol. *111*, 112–119.

Stretton, S., Techkarnjanaruk, S., McLennan, A.M., and Goodman, A.E. (1998). Use of green fluorescent protein to tag and investigate gene expression in marine bacteria. Appl. Environ. Microbiol. *64*, 2554–2559.

Studier, F.W., and Moffatt, B.A. (1986). Use of bacteriophage T7 RNA polymerase to direct selective high-level expression of cloned genes. J. Mol. Biol. *189*, 113–130.

Sugihara, S., Orikasa, Y., and Okuyama, H. (2008). An EntD-like phosphopantetheinyl transferase gene from Photobacterium profundum SS9 complements pfa genes of Moritella marina strain MP-1 involved in biosynthesis of docosahexaenoic acid. Biotechnol. Lett. *30*, 411–414.

Suutari, M., and Laakso, S. (1994). Microbial fatty acids and thermal adaptation. Crit. Rev. Microbiol. *20*, 285–328.

Takeuchi, K., and Wagner, G. (2006). NMR studies of protein interactions. Curr. Opin. Struct. Biol. *16*, 109–117.

Thevenieau, F., and Nicaud, J.-M. (2013). Microorganisms as sources of oils. OCL *20*, D603.

Touchstone, J.C. (1992). Practice of Thin Layer Chromatography (John Wiley & Sons).

Towbin, H., Staehelin, T., and Gordon, J. (1979). Electrophoretic transfer of proteins from polyacrylamide gels to nitrocellulose sheets: procedure and some applications. Proc. Natl. Acad. Sci. *76*, 4350–4354.

Trujillo, U., Vázquez-Rosa, E., Oyola-Robles, D., Stagg, L.J., Vassallo, D.A., Vega, I.E., Arold, S.T., and Baerga-Ortiz, A. (2013). Solution Structure of the Tandem Acyl Carrier Protein Domains from a Polyunsaturated Fatty Acid Synthase Reveals Beads-on-a-String Configuration. PLoS ONE *8*, e57859.

Untergasser, A., Cutcutache, I., Koressaar, T., Ye, J., Faircloth, B.C., Remm, M., and Rozen, S.G. (2012). Primer3—new capabilities and interfaces. Nucleic Acids Res. gks596.

Uthoff, S., Bröker, D., and Steinbüchel, A. (2009). Current state and perspectives of producing biodiesel-like compounds by biotechnology. Microb. Biotechnol. *2*, 551–565.

Valenzuela, R., and Valenzuela, A. (2013). Overview About Lipid Structure. In Lipid Metabolism, R. Valenzuela Baez, ed. (InTech),.

Vanhercke, T., El Tahchy, A., Shrestha, P., Zhou, X.-R., Singh, S.P., and Petrie, J.R. (2013). Synergistic effect of WRI1 and DGAT1 coexpression on triacylglycerol biosynthesis in plants. FEBS Lett. *587*, 364–369.

Venkitakrishnan, R., Benard, O., Max, M., Markley, J., and Assadi-Porter, F. (2012). Use of NMR Saturation Transfer Difference Spectroscopy to Study Ligand Binding to Membrane Proteins. In Membrane Protein Structure and Dynamics, N. Vaidehi, and J. Klein-Seetharaman, eds. (Humana Press), pp. 47–63.

Viegas, A., Manso, J., Nobrega, F.L., and Cabrita, E.J. (2011). Saturation-Transfer Difference (STD) NMR: A Simple and Fast Method for Ligand Screening and Characterization of Protein Binding. J. Chem. Educ. *88*, 990–994.

Villa, J.A., Cabezas, M., de la Cruz, F., and Moncalian, G. (2014). Use of limited proteolysis and mutagenesis to identify folding domains and sequence motifs critical for wax ester synthase/acyl coenzyme A:diacylglycerol acyltransferase activity. Appl. Environ. Microbiol. *80*, 1132–1141.

Villa Torrecilla, J.A. (2012). Producción y acumulación de triglicéridos en procariotas.

Viola, P., and Viola, M. (2009). Virgin olive oil as a fundamental nutritional component and skin protector. Clin. Dermatol. *27*, 159–165.

Vlahov, G. (1999). Application of NMR to the study of olive oils. Prog. Nucl. Magn. Reson. Spectrosc. *35*, 341–357.

Wahlen, B.D., Morgan, M.R., McCurdy, A.T., Willis, R.M., Morgan, M.D., Dye, D.J., Bugbee, B., Wood, B.D., and Seefeldt, L.C. (2013). Biodiesel from Microalgae, Yeast, and Bacteria: Engine Performance and Exhaust Emissions. Energy Fuels *27*, 220–228.

Wallis, J.G., Watts, J.L., and Browse, J. (2002). Polyunsaturated fatty acid synthesis: what will they think of next? Trends Biochem. Sci. *27*, 467.

Wältermann, M., and Steinbüchel, A. (2005). Neutral Lipid Bodies in Prokaryotes: Recent Insights into Structure, Formation, and Relationship to Eukaryotic Lipid Depots. J. Bacteriol. *187*, 3607–3619.

Wältermann, M., and Steinbüchel, A. (2006). Wax Ester and Triacylglycerol Inclusions. In Inclusions in Prokaryotes, D.J.M. Shively, ed. (Springer Berlin Heidelberg), pp. 137–166.

Wältermann, M., Luftmann, H., Baumeister, D., Kalscheuer, R., and Steinbüchel, A. (2000). Rhodococcus opacus strain PD630 as a new source of high-value single-cell oil? Isolation and characterization of triacylglycerols and other storage lipids. Microbiol. Read. Engl. *146 (Pt 5)*, 1143–1149.

Wältermann, M., Hinz, A., Robenek, H., Troyer, D., Reichelt, R., Malkus, U., Galla, H.-J., Kalscheuer, R., Stöveken, T., Von Landenberg, P., et al. (2005). Mechanism of lipid-body formation in prokaryotes: how bacteria fatten up. Mol. Microbiol. *55*, 750–763.

Wältermann, M., Stöveken, T., and Steinbüchel, A. (2007). Key enzymes for biosynthesis of neutral lipid storage compounds in prokaryotes: properties, function and occurrence of wax ester synthases/acyl-CoA: diacylglycerol acyltransferases. Biochimie *89*, 230–242.

Ward, O.P., and Singh, A. (2005). Omega-3/6 fatty acids: Alternative sources of production. Process Biochem. *40*, 3627–3652.

Wilken, H.C., Rogge, S., Götze, O., Werfel, T., and Zwirner, J. (1999). Specific detection by flow cytometry of histidine-tagged ligands bound to their receptors using a tag-specific monoclonal antibody. J. Immunol. Methods *226*, 139–145.

Williamson, M.P. (2008). The Nuclear Overhauser Effect. In Modern Magnetic Resonance, G.A. Webb, ed. (Springer Netherlands), pp. 409–412.

Xu, J., Du, W., Zhao, X., Zhang, G., and Liu, D. (2013). Microbial oil production from various carbon sources and its use for biodiesel preparation. Biofuels Bioprod. Biorefining *7*, 65–77.

Yazawa, K. (1996). Production of eicosapentaenoic acid from marine bacteria. Lipids *31 Suppl*, S297–S300.

Zhang, F., Ouellet, M., Batth, T.S., Adams, P.D., Petzold, C.J., Mukhopadhyay, A., and Keasling, J.D. (2012). Enhancing fatty acid production by the expression of the regulatory transcription factor FadR. Metab. Eng. *14*, 653–660.

(2015). FAO Globefish.

PHYRE2 Protein Fold Recognition Server.

PyMOL | www.pymol.org.

PUBLICATIONS

8. Publications

8.1. Patent

Heat-stable triacylglycerol synthases and use thereof.
Gabriel Moncalián Montes, Fernando de la Cruz Calahorra, Juan Antonio Villa Torrecilla, Beatriz Lázaro Pinto and Matilde Andrea Cabezas Isidro.
University of Cantabria.

Patentscope: WO2014049180 A1, April 03, 2014.
Also published as: ES2457665 B1, November 13, 2014.

8.2. Scientific papers in preparation

Heterologous expression of a thermophilic acyltransferase sparks oil accumulation in Escherichia coli.
Beatriz Lázaro, Juan A. Villa, Omar Santín, Matilde Cabezas, Fernando de la Cruz and Gabriel Moncalián.

A gene deletion increases DHA production in Escherichia coli *expressing Pfa genes.*
Laura Giner, Irene Gonzalez, Beatriz Lázaro, Fernando de la Cruz and Gabriel Moncalián.

Nutrient starvation leading to triglyceride accumulation activates the Entner Doudoroff pathway in Rhodococcus jostii *RHA1.*
Antonio Juarez, Juan A. Villa, Val F. Lanza, Beatriz Lázaro, Fernando de la Cruz, Héctor M. Alvarez and Gabriel Moncalián.

(19) OFICINA ESPAÑOLA DE PATENTES Y MARCAS

ESPAÑA

(11) Número de publicación: **2 457 665**

(21) Número de solicitud: 201200967

(51) Int. Cl.:

C12N 9/10 (2006.01)
C12N 1/21 (2006.01)
C12P 7/64 (2006.01)

(12) PATENTE DE INVENCIÓN B1

(22) Fecha de presentación:

28.09.2012

(43) Fecha de publicación de la solicitud:

28.04.2014

Fecha de la concesión:

05.11.2014

(45) Fecha de publicación de la concesión:

13.11.2014

(73) Titular/es:

UNIVERSIDAD DE CANTABRIA (100.0%)
Pabellón de Gobierno, Avda. de los Castros s/n
39005 Santander (Cantabria) ES

(72) Inventor/es:

MONCALIÁN MONTES, Gabriel;
DE LA CRUZ CALAHORRA, Fernando;
VILLA TORRECILLA, Juan Antonio ;
LÁZARO PINTO , Beatriz y
CABEZAS ISIDRO, Matilde Andrea

(54) Título: **Triacilglicerol sintasas termoestables y usos de las mismas**

(57) Resumen:
Polinucleótido aislado que presenta al menos un 75% de homología con la secuencia SEQ ID NO 1. Polipéptido codificado por el polinucleótido anterior, que presenta actividad triacilglicerol sintasa. Vector que comprende el polinucleótido anterior. Célula hospedadora transformada con dicho vector. Método para la obtención de TAGs basado en la expresión del polipéptido codificado por el polinucleótido anterior mediante el cultivo de la célula hospedadora transformada anterior en un medio que comprende residuos o desechos industriales como fuente de carbono. Empleo de los TAGs obtenidos en dicho método como biocombustible o como material de partida para la obtención de biocombustible.

ES 2 457 665 B1